Stability domains computation and stabilization of nonlinear systems: implications for biological systems

PROEFSCHRIFT

ter verkrijging van de graad van doctor aan de
Technische Universiteit Eindhoven, op gezag van de
rector magnificus, prof.dr.ir. F.P.T. Baaijens, voor een
commissie aangewezen door het College voor
Promoties, in het openbaar te verdedigen
op dinsdag 4 oktober 2016 om 16.00 uur

door

Alina Ionela Doban

geboren te Târgu Frumos, Roemenië

Dit proefschrift is goedgekeurd door de promotoren en de samenstelling van de promotiecommissie is als volgt: :

voorzitter:	Prof.dr.ir. J.H. Blom
1e promotor:	Prof.dr.ir. P.M.J. Van den Hof
copromotor:	Dr. M. Lazar
leden:	Prof.dr.rer.nat. S.F. Hafstein (Reykjavik University, Iceland)
	Prof.dr.ing. O.C. Pastravanu ("Gh. Asachi" Technical University of Iasi, Romania)
	Prof.dr.ir. R.L.M. Peeters (Maastricht University)
	Prof.dr.ir. N.A.W. van Riel
	Prof.dr. A.J. van der Schaft (Rijksuniversiteit Groningen)

Het onderzoek dat in dit proefschrift wordt beschreven is uitgevoerd in overeenstemming met de TU/e Gedragscode Wetenschapsbeoefening.

Stability domains computation and stabilization of nonlinear systems: implications for biological systems

Motto:

"*Do not fear to be eccentric in opinion,*
for every opinion now accepted was once eccentric."

Bertrand Russell

The research reported in this thesis forms a part of the research program of the Dutch Institute of Systems and Control (DISC). The author has successfully completed the educational program of the DISC Graduate School.

Nederlandse Organisatie voor Wetenschappelijk Onderzoek

This work is part of the research programme "DISC Graduate Programme" with project number 022.002.025, which is financed by the Netherlands Organisation for Scientific Research (NWO).

A catalogue record is available from the Eindhoven University of Technology Library.

Stability domains computation and stabilization of nonlinear systems:
implications for biological systems
by Alina Doban.
Eindhoven : Technische Universiteit Eindhoven, 2016. Proefschrift.

ISBN: 978-90-386-4133-1 NUR: 959.

Cover design: Razvan Constantin Cercel.
Reproduction: Printservice, Eindhoven University of Technology.

Contents

Summary

Stability domains computation and stabilization of nonlinear systems: implications for biological systems

The research presented in this thesis considers the stability analysis and feedback stabilization of nonlinear continuous time dynamical systems that arise in biomedical and biological applications. In particular, these applications can be classified in two categories with respect to the modelling approach. Thus, we consider evolutionary (population interaction) models, which are used for characterizing tumor or HIV dynamics and biochemical reactions models, which are common for describing feedback loops in regulating organ functions, as it is the case of the hypothalamic–pituitary–adrenal (HPA) axis, or the genetic toggle switch in gene regulatory networks. These classes of models are either polynomial or rational (involving Hill type of rational terms). Such nonlinear models exhibit multiple equilibria corresponding to healthy or non–healthy clinical situations. The analysis of the stability properties of these equilibria is useful for diagnosis and treatment assessment, while by feedback stabilization an optimal personalized treatment strategy can be indicated to clinicians.

The stability analysis problem for the underlying classes of systems translates into computing domains of attraction of equilibria of interest. The feedback stabilization problem is aimed at either enlarging the domain of attraction or at destabilizing one equilibrium and stabilizing another, i.e. by steering the system trajectories that are already converging to a particular equilibrium to another equilibrium. The tool for answering the problems above consists of Lyapunov functions. Despite the extensive ongoing research in the community for providing either explicit forms of Lyapunov functions or constructive computational methods aimed at estimating domains of attraction, a general, systematic methodology has not yet been proposed for nonlinear systems. In order to use Lyapunov functions as a computational tool for challenging, nonlinear dynamics arising in mathematical biology, drawbacks of existing methods such as conservativeness and computational complexity need to be addressed.

We proceed, in *Chapter 1*, by providing a motivating example relating biological processes to aspects from nonlinear systems theory, together with an overview of the types of dynamics considered and related Lyapunov stability theory concepts. The chapter concludes with a summary of the contributions and corresponding publications.

In *Chapter 2*, one of the constructive results for computing domains of attraction based

on rational Lyapunov functions will be described. Similar to other type of Zubov's method approaches, this result yields a recursive approach towards estimating a maximal Lyapunov function. Based on this, we provide a procedure which generates a rational control Lyapunov function and a polynomial stabilizer. For polynomial systems, we indicate that the existence of a polynomial feedback stabilizer is guaranteed by the existence of a rational control Lyapunov function. Furthermore, rational Lyapunov functions lead to a Lyapunov condition that can be verified in a tractable manner. We illustrate the proposed procedure for the stabilization of the population co–existence equilibrium of a predator–prey model describing tumor dynamics.

In *Chapter 3*, we derive a new stabilization approach which can be used for tumor immunotherapy and it is based on a switching control strategy defined on domains of attraction of equilibria of interest. For this, we consider a recently derived model which captures the interaction between the tumor cells and immune system through predator–prey competition terms. Additionally, it incorporates the immune system's mechanism for producing hunting immune cells, which makes the model suitable for immunotherapy strategies analysis and design. For computing the domain of attraction of an equilibrium of interest, maximal rational Lyapunov functions are employed, which can be systematically computed for nonlinear systems as shown in Chapter 2. The proposed procedure confirms observations from medical practice and provides a useful support tool for model–based cancer therapy design and testing. The analysis and stabilization methods described above, which are based on rational Lyapunov functions are tailored to provide nonconservative results for polynomial systems.

To address nonpolynomial nonlinear dynamics, in *Chapter 4*, we derive a new, Massera–type Lyapunov converse construction which can be applied to systems with any type of nonlinearity, as long as some regularity conditions are satisfied. This construction is enabled by imposing a finite–time criterion on the integrated function. Compared to standard converse theorems, which either integrate up to infinity or assume global exponential stability and integrate over a finite time interval, we relax the assumption of exponential stability to $\mathcal{KL}$–stability, while still allowing integration over a finite time interval. The resulting Lyapunov function can be computed based on any $\mathcal{K}_\infty$–function of the norm of the solution of the system. In addition, we show how the developed converse theorem can be used to construct an estimate of the domain of attraction. A similar Yoshizawa–type construction which offers a computationally attractive alternative to the Massera construction, as there is no integral to compute, is also developed. The freedom to choose any norm as a candidate function, which is allowed by the finite–time criterion, in turn, requires knowledge of the system's solution over a finite period of time. This offers a trade–off between the classical Lyapunov construction, where the solution is not needed, but the candidate function cannot be chosen as freely.

To enable construction of Lyapunov functions via the converse results proposed in Chapter 4, in *Chapter 5* two finite–time verification and computation methods are proposed. The first one is based on piecewise affine approximations of the solution of the system and numerical approximations of the Massera–type Lyapunov function. This leads to continuous and piecewise affine Lyapunov function candidates, for which an optimization problem is solved to validate the obtained domain of attraction estimate. When obtaining a numerical approximation of the solution is computationally tedious, as it can be the case for higher order nonlinear systems, then we propose an indirect type of approach, starting from the linearized dynamics, however in terms of the finite–time Lyapunov function concept.

In *Chapter 6*, the nonevolutionary biological applications are considered. More specifically, the tools developed in Chapters 4 and 5 are used to compute domains of attraction for models which are aimed at describing the HPA axis behavior and genetic regulatory networks such as the toggle switch and the repressillator. The toggle switch is characterized by bistability, while bistability in the case of the HPA corresponds to hypocortisolic or hypercortisolic equilibria and relates to disorders such as type 2 diabetes. The stabilization problem for this class of systems is also addressed, via the Massera construction.

Since biological systems are subject to uncertainties coming from parameter estimation errors, for example, and disturbances, in *Chapter 7*, we address robustness issues when computing Lyapunov functions as developed in Chapter 4, by means of the (input to state stability) ISS framework. As such, we provide an ISS LF construction procedure and we consider the problem of ISS stabilization by using Sontag's universal controller formula.

Chapter 8 concludes the thesis with a concise overview of the main achievements and an outlook to open problems, relevant future research directions and possible implications for medical practice of the developed tools and results.

Basic notation and definitions

Sets, set operations and real numbers

The following standard sets and set operations are considered:

$\mathbb{N}$, $\mathbb{R}$, $\mathbb{R}_{\geq 0}$, $\mathbb{R}_{>0}$, $\mathbb{Z}$, $\mathbb{Z}_{\geq 0}$, $\mathbb{Z}_{>0}$	The set of natural numbers, real numbers, of nonnegative reals, of positive reals, of integers, of nonnegative integers and of positive integers;
$\mathbb{R}^n_+$	The positive orthant;
$\mathcal{S}^\circ$, $\partial\mathcal{S}$, $\overline{\mathcal{S}}$	The interior, boundary and closure of $\mathcal{S}$;
$\mathbb{N}_{[a:b]}$	The set defined by $\{a, a+1, \ldots, b-1, b\}$, $a, b \in \mathbb{N}$, $a < b$;
$\mathbb{Z}_{[a:b]}$	The set defined by $\{a, a+1, \ldots, b-1, b\}$, $a, b \in \mathbb{Z}$, $a < b$;
$\lfloor x \rfloor$	The largest integer which is less or equal than x.

- A subset $\mathcal{S}$ of a topological space $\mathbb{X}$ is called *compact* if every open cover of $\mathcal{S}$ has a finite subcover. Every closed, bounded subset of $\mathbb{R}^n$ is compact.

- A set $\mathcal{S} \subseteq \mathbb{R}^n$ is called *proper* if it contains the origin in its interior.

- By $p \in \mathbb{R}[x_1, x_2, \ldots, x_n]$ we say that p belongs to the set of all polynomials in $x_1, \ldots, x_n$ with coefficients in $\mathbb{R}$. A subset of $\mathbb{R}^n$ is called *semialgebraic* [63] if it is a finite union of finite intersections of sets defined by a polynomial equation or inequality.

Vectors, matrices and norms

The following definitions regarding vectors and matrices are used:

$\lambda_{\text{max}}(Z)$, $\lambda_{\text{min}}(Z)$	The largest and the smallest eigenvalue of the symmetric matrix Z;
$\|x\|$, $\|A\|$	An arbitrary norm of $x \in \mathbb{R}^n$ and the induced norm of A, i.e., $\max\{\|Ax\| : x \in \mathbb{R}^n, \|x\| = 1\}$;
$\|x\|_p$, $\|x\|_\infty$	The p-norm, $p \in \mathbb{Z}_{\geq 1}$ and the infinity-norm of the vector x, i.e., $(\sum_{i=1}^n \|[x]_i\|^p)^{\frac{1}{p}}$ and $\max_{i \in \mathbb{Z}_{[1,n]}} \|[x]_i\|$, respectively;
$\mu(A)$	The logarithmic norm of a matrix (or the matrix measure), i.e., $\mu(A) = \lim\limits_{h \to 0+} \frac{\|I + hA\| - 1}{h}$;
$\mu_2(A)$, $\mu_{2,P}(A)$	The logarithmic norm induced by the 2–norm, and by the 2–weighted norm, i.e., $\mu_2(A) = \lambda_{\text{max}}(\frac{1}{2}(A + A^\top))$, $\mu_{2,P}(A) = \lambda_{\text{max}}(\frac{\sqrt{P}A\sqrt{P}^{-1} + (\sqrt{P}A\sqrt{P}^{-1})^\top}{2})$;
$Z \succ 0$, $Z \succeq 0$	The symmetric matrix $Z \in \mathbb{R}^{n \times n}$ is positive definite and positive semidefinite.

Furthermore, let $\mathbb{B}_\rho(p)$ denote the ball of radius ρ centered in $p \in \mathbb{R}^n$, defined as $\mathbb{B}_\rho(p) = \{x \in \mathbb{R}^n \mid \|x - p\| \leq \rho\}$. Given a point $p \in \mathbb{R}^n$ we define a neighborhood of p, $\mathcal{N}(p)$, as the ball $\mathbb{B}_\rho(p)$ for some radius ρ. By $\mathcal{N}(p)^+$ the projection of $\mathcal{N}(p)$ on $\mathbb{R}^n_{\geq 0}$ is denoted.

Basic functions and classes of functions

The following definitions and classes of functions are distinguished:

id	The identity function, i.e., $\mathrm{id} : \mathbb{R} \to \mathbb{R}$, such that $\mathrm{id}(s) = s$.
$\alpha \circ \tilde{\alpha}(\cdot)$	The composition of $\alpha : \mathbb{R} \to \mathbb{R}$ with $\tilde{\alpha} : \mathbb{R} \to \mathbb{R}$, i.e., such that $\alpha \circ \tilde{\alpha}(r) := \alpha(\tilde{\alpha}(r))$ for all $r \in \mathbb{R}$;
$\mathcal{K}$, $\mathcal{K}_\infty$	The class of all functions $\alpha : \mathbb{R}_{[0,a)} \to \mathbb{R}_{\geq 0}$, $a \in \mathbb{R}_{>0}$ that are continuous, strictly increasing and satisfy $\alpha(0) = 0$ and the class of all functions $\alpha \in \mathcal{K}$ with $a = \infty$ and such that $\lim_{r\to\infty} \alpha(r) = \infty$;
$\mathcal{L}$	The class of all continuous functions $\sigma : \mathbb{R}_{\geq 0} \to \mathbb{R}_{\geq 0}$ which are strictly decreasing and $\lim_{s\to\infty} \sigma(s) = 0$;
$\mathcal{KL}$	The class of all continuous functions $\beta : \mathbb{R}_{[0,a)} \times \mathbb{Z}_{\geq 0} \to \mathbb{R}_{\geq 0}$, $a \in \mathbb{R}_{>0}$ such that for each fixed $s \in \mathbb{Z}_{\geq 0}$, $\beta(r, s) \in \mathcal{K}$ with respect to r and for each fixed $r \in \mathbb{R}_{[0,a)}$, $\beta(r, s)$ is decreasing with respect to s and $\lim_{s\to\infty} \beta(r, s) = 0$.

- A function $V : \mathcal{A} \to \mathbb{R}$, where $\mathcal{A} \subseteq \mathbb{R}^n$ is a proper set, is called *positive definite* (positive semidefinite) on $\mathcal{A}$ if

$$V(0) = 0 \quad \text{and} \quad V(x) > 0 \, (V(x) \geq 0),$$

  for any $x \in \mathcal{A} \backslash \{0\}$. $V(x)$ is called *negative definite* (negative semidefinite) if $-V(x)$ is positive definite (positive semidefinite).

- A function $f : \mathbb{R}^n \to \mathbb{R}^n$ is called *$\mathcal{K}$–bounded* if there exists a function $\alpha \in \mathcal{K}$ such that

$$\|f(x)\| \leq \alpha(\|x\|), \quad \forall x \in \mathbb{R}^n.$$

List of abbreviations

The following abbreviations are used throughout this thesis:

AS	asymptotically stable
GAS	globally AS
LF	Lyapunov function
CLF	control Lyapunov function
RCLF	rational control Lyapunov function
DOA	domain of attraction
PWA	piecewise affine
CPA	continuous piecewise affine
FTLF	finite time Lyapunov function
ISS	input to state stable
HPA	hypothalamic-pituitary-adrenal
RNA	ribonucleic acid
mRNA	messenger RNA
SOS	sum of squares

Chapter 1

Introduction

1.1 Background

Mathematical biology can be essentially defined as the research field of applied mathematics to the biomedical sciences including biology, biotechnology, medicine and even psychology. Mathematical models have as main purpose the deductive explanation of the underlying biological processes that occur in a particular observed phenomenon. Consequently, models which are able to capture the essence of various interactions, whether occurring in competing populations in evolutionary processes or in biochemical reactions, provide an understanding and predictions of the outcome of these interactions. For a comprehensive overview of problems arising in biology which can be addressed and understood by means of deterministic dynamical models (i.e., continuous–time differential equations) see for example, [94] and [73]

When the purpose of studying biological processes is to facilitate societal tasks such as: disease diagnosis, disease monitoring and predictions, and ultimately, optimal treatment design and biotechnologies, the a very suitable approach is to analyze their dynamical models. Whether these processes are inherently occurring in nature, or they are synthetically engineered to generate new systems or to mimic existing ones, they often lead to complex, nonlinear system descriptions.

The nonlinear differential equations models which arise from biological processes are most often derived from applying the following principles. Generally, for systems regulating a certain substance, the law of mass action is applied for the biochemical reaction networks characterizing the process, which together with the involved feedback loops lead to Hill function types of nonlinearities [36]. When population interactions are involved, a population ecology perspective is used for deriving evolutionary models with predator–prey/competing type of dynamics. As for systems used to model and design synthetic gene networks, biochemical rate equations formulations of gene expressions provide models with Hill–type nonlinearities.

Although biological processes are relevant in a broad range of application areas, i.e., from the (bio)medical domain to synthetic fuel production, in this thesis the focus is on biomedical systems. Namely, a nonlinear systems theory approach is considered for establishing supporting tools for disease diagnosis and qualitative predictions, as well as for treatment design.

In the recent years, with the exponential increase in incidence cases of chronic diseases like type two diabetes or becoming chronic diseases such as cancer, mathematical tools have become more and more popular in the study of such diseases [88], [38]. This is because mathematical models can provide information beyond sequential diagnostics or check-ups, which is concerned with the dynamical evolution of a disease or dysfunction.

The human body is the most complex and efficient existing control system. It is composed of switching positive and negative feedback loops which act at maintaining optimal organ functioning and optimal hormone values, fast response to stress and rejection of viruses and bacteria; thus, maintaining homeostasis [116]. At a cellular level, immune cell populations are constantly competing with invader populations such as tumor cells or bacteria in a predator–prey type of interaction [93]. All of these functions, but also corresponding disorders, can be described by nonlinear dynamics. Take for example the Hypothalamus–

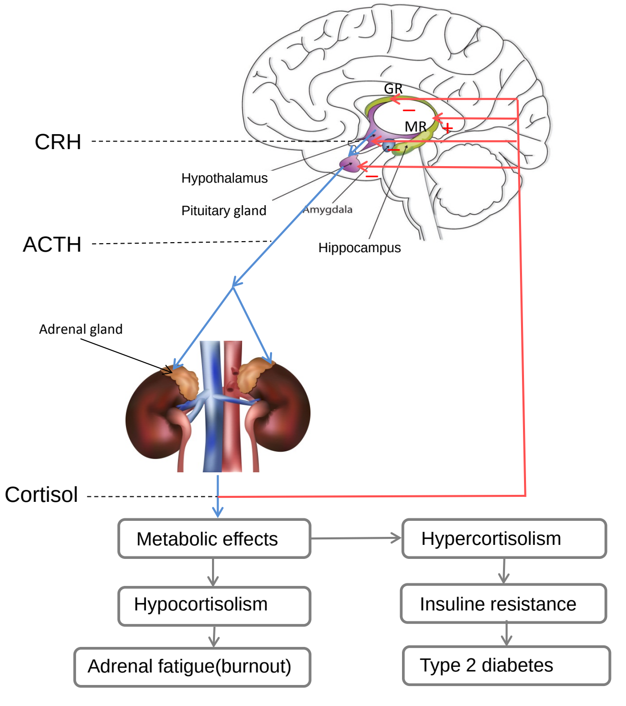

Figure 1.1: The HPA axis and disorder effects.

Pituitary–Adrenal Axis (HPA) system depicted in Figure 1.1. The three components interact via three hormones: corticotropin release hormone (CRH), adrenocorticotropic hormone (ACTH) and cortisol. While the secretion of CRH in the hypothalamus is stimulated by the hippocampus, cortisol inhibits the secretion of CRH with a negative feedback both at the hypothalamus level, as well as through a negative feedback with the glucocorticoid receptors (GR) in the hypothalamus. In turn, the hypothesis that cortisol exhibits a positive feedback with the mineralcorticoid receptors (MR) in the hippocampus has led to better patient data fit in the literature [6]. Cortisol also inhibits the secretion of ACTH in the pituitary gland, which is stimulated by CRH. All these feedback mechanisms work simultaneously in the HPA axis to maintain an optimum level of cortisol. Whenever the HPA axis is not functioning properly, too high or too low levels of cortisol have many metabolic effects that can lead to insulin resistance and diabetes, as an example in the case of hypercortisolism, or to adrenal fatigue, as an example in the case of hyporcortisolism. Other consequences are related to heart diseases or tyroid disfunctions.

The correspondence between problems in biological systems and nonlinear systems theory is summarized in Table 1.1 and will be elaborated as follows. Maintaining homeostasis in certain systems in the body, or at a tissue level in the case of diseases such as cancer, translates to maintaining a stable, "healthy" equilibrium of their corresponding dynamical models. Information about the set of all possible initial states which converge to the stable equilibrium is relevant for diagnosis but also for predictions. This set is called the *domain of*

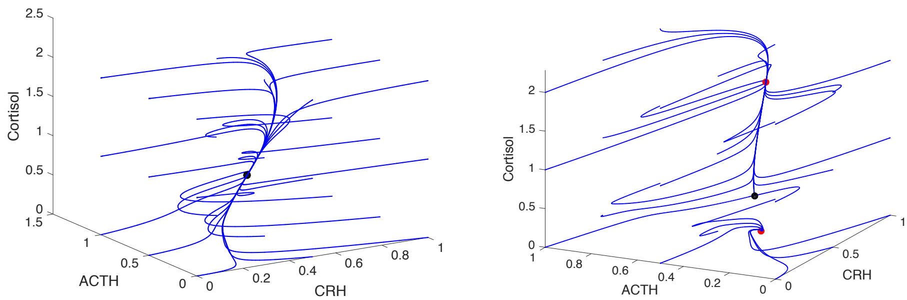

(a) (b)

Figure 1.2: HPA axis: (a) - unique stable equilibrium marked with black and a set of trajectories, bistability; (b) - bistability: hypercortisolic (upper red) stable equilibrium, hypocortisolic (lower red) equilibrium and healthy cortisol value unstable equilibrium (black).

stability or *the domain of attraction* (DOA) of the equilibrium of interest. Throughout this thesis, the diagnosis and prediction problem is closely related to the problem of computing the DOA. For example, in Figure 1.2(a) we illustrate the case when the HPA axis system has a healthy cortisol level as the only stable equilibrium, shown with black in the plot. This stable equilibrium value corresponds to a well functioning HPA axis, which is able to maintain homeostasis. Specifically, this means that if the body is subject to stress (physical or psychological) the homeostasis state is disrupted and the cortisol level is affected, but the HPA axis is able to bring the cortisol value back to normal. The trajectories displayed in Figure 1.2(a) correspond to a set of initial states from which the HPA axis will always converge to the healthy equilibrium. Thus, the displayed set of initial states is a subset of the DOA of the black equilibrium.

In general, nonlinear systems exhibit multiple stable and unstable equilibria. In the case of nonlinear biological systems, bistability, i.e., two stable equilibria, is most often encountered. For the particular case of the HPA system introduced above, the hypercortisolic and hypocortisolic case correspond to two stable equilibria with high/low cortisol values as shown in Figure 1.2(b). In this case the black (healthy) equilibrium is unstable. Some trajectories will converge to the hypercortisolic equilibrium and some to the hypocortisolic one, depending on the initial state. However, for certain initial conditions, the corresponding trajectories will first converge to the healthy equilibrium state (black), and since this one is unstable, they will further converge to either one of the nonhealthy ones. Therefore, if a patient is to be diagnosed based only on measuring the level of cortisol, that patient may appear to be healthy (while the HPA axis is dysfunctional), and after some time he/she will become hypocortisolic depressed, for example, and cannot be treated without drug influence.

The switch to bistability occurs in the case of HPA axis dysfunction and it is related to changes in the parameter values of its corresponding model. In such cases, the purpose of the treatment is to either control the states of the system to the DOA of the healthy equilibrium, or to prevent trajectories from converging to an undesired equilibrium. Thus the treatment design problem translates into a stabilization problem for the considered models.

In Table 1.1 we summarize the key aspects from biological systems, described above, which can be best understood by investigating their dynamical models. In particular, we map concepts and problems from the biological domain to corresponding concepts and problems in the nonlinear systems theory area.

Mapping of research problems	
Biological systems	Nonlinear systems theory
predator–prey models	polynomial nonlinearities
biochemical reaction networks	rational nonliniearities (Hill type)
maintaining homeostasis	stable equilibrium
diagnosis and prediction	compute the DOAs and stability boundary
treatment design case 1	stabilization of unstable equilibrium
treatment design case 2	enlarge DOA of stable equilibrium

Table 1.1: A summary of problems in the biological domain which can be addressed by means of dynamical systems.

1.2 Research objectives

Lyapunov functions (LFs) are the main tool for nonlinear systems stability analysis. The construction or computation of LFs has been long studied in the literature since they were first introduced in [84] as they provide information about the solution of a nonlinear system without computing it. See in Figure 1.3(a) an illustration of the LF concept, with respect to the time evolution of the states of a second order dynamical system. Specifically, a given candidate function is a LF if it decreases in time with respect to the system's solutions for all positive time values. In Figure 1.3(b) we show an example of a function which is not a LF with respect to the shown system's solutions. Naturally, the decrease condition should hold for all initial conditions in some set around the origin when we talk about local LFs, and for all initial conditions in $\mathbb{R}^n$ when we talk about global LFs. Formally, we say that a function $W : \mathbb{R}^n \to \mathbb{R}_{\geq 0}$ is a LF for a system $\dot{x} = f(x)$ if

a) $W(x)$ is positive definite and radially unbounded on $\mathbb{R}^n$, and,

b) its derivative along the trajectories of $\dot{x} = f(x)$, $\dot{W}(x) = \nabla W^\top f(x)$, is negative definite on some proper set $\mathcal{A} \in \mathbb{R}^n$.

Computing LFs is relevant for the problems in Table 1.1 because their level sets provide approximations of the DOA of an equilibrium. Generally, in the case of nonlinear systems a given function is a valid LF for that system only in a region around the equilibrium where the function is decreasing with respect to the system's solutions, i.e. $\dot{W}(x) < 0$. This region will be defined by the largest level set of the LF such that the decrease condition is satisfied.

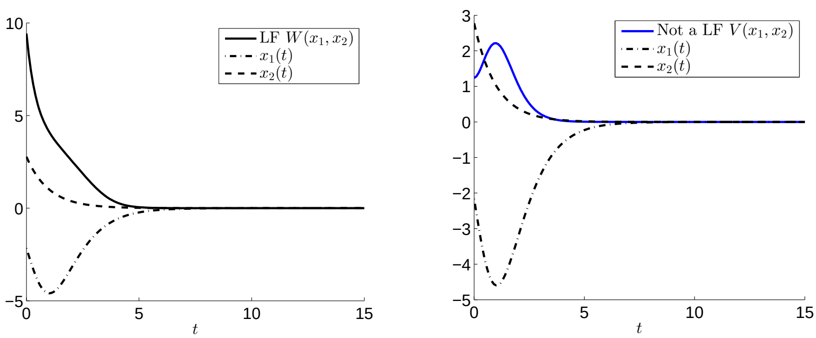

(a)

(b)

Figure 1.3: Illustration of the Lyapunov function concept.

Often, computing LFs is very difficult if not impossible for nonlinear systems. We refer to the books [77] and [80] for an extensive introduction, and to [60], [121], [122] for a more in depth exposition of the LF concept and related methods. For systems which are subject to control inputs, control Lyapunov functions (CLFs) enable the computation of feedback stabilizers. While LFs based tools are useful for analysis and stabilization of nonlinear systems without knowledge of the system's solutions, constructing such functions is a very challenging problem. In particular, when the computed LFs should lead to nonconservative DOA estimates.

By *nonconservative* DOA estimates, in this thesis, it is meant that the resulting DOA estimate generated by the LF satisfies one of the following criteria. In the case of an unique stable equilibrium, the estimate captures the largest state space region when a comparison is possible, or its boundary is sufficiently close to possibly existing unstable equilibria [28]. In the bistability case, as shown in Figure 1.2(b), the DOA estimates of the two stable equilibria are called nonconservative if their boundaries are sufficiently close to the separating unstable equilibrium [29].

Local stability of equilibria can be easily inferred based on Lyapunov's indirect method which uses the system's linearization around the equilibria, or even by the Lyapunov direct method. The latter guarantees stability in the set where there exists a valid LF. Albeit a quadratic LF can be computed for a general nonlinear system, it will provide stability guarantees (DOA estimate) only in a small area around the origin. In turn, converse Lyapunov theorems are concerned with the construction and computation of LFs under stability assumptions.

For the class of biological systems considered in this thesis, as good as possible DOA estimates are needed both for accurate diagnosis and prediction and for control design. Consider again the HPA example. If a patient's measured cortisol level is outside of the healthy range, but it belongs to the DOA estimate of a healthy equilibrium, then it is known that the HPA axis will naturally regulate the cortisol level after some time, without the influence of treatment. While, without this information, applying treatment might in fact destabilize the healthy equilibrium and have the opposite effect.

In this thesis, the focus is on the construction of LFs such that they lead to nonconservative DOA estimates and facilitate the computation of feedback stabilizers, when local stability properties are known. As such, we consider results based on the converse of Lyapunov's second method (or direct method) for general nonlinear systems. Work on converse based constructions has started around the 1950s with the crucial results in [90] and later the alternative [121], which led to a considerable amount of subsequent work, out of which we point out to the more recent contributions in [87], [115] and [76]. As for existing results which are specifically aimed at providing relevant DOA estimates while computing a LF, we refer to the approach of Zubov in [122], which yields an analytic formula for a LF. Stemming from Zubov's method, a recursive procedure for constructing a rational LF, which has computational advantages with respect to the one in [122], was proposed in [118].

In the case of nonlinear systems which are polynomial, a significant amount of research has been dedicated for computing polynomial LFs. We refer to [96] and developments of the authors of [96]. The therein developed tools were enabled by the fact that polynomial nonlinearities in the systems allow to formulate the LF computation problem in terms of sum–of–square inequalities. However, the applicability of sum–of-square tools is limited even within the polynomial systems class, since there exist polynomial systems which are stable and do not admit a polynomial LF [3]. The advantage of sum–of–square type of methods is that they allow to formulate the involved optimization problems as Linear Matrix Inequalities [25], [26], [61]. Nevertheless, similarly to Zubov type of approaches, for general nonlinear systems, conservativeness is introduced in the computations due to Taylor approximations of the dynamics.

For what concerns state–of–the–art LF numerical, constructive methods, see the recent developments of the author of [57] and subsequent works, out of which we single out [12] and the subsequent [15], where the Massera construction is exploited for generating piecewise affine LFs and [59] and the subsequent [58] where the Yoshizawa construction is used. These constructions do not depend on the type of nonlinearity, however they rely on state space simplicial partitions which can lead to a heavy computational load for higher order complex systems.

Despite the extensive work on the topic of providing a converse to Lyapunov's theorem, the existing constructive approaches have two main drawbacks. Either they are specific to classes of systems, e.g. polynomial or homogeneous [97], which renders them unapplicable to other classes, or they will provide conservative results, due to approximations. In the case of general computational approaches, the most recent ones involve state space partitions and, thus either scalability with the state space dimension might be problematic, or for more complex systems, such as those from with biological applications, very fine partitions are needed, leading to high computational demands.

For the problem of stabilization, in [7] it was shown that the existence of a smooth stabilizer is equivalent with the existence of a smooth CLF for a given nonlinear control system, thus allowing for computing feedback stabilizers by means of CLFs. Consequently, in [106] a general formula for computing the stabilizer was provided. However, either the CLF or the stabilizer need to be known to compute a stabilizer or a CLF, respectively.

As for the underlying application, there is more and more research oriented at using mathematical or system theory based tools for answering problems in biology and/or biomedical systems. A more comprehensive overview will be given in the corresponding chapters. However, we single out here the opinion papers [42] and [67], which advocate the need for integrating control theory and information from dynamical models when designing treatment strategies for cancer. The relevance of computing trapping regions (DOAs) in the case of HPA dysfunctions related to diseases such as adrenal fatigue and diabetes is promoted in [6] and [54].

1.2.1 Research question

If mathematical tools, and in particular dynamical models are to be considered for providing an understanding of the underlying biological processes behind certain diseases, dysfunctions or when engineering genetic systems with specific properties, then nonlinear systems specific concepts and problems need to be addressed.

For the biomedical subclass of biological systems, the problems of diagnosis, treatment evaluation or disease evolution prediction correspond to the problem of analysis of properties of equilibria of their dynamical descriptions. The corresponding task is the computation of DOAs. Since diseases can be related to stability properties of equilibria of nonlinear models, the treatment design problem is related to the problem of feedback stabilization. In view of the fact that in this thesis we divide the considered biological models into polynomial (evolutionary models) and rational (biochemical reactions models), for these classes of systems we formulate the following research question.

Can we compute nonconservative DOAs and stabilizing feedback laws in a systematic, reasonably computationally manner for nonlinear polynomial and rational systems?

In order to provide an answer to the research question the following subproblems are addressed in the thesis.

Since a large set of biological systems can be described by polynomial models, Zubov method type of approaches which rely on polynomial approximations of the dynamics, such as the one in [118], are good candidates. Moreover, the procedure yielding a RLF is systematic, works at maximizing the estimate of the DOA in an iterative manner and it is not computationally demanding. Furthermore, the polynomial models of the considered biological applications are rendered by evolutionary arguments, which often lead to a low number of interacting populations, ergo low system dimension. The drawback of this type of approaches, and in fact of any constructive procedure, is that in most cases the level set value of the resulting LF candidate which is included in the true DOA of the system, is not known. Usually it is computed a posteriori via a nonlinear optimization problem. Compared to other methods specifically developed for polynomial systems, such as those relying on SOS formulations which yield a polynomial LF, the RLFs are more advantageous because they are specifically constructed to provide approximates of the true DOA of the system. Nonetheless, often for assessing the stability properties of biological/biochemical systems, LF candidates which take into account the physical structure of the systems are considered. Such functions are the Gibbs free energy functions [117]. The drawback of these functions is that they rely on very good knowledge of the physical properties of the system.

RLFs enable two stabilization procedures derived in this thesis. Firstly, due to the iterative constructive property of the computation algorithm, a feedback stabilizer can be simultaneously computed with the RLF. This will address the problem of enlarging the DOA of an equilibrium, and consequently, the treatment design case 2 research problem in Table 1.1. Secondly, a switching control law defined on DOAs of successive equilibria is developed in order to steer trajectories from an unhealthy equilibrium to a healthy one, and thus addressing the treatment design case 2 research problem in Table 1.1.

As for models describing biological systems which are not polynomial, they cannot be studied by means of the same tools as those mentioned above without having to deal with approximation errors. The alternative is to use constructions which are based on functions of the state of the system, similar to Massera/Yoshizawa formulations [90], [121], computed over finite or infinite time intervals. To allow computability, often such methods are based on estimates of the solution which in turn reduce the class of systems that can be considered in terms of the stability type (e.g. exponential). This problem is addressed in the thesis and alternative constructions are proposed.

When the framework for computing LFs relies on the solutions of the system, the observation that a given function need not be strictly decreasing to ensure stability (as shown in Figure 1.3(b)) is in order. In [2] and [71] this observation was exploited to derive alternative "Lyapunov" conditions for stability. In fact, when the purpose is to compute non-conservative DOAs, the very strict decrease condition $\dot{V} < 0$ might introduce conservativeness [22], [4] when constructing a function of a certain type which iteratively expands the DOA estimate. The key problem to be addressed here is the relaxation of the LF decrease condition such that it allows for true LF constructions (of Massera/Yoshizawa type) and a systematic verification approach which is applicable to the considered class of biological systems.

Lastly, as one of the broad scopes of the mathematical biology area, and also of this thesis to a certain extent, is to provide information about biological processes which can be used for predictions and support (treatment) design, the developed tools should accommodate modelling uncertainties and disturbances. To this end, the ISS framework is considered.

1.3 Outline of the thesis

The research framework and objectives formulated in Section 1.2 can be decomposed in terms of the following problems: construction of LFs, computation/verification of LFs, stabilization by means of CLFs and applicability of the above to the considered biological applications. Consequently, the answer to the research question posed in Section 1.2.1 will be elaborated in the remainder of this thesis following the outline below.

In *Chapter 2* we consider one of the constructive results for computing LFs, which then leads to computing domains of attraction. We rely on a procedure based on constructing a rational LF, iteratively (similarly to the Zubov method) with the purpose of estimating a maximal LF. The latter function converges to infinity when the state is close to the boundary of the DOA. Furthermore, it is based on polynomial approximations of the function describing the system. Following a similar reasoning, for addressing the stabilization problem we propose a procedure which generates a rational control LF and a polynomial stabilizer. For polynomial systems, we indicate that the existence of a polynomial feedback stabilizer is guaranteed by the existence of a rational control Lyapunov function. Two examples, the Van der Pol oscillator and the stabilization of the population co–existence equilibrium and of the healthy state equilibrium (in the case of bistability) of a tumor dynamics model, are shown for illustration purposes. This procedure, in general, is guaranteed to yield the best results in terms of DOA computation and feedback stabilization for polynomial systems. Whilst the same procedure can be applied to nonpolynomial systems, the resulting DOA estimates will be highly dependent on the type of nonlinearity in the dynamics, and thus, the approximating error terms in Taylor series expansion.

For polynomial models describing tumor growth, we make use of the RLF as a tool for analysis and immunotherapeutic strategies design in *Chapter 3*. We propose a multiple LFs approach for stabilizing the tumor dormancy equilibrium of evolutionary tumor growth models, with emphasis on tumor immunotherapy considerations. The stabilizing control law is based on a switching control strategy defined on domains of attraction of equilibria of interest. We consider two evolutionary tumor growth models from the literature and we point out their drawbacks with respect to treatment design considerations. As such, by similar evolutionary considerations, we derive a new model which captures the mutual effects of the tumor cells immune system interactions, through predator–prey competition terms. Additionally, it incorporates the immune system's mechanism for producing hunting immune cells, which makes the model suitable for immunotherapy strategies analysis and design. The advantage of considering RLF for analysis and treatment synthesis is that they can be systematically computed. The proposed procedure confirms observations from medical practice and provides a possibly useful supporting tool for cancer therapy design and testing.

The analysis and stabilization methods described above, which are based on RLFs are tailored to provide nonconservative results for polynomial systems. Many biological applications are not modelled by polynomial functions or their dynamics cannot be captured by relatively low order polynomial functions. Therefore, in *Chapter 4*, we revisit constructions stemming from Lyapunov converse results. Specifically, we look at Massera and Yoshizawa type of LFs, enabled by imposing a finite–time decrease criterion on the involved function of the state. This function will be called a finite time LF (FTLF). For a graphical illustration see Figure 1.3(b); the function V whose values in time, with respect to the depicted solutions are plotted in blue, is a FTLF, which decreases after a finite time interval, unlike a LF, which decreases at all times. By means of this approach, we relax the assumptions of exponential stability on the system dynamics, while still allowing computation over a finite time interval. The resulting LF can be computed based on any $\mathcal{K}_\infty$–function of the norm of the solution of the system, in contrast with classical LFs which are generally defined by special, complex functions. In addition, we show how the developed converse theorem can be used to construct an estimate of the DOA. However, for either constructions the solution needs to be known up to some finite time value.

The freedom in construction allowed by the finite–time criterion in turn, requires knowledge of the system's solution over a finite period of time in order to verify the finite–time condition. In *Chapter 5*, we develop two options to address the verification problem. One is based on linearization of the system around the equilibrium and computing a finite–time integral/maximum of an "expanded" FTLF. The other option relies on previously introduced ODE solutions approximation techniques by means of piecewise affine (PWA) approximations of the dynamics over a state space region. While the linearization approach leads to an analytical form of a LF, the second case results in values of a LF which are interpolated towards constructing a continuous PWA (CPA) LF.

In *Chapter 6* the nonevolutionary biological applications are considered. More specifically, the tools developed in Chapters 4 and 5 are used to compute DOAs for models which are aimed at describing the HPA axis behavior and genetic regulatory networks such as the toggle switch and the represillator. The toggle switch is characterized by bistability, while bistability in the case of the HPA corresponds to hypocortisolic or hypercortisolic equilibria and relates to disorders such as type 2 diabetes. The stabilization problem for this class of systems, via the Massera construction can be essentially addressed via the universal controller proposed by Sontag in [106].

Since biological systems are subject to uncertainties coming from parameter estimation errors, for example, and disturbances, in *Chapter 7*, we address robustness issues when computing LF based on FTLFs by means of the (input to state stability) ISS framework. We show that existence of ISS FTLFs implies ISS and it is equivalent with existence of ISS LFs. As such, we provide an ISS LF construction procedure and we consider the problem of ISS stabilization by using Sontag's universal controller formula. The computational aspects are handled via inherent (FT) ISS LF considerations.

Finally, in *Chapter 8* a discussion on the developments in the thesis, applicability to real–life applications from the biological and biomedical fields, drawbacks and future prospects is reported.

1.4 Summary of publications

The results that are presented in this thesis have appeared in the publications listed below.

Chapter 2 contains results that were presented in:

- A.I. Doban and M. Lazar, "Domain of attraction computation for tumor dynamics", in the proceedings of the 53rd IEEE Conference on Decision and Control (CDC), Los Angeles, 2014, pp. 6987-6992;

- A.I. Doban and M. Lazar, "Feedback stabilization via Rational Control Lyapunov functions", in the proceedings of the 54th IEEE Conference on Decision and Control (CDC), Osaka, 2015, pp. 1148-1153.

Chapter 3 contains results that were presented in:

- A.I. Doban and M. Lazar, “A switched systems approach to cancer therapy”, in the proceedings of the 14th annual European Control Conference (ECC), Linz, 2015, pp. 2723-2729;
- A.I. Doban and M. Lazar, “An evolutionary-type model for tumor immunotherapy”, in the proceedings of the 9th IFAC Symposium on Biological And Medical Systems (BMS), Berlin, 2015, pp. 575-580;
- A.I. Doban and M. Lazar, “A Lyapunov-methods approach for tumor immunotherapy”, accepted for publication in Mathematical Biosciences, submitted 2016.

Chapter 4 and Chapter 6 contain results that were presented in:

- A.I. Doban and M. Lazar, “Computation of Lyapunov functions for nonlinear differential equations via a Massera-type construction”, submitted for publication to a journal, 2016; online version can be found at *http://arxiv.org/abs/1603.03287*.
- A.I. Doban, M. Lazar, “Computation of Lyapunov functions for nonlinear systems via a Yoshizawa-type construction”, accepted for publication in the proceedings of the 10th IFAC Symposium on Nonlinear Control Systems (NOLCOS) 2016.

Chapter 5 contains results that were presented in:

- T.R.V. Steentjes, A.I. Doban and M. Lazar, “Construction of continuous and piecewise affine Lyapunov functions via a finite-time converse”, accepted for publication in the proceedings of the 10th IFAC Symposium on Nonlinear Control Systems (NOLCOS) 2016.

A discrete–time counterpart of the results in Chapter 4 where presented in:

- A.I. Doban and M. Lazar, “Stability analysis of discrete-time general homogeneous systems”, in IFAC 19th Triennial World Congress, Cape Town, South Africa, 2014, pp. 8642–8647.

Chapter 2

Analysis and feedback stabilization via rational Lyapunov functions

In this chapter, we consider the problem of computing nonconservative domains of attraction and feedback stabilizers for polynomial systems. One of the constructive results for computing domains of attraction based on rational Lyapunov functions is presented. Similar to other type of Zubov's method approaches, this result yields a recursive routine towards estimating a maximal Lyapunov function. Based on this, we provide a procedure which generates a rational control Lyapunov function and a polynomial stabilizer for nonlinear systems described by analytic functions satisfying some regularity conditions. Furthermore, an improved estimate of the domain of attraction of the closed–loop system can be computed by means of previously introduced rational Lyapunov functions. For polynomial systems, we show that the existence of a polynomial feedback stabilizer is guaranteed by the existence of a rational control Lyapunov function. We illustrate the proposed procedure for the stabilization of the population co–existence equilibrium of a predator–prey model describing tumor dynamics.

2.1 Introduction

Computing an estimate of the DOA for general nonlinear systems is a very complex problem, as indicated in Chapter 1. For some of the existing approaches, we refer to the work in [29], where the computation of the DOA is based on some topological considerations, or the work in [30], where some gridding techniques are used. Some other works include [47], where ellipsoidal estimates of the DOA of second order nonlinear systems with certain model properties are considered. Except for the method proposed in [29], the above cited papers are based on the use of quadratic LFs. Often the level sets of these functions are unable to capture the nonlinear behavior of the system outside a small region around the origin. The difficulty in computing DOA estimates for nonlinear systems is inherited from the problem of finding an explicit form of a suitable LF. We single out, Zubov's method [122] for providing an analytic expression of a LF, which is iteratively updated towards improving the DOA estimate that it generates. Stemming from this method, in [118], the concept of a maximal LF has been introduced, which can be used to estimate the DOA exactly, and an iterative procedure based on RLFs has been developed. This approach is particularly advantageous because it can provide an analytic expression of the boundary of the DOA (estimate) and it converges after very few iterations.

As introduced in Chapter 1, the problem of computing the DOA is aimed at answering the analysis problem for the class of systems considered in this thesis, namely nonlinear systems describing biological and biomedical processes. However, for enlarging the computed DOA or for destabilizing one equilibrium and stabilizing another, the computation of feedback stabilizers is considered.

The classical problem of stabilization of nonlinear systems has been substantially studied in the control theory community. We refer to [107] for a review of some of the main stabilization techniques. One of the major results was established in [7], where it was shown that the existence of a smooth stabilizer is equivalent with the existence of a control Lyapunov function (CLF) for a given nonlinear control system, thus allowing for computing feedback stabilizers by means of LFs. Stemming from this result, in [106] a general formula for computing the stabilizer by using a CLF is given. However, the CLF needs to be known in advance, which again requires LF computing/constructing techniques for general nonlinear systems. Nonetheless, certain properties of the system dynamics can be exploited to establish general results. In [97] it has been shown that a homogeneous vector field admits a homogeneous LF. In [53] it has been shown that there exists a homogeneous CLF for any asymptotically controllable (AC) control system, and this result can be applied to check local AC for nonlinear systems which can be approximated by AC homogeneous systems. In [101] a condition for stabilization of nonlinear systems has been derived, provided that there exists a homogeneous LF for the closed–loop system. Recently, a procedure by which a continuous piecewise affine parametrization for CLFs is computed for nonlinear systems on a simplicial triangulation of the state space was proposed in [9], however it leads to a mixed integer linear program.

For polynomial vector fields, the usual go–to approach is to use sum–of–squares (SOS) techniques to compute a polynomial LF, [96]. Using similar techniques, in [27], rational LFs defined as the fraction between polynomial expressions computed using SOS methods have been derived. Some novel results [102], consider for the computation of polynomial LFs/polynomial feedback law the Bernstein polynomial basis, as it allows for checking positivity of polynomials on simplices simply by checking positivity of some coefficients. However, there exist asymptotically stable polynomial systems which do not admit a polynomial LF [3].

When the purpose of computing LFs is to estimate the DOA of a given nonlinear system, a LF which generates the best estimate of the DOA is needed. For nonautonomous systems, a CLF needs to be constructed such that the DOA of the closed loop system satisfies certain requirements. For example, in constrained stabilization it should cover the constraint set as good as possible. As for existing Zubov type results, CLFs can also be constructed as the solution to a generalized version of the Zubov equation as proposed in [24] and the references therein.

In this chapter, we consider the problem of feedback stabilization for continuous–time nonlinear systems by means of rational control Lyapunov functions (RCLFs) of the form

$$V(x) = \frac{\sum_{i=2}^{\infty} R_i(x)}{1 + \sum_{i=1}^{\infty} Q_i(x)},$$

where R_i and Q_i are homogeneous polynomials of order i. We develop a recursive procedure that generates simultaneously the coefficients of the polynomials in the RCLF V, and the coefficients of a polynomial feedback stabilizer

$$k(x) = \sum_{i=1}^{\infty} K_i(x),$$

provided that the system to be stabilized is described by an analytical, sufficiently regular function and it is affine in the control input. Analytical functions can be expressed as infinite sums of homogeneous polynomials (as for example Taylor series expansion), thus allowing for the constraints in the above mentioned recursive procedure to be linear. For polynomial systems, it will be shown that if the system admits a RCLF, then there always exists a polynomial feedback stabilizer for that system.

The introduced approach yields a feedback stabilizer while computing a RCLF. Then, by computing a RLF for the controlled system in closed loop with the stabilizer, the best DOA estimate for that $k(x)$ will be produced.

The proposed procedure will be illustrated first on the Van der Pol oscillator and then on a model from biomedical systems which describes the predator–prey type of interaction between normal cell and cancer cells in tumor development. This model has three equilibria, and depending on the model parameters one or two of the equilibria are stable. We will consider computing a feedback stabilizer for the tumor dynamics model, with respect to a desired healthy equilibrium. From a biomedical interpretation, the role of the stabilizer could be represented, for example, by immunotherapy in clinical treatment.

2.2 Computation of DOAs based on RLFs

Consider the continuous–time nonlinear autonomous system

$$\dot{x} = f(x), \tag{2.1}$$

where $f : \mathbb{X} \to \mathbb{R}^n$ is a locally Lipschitz map from the domain $\mathbb{X} \subset \mathbb{R}^n$ into $\mathbb{R}^n$.

Definition 2.1 The origin is an asymptotically stable (AS) equilibrium for the system (2.1) in the proper set $\mathcal{S} \subseteq \mathbb{R}^n$, if, for each $\varepsilon > 0$, there exists $\delta = \delta(\varepsilon) > 0$ such that $x(0) \in \mathcal{S}$ and:

$$\|x(0)\| < \delta \Rightarrow \|x(t)\| < \varepsilon, \quad \forall t \in \mathbb{R}_{\geq 0}, \tag{2.2}$$

and for all $x(0) \in \mathcal{S}$ it holds that $\lim_{t\to\infty} x(t) = 0$. If the set $\mathcal{S} = \mathbb{R}^n$, then we say that the origin is globally AS (GAS).

Definition 2.2 The origin is a $\mathcal{KL}$–stable equilibrium for the system (2.1) in the proper set $\mathcal{S} \subseteq \mathbb{R}^n$, if there exists a function $\beta \in \mathcal{KL}$ such that for all $x(0) \in \mathcal{S}$,

$$\|x(t)\| \leq \beta(\|x(0)\|, t), \quad \forall t \in \mathbb{R}_{\geq 0}. \tag{2.3}$$

If the set $\mathcal{S} = \mathbb{R}^n$, then we say that the origin is globally $\mathcal{KL}$–stable.

In [87, Proposition 2.5] (see also [77, Lemma 4.5]) it was shown that uniform AS is equivalent with $\mathcal{KL}$–stability in the set $\mathcal{S}$. This also holds for autonomous systems of the type (2.1), i.e. f is not time dependent, since for these systems AS of the origin is uniform with respect to the initial time t_0.

In the remainder of the thesis we will use *$\mathcal{KL}$–stability* to refer to $\mathcal{KL}$–stability in $\mathcal{S}$ or, equivalently to AS, as defined above. When $\mathcal{S} = \mathbb{R}^n$, then we use the term global $\mathcal{KL}$–stability.

Assumption 2.1 $x = 0$ is an asymptotically stable equilibrium point of the system (2.1).

Consider the concept of *domain of attraction* introduced for example in [60].

Definition 2.3 The domain of attraction of the origin for the system (2.1) is the set

$$\mathcal{S} := \{x_0 \in \mathbb{R}^n \, : \, \lim_{t\to\infty} x(t, x_0) = 0\}, \tag{2.4}$$

where $x(\cdot, x_0)$ denotes the solution of (2.1) corresponding to the initial condition x_0.

Definition 2.4 A set $\mathcal{S} \in \mathbb{R}^n$ is called a forward invariant set w.r.t. (2.1) if for any initial condition $x_0 = x(0) \in \mathcal{S}$, it holds that $x(t, x_0) \in \mathcal{S}$ for all $t > 0$.

In the remainder of this thesis, for simplicity, we will use invariant set to refer to a forward invariant set. The DOA of an equilibrium for a given system is inherently an invariant set.

Definition 2.5 Let $V : \mathcal{A}^\dagger \to \mathbb{R}$, with $\mathcal{A}^\dagger \subseteq \mathbb{R}^n$ containing the origin, be a continuously differentiable function with $V(0) = 0$ and the following properties:

a) $V(x)$ is positive definite on $\mathcal{A}^\dagger$ and radially unbounded, i.e. $V(x) \to \infty$ as $\|x\| \to \infty$

b) its derivative along the trajectories of (2.1), $\dot{V}(x) = \nabla V^\top f(x)$, is negative definite on $\mathcal{A}^\dagger$.

Then V is called a Lyapunov function for the system (2.1).

The following result is a consequence of [80, Theorem 1] and will be instrumental in the procedure for estimating the DOA of the origin of the system (2.1).

Theorem 2.1 Let $V(x)$ be a Lyapunov function for the system (2.1) and consider the region

$$\mathcal{A} = \{x \, : \, \dot{V}(x) \leq 0\}. \tag{2.5}$$

Furthermore, let C^* be the largest positive value such that the level set $V(x) = C^*$ is contained in $\mathcal{A}$. Then, the set

$$\mathcal{S}_\mathcal{A} = \{x \in \mathcal{A} \, : \, V(x) < C^*\} \tag{2.6}$$

is contained in the DOA of the origin of (2.1), $\mathcal{S}$.

Proof: The proof is based on the following steps. First, since $\dot{V}(x)$ is negative semidefinite on $\mathcal{S}_{\mathcal{A}} \subset \mathcal{A}$ it implies that $\mathcal{S}_{\mathcal{A}}$ is an invariant set for (2.1), which means that the solution $x(t, x_0)$ of (2.1), $x_0 \in \mathcal{S}_{\mathcal{A}}$, will stay in $\mathcal{S}_{\mathcal{A}}$ for all times. Furthermore, it will not escape to infinity since $\mathcal{S}_{\mathcal{A}}$ is bounded (included in $\mathcal{A}$). Finally, $x(t, x_0) \to 0$ as $t \to \infty$, which follows from the fact that $\dot{V}(x) < 0$, for $x \in \mathcal{S}_{\mathcal{A}} \backslash \{0\}$ via the Asymptotic Stability Theorem from [80, page 37]. ■

In [118], it is shown that if f is continuously differentiable in a neighborhood of the origin, then there exists a *maximal* LF which can be used to estimate the DOA exactly [118, Theorem 2]. This function tends to infinity as x approaches the boundary $\partial\mathcal{S}$ of the DOA $\mathcal{S}$.

Definition 2.6 [118] A function $V_m : \mathbb{R}^n \to \mathbb{R}_+ \cup \{\infty\}$ is called a *maximal Lyapunov function* for the system (2.1) if

a) $V_m(0) = 0$, $V_m(x) > 0$, for any $x \in \mathcal{S} \setminus \{0\}$

b) $V_m(x) < \infty$ if and only if $x \in \mathcal{S}$

c) $V_m(x) \to \infty$ as $x \to \partial\mathcal{S}$ and/or $\|x\| \to \infty$

d) $\dot{V}_m$ is well defined and negative definite over $\mathcal{S}$.

When f is continuously differentiable, then $V_m(x) \to \infty$ as $x \to \partial\mathcal{S}$. If f is Lipschitz continuous on $\mathcal{S}$, then V_m can be taken continuously differentiable on $\mathcal{S}$ and then $V_m(x) \to \infty$ as $\|x\| \to \infty$.

Remark 2.1 In [118, Theorem 1] it is shown that if it is possible to find a set $\mathcal{A}$ containing the origin in its interior and a continuous function satisfying the properties of a maximal LF on that set, then $\mathcal{A}$ is the same as the DOA $\mathcal{S}$ defined in (2.4). This result implicitly assumes that there does not exist a $\xi \in \mathcal{S}^\circ$ such that $\lim_{x \to \xi} V(x) = \infty$. For any proper candidate LF, i.e. radially unbounded, thus which is upper and lower bounded by class $\mathcal{K}_\infty$ functions, this property obviously holds. As such, we consider in the definition above of a maximal LF, item c) the case when both $V_m(x) \to \infty$ as $x \to \partial\mathcal{S}$ and as $\|x\| \to \infty$ hold.

Thus, the DOA can be computed if a function V which is a maximal LF for the considered system can be constructed, since the boundary of the DOA is defined by $V(x) \to \infty$. In [118], in order to satisfy the condition (c), rational LFs were considered as candidates. More specifically, functions of the form

$$V(x) = \frac{N(x)}{D(x)}, \tag{2.7}$$

with $N(x)$ and $D(x)$ polynomials in x, were considered. Thus, when $D(x) = 0$, $x \to \partial\mathcal{S}$. Therein, a recursive procedure is proposed, to construct both an approximation of the maximal LF, which is shown to be a true LF, and based on its level set to provide a close approximation of the DOA, based on the result in Theorem 2.1.

The steps of the procedure in [118] have been addressed in detail in [99], [95], [56]. They are based on expressing f as

$$f(x) = \sum_{i=1}^{\infty} F_i(x), \tag{2.8}$$

where $F_i(\cdot)$ is a homogeneous function of degree i and V as

$$V(x) = \frac{\sum_{i=2}^{\infty} R_i(x)}{1 + \sum_{i=1}^{\infty} Q_i(x)}, \tag{2.9}$$

where R_i, Q_i are homogeneous functions of degree i. The procedure results in an approximation of V of the form:

$$V_n(x) = \frac{\sum_{i=2}^{n} R_i(x)}{1 + \sum_{i=1}^{n-2} Q_i(x)}, \tag{2.10}$$

and it was shown that $V_n(x)$ is a Lyapunov function for all $n \geq 2$.

More details related to the computation of the coefficients of the polynomials in (2.10) will be given in Section 2.2.1. The main attribute of the procedure is that it converges in a rather small number of steps, usually $n = 4$ is sufficient.

Next, we shall focus on the steps to determine the maximal level set of V_n which renders the approximation of $\mathcal{S}$.

2.2.1 DOA computation

Consider the RLF candidate as defined in (2.10). From Theorem 2.1 we have that the interior of the largest level set of V_n which is included in the state space area where its derivative is negative definite is a subset of the DOA of the considered system. This translates into the optimization problem:

$$\begin{aligned} \max_{c,x} \quad & c \\ \text{subject to} \quad & V_n(x) - c = 0 \\ & \dot{V}_n(x) \leq 0 \\ & c > 0, \end{aligned}$$

or equivalently, from [60]:

$$\begin{aligned} \min_{c,x} \quad & c \\ \text{subject to} \quad & V_n(x) - c = 0 \\ & \dot{V}_n(x) = 0 \\ & c > 0. \end{aligned} \tag{2.11}$$

The formulation in problem (2.11) is based on a result from [60], which says that if the level set $V(x) = c$ lies entirely on the closed hypersurface where $\dot{V}(x) = 0$, i.e. the level set $\dot{V}(x) = 0$, then the domain defined by $V(x) \leq c$ is a subset of the DOA.

For the considered RLFs the above optimization problem turns out to be nonconvex, which means that local optima need to be avoided when searching for the best DOA approximation. The problem (2.11) was considered in [56] where an LMI estimation method based on the theory of moments was proposed. Therein the problem was re-written by means of a polynomial objective function and constraints as:

$$\begin{aligned} \min_{c,x} \quad & c \\ \text{subject to} \quad & N_n(x) - cD_n(x) = 0 \\ & \hat{N}_n(x) = 0,\ \hat{D}_n(x) \neq 0,\ x \neq 0 \\ & c > 0, \end{aligned} \tag{2.12}$$

where $V_n(x) = \frac{N_n(x)}{D_n(x)}$ and $\dot{V}_n(x) = \frac{\hat{N}_n(x)}{\hat{D}_n(x)}$ (from the derivation of fractions rule). Furthermore, in order to avoid dummy solutions of the above problem, in [91], additional constraints have been proposed. As such, the problem in (2.12) becomes:

$$\begin{aligned} \min_{c,x,\varepsilon} \quad & c \\ \text{subject to} \quad & N_n(x) - cD_n(x) = 0 \\ & \hat{N}_n(x) = 0 \\ & \nabla(N_n(x) - cD_n(x)) = \varepsilon\nabla(\hat{N}_n(x)) \\ & N_n(x) > 0,\ D_n(x) > 0,\ x \neq 0 \\ & c > 0. \end{aligned} \tag{2.13}$$

In problem (2.13), the estimation of the DOA is obtained by minimizing the level set of V_n until it is tightly included in the level set $\dot{V}(x) = 0$. This reasoning is based on the assumption that one can find a closed surface where $\dot{V}(x) = 0$. However this is not generally valid. For the tumor growth system it turned out that solving the optimization problem to find the DOA estimate with a less restrictive formulation is more stable numerically. It is then more numerically robust to maximize c as long as the level set of V_n remains included in the set $\mathcal{A}$ defined in (2.5). In this way irregularities in the level set surface of $\dot{V}_4 = 0$, such as corresponding to singularity points of $\dot{V}_4$ (see the empty areas within the interior of the red surface plotted in Figure 3.1(b) are avoided. The optimization problem then becomes:

$$\begin{aligned} \max_{c,x,\varepsilon} \quad & c \\ \text{subject to} \quad & N_n(x) - cD_n(x) = 0 \\ & \hat{N}_n(x) \leq 0 \\ & \nabla(N_n(x) - cD_n(x)) = \varepsilon\nabla(\hat{N}_n(x)) \\ & N_n(x) > 0,\ D_n(x) > 0,\ x \neq 0 \\ & c > 0. \end{aligned} \tag{2.14}$$

In what follows the procedure proposed in [118] for constructing a RLF and an approximation of the DOA of the origin equilibrium of (2.1) will be recalled.

- $n = 2$

$$V_2(x) = R_2(x),$$

from (2.8), $F_1 = Ax$, where A is the linearization matrix around the origin and the matrix $P \succ 0$ is computed as the solution of $A^\top P + PA = -Q$, $Q \succ 0$. Typically, Q is taken as the identity matrix of corresponding size.

- $n = 3$

$$V_3(x) = \frac{R_2(x) + R_3(x)}{1 + Q_1(x)},$$

the recursive relation in [118, (60)] needs to be satisfied, i.e.:

$$(\nabla R_2)^\top F_2 + ((\nabla R_3)^\top + Q_1(\nabla R_2)^\top - (\nabla Q_1)^\top R_2)F_1 = -x^\top Qx(2Q_1). \tag{2.15}$$

- $n = 4$

$$V_4(x) = \frac{R_2(x) + R_3(x) + R_4(x)}{1 + Q_1(x) + Q_2(x)},$$

the recursive relation is:

$$(\nabla R_2)^\top F_3 + ((\nabla R_3)^\top + Q_1(\nabla R_2)^\top - (\nabla Q_1)^\top R_2)F_2 + ((\nabla R_4)^\top + Q_1(\nabla R_3)^\top - (\nabla Q_1)^\top R_3 + Q_2(\nabla R_2)^\top - (\nabla Q_2)^\top R_2)F_1 = -x^\top Qx(2Q_2 + Q_1^2). \tag{2.16}$$

For each step $n \geq 3$ a constrained minimization problem is solved in order to obtain the coefficients of the polynomials in the RLF. The constraints are linear equalities in terms of the coefficients of the polynomials in V_n and come from the recursive relations above. The cost function to minimize comes from the expression of the derivative of V_n. It is shown in [118] that $\dot{V}_n$ can be written as:

$$\dot{V}_n = -x^\top Qx + \frac{\{\text{terms of degree} \geq n+1\}}{(1 + \sum_{i=1}^{n-2} Q_i)^2}, \tag{2.17}$$

which implies that $\dot{V}_n$ is negative definite in a small region around the origin. The error/cost function to minimize is then defined as:

$$e_n = \|\text{coefficients of the numerator terms in (2.17)}\|_2^2, \tag{2.18}$$

which allows to maximize the estimate of the DOA, by the choice of the coefficients of the polynomials in V_n. Once the homogeneous polynomials R_n and Q_{n-2} are chosen from the constrained minimization problem, an estimate of the DOA can be computed by solving the problem (2.14).

2.3 Stabilizability of polynomial systems

2.3.1 Instrumental concepts

Consider continuous–time nonlinear control systems described by

$$\dot{x} = \hat{f}(x, u), \tag{2.19}$$

where $x \in \mathbb{X} \subseteq \mathbb{R}^n$ denotes the state, $u \in \mathbb{U} \subseteq \mathbb{R}^m$ denotes the input and $\hat{f} : \mathbb{X} \times \mathbb{U} \to \mathbb{R}^n$ is a sufficiently regular map from the domain $\mathbb{X} \times \mathbb{U} \subset \mathbb{R}^n$ into $\mathbb{R}^n$ with $f(0,0) = 0$.

We are concerned with systems where $\hat{f}(x,u)$ is defined as $\hat{f}(x,u) = f(x) + g(x)u$, thus (2.19) becomes

$$\dot{x} = f(x) + g(x)u. \tag{2.20}$$

Let $x(t, x_0, u)$ denote the solution of (2.20) corresponding to the initial value x_0 and control u.

Definition 2.7 Let $k : \mathbb{R}^n \to \mathbb{U}$ be a mapping, smooth on $\mathbb{R}^n$ with $k(0) = 0$. k is called a *feedback stabilizer* for the system (2.19), with $u = k(x)$, if the closed–loop system

$$\dot{x} = f(x) + g(x)k(x) \tag{2.21}$$

is asymptotically stable (AS) on $\mathbb{X}$.

We define the set of stabilizers for the system (2.19) as:

$$\mathscr{K} := \{k : \mathbb{R}^n \to \mathbb{U} : \hat{f}(x, k(x)) \text{ is AS on } \mathbb{X}\}. \tag{2.22}$$

Definition 2.8 The *domain of attraction* (DOA) of the origin for the system (2.19) where $u = k(x)$, $k \in \mathscr{K}$ is the set defined by:

$$\mathcal{S}_k := \{x_0 \in \mathbb{R}^n : \lim_{t\to\infty} x(t, x_0, k(x)) = 0\}. \tag{2.23}$$

Definition 2.9 The *domain of stabilizability* (DOS) of the origin for the system (2.19) is the set defined by

$$\mathcal{S} := \bigcup_{k \in \mathscr{K}} \mathcal{S}_k. \tag{2.24}$$

Next we recall the concept of a control Lyapunov function (CLF), as defined in [106].

Definition 2.10 Let $V : \mathbb{R}^n \to \mathbb{R}_{\geq 0}$ be a continuously differentiable function with $V(0) = 0$ and the following properties:

a) $V(x)$ is positive definite and radially unbounded, i.e. $V(x) \to \infty$ as $\|x\| \to \infty$[1], for all $x \in \mathbb{R}^n$;

b) its derivative along the trajectories of (2.19), $\dot{V}(x) = \nabla V^\top \hat{f}(x,u)$, is negative definite, i.e.

$$\nabla V(x)^\top f(x) + \nabla V(x)^\top g(x)u < 0, \quad \forall x \in \mathbb{R}^n,\ x \neq 0. \tag{2.25}$$

Then V is a CLF for the system (2.19).

[1] This condition corresponds to condition (4.2) in Chapter 4.

The condition (b) above is equivalent with the statement that

$$\nabla V(x)^\top g(x) = 0 \Rightarrow \nabla V(x)^\top f(x) < 0, \quad \forall x \in \mathbb{R}^n.$$

As indicated in Theorem 2.1, CLFs enable the computation of a DOA estimate, $\mathcal{S}_k$ for a given $k \in \mathscr{K}$ for (2.20).

Similarly, the concept of a *maximal Lyapunov function* for the closed loop system (2.19) with $u = k(x)$, $k \in \mathscr{K}$ is defined as in Definition 2.6, but with respect to the set $\mathcal{S}_k$.

In [7] it has been shown that the existence of a smooth feedback stabilizer is equivalent with the existence of a smooth CLF. Further, in [106] an explicit proof of the fact that the existence of a smooth CLF implies the existence of a smooth feedback stabilizer was given. A "universal" formula for the stabilizer has been used. Furthermore, it has been shown that if the considered system is described by a rational map and there exists a RCLF for that system, then there exists a rational feedback stabilizer [106, Theorem 2]. In what follows we will establish that for polynomial systems, if there exists a RCLF, then there exists a polynomial feedback stabilizer. For this purpose, we recall the following algebraic geometry result proposed in [106, Lemma 3.1].

Lemma 2.1 Consider a closed semialgebraic subset of $\mathbb{R}^n$, T and two polynomials β, a belonging to $\mathbb{R}[x_1, x_2, \ldots, x_n]$ so that $\beta(x) > 0$ on T. Then there exists a polynomial $d \in \mathbb{R}[x_1, x_2, \ldots, x_n]$ such that

$$\beta(x)d(x) > a(x), \quad x \in \mathbb{R}^n. \tag{2.26}$$

2.3.2 *Existence result*

Theorem 2.2 Consider the system (2.20), where $f(x)$ and $g(x)$ are polynomial functions. If there exists a RCLF for (2.20), then there exists a polynomial feedback stabilizer $k \in \mathscr{K}$, $k = \begin{pmatrix} k_1 & k_2 & \ldots & k_m \end{pmatrix}^\top$, for (2.20).

Proof: Let $V = \frac{N(x)}{D(x)}$, well–defined on $\mathbb{R}^n$ ($D(x)$ has no poles in zero), be a rational CLF for (2.20). Then it holds that

$$\frac{(D\nabla N^\top - \nabla D^\top N)f + (D\nabla N^\top - \nabla D^\top N)gu}{D^2} < 0,$$

which is equivalent to

$$\begin{aligned}&(D\nabla N^\top - \nabla D^\top N)f + u_1(D\nabla N^\top - \nabla D^\top N)g_1 + u_2(D\nabla N^\top - \nabla D^\top N)g_2 + \\ &\ldots + u_m(D\nabla N^\top - \nabla D^\top N)g_m < 0,\end{aligned}$$

since D^2 is always positive and $u_1, \ldots, u_m$ are the components of u and $g_1, \ldots, g_m$ are the components of g. Denote by $a(x) := (D\nabla N^\top - \nabla D^\top N)f$ and $b_i(x) := (D\nabla N^\top - \nabla D^\top N)g_i$ and let $k_i(x)$ be of the polynomial form

$$k_i(x) = -c(x)b_i(x), \tag{2.27}$$

where $c(x)$ is a polynomial function, $i = 1, \ldots, m$. We need to prove that

$$a(x) - c(x)\beta(x) < 0, \tag{2.28}$$

for all $x \neq 0$ with $\beta(x) := \sum_{i=1}^{m} b_i^2(x)$. We follow the same reasoning as used in proving Theorem 2 in [106]. Since $\beta(x) > 0$, (2.28) is equivalent to

$$c(x) > \frac{a(x)}{\beta(x)}.$$

Consider the closed semialgebraic set

$$T := \{(x, y) \in \mathbb{R}^{n+1} \ : \ a(x) \geq 0 \,\text{and}\, y - \|x\|_2^2 = 0\}. \tag{2.29}$$

The CLF condition (2.25) is equivalent with requiring that $b(x) = 0$ implies that $a(x) < 0$, for all nonzero x. The rational function $\frac{a(x)}{\beta(x)}$ is well–defined in T. This follows from the fact that if there exists some y so that $(x, y) \in T$, then for $x \neq 0$, $a(x) \geq 0$ and from the CLF condition this implies that $\beta(x) \neq 0$. Therefore, we can now use the result in Lemma 2.1, which guarantees that there exists a polynomial function $d \ : \ \mathbb{R}^{n+1} \ \rightarrow \ \mathbb{R}$, so that $d > 0$ everywhere and

$$d(x, y) \geq \frac{a(x)}{\beta(x)},$$

for $(x, y) \in T$. Consider now

$$c(x) := d(x, \|x\|_2^2).$$

If we assume that $\beta(x) > 0$ for $x \neq 0$, and $a(x) \geq 0$, then $(x, \|x\|_2) \in T$ and therefore (2.28) holds. ∎

Remark 2.2 If the semialgebraic set T is defined by

$$T := \{(x, y) \in \mathbb{R}^{n+1} \ : \ a(x) \geq 0 \,\text{and}\, \|x\|_2^2 y = 1\},$$

as it was defined in [106], then $c(x)$ becomes rational and thus leading to a rational feedback stabilizer $k(x)$.

2.4 Rational Control Lyapunov Functions

In this section we consider a particular form of CLFs, namely described by rational functions as introduced in [118]. Let V be of the form:

$$V(x) = \frac{\sum_{i=2}^{\infty} R_i(x)}{1 + \sum_{i=1}^{\infty} Q_i(x)}. \tag{2.30}$$

Further, let f and g in (2.20) be analytical, thus the system (2.20) can be written as:

$$\dot{x} = \sum_{i=1}^{\infty} F_i + \sum_{i=1}^{\infty} G_i u, \tag{2.31}$$

where F_i, G_i are homogeneous polynomials of order i.

Let u be a feedback stabilizer $u = k(x)$, $k \in \mathscr{K}$. Then V is a CLF for (2.30) if

$$\nabla V(x)^\top f(x) + k(x)\nabla V(x)^\top g(x) = -x^\top Qx < 0, \tag{2.32}$$

holds for some fixed matrix $Q \succ 0$. In this section we consider the case when $m = 1$, thus u in (2.31) is scalar. However, all the derivations that follow can be mutatis mutandis extended to the multivariable case.

By the result in Theorem 2.2, we know that if V is a RCLF, then there exists a polynomial feedback stabilizer $k \in \mathscr{K}$ for (2.31). Let k be described by

$$k(x) = \sum_{i=1}^{\infty} K_i(x), \tag{2.33}$$

where $K_i(x)$ are homogeneous polynomials of order i. Since $k(x)$ needs to satisfy $k(0) = 0$, we do not consider the case when $i = 0$, i.e., $k(x) =$ constant, in the expression above, as it would lead $k(0) = K_0(0) + K_1(0) + K_2(0) + \ldots =$ constant $+ 0 \neq 0$.

Then, by applying the standard derivation rules, equation (2.32) can be written as follows (similarly to equation (42) in [118]):

$$\begin{aligned}
&\sum_{i=2}^{\infty}\sum_{k=1}^{\infty} \nabla R_i^\top F_k + \sum_{i=1}^{\infty}\sum_{j=2}^{\infty}\sum_{k=1}^{\infty} Q_i \nabla R_j^\top F_k - \sum_{i=1}^{\infty}\sum_{j=2}^{\infty}\sum_{k=1}^{\infty} \nabla Q_i^\top R_j F_k + \\
&\sum_{i=1}^{\infty}\sum_{j=2}^{\infty}\sum_{k=1}^{\infty} K_i \nabla R_j^\top G_k + \sum_{i=1}^{\infty}\sum_{j=1}^{\infty}\sum_{k=2}^{\infty}\sum_{l=1}^{\infty} K_i Q_j \nabla R_k^\top G_l - \\
&\sum_{i=1}^{\infty}\sum_{j=1}^{\infty}\sum_{k=2}^{\infty}\sum_{l=1}^{\infty} K_i \nabla Q_j^\top R_k G_l = -x^\top Qx(1 + 2\sum_{i=1}^{\infty} Q_i + \sum_{i=1}^{\infty}\sum_{j=1}^{\infty} Q_i Q_j).
\end{aligned} \tag{2.34}$$

For equality (2.34) to hold, the left hand side and right hand side coefficients corresponding to each order term in the polynomials should be equal. By equating the coefficients of the same degrees on the left and right hand side of the equality, we obtain:

$$\nabla R_2^\top F_1 = -x^\top Qx, \qquad \text{for } k = 2 \tag{2.35}$$

$$\begin{aligned}
&\sum_{i=2}^{k} \nabla R_i^\top F_{k+1-i} + \sum_{i=1}^{k-2}\sum_{j=2}^{k-1} (Q_i \nabla R_j^\top - \nabla Q_i^\top R_j) F_{k+1-i-j} + \\
&\sum_{i=1}^{k-2}\sum_{j=2}^{k-1} K_i \nabla R_j^\top G_{k-i-1} + \sum_{i=1}^{k-3}\sum_{j=2}^{k-2} K_i (Q_i \nabla R_j^\top - \nabla Q_i^\top R_j) G_{k-i-j} \\
&= -x^\top Qx(2Q_{k-2} + \sum_{i=1}^{k-3} Q_i Q_{k-2-i}), \quad \text{for } k \geq 3.
\end{aligned} \tag{2.36}$$

We can further re–write (2.35) as

$$\nabla R_2^\top F_{k-1} + \sum_{j=3}^{k}\left(\nabla R_j^\top + \sum_{i=1}^{j-2}(Q_i\nabla R_{j-1}^\top - \nabla Q_i^\top R_{j-1})\right)F_{k-j+1}+$$
$$\sum_{i=1}^{k-2} K_i\nabla R_2^\top G_{k-1-i} + \sum_{j=3}^{k-1}\left(\sum_{i=1}^{j-2}K_i\nabla R_j^\top + \sum_{i=1}^{j-1}K_i(Q_i\nabla R_{j-1}^\top - \nabla Q_i^\top R_{j-1})\right)G_{k-j}$$
$$= -x^\top Qx(2Q_{k-2} + \sum_{i=1}^{k-3}Q_iQ_{k-2-i}), \quad \text{for } k \geq 3. \tag{2.37}$$

Next, we will show that by using the above recursive relations, approximations of V and k can be computed which will satisfy the RCLF conditions.

Theorem 2.3 Consider the system defined in (2.31). Let $\dot{x} = F_1 = Ax$ be AS and let the polynomials R_i, Q_i, K_i satisfy the equations (2.35) and (2.37), where $Q \succ 0$ is a fixed matrix. Then $V_n(x) = \frac{\sum_{i=2}^{n} R_i}{1+\sum_{i=1}^{n-2} Q_i}$ is a CLF for (2.31) for all $n \geq 2$ and with $u = k(x) = \sum_{i=1}^{n-2} K_i(x)$.

Proof: Denote $U = (1 + \sum_{i=1}^{n-2} Q_i)^2$. With $u = k(x) = \sum_{i=1}^{n-2} K_i$, we can write the expression of $\dot{V}_n$ as follows:

$$\dot{V}_n = \frac{1}{U}\big(\nabla R_2^\top + \nabla R_3^\top + \ldots + \nabla R_n^\top + \sum_{i=1}^{n-2}\sum_{j=2}^{n}(Q_i\nabla R_j^\top - \nabla Q_i^\top R_j)\big)\sum_{k=1}^{\infty} F_k +$$
$$\frac{1}{U}\sum_{i=1}^{n-2} K_i\big(\nabla R_2^\top + \nabla R_3^\top + \ldots \nabla R_n^\top + \sum_{i=1}^{n-2}\sum_{j=2}^{n}(Q_i\nabla R_j^\top - \nabla Q_i^\top R_j)\big)\sum_{k=1}^{\infty} G_k$$
$$= \frac{1}{U}\Big[\nabla R_2^\top F_1 + \sum_{k=3}^{n}\nabla R_2^\top F_{k-1} +$$
$$\sum_{j=3}^{k}\big(\nabla R_j^\top + \sum_{i=1}^{j-2}(Q_i\nabla R_{j-1}^\top - \nabla Q_i^\top R_{j-1})\big)F_{k-j+1} + \sum_{k=3}^{n}\sum_{i=1}^{k-2}K_i\nabla R_2^\top G_{k-1-i} +$$
$$\sum_{j=3}^{k-1}\big(\sum_{i=1}^{j-2}K_i\nabla R_j^\top + \sum_{i=1}^{j-1}K_i(Q_i\nabla R_{j-1}^\top - \nabla Q_i^\top R_{j-1})\big)G_{k-j}\Big] +$$
$$\frac{1}{U}\Big[\sum_{k=n+1}^{\infty}\nabla R_2^\top F_{k-1}\sum_{j=3}^{k}\big(\nabla R_j^\top + \sum_{i=1}^{j-2}(Q_i\nabla R_{j-1}^\top - \nabla Q_i^\top R_{j-1})\big)F_{k-j+1} +$$
$$\sum_{k=n+1}^{\infty}\sum_{i=1}^{k-2}K_i\nabla R_2^\top G_{k-1-i} +$$

$$\sum_{j=3}^{k-1}\Big(\sum_{i=1}^{j-2}K_i\nabla R_j^\top+\sum_{i=1}^{j-1}K_i(Q_i\nabla R_{j-1}^\top-\nabla Q_i^\top R_{j-1})\Big)G_{k-j}\Big].$$

We can substitute equations (2.35) and (2.37) above and we obtain:

$$\begin{aligned}\dot{V}_n =& \frac{1}{U}\Big[-x^\top Qx - x^\top Qx\big(2Q_{k-2}+\sum_{i=1}^{k-3}Q_iQ_{k-2-i}\big)\Big]+\\ &\frac{1}{U}\big[\text{terms of degree}\geq n+1\big].\end{aligned}$$

Notice that in $\big(2Q_{k-2}+\sum_{i=1}^{k-3}Q_iQ_{k-2-i}\big)$ terms of U appear, thus, we further obtain

$$\begin{aligned}\dot{V}_n =& \frac{1}{U}\Big[-x^\top Qx - x^\top Qx\big(U-1-\sum_{k=3}^{n}\sum_{i=1}^{k-3}Q_iQ_{k-1-i}\big)\Big]+\\ &\frac{1}{U}\big[\text{terms of degree}\geq n+1\big]\\ =& \frac{1}{U}\Big[-x^\top Qx\big(1+U-1-\sum_{k=3}^{n}\sum_{i=1}^{k-3}Q_iQ_{k-1-i}\big)\Big]+\\ &\frac{1}{U}\big[\text{terms of degree}\geq n+1\big]\\ =& -x^\top Qx+\frac{1}{U}(-x^\top Qx)\underbrace{\big(-\sum_{k=3}^{n}\sum_{i=1}^{k-3}Q_iQ_{k-1-i}\big)}_{\text{terms of degree}\leq n-1}+\\ &\frac{1}{U}\big[\text{terms of degree}\geq n+1\big]\\ =& -x^\top Qx+\frac{1}{U}\big[\text{terms of degree}\geq n+1\big].\end{aligned}\tag{2.38}$$

From (2.38), we get that $\dot{V}_n$ is negative definite over a small neighborhood around the origin, thus V_n is a Lypunov function for the closed loop system with $u=k(x)$, and further it is a CLF function for (2.31).

When the error to be minimized during the recursive procedure for computing the coefficients of V_n is defined as

$$e_n = \|\text{coeffs of terms of numerator in (2.38)}\|^2, \tag{2.39}$$

then the region where $\dot{V}_n$ is negative definite is maximized.

Remark 2.3 In Theorem 2.3, it has been required that $\dot{x}=F_1=Ax$ is asymptotically stable. However the above procedure for computing RCLF can also be applied for systems for which this assumption does not hold. Then a pre–stabilizing step is required, for example by computing a state feedback $u'=Kx$, $K\in\mathbb{R}^{1\times n}$ for the linearization of (2.20). Then $F_1=(A+BK)x$, where A and B are matrices resulting from the linearization of (2.20) around a fixed point.

As a result of Theorem 2.3, the maximal approximation order for $k(x)$ is $n-2$. The recursive procedure that is generated by (2.35), (2.37) and (2.39) usually converges after a few iterations, i.e. the error becomes small enough for $n=4$. Thus, terms of order up to $n-2=2$ appear in the constraints expressions, even if $k(x)$ would be defined up to order n. The result of Theorem 2.3 still holds for $k(x)=\sum_{i=1}^{n} K_i(x)$.

Remark 2.4 By applying the result in Theorem 2.3, a RCLF and a feedback stabilizer are generated during the same optimization procedure. While allowing this, although V_n is a valid RCLF, it will not be the maximal one. Once a $k(x)$ is computed, a RLF can be computed for the closed–loop system to obtain a better estimate of the DOA of the closed loop system, $\mathcal{S}_k$.

2.5 Illustrative applications

2.5.1 Van der Pol oscillator

Let us consider the Van der Pol oscillator described by

$$\begin{aligned} \dot{x}_1 &= -x_2 \\ \dot{x}_2 &= x_1 + (1+u)x_2(x_1^2-1), \end{aligned} \tag{2.40}$$

so that when $u=0$ the origin is locally stable equilibrium, with the estimate of the DOA depicted in Figure 2.1(a) in blue and defined by $V_4=3.8$. The derivative level set $\dot{V}_4=0$ is shown in red. By applying the procedure in Section 2.4, we obtained the RCLF

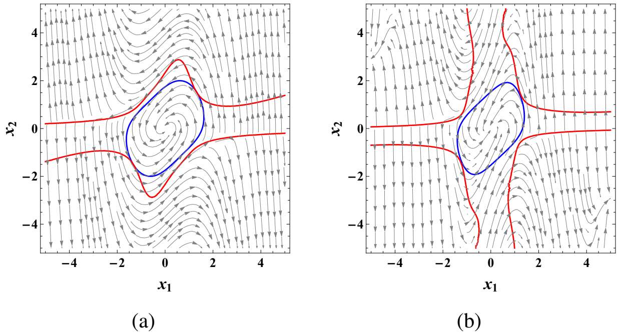

Figure 2.1: Vector fields, RLF–blue level set and derivative–red level set for autonomous–(a) and controlled–(b) case.

$$V_4 = \frac{1.5x_1^2 + 0.0394355x_1^4 - x_1x_2 + 0.451638x_1^3x_2 + x_2^2 + 0.0856408x_1^2x_2^2 -}{1 + 0.023885x_1^2 + 0.317015x_1x_2 - 0.0735786x_2^2} + \frac{0.0132402x_1x_2^3 - 0.0290605x_2^4}{1 + 0.023885x_1^2 + 0.317015x_1x_2 - 0.0735786x_2^2},$$

and the polynomial feedback stabilizer

$$k(x) = 0.0361545x_1^2 + 0.262089x_1x_2 + 0.112881x_2^2.$$

The level sets $V_4 = 2.65$–blue and $\dot{V}_4 = 0$–blue are shown in Figure 2.1(b). An improved approximation of the DOA for the Van der Pol system was obtained by computing a RLF for the closed–loop system with $k(x)$ defined above. The improved DOA is described by $V_{4,k} = 2$, where

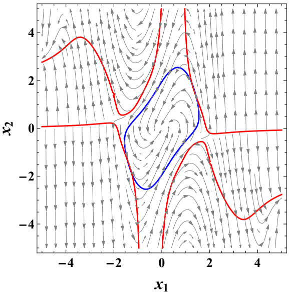

Figure 2.2: Phase plot and new DOA estimate for the closed–loop system.

$$V_{4,k} = \frac{1.5x_1^2 - 0.209208x_1^4 - x_1x_2 + 0.556388x_1^3x_2 + x_2^2/2 + 0.0418157x_1^2x_2^2}{1 + 0.0435481x_1^2 + 0.399957x_1x_2 - 0.00857623x_2^2} + \frac{0.043728x_1x_2^3 + 0.00220517x_2^4}{1 + 0.0435481x_1^2 + 0.399957x_1x_2 - 0.00857623x_2^2},$$

and it is plotted in Figure 2.2–blue.

2.5.2 *Tumor dynamics*

We will consider the model proposed in [41] to describe the tumor–host interaction dynamics. The principles of population ecology are exploited in this model, namely to describe population interactions between tumor and normal cells. As such, we consider the tumor dynamics system to be defined as follows:

$$\begin{aligned} \dot{N}_N &= R_N N_N - \frac{R_N}{K_N} N_N^2 - \frac{R_N \alpha_{NT}}{K_N} N_T N_N \\ \dot{N}_T &= R_T N_T - \frac{R_T}{K_T} N_T^2 - \frac{R_T \alpha_{TN}}{K_T} N_T N_N, \end{aligned} \tag{2.41}$$

where N_N represents the normal cells population and N_T represents the tumor cells population. The system above has three possible equilibria (if we eliminate the one in the origin since it doesn't make sense from a biological perspective) corresponding to extinction of the normal cells, extinction of the tumor cells and coexistence of the two species, or so–called tumor dormancy. The stability properties of equilibria depend on the parameters, allowing for local bistability of the extreme equilibria or local stability of each of the three. The parameters in (2.41) which have an impact on the stability of the equilibria and can be directly influenced through treatment (drugs or immunotherapy) are α_{NT}, which represents the effect that the tumor cells have on the normal cells, and α_{TN}, which represents the predation rate of the tumor cells by the normal cells.

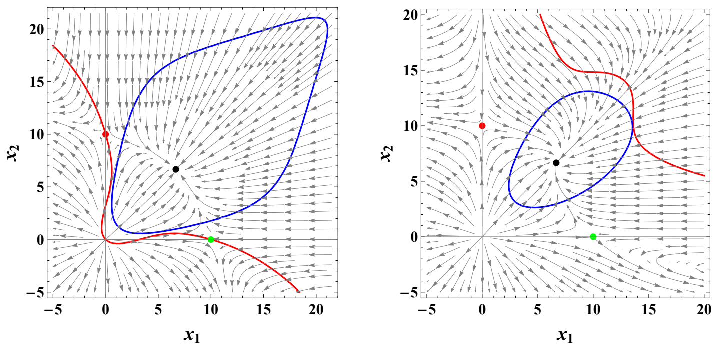

(a)

(b)

Figure 2.3: Vector fields, RLF–blue level set and derivative–red level set for autonomous–(a) and controlled–(b) case.

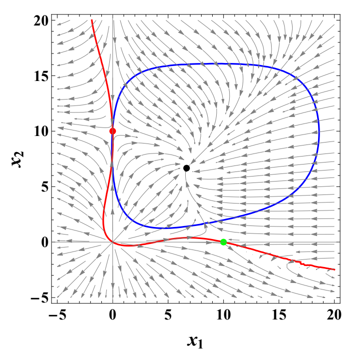

Figure 2.4: Phase plot and new DOA estimate for the closed–loop system.

Let the controlled tumor system be:

$$\begin{aligned} \dot{N}_N &= R_N N_N - \frac{R_N}{K_N} N_N^2 - \frac{R_N}{K_N}(\alpha_{NT} + u) N_T N_N \\ \dot{N}_T &= R_T N_T - \frac{R_T}{K_T} N_T^2 - \frac{R_T \alpha_{TN}}{K_T} N_T N_N. \end{aligned} \tag{2.42}$$

For $u = 0$ and the parameter values $R_N = R_T = 0.9$, $K_T = K_N = 10$ and $\alpha_{NT} = \alpha_{TN} = 0.5$, the equilibria of the system are $E_1 = (0, 10)$, $E_2 = (6.66667, 6.66667)$ and $E_3 = (10, 0)$. The only stable equilibrium is E_2. See a plot of the DOA estimate using a RLF for E_2, which was computed in [35], in Figure 2.3(a). The zero level set of the derivative of the RLF is shown in red. In what follows we will compute a feedback stabilizer $u = k(x)$ as shown in Section 2.4 such that E_2 is a stable equilibrium on the positive orthant for (2.42). Naturally, first a state transformation is required for (2.42) with respect to E_2, such that the new system has the equilibrium in the origin. Let x_1 denote N_N and x_2 denote N_T. For the transformed system, by applying the procedure in Section 2.4, the RCLF

$$V_4(x) = \frac{R_2 + R_3 + R_4}{1 + Q_1 + Q_2},$$

with

$$\begin{aligned}
R_2 =& 49.3827 - 7.40741x_1 + 1.11111x_1^2 - 7.40741x_2 - 1.11111x_1x_2 + 1.11111x_2^2 \\
R_3 =& 6.48163 + 0.813352x_1 + 0.411231x_1^2 - 0.0188696x_1^3 - 3.73008x_2 - \\
& 1.06647x_1x_2 - 0.00507587x_1^2x_2 + 1.09275x_2^2 + 0.0850609x_1x_2^2 - 0.0829909x_2^3
\end{aligned}$$

$$\begin{aligned}
R_4 =& 0.901174 + 1.8253x_1 - 0.250225x_1^2 + 0.0134279x_1^3 - 0.0000345885x_1^4 - \\
& 2.366x_2 - 0.320935x_1x_2 + 0.0347837x_1^2x_2 - 0.00187583x_1^3x_2 + 0.692818x_2^2 + \\
& 0.0133567x_1x_2^2 + 0.000204973x_1^2x_2^2 - 0.0737341x_2^3 - 0.000804481x_1x_2^3 + \\
& 0.00296615x_2^4 \\
Q_1 =& -0.535414 + 0.0632948x_1 + 0.0170173x_2 \\
Q_2 =& -0.124567 - 0.0102211x_1 + 0.0000549605x_1^2 + 0.0475912x_2 + \\
& 0.00142325x_1x_2 - 0.00428096x_2^2,
\end{aligned}$$

has been obtained together with the feedback stabilizer

$$\begin{aligned}
k(x) =& 0.00162532 + 0.0704234x_1 + 0.00408656x_1^2 - 0.0704234x_2 + \\
& 0.00230886x_1x_2 - 0.00643199x_2^2.
\end{aligned}$$

Note that the above polynomials are not homogeneous, since we are reporting the results with respect to the nonzero equilibrium E_2. In Figure 2.3(b) the level sets defined by $V_4(x) = 23$–blue and $\dot{V} = 0$–red are shown. As a consequence of Remark 2.4, see in Figure 2.4 a plot of the level set $V_{4,k} = 50$–blue and $\dot{V}_{4,k} = 0$–red, with

$$\begin{aligned}
V_{4,k} =& (53.6869 - 8.45252x_1 + 1.8274x_1^2 - 0.113701x_1^3 + 0.00284881x_1^4 - \\
& 8.73687x_2 - 1.63786x_1x_2 + 0.027169x_1^2x_2 + 0.000838963x_1^3x_2 + \\
& 1.40989x_2^2 + 0.138567x_1x_2^2 - 0.00354257x_1^2x_2^2 - 0.0963518x_2^3 - \\
& 0.00145082x_1x_2^3 + 0.00280129x_2^4)/(0.346669 + 0.0252582x_1 - \\
& 0.00166945x_1^2 + 0.0748148x_2 + 0.00442781x_1x_2 - 0.00306936x_2^2).
\end{aligned}$$

The invasive tumor growth equilibrium E_1 of the uncontrolled tumor system (2.41) remains an (unstable) equilibrium of (2.42) in closed–loop with $k(x)$. The zero level set of $\dot{V}_{4,k}$ is tangent to the Ox_2 axis in E_1, $\dot{V}_{4,k}(E_1) = -8.3904 \times 10^{-14}$. This implies that the distance between the DOA estimate S_k of E_2 and E_1 is infinitesimally small. In consequence, all trajectories which are on the stable manifolds of E_1 and get sufficiently close to the boundary of the DOA of E_2 will converge to E_2 instead of E_1, via the unstable directions of E_1. This is particularly relevant from a clinical perspective, as it implies that critical states can be steered to dormancy.

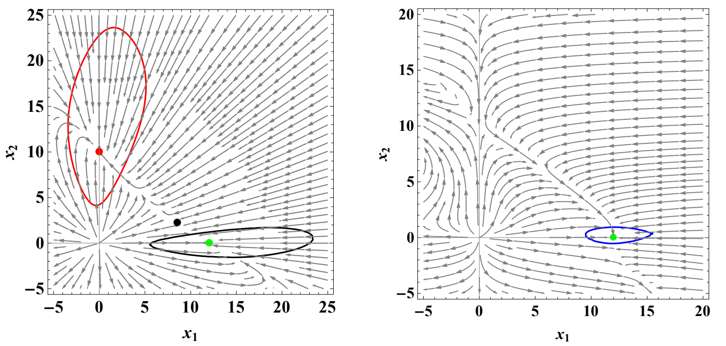

(a) (b)

Figure 2.5: (a): Vector fields, DOA estimate of E_1–red countour, DOA estimate of E_3–black contour. (b): Stabilized E_3 equilibrium and corresponding DOA estimate–blue contour.

Now consider the case when $u = 0$ and the parameter values $R_N = R_T = 0.9$, $K_T = 10$, $K_N = 10$ and $\alpha_{NT} = 1.5$, $\alpha_{TN} = 0.9$. The equilibria of the system are $E_1 = (0, 10)$, $E_2 = (8.5714, 2.28571)$ and $E_3 = (12, 0)$. For this set of parameters, E_1 and E_3 are stable and E_2 is unstable. See a plot of the DOA estimates using RLFs for E_1, and E_3 in Figure 2.5(a). The zero level set of the derivative of the RLF is shown in red. A feedback stabilizer $u = k(x)$ was computed for stabilizing the healthy state equilibrium E_3. The vector field plot of the controlled system is shown in Figure 2.5(b) together with the DOA estimate generated by the corresponding RLF. Note that in this case, the intersection of the estimated DOAs, computed via RLFs, with the positive orthant are the biologically realistic sets to consider. This is allowed due to the fact that the positive orthant is invariant for the tumor system (see also Theorem 5.1).

2.6 Conclusions

In this chapter, a new approach to compute RCLFs and polynomial stabilizers for nonlinear continuous–time systems has been introduced. The approach is based on a recursive procedure in which at each step an optimization problem with linear constrains is solved, generating coefficients of polynomials in the rational function and the coefficients of the polynomial feedback. For polynomial systems, it was shown that there always exists a polynomial feedback stabilizer, provided that there exists a RCLF. This procedure should generally, yield the best results in terms of DOA computation and feedback stabilization for polynomial systems due to the fact that Taylor approximations are exact for polynomial functions. Nonetheless, the same procedure can be applied to nonpolynomial systems, however it will be highly dependent on the type of nonlinearity and how much of the dynamics information can be captured by low order approximations, for initial states far from the equilibrium. A very high order approximation might be problematic in terms of computational effort. However, since the central objective of the feedback law is stabilization whether it is based on a CLF valid in a larger or smaller area around the origin is not very relevant, as long as the system is stabilized. This will not be the case when the purpose of the stabilization control law is to enlarge the DOA estimate.

Chapter 3

Switching control strategies with a perspective on tumor immunotherapy

In this chapter we investigate the problem of stabilizing an unstable equilibrium by means of a switching control strategy defined on domains of attraction of equilibria of interest. In particular, we consider polynomial systems describing tumor dynamics, therefore the implications of the proposed stabilization strategy on tumor immunotherapy are also analyzed. For this, we derive a new model which captures the effects of the tumor cells on the immune system and viceversa, through predator–prey competition terms. Additionally, it incorporates the immune system's mechanism for producing hunting immune cells, which makes the model suitable for immunotherapy strategies analysis and design. For computing domains of attraction for the tumor nonlinear dynamics, and thus, for indicating immunotherapeutic strategies we employ rational Lyapunov functions. Finally, we apply the switching control strategy to destabilize an invasive tumor equilibrium and steer the system trajectories to tumor dormancy.

3.1 Introduction

Developing dynamical models which can be employed to describe and predict tumor evolution has been the focus of a considerable amount of research work in the past decades. The majority of this work is based on capturing the competition interaction between the immune cells and cancer cells, which turns out to be dynamical and nonlinear. See [1] for a collection of such models, or the more recent [38] for a more specific survey focused on tumor dormancy. This interaction is best understood if seen from an evolutionary perspective, as the competition of two populations for space in the tissue. Such models have been developed and studied in [41] and [43]. Although the model proposed therein is a two states Lotka–Volterra model, it is able to effectively capture certain phases in tumor development and growth. Some other type of models take into account also the immune system's mechanism of producing hunting immune cells (killer T–cells) by conversion from resting immune cells (helper T–cells). See for example the model proposed in [100]. This type of models is particularly interesting for immunotherapy.

Immunotherapy is a type of treatment which uses certain parts of the immune system to fight tumor growth and can act towards boosting the immune system in a general way or by helping it to attack cancer cells specifically. If the mechanism which produces hunting immune cells acts optimally, this has great influence on helping eradicating cancer or at least on driving it to dormancy. The usefulness of a dynamical model which incorporates this mechanism comes from the fact that such a model allows for assessment of immunotherapy effectiveness and for designing new strategies.

In this chapter, we consider three different evolutionary models for describing tumor dynamics. Two of the models have been introduced in the literature to study different mechanisms in tumor growth. Starting from the literature, we developed a model which also incorporates the dynamics driving the immune system itself, i.e. the conversion of resting cells to hunting ones, and the mutual effects the immune cells and the tumor cells have on each other. For predicting treatment outcome or designing treatment strategies, it is not sufficient to assess whether a certain equilibrium becomes stable or unstable under treatment. On one hand, it is also necessary to be able to say from which set of initial conditions the system will converge to that certain equilibrium, i.e. by computing the domain of attraction. And on the other hand, treatment strategies should take into account destabilizing unhealthy equilibria and adapting therapies until the desired equilibrium is reached, with minimal side effects to the patient. Thus, the focus on immunotherapies, and consequently on the model parameters which are responsible for boosting the immune response against cancer.

The idea that maintaining a stable dormant tumor might actually increase a patient's survival chances more than by trying to completely eradicate the tumor was proposed, for example, in [42]. In terms of tumor dynamical models, this implies that the optimal treatment tactic would be to try to maintain the stable tumor dormancy equilibrium. Therefore, the goal of the proposed DOA based immunotherapy strategy is to steer the tumor growth dynamics to the tumor dormancy equilibrium of the proposed model.

The tools developed in Chapter 2 in Section 2.2 will be used to compute estimates of the DOAs in the control strategy. This proposed switching strategy comes as an alternative to the feedback stabilization law developed in Chapter 2 in Section 2.4 based on RCLFs, which was applied on the tumor dynamics model from [41]. The switching strategy will also be illustrated on this model in the current chapter. We refer to the control strategy developed in this chapter as a switching control strategy because it involves switching the parameters of the system, thus the system dynamics, when the solution trajectory crosses to the DOA corresponding to the next systems parameters in a predefined parameter sequence. The motivation for considering the switching strategy comes from clinical arguments. It is expected that treatment will be applied at certain time moments, thus in a discrete manner, affecting the model's parameters and equilibria, and will have a continuous influence on the dynamics until the next treatment instance.

Maximal Lyapunov functions approximated by RLFs have been considered due to the fact that predator–prey type of considerations when developing tumor growth models lead to polynomial systems. These models are exactly approximated by Taylor series expansions which are at the basis of the RLF computation procedure.

When the purpose of analyzing such biological systems, resulting from applying the laws of mass action kinetics for biochemical reaction networks and/or competing populations principles, is to assess their stability properties, often LF candidates which take into account the physical structure of the systems are considered. Such functions are the Gibbs free energy functions [117]. These functions represent a thermodynamical potential that is minimized when a system reaches chemical equilibrium, at a constant temperature and pressure. Although Gibbs free energy functions define global LFs on the positive orthant, constructing such functions requires knowledge of the physical properties of the system. In turn, RLFs can be applied directly to the differential equations describing the system.

3.2 Tumor growth dynamical models

In this section we will first present two models of interacting populations from the literature (proposed in [41] and [100]), which have led to a new developed model in this thesis [34]. We will briefly analyze these models and their parameters and equilibria together with their clinical interpretations.

3.2.1 An immune cells–tumor cells competition model with 3 states

Consider the prey–predator type model proposed in [100] for the spontaneous regression and progression of a malignant tumor:

$$
\begin{aligned}
\dot{M} &= q + rM(1-\frac{M}{k_1}) - \alpha MN \\
\dot{N} &= \beta NZ - d_1 N \\
\dot{Z} &= sZ(1-\frac{Z}{k_2}) - \beta NZ - d_2 Z.
\end{aligned} \tag{3.1}
$$

For this type of models, the prey population is represented by the malignant cells (M), which is attacked by the predator cells (N and Z). The latter ones perform the immune response against the tumor and they are of two types: resting predator cells (Z) and hunting predator cells (N). The predator cells consist of cytotoxic T–lymphocytes and macrophages and the prey cells consist of the malignant cells. The macrophages detect and absorb tumor cells, eat them and release cytokines which activate the resting T–lymphocytes, which coordinate the counter attack. The resting cells are converted to a special type of T–lymphocytes, natural killers/hunting cells, and begin to multiply and release other cytokines which stimulate more resting cells. In this model, the hunting cells are the cytotoxic T–lymphocytes and the resting cells are the T–helper cells. The resting predator cells can become active predators when an activation signal is sent. The state variables in the model (3.1) represent densities of cells, therefore number of cells per unit volume of tissue.

Due to biological considerations, all the states and parameters in the model are in the positive real orthant. The parameters represent the following: r–the growth rate of tumor cells, q–the conversion of normal cells to malignant cells, k_1–the maximum carrying or packing capacity of tumor cells, k_2–the maximum carrying capacity of resting cells ($k_1 > k_2$), α–the rate of predation/destruction of tumor cells by the hunting cells, s–the growth rate of resting predator cells, d_1–the natural death of hunting cells, d_2–the natural death of resting cells. The system described in (3.1) has three equilibrium points, E_1, E_2, E_3, which correspond to zero N and Z cell populations and nonzero M cell population, i.e., $E_1 = (M^*, 0, 0)$, nonzero M and Z populations and zero N population, i.e., $E_2 = (M^*, 0, Z^*)$, and all nonzero populations, i.e., $E_3 = (M^*, N^*, Z^*)$, respectively. The local stability properties of the equilibria are described in more detail in [100] and in [92]. The following cases can occur:

(i) E_1 is stable if there exists no E_2 and no E_3.

(ii) E_1 is unstable, then there exists E_2, which if stable then there is no E_3.

(iii) E_1 unstable, then if E_2 is unstable, there exists E_3 which is stable.

We say that a certain equilibrium does not exist when it has values which are not in $\mathbb{R}_{>0}$, and, therefore, are not biologically admissible. In order to study the regression and progression of the tumor, it is of interest to consider the cases when E_3 exists, as for this equilibrium all cell populations are present. This means that information on the DOA of E_3 could then be used twofold. On one hand, for diagnosis or treatment assessment, i.e. is the tumor in regression or progression mode, and on the other hand to design optimal treatment strategies. The latter can be achieved through the interaction with the immune cell populations.

In what follows we consider the parameter values given in [92], $q = 10$, $r = 0.9$, $\alpha = 0.06$, $k_1 = 0.8$, $\beta = 0.1$, $d_1 = 0.02$, $s = 0.8$, $k_2 = 0.7$ and $d_2 = 0.03$. For these parameter values E_1 and E_2 are unstable and E_3 is stable. Furthermore, let x_1 denote M, x_2 denote N and x_3 denote Z. This system was studied in detail in [32], where the procedure in Chapter 2 was applied to compute a RLF V_4 and estimate the corresponding DOA estimate for E_3. It resulted that the set $\mathcal{S}_{\mathcal{A}} = \{x : V(x) < C^*\}$ for $C^* = 4.21466$, belongs to the true DOA of the equilibrium E_3, which is equal to $\begin{pmatrix} 3.25 & 5.41 & 0.2 \end{pmatrix}^\top$ for the considered parameter values. A plot of the level set $V_4(x) = 4.21466$ in a neighborhood around E_3 is shown in Figure 3.1(a). In Figure 3.1(b), the level set $\dot{V}_4 = 0$, which includes the level set $V_4(x) = 4.21466$, is also shown. Although the proposed procedure can be

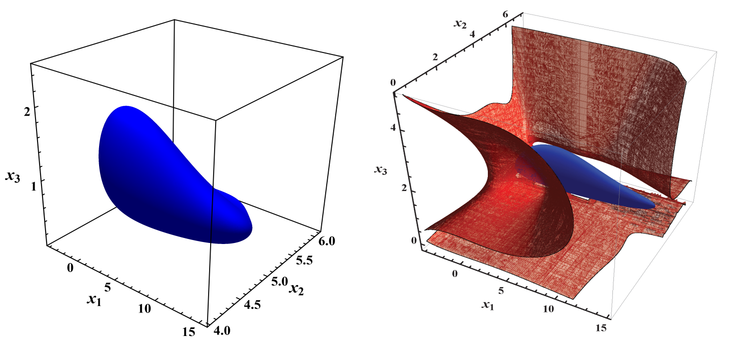

(a)

(b)

Figure 3.1: Estimation of the DOA of (3.3) bounded by the level set $V_4(x) = 4.21466$–(a) and together with the level set $\dot{V}_4 = 0$–(b).

extended to designing a control strategy which can parameterize, for example the predation rate of the tumor cells by the hunting cells α, the influence on the dynamics would not be significant. This is due to the fact that the model (3.1) does not incorporate the influence of the malignant cells on the immune cells. Therefore, the model needs to be modified if the purpose is to use α as a control parameter. Otherwise, if for example, the growth rate of the resting immune cells s, can be considered for control, the parametrization should be a function also of the tumor population state.

3.2.2 An immune cells–tumor cells competition model with 2 states

This model, proposed in [41] was further studied in [43] with the purpose to gain insight into the effectiveness of certain treatment approaches and the limitations of therapies based only on cytotoxic drugs aimed at killing the cancer cells, as well as to suggest new therapy strategies. Similarly to other models proposed in the literature such as (3.1), proposed in [100], the principles of population ecology are exploited also in this case, namely to describe population interactions of predator–prey type, i.e. by Lotka–Volterra models [62]. The difference is that in this model the effects of the tumor cells on the immune cells are also incorporated. As such, we consider the tumor dynamics system to be defined as follows:

$$\begin{aligned} \dot{N}_N &= R_N N_N - \frac{R_N}{K_N} N_N^2 - \frac{R_N \alpha_{NT}}{K_N} N_T N_N \\ \dot{N}_T &= R_T N_T - \frac{R_T}{K_T} N_T^2 - \frac{R_T \alpha_{TN}}{K_T} N_T N_N, \end{aligned} \tag{3.2}$$

where N_T represents the dominant tumor cells population which interacts with the normal cells population N_N. The model parameters have biological significance as follows. α_{TN} represents a variety of host defenses, including the immune response, that have as effect the decrease of the growth of the tumor populations, while α_{NT} represents the negative effect of the tumor on normal tissue. R_N and R_T are the maximum growth rates of normal and tumor cells, respectively, and K_N and K_T denote the maximal normal and tumor cells densities. The latter parameters correspond to the so–called carrying capacity terms in the model. This term represents the maximum population size that the tissue can sustain.

The system (3.2) can exhibit multiple fixed points which, depending on conditions on the parameters, have different stability properties. These aspects have been analyzed in [43] and will be briefly recalled next.

1. $E = (0, 0)$ will always be an equilibrium for the system, independently of parameter values, however it is not biologically relevant.

2. $E = (K_N, 0)$, which corresponds to normal tissue with no tumor cells present. This is an asymptotically stable equilibrium if $\frac{\alpha_{TN} K_N}{K_T} > 1$ and $\frac{\alpha_{NT} K_T}{K_N} < 1$ are satisfied.

3. $E = (\frac{K_N - \alpha_{NT} K_T}{1 - \alpha_{NT}\alpha_{TN}}, \frac{K_T - \alpha_{TN} K_N}{1 - \alpha_{NT}\alpha_{TN}})$, which corresponds to a stable coexistence of both tumor and normal cells, i.e. a benign, noninvasive tumor. This is an asymptotically stable equilibrium if $\frac{\alpha_{TN} K_N}{K_T} < 1$ and $\frac{\alpha_{NT} K_T}{K_N} < 1$.

4. $E = (0, K_T)$, which corresponds to an invasive cancer, with the normal cells being completely overgrown by the tumor cells. This is an asymptotically stable equilibrium if $\frac{\alpha_{TN} K_N}{K_T} < 1$ and $\frac{\alpha_{NT} K_T}{K_N} > 1$ are satisfied.

A detailed analysis of this model was carried in [35] and it resulted that mainly depending on the competition parameters, α_{TN} and α_{NT}, the tumor dynamics system may exhibit different stable equilibria (corresponding to different tumor dynamics situations) which then naturally change the vector field of the system. These equilibria correspond to either an invasive tumor, no tumor, or tumor dormancy (stable, noninvasive tumor) behavior. Naturally, the invasive tumor case will be favored if $K_T > K_N$. For the sake of illustration of the

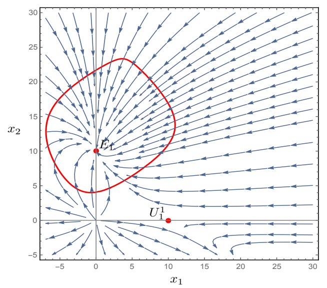

(a) Vector fields plot, the DOA $\mathcal{S}_1$ of the equilibrium E_1 of the system (3.2) for Case 1 and the unstable equilibrium U_1^1.

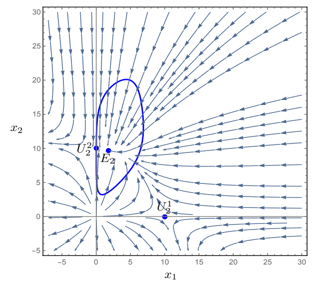

(b) Vector fields plot, the DOA $\mathcal{S}_2$ of the equilibrium E_2 of the system (3.2) for Case 2 and the unstable equilibria U_2^1 and U_1^2.

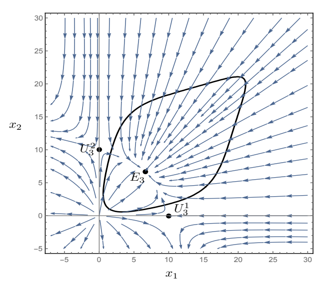

(c) Vector fields plot, the DOA $\mathcal{S}_3$ of the equilibrium E_3 of the system (3.2) for Case 3 and the unstable equilibria U_3^1 and U_3^2.

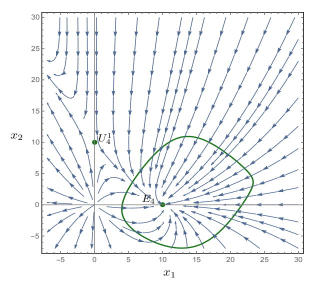

(d) Vector fields plot, the DOA $\mathcal{S}_4$ of the equilibrium E_4 of the system (3.2) for Case 4 and the unstable equilibrium U_4^1.

Figure 3.2: Estimates of DOA's of equilibria of (3.2) for different parameter values.

three behaviors or stages of tumor development let us consider the fixed parameters to have values $K_N = K_T = 10$ and $R_N = R_T = 0.9$ and the following cases for α_{TN} and α_{NT}:

- Case 1: $\alpha_{NT} = 2$, $\alpha_{TN} = 0.5$, when the stable equilibrium is $E_1 = (0, 10)$ and the vector fields are as shown in Figure 3.2(a);

- Case 2: $\alpha_{NT} = 0.847$, $\alpha_{TN} = 0.163$, with the stable equilibrium $E_2 = (1.76, 9.71)$ and the vector fields are as shown in Figure 3.2(b);

- Case 3: $\alpha_{NT} = 0.5$, $\alpha_{TN} = 0.5$, with the stable equilibrium $E_3 = (6.67, 6.67)$ and the vector fields are as shown in Figure 3.2(c);
- Case 4: $\alpha_{NT} = 0.5$, $\alpha_{TN} = 2$, when the stable equilibrium is $E_4 = (10, 0)$ and the vector fields are as shown in Figure 3.2(d).

Each of the above cases corresponds to a different dynamical behavior of the tumor–normal cells interaction, out of which cases 1, 3 and 4 represent the extremes. In this work we consider the tumor dormancy equilibrium, E_3 to be the desired equilibrium, thus the therapy strategy should meet the following specifications. Firstly, as discussed above, the treatment needs to steer the system trajectories to the DOA of E_3 and, secondly, to maintain this stable coexistence of tumor and cancer cells [42]. To design the control law achieving the above therapy strategy, the best possible approximation of the DOA of a given equilibrium is needed. To compute the closest DOA approximation, the results in Chapter 2 will be employed. For the system (3.2), when the maximal Lyapunov function is taken as a RLF, we obtained the following results for the Cases 1–4 in Figure 3.2. For the computational details we refer to the paper [35].

All biological systems are positive systems. We cannot allow the trajectories to become negative while initiated in the positive orthant, because this would imply that the states, which represent population densities or concentrations of substances become negative. A formal definition of a positive system is given below [11].

Definition 3.1 A system defined as in (2.1) is called *positive* if for any initial state x_0 in $\mathbb{R}^n_+$, the solution $x(t, x_0)$ will remain in $\mathbb{R}^n_+$, for any $t > 0$.

Therefore, the positive orthant is an invariant set for a positive system. Furthermore, a system is positive if the vector field at any state on the boundary of the positive orthant points into the interior of the positive orthant or along the boundary of the positive orthant. Notice that in Figure 3.2(d) for example, the computed level set of the LF V_4 is intersecting with the positive orthant boundary and contains states outside the positive orthant. In that case, the valid DOA estimate consists of the intersection of the corresponding level set of V_4 with the positive orthant. This is allowed by Theorem 5.1.

While the model (3.2) is suitable for designing a treatment strategy in terms of the inter-influence parameters α_{TN} and α_{NT} between the two competing cell populations, it does not include the mechanism that drives resting immune cells to convert to hunting immune cells. As this process is relevant for immunotherapy the model in the next section was developed.

3.2.3 A hunting–resting immune cells–tumor cells competition model

Let the system below describe the hunting–resting immune cells–tumor cells competition:

$$\begin{aligned} \dot{T} &= R_T T - (R_T/K_T)T^2 - (R_T/K_T)\alpha_{TN} NT \\ \dot{N} &= -\alpha_{NT} NT + \beta NZ \\ \dot{Z} &= R_Z Z - (R_Z/K_Z)Z^2 - (R_Z/K_Z)\beta NZ. \end{aligned} \tag{3.3}$$

In this model, the tumor cells population T and the immune cells, N and Z, are in a predator–prey type of interaction. The same interpretation for the states variable from (3.1) stands valid for this model. The proposed model (3.3) can be seen as an extension of the model (3.2), in the sense that the proposed model also incorporates the conversion mechanism of the T–cells from resting to hunting. A similar reasoning was applied when deriving the model in [100] (3.1). However, the model in [100] is conservative since the effect of the tumor cells on the immune cells is not illustrated in the differential equations. This effect is particularly important, since it can be related to treatment resistance. In many cases, whether the treatment is specifically targeted to destroy the cancer cells or whether it is aimed at stimulating the immune cells to either multiply faster or to strengthen the immune response, the tumor is resisting the treatment. This is due to the fact that the tumor cells also have a mechanism to fight back, which is illustrated in the model (3.3) by the term $-\alpha_{NT}NT$.

The parameters in (3.3) have the following interpretations. R_T and R_Z, represent, respectively, the growth rate of the tumor cells and the resting immune cells, while K_T and K_Z are their respective carrying capacities. The parameter α_{TN} illustrates the effect of the immune cells on the tumor cells, while α_{NT} represents the effect of the tumor cells on the immune cells. Finally, β represents the conversion rate of the resting immune cells to hunting immune cells. This parameter is of interest, particularly for treatment evaluation and treatment design, since on one hand, it controls the immune system dynamics and on the other hand, along with α_{TN} it defines the aggressiveness of the immune response and/or drugs against the invader cells, which in this case are the cancer cells.

The system (3.3) has multiple equilibrium points, including the one in the origin which is irrelevant from a biological perspective. The other equilibria are given by: $E_1 = \begin{pmatrix} 0 & p & 0 \end{pmatrix}^\top$, $p \in \mathbb{R}_{>0}$, $E_2 = \begin{pmatrix} E_2^1 & E_2^2 & E_2^3 \end{pmatrix}^\top$, $E_2^1 = -\frac{\beta^2 K_T - \alpha_{TN}\beta K_Z}{\alpha_{NT}\alpha_{TN} - \beta^2}$, $E_2^2 = -\frac{\alpha_{NT}K_T - \beta K_Z}{-\alpha_{NT}\alpha_{TN} + \beta^2}$, $E_2^3 = -\frac{\alpha_{NT}(\beta K_T - \alpha_{TN}K_Z)}{\alpha_{NT}\alpha_{TN} - \beta^2}$, $E_3 = \begin{pmatrix} 0 & 0 & K_Z \end{pmatrix}^\top$, $E_4 = \begin{pmatrix} K_T & 0 & K_Z \end{pmatrix}^\top$ and $E_5 = \begin{pmatrix} K_T & 0 & 0 \end{pmatrix}^\top$.

In all the computations in the remainder of this chapter, we will denote T by x_1, N by x_2 and Z by x_3. The Jacobian matrix is $A = \begin{pmatrix} a_{11} & -\frac{\alpha_{TN}R_T x_1}{K_T} & 0 \\ -\alpha_{NT}x_2 & -\alpha_{NT}x_1 + \beta x_3 & \beta x_2 \\ 0 & -\frac{\beta R_Z x_3}{K_Z} & a_{33} \end{pmatrix}$, where $a_{11} = R_T - \frac{2R_T x_1}{K_T} - \frac{\alpha_{TN}R_T x_2}{K_T}$, and $a_{33} = R_Z - \frac{\beta R_Z x_2}{K_Z} - \frac{2R_Z x_3}{K_Z}$. Based on the Jacobian matrix, we can directly assess the local stability properties of some of the equilibria, as follows.

- E_1 corresponds to a healthy equilibrium situation, however it doesn't make sense from a biological point of view, since it contains nonzero hunting cells populations, whereas the tumor and resting cells populations are zero. For this reason, it will be discarded from the analysis.

- The eigenvalues of the Jacobian matrix for E_3 are:

$$\lambda_3 = (\beta K_Z, R_T, -R_Z),$$

  thus E_3 is always unstable since $R_T > 0$.

- The eigenvalues of the Jacobian matrix for E_4 are:

$$\lambda_4 = (-\alpha_{NT}K_T + \beta K_Z, -R_T, -R_Z)\,.$$

If $\beta > \frac{\alpha_{NT}K_T}{K_Z}$, then E_4 is unstable.

- The eigenvalues of the Jacobian matrix for E_5 are:

$$\lambda_5 = (-\alpha_{NT}K_T, -R_T, R_Z)\,,$$

thus E_5 is always unstable since $R_Z > 0$.

- The eigenvalues of the Jacobian matrix for E_6 are:

$$\lambda_6 = \left(0, 0, \frac{(-\beta K_T + \alpha_{TN}K_Z)R_Z}{\alpha_{TN}K_Z}\right),$$

thus E_6 is always unstable.

Immunotherapy acts mainly towards boosting the body's immune response to fight diseases such as cancer. Specifically, immunotherapy targets certain proteins in cells which are stimulated so that the immune response against cancer is stronger. If we consider the model (3.3), the key parameters in boosting the response of the immune cells against cancer are α_{TN}, α_{NT} and β. Therefore, one strategy for immunotherapy is to target the above mentioned parameters. How these parameters influence the immune response, and therefore the dynamical behavior of the tumor–immune cells interaction, can be determined by looking into stability of equilibria of interest. Moreover, for treatment purposes it is not sufficient to have only information on the equilibria of the tumor dynamics and their respective stability. It is of crucial importance to be able to assess whether from a certain initial condition, the trajectory of the tumor dynamics will converge to a specific equilibrium. This can help making the distinction from a patient which is on the path of being cured, or who is converging towards a stable, noninvasive tumor, or one which has a tumor that will malignantly grow. This distinction can be done or estimated, by computing the DOA of an equilibrium of interest.

In this chapter, we consider the analysis of the tumor dormancy equilibrium (E_2) and the invasive tumor equilibrium (E_4) of the proposed model (3.3). More specifically, first we focus on how their properties are influenced by the relevant parameters which can be driven through immunotherapy. This will be addressed by means of computing the DOAs of these equilibria. Then, we develop a switching strategy design for immunotherapy, when the goal is to steer the states to tumor dormancy (E_2) and maintain this equilibrium.

3.3 Therapy strategy design methods

3.3.1 Parameter analysis for immunotherapy

In what follows we will make use of the tools in Chapter 2 for computing RLFs and corresponding DOA estimates. Further, we will focus on analyzing the properties of the tumor dormancy and invasive tumor equilibria of the system (3.3). To this end, we recall three possible cases with respect to the effects that the immune cells and the tumor cells have on each other, and analyze the influence of the rate of conversion of hunting immune cells from resting ones on the overall dynamics [34]. More specifically, we consider β as the parameter which can be driven by immunotherapy and we look into how β influences the two equilibria of interest.

3.3.1.1 Case I: influence of tumor cells on immune cells is equal to the influence of immune cells on tumor cells: $\alpha_{TN} = \alpha_{NT} = 0.5$.

For the known parameter values, the eigenvalues of E_4 as a function of the β parameter will become $\lambda_4 = (-0.9, -0.9, -5 + 10\beta)$, therefore for values of $\beta < 0.5$, E_4 will be stable. If we evaluate the eigenvalues of the Jacobian for $\beta < 0.5$ and E_2, it results that E_2 will be unstable. For $\beta > 0.5$, E_4 becomes stable, and the corresponding Jacobian will have complex eigenvalues. Therefore, if the conversion rate from resting predators to hunting predators is high enough, this will lead to a stable confined tumor. Let β be equal to 0.9. Then $E_2 = \begin{pmatrix} 6.42857 & 7.14286 & 3.57143 \end{pmatrix}^\top$ is stable and $E_4 = \begin{pmatrix} 10 & 0 & 10 \end{pmatrix}^\top$ is unstable. For E_2 a RLF of order 4 was computed and an approximation of the DOA of E_2 defined by the level set value $C^* = 83.102$ of V_4 is shown in Figure 3.3 together with a left–angle view of the set and a vector field plot of (3.3). The value of C^* was computed via the optimization problem (15) in [32]. Let now $\beta = 0.2$. Then $E_2 = \begin{pmatrix} 2.85714 & 14.2857 & 7.14286 \end{pmatrix}^\top$ is an unstable dormancy equilibrium, while $E_4 = \begin{pmatrix} 10 & 0 & 10 \end{pmatrix}^\top$ is stable. By a similar procedure, an approximation of the DOA of E_4 was computed for the level set value $C^* = 36$. This is shown in Figure 3.4 together with a left–angle view of the set and a vector field plot of (3.3). Note that for this case the realistic DOA approximation is a subset of the set displayed in Figure 3.4 which results from its intersection with the positive axes. This is allowed by Theorem 5.1, since the tumor system (3.3) is positive and the positive axes are an invariant set for this system.

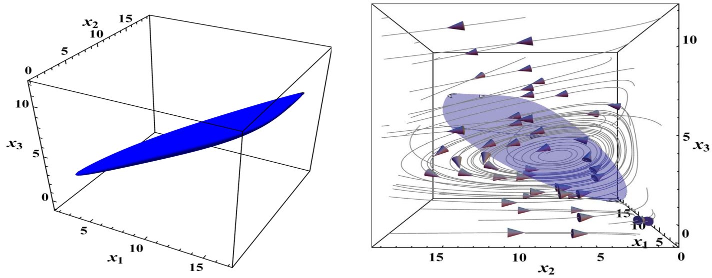

(a) (b)

Figure 3.3: Case I: Level set plot $V_4(x) = 83.102$ for $\beta = 0.9$, i.e. stable tumor dormancy–(a) and with vector fields–(b).

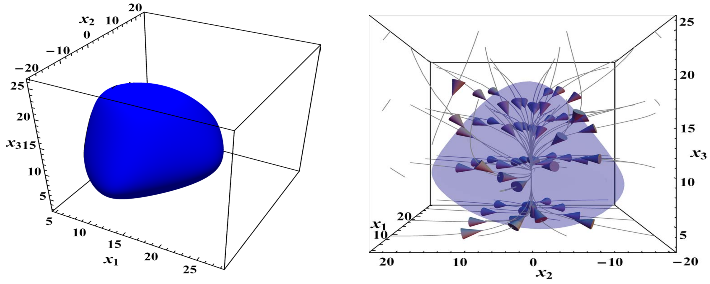

(a) (b)

Figure 3.4: Case I: Level set plot $V_4(x) = 36$ for $\beta = 0.2$, i.e. stable invasive tumor–(a) and with vector fields–(b).

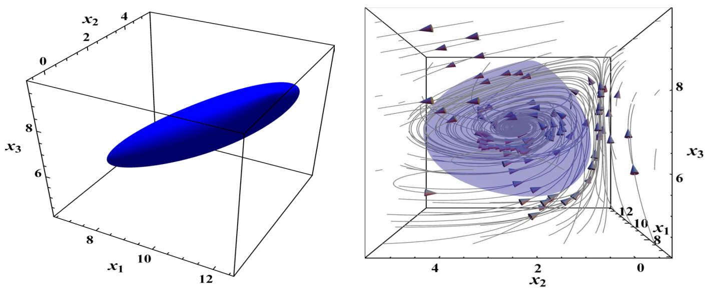

(a) (b)

Figure 3.5: Case II: Level set plot $V_4(x) = 5.2$ for $\beta = 1.2$, i.e. stable tumor dormancy–(a) and with vector fields–(b).

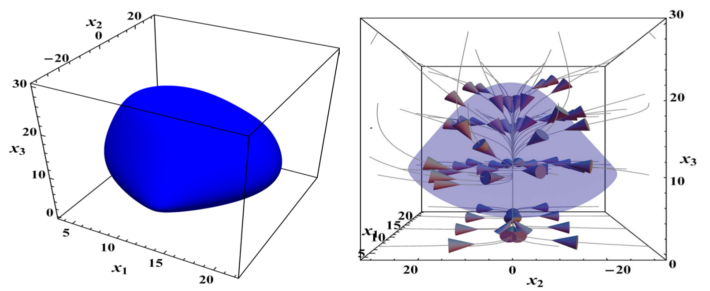

(a) (b)

Figure 3.6: Case II: Level set plot $V_4(x) = 40$ for $\beta = 0.2$, i.e. stable invasive tumor–(a) and with vector fields–(b).

3.3.1.2 Case II: influence of tumor cells on immune cells is stronger than the influence of immune cells on tumor cells: $\alpha_{TN} = 0.2$; $\alpha_{NT} = 0.9$.

Similarly as in the previous case, we get $\lambda_4 = (-0.9, -0.9, -9 + 10\beta)$, therefore for $\beta < 0.9$, E_4 will be stable and E_2 unstable. For $\beta = 0.91$, the Jacobian corresponding to E_2 has stable, real eigenvalues and complex for $\beta > 0.91$, thus we pick $\beta = 1.2$ to illustrate the complex eigenvalues case as well. The DOA of the stable equilibrium $E_2 = \begin{pmatrix} 9.52381 & 2.38095 & 7.14286 \end{pmatrix}^\top$ is shown in both plots from Figure 3.5. In Figure 3.5(b) a left angle view of the set is shown together with the corresponding vector field plots. For $\beta = 0.2$, the stable equilibrium is E_4, while $E_2 = \begin{pmatrix} 0 & 50 & 0 \end{pmatrix}^\top$–unstable can be discarded since it is not realistic. The corresponding DOA is displayed in Figure 3.6. The same set is plotted from a left angle view together with the system's vector fields in Figure 3.6(b).

3.3.1.3 Case III: influence of tumor cells on immune cells is weaker than the influence of immune cells on tumor cells: $\alpha_{TN} = 0.9$; $\alpha_{NT} = 0.2$.

By the same reasoning as in the previous two cases, it can be concluded that for $\beta < 0.2$, E_4 is stable. However, in this case, E_2 will remain unstable, irrespective of the value of β. For $\beta = 0.05$, $E_2 = \begin{pmatrix} 2.39437 & 8.4507 & 9.55746 \end{pmatrix}^\top$. We exclude here the cases which generate stable E_2, but with negative equilibrium values, which are not biologically admissible. As such, an estimation of the DOA of E_4 was computed for $\beta = 0.05$. The computed set is shown in Figure 3.8(a) and in Figure 3.8(b) together with vector field plots. As for what concerns E_2, if we allow for the parameters K_T and K_Z to be different, we can achieve stability. For example for $K_T = 10$ and $K_Z = 5$, then $E_4 = \begin{pmatrix} 10 & 0 & 5 \end{pmatrix}^\top$ will be stable for $\beta < 0.4$ and E_2 will be stable for $\beta > 0.4$. If $\beta = 1.2$, then $E_2 = \begin{pmatrix} 7.14286 & 3.1746 & 1.19048 \end{pmatrix}^\top$ with the estimated DOA shown in Figure 3.7.

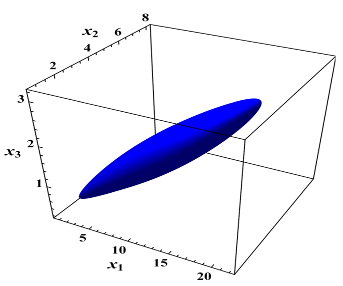

(a)

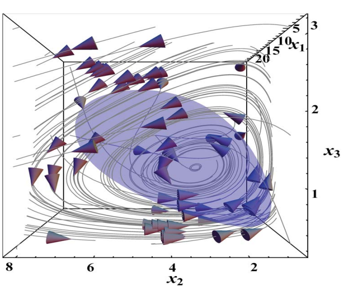

(b)

Figure 3.7: Case III: Level set plot $V_4(x) = 40$ for $\beta = 1.2$, i.e. stable tumor dormancy–(a) and with vector fields–(b).

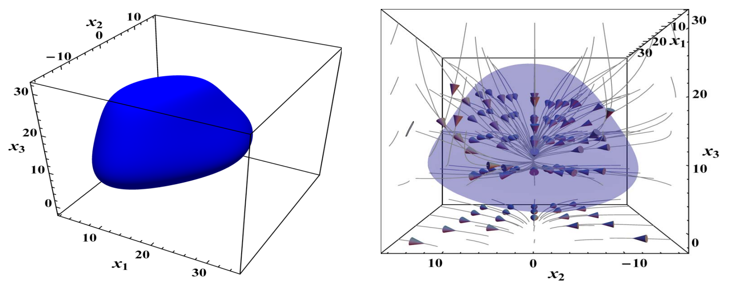

(a) (b)

Figure 3.8: Case III: Level set plot $V_4(x) = 60$ for $\beta = 0.05$, i.e. stable invasive tumor–(a) and with vector fields–(b).

3.3.2 Tools for therapy strategy design

From the above analysis it follows that the parameter β influences the stability of the equilibria of interest in different cases depending on the interinfluence parameters $(\alpha_{NT}, \alpha_{TN})$. Ideally, the treatment strategy should be able to steer the dynamics from Case 3.3.1.2 to Case 3.3.1.3 with E_2 stable, or worst case, to Case 3.3.1.1 with E_2 stable, via a switching sequence based on the parameters $(\beta, \alpha_{NT}, \alpha_{TN})$. However, as it will be seen in the remainder of this chapter, more (possibly all) model parameters need to be influenced for the model (3.3).

Let

$$\sigma_i = \begin{pmatrix} p_{i1} & p_{i2} & \dots & p_{ij} \end{pmatrix}^\top, \quad i = 1, \dots, M,\ j = 1, \dots Q.$$

Each σ_i defines a new system of differential equations describing the tumor dynamics which will have a corresponding stable equilibrium E_i. Q denotes here the number of system parameters that define each σ_i and M denotes the number of needed switching parameter sets. Let us denote the vector field describing the dynamics by f_i, which will be a function of the state vector x_i and of the parameter vector σ_i. We define the finite sequence of parameters $\Lambda = \{\sigma_1, \sigma_2, \dots, \sigma_M\}$ such that

$$\sigma_M = \sigma^*,\ E_M = E^*,\ f_M = f^*,$$

where σ^*, E^* and f^* denote, respectively, the desired set of parameters which define the desired equilibrium value and the desired dynamics. Furthermore, if we consider the corresponding DOAs for each of the equilibria above, then the sequence of DOAs should converge to the DOA of $E_M = E^*$, denoted by $\mathcal{S}^*$. If we consider the worst case scenario, when the system parameters correspond to the case which has as stable equilibrium the invasive cancer state (with zero normal cells), then we also have information about σ_1. Therefore, the switching law is initiated by identifying the DOA where the initial state of the system is to be considered. Furthermore, the overall cancer dynamics system, with varying parameters σ_i is in fact an autonomous switched nonlinear system [19].

In what follows we will derive a therapy strategy for steering the parameters from the invasive cancer dynamics to the dormant tumor dynamics, which is based on the DOAs of the individual corresponding dynamics. Equivalently, this implies that the switching rule is designed based on DOAs of the switched system and the finite dynamics is defined on a predefined finite set of values of parameters. Consider the following sets:

$$\Lambda = \{\sigma_1, \sigma_2, \ldots, \sigma_M\} \tag{3.4}$$

$$\mathbb{S} = \{\mathcal{S}_1, \mathcal{S}_2, \ldots, \mathcal{S}_M\} \tag{3.5}$$

$$\mathbb{E} = \{E_1, E_2, \ldots, E_M\} \tag{3.6}$$

$$\mathcal{I} = \{1, 2, \ldots, M\}, \tag{3.7}$$

where $M > 0$, denotes the finite number of switchings among parameters and consequently, among vector fields over DOAs, i.e. the subsets of $\mathbb{S}$. $\mathbb{E}$ represents the set of equilibria of the switching systems and $\mathcal{I}$ defines an index set.

Next, consider the following system

$$\begin{aligned} \dot{x} &= \widetilde{f}(x(t), \sigma(t)) \\ \sigma(t) &= \nu(x(t)), \end{aligned} \tag{3.8}$$

where $x(t) \in \mathbb{R}^n$, $\sigma(t) \in \Lambda$. The maps $\widetilde{f}(\cdot, \sigma) : \mathbb{R}^n \to \mathbb{R}^n$ are Lipschitz continuous for any $\sigma \in \Lambda$ and $\widetilde{f}(\cdot, \sigma) = f_i(x)$, for any $i \in \mathcal{I}$. For certain values of parameters of interest, f_i denotes the vector field describing dynamics of the form $\dot{x} = f_i(x)$. $\nu : \mathbb{R}^n \to \Lambda$ is the discrete dynamics, which is defined as

$$\nu(x(t)) = \sigma_{i^*}, \text{ if } x(t) \in \mathcal{S}_{i^*}, \tag{3.9}$$

for any $\sigma_i \in \Lambda$, with the switching rule

$$i^* := \max\{i \,|\, x(t) \in \mathcal{S}_i\}. \tag{3.10}$$

Theorem 3.1 Consider the switched system described in (3.8)–(3.10) where $E_i \in \mathbb{E}$ are such that for any $i \in \mathcal{I}$, $\widetilde{f}(E_i, \sigma_i) = f_i(E_i) = 0$, and the sets $S_i \in \mathbb{S}$ represent DOAs of the equilibria E_i. Furthermore let the following conditions

$$\mathcal{N}(E_i)^+ \subseteq \mathcal{S}_i \cap \mathcal{S}_{i+1} \tag{3.11}$$

hold for all $i \in \mathcal{I}$ and define $\widetilde{\mathcal{S}} := \bigcup_i \mathcal{S}_i$. Then E_M is an asymptotically stable equilibrium for the switched system (3.8)–(3.10) with DOA $\widetilde{\mathcal{S}}$.

Proof: Take any initial condition $x_0 \in \widetilde{\mathcal{S}}$. Then according to (3.9) and (3.10) there exists an index i such that $x_0 \in \mathcal{S}_i$. Let $i^* = \max\{i \,|\, x_0 \in \mathcal{S}_i\}$. Then we can have the next two situations.

If $i^* = M$, then $\mathcal{S}_M$ is a DOA for the considered switched system with $\nu(x(t)) = \sigma_M$. This follows from the fact that for any $x_0 \in \mathcal{S}_M$, $\max\{i \,|\, x(t, x_0) \in \mathcal{S}_i\} = M$, for any $t \geq 0$ and $\mathcal{S}_M$ is a DOA for E_M and the system $\dot{x}(t) = f(x(t), \sigma_M) = f_M(x(t))$ by construction.

If $i^* \neq M$ then it can only be that $i^* < M$. Thus, let $x_0 \in \mathcal{S}_{i^*}$. This implies that $\lim_{t\to\infty} x(t, x_0) = E_{i^*}$ and $x(t, x_0) \in \mathcal{S}_{i^*} \subseteq \mathbb{R}^n_+$ for some $t > 0$, since S_{i^*} is a DOA defined by the RLF $V_{i^*}(x)$. Suppose there does not exist a $t_{i^*+1} \in \mathbb{R}_{>0}$ such that $x(t_{i^*+1}, x_0) \in \mathcal{N}(E_{i^*})^+$. Further, let $\mathbb{B}_\rho(E_{i^*})^+$ denote the projection on $\mathbb{R}^n_+$ of a ball of radius $\rho > 0$ and centered in E_{i^*} which is contained in $\mathcal{N}(E_{i^*})^+$. Hence, $\|x(t, x_0) - E_{i^*}\| \geq \rho$, for any $t > 0$, which contradicts the convergence to the equilibrium. Therefore, at t_{i^*+1} we have that $x(t_{i^*+1}, x_0) \in \mathcal{N}(E_{i^*})^+ \subseteq \mathcal{S}_{i^*} \cap \mathcal{S}_{i^*+1}$, which implies that $\nu(x(t_{i^*+1}, x_0)) = \sigma_{i^*+1}$.

By iterating the reasoning above, it results that there exists $t_M > 0$, such that

$$\nu(x(t_M, x_0)) = \sigma_M$$

and, moreover, that $\lim_{t\to\infty} x(t, x_0) = E_M \in \mathcal{S}_M$. Therefore, for any $x_0 \in \widetilde{\mathcal{S}}$, $x(t, x_0)$ will converge to E_M, while never leaving $\widetilde{\mathcal{S}}$ since it will never leave $\bigcup_i \mathcal{S}_i$. This implies that E_M is an asymptotically stable equilibrium for the switched system (3.8)–(3.10) with DOA $\widetilde{\mathcal{S}}$.

■

Notice that the switching rule (3.10) together with condition (3.11) guarantee that E_i is not an equilibrium of $\dot{x} = \widetilde{f}(x(t), \sigma_{i+1})$, thus the trajectories of this system can never converge to E_i in $\mathcal{S}_i$.

Remark 3.1 In order to ensure some robustness for the switching control law, i.e., to avoid chattering around the switching boundary one can redefine the parametric switching function ν in (3.9) and the switching rule (3.10) as

$$\nu(x(t)) = \sigma_{i^*},\ x(t) \in \varepsilon\mathcal{S}_{i^*}, \tag{3.12}$$

and

$$i^* = \max\{i \,|\, x(t) \in \varepsilon\mathcal{S}_i\}, \tag{3.13}$$

for any $\sigma_i \in \Lambda$, with $0 < \varepsilon < 1$ as scaling factor. However, it is possible that, for a certain value of ε and for some initial conditions, the trajectories will never reach the boundary of the set $\varepsilon\mathcal{S}_{i+1}$ before converging to E_i. This implies that a trade–off between the degree of robustness with respect to switching and certain restrictions with respect to the set of possible initial conditions must be made.

3.3.3 Application of immunotherapeutic strategies design

In this section, the switching control law described in Section 3.3.2 will be applied to the models (3.2) and (3.3).

3.3.3.1 Immune cells–tumor cells competition model

The parameter based switching control law described in Subsection 3.3.2 will be illustrated next for the tumor dynamics system (3.2) to design a therapy strategy for invasive tumor growth. Thus, let the σ parameters in the model (3.2) be such that $E_1 = (0, 10)$ is the asymptotically stable equilibrium and let the desired equilibrium be $E_3 = (6.66667, 6.66667)$. As such, the set Λ is defined by the parameter pairs $\sigma_1 = (2, 0.5)$,

$\sigma_2 = (0.847, 0.163)$, $\sigma_3 = (0.5, 0.5)$. With this sequence of parameters we can compute the sequence of corresponding DOAs, $\mathbb{S} = \{\mathcal{S}_1, \mathcal{S}_2, \mathcal{S}_3\}$. The sets are shown in Figure 3.9 with red, blue and black contour, respectively. As shown also in the plots, the generated set sequence satisfies the condition (3.11) in Theorem (3.1). In particular, for E_1, $\mathcal{N}(E_i)^+ = [a_1, b_1]$, where $a_1 = (0, 6.06)$ and $b_1 = (0, 10.6)$, which are the intersection points of the set $\{x \in \mathbb{R}^n \,|\, V_2(x) \leq C_2\}$ with the positive orthant, therefore (3.11) holds. Note that E_2 belongs to the interior of the set $\mathcal{S}_2$ and that $\mathcal{S}_i$, for any $i \in \mathcal{I}$, are the intersections of the sets with contours shown in Figure 3.9 with the positive orthant. In Figure 3.9(b), the trajectories corresponding to the initial conditions $x_0^1 = (1.35 \quad 21.26)^\top$ and $x_0^2 = (7.429 \quad 19.91)^\top$ are shown. We considered the switching rule as defined by (3.12) and (3.13) with $\varepsilon = 0.8$ when the trajectory switches from $\mathcal{S}_1$ to $\mathcal{S}_2$ and $\varepsilon = 0.95$ when the trajectory switches from $\mathcal{S}_2$ to $\mathcal{S}_3$. For the first switch, due to the robustness condition, if in the initial state the number of normal cells is too low, then it is possible that the trajectory will never hit $\varepsilon\mathcal{S}_1$. This means that it will converge to E_1, therefore a safety initial condition margin is required. In the illustrated case, the first element of x_0^1 is equal to 1.35, which suggests that this distance from zero on the x_1 axis is safe.

In terms of clinical interpretation, the results shown above imply that pre–therapy, which can allow the number of normal cells to grow, although the number of cancer cells will also grow, is needed before the proposed therapy design procedure can be used. However, this is only necessary if robustness is enforced. Moreover, a trade–off between the robustness margin and the initial safety bound is required. Due to the condition in (3.11) if robustness is not of interest, then for any initial state which belongs to $\mathcal{S}_1$ and it is arbitrarily close to E_1, the proposed switching rule will steer the trajectory to E_4.

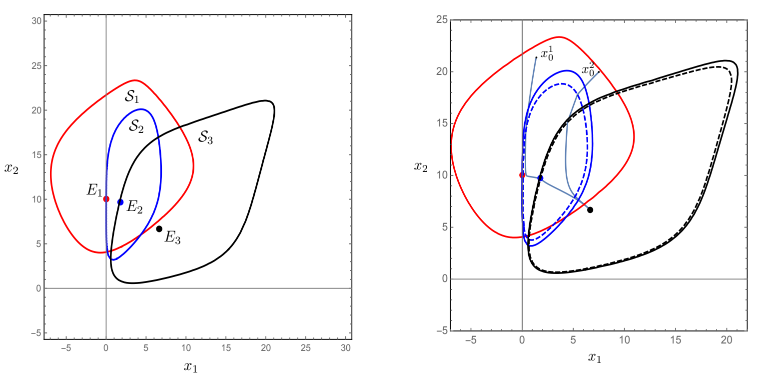

(a) Estimation of the DOAs of E_1–red, E_2–blue and E_3–black together with corresponding equilibrium values.

(b) Estimation of the DOAs of E_1–red, E_2–blue and E_3–black together with corresponding equilibrium values and two switched systems trajectories.

Figure 3.9: An example of applying the switching control law to the two states tumor dynamics model (3.2).

3.3.3.2 Hunting–resting immune cells–tumor cells competition model

Let us apply the switching law described in Section 3.3.2 for the model (3.3). We consider the following scenario. Let the parameters of the model correspond to Case 3.3.1.2, when E_4 is the stable equilibrium, i.e. $\beta = 0.2$. The goal is to steer the states away from this equilibrium, and its corresponding DOA to a dormancy equilibrium, similar to the Case 3.3.1.1, when the values of α_{TN} and α_{NT} are equal or very close to each other.

Although the major influence on immunotherapy is carried by the parameters α_{TN}, α_{NT} and β, in order to shift the dynamics from one which exhibits a stable invasive tumor equilibrium (E_4) with zero hunting cells to one intermediate dynamics which exhibits a stable equilibrium with nonzero hunting cells (E_2), all model parameters need to be influenced. Note that the growth rates R_T and R_Z do not have an influence on the values of E_2 and E_4, however they come in play in the linearization matrix which determines the local stability properties of these equilibria [34]. As such, let $M = 6$ and $Q = 7$ and

$$\sigma_i = \begin{pmatrix} \alpha_{NT}^i & \alpha_{TN}^i & \beta^i & K_T^i & K_Z^i & R_T^i & R_Z^i \end{pmatrix}^\top, \quad i = 1, \ldots, M.$$

For

$$\sigma_1 = \begin{pmatrix} 0.9 & 0.2 & 0.2 & 10 & 10 & 0.9 & 0.9 \end{pmatrix}^\top,$$

the corresponding stable equilibrium $E_4^1 = \begin{pmatrix} 10 & 0 & 10 \end{pmatrix}^\top$ has as corresponding DOA estimate the set depicted in red in Figure 3.10(a).

Let the desired equilibrium be $E_2^6 = \begin{pmatrix} 6.74562 & 6.50877 & 4.07702 \end{pmatrix}^\top$, and the target set of parameters

$$\sigma_6 = \begin{pmatrix} 0.55 & 0.5 & 0.91 & 10 & 10 & 0.9 & 0.9 \end{pmatrix}^\top,$$

for which the corresponding DOA estimate is shown in Figure 3.10(e) with green. In order to steer the trajectories to the set $\mathcal{S}_6$, first we switch from E_4^1 to a lower x_3 value equilibrium $E_4^2 = \begin{pmatrix} 10 & 0 & 6.6 \end{pmatrix}$. Thus, for

$$\sigma_2 = \begin{pmatrix} 0.9 & 0.2 & 0.5 & 10 & 6.6 & 0.9 & 0.9 \end{pmatrix}^\top,$$

a new DOA estimate $\mathcal{S}_2$ is obtained, shown in yellow in Figures 3.10(a) and 3.10(b). In Figure 3.10(a) a trajectory initiated in $x_0 = (20, 6, 7)^\top$, $x_0 \in \mathcal{S}_1$, is shown with red. When the trajectory hits the boundary of $\mathcal{S}_2$, then the dynamics is switched to $\dot{x} = f_2(x)$, as shown in Figure 3.10(b) with black.

In order to steer the trajectory away from the boundary of the positive orthant defined by $x_2 = 0$, a new equilibrium E_2^3 needs to be assigned such that its corresponding DOA estimate, $\mathcal{S}_3$ contains E_4^2, according to (3.11). For this to hold, E_2^3 can't be assigned with the x_2 value very far from $x_2 = 0$ and there must exist a level set value C_3 for $V_4^3(x)$ such that $\mathcal{S}_3 \cap \mathcal{P} \cap \mathcal{N}(E_2^3)^+ \neq \emptyset$, where $\mathcal{P}$ denotes the positive orthant. However, for C_3 to exist, we must allow that the set $\mathcal{S}_3 = \{x \in \mathbb{R}^n \,|\, V_4^3(x) \leq C_3\}$ intersects the zero level

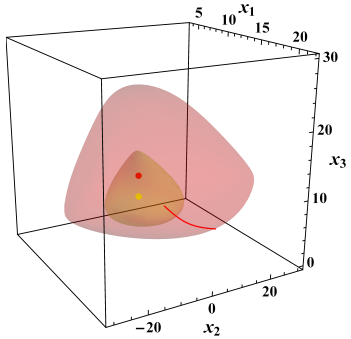

(a) Estimation of the DOAs of E_4^1–red and E_4^2–yellow and a switched system trajectory.

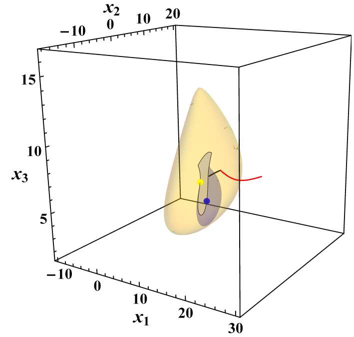

(b) Estimation of the DOAs of E_4^2–yellow and E_2^3–blue and a switched system trajectory.

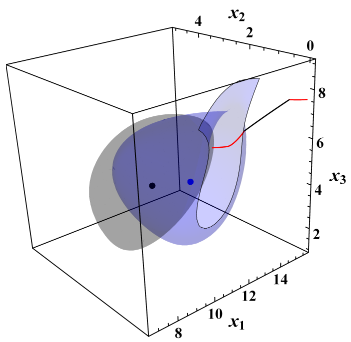

(c) Estimation of the DOAs of E_2^3–blue and E_2^4–black and a switched system trajectory.

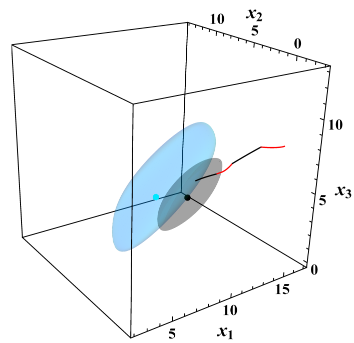

(d) Estimation of the DOAs of E_2^4–black and E_2^5–cyan and a switched system trajectory.

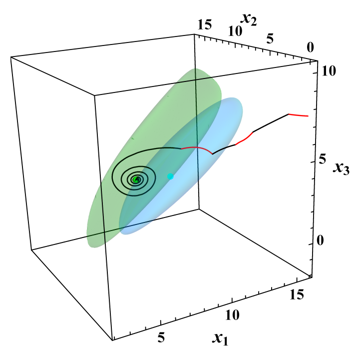

(e) Estimation of the DOAs of E_2^5–cyan and E_2^6–green and a switched system trajectory.

Figure 3.10: An example of applying the switching control law to the two states tumor dynamics model (3.3).

set of $\dot{V}_4^3(x)$, for $x \in \mathbb{R}^n \setminus \mathcal{P}$. This is allowed, since the positive orthant is an invariant set for the tumor system. A formal proof can be found in [114, Theorem 2.3]. We consider $E_2^3 = \begin{pmatrix} 10.6875 & 1.04151 & 5.02943 \end{pmatrix}^\top$, and

$$\sigma_3 = \begin{pmatrix} 0.8 & 0.3 & 1.7 & 11 & 6.8 & 0.5 & 1 \end{pmatrix}^\top,$$

with the corresponding DOA estimate shown in Figure 3.10(b) and Figure 3.10(c) with blue. Note that, as expected the level of α_{TN} is slightly increased, while α_{NT} is slightly decreased showing that the effect of the immune cells on the tumor cells is slightly stronger, the carrying capacity of the resting immune cells, K_Z is still close to the previous low value while, rather unintuitively K_T is increased. In turn, the conversion rate β is much higher. As the growth rates R_T and R_Z have an influence on the eigenvalues of the linearization matrix around E_2^3, decreasing R_T and increasing R_Z, have an influence on the shape of the set $\mathcal{S}_3$, thus facilitating the inclusion of the unhealthy equilibrium E_4^2. The trajectory defined by the new map $f_3(x)$ is shown in Figure 3.10(c).

Since E_2^3 is very close to the undesired equilibrium, E_4^1, we propose two more intermediate steps, which correspond to switching between stable tumor dormancy equilibria until the "safe" dormancy equilibrium E_4^6 is reached. As such, for

$$\sigma_4 = \begin{pmatrix} 0.7 & 0.45 & 1.3 & 10 & 7 & 0.9 & 0.9 \end{pmatrix}^\top,$$

the DOA estimate of $E_2^4 =$ is shown in Figures 3.10(c) and 3.10(d) with black, and the trajectory defined by $f_4(x)$ is plotted in Figure 3.10(d) with black. Next, for

$$\sigma_5 = \begin{pmatrix} 0.65 & 0.5 & 1.14 & 10 & 9 & 0.9 & 0.9 \end{pmatrix}^\top,$$

the DOA estimate of $E_2^5 =$ is shown in Figures 3.10(d) and 3.10(e) with cyan, and the trajectory defined by $f_5(x)$ is plotted in Figure 3.10(e) with red. Finally, the trajectory converging to the desired equilibrium E_2^6 is shown with black in Figure 3.10(e).

In Figure 3.11(a) a plot with all the sets together is shown, together with one trajectory of the controlled tumor dynamics. Since all the other sets are rather small compared to $\mathcal{S}_1$(red) a left view plot of the sets and trajectory is shown in Figure 3.11(b).

Note that in the case of the last three switching systems corresponding to the parameters in σ_4, σ_5 and σ_6, the values of α_{TN} and α_{NT} are slowly converging to each other, showing that the predator–prey type of interaction between the tumor cells and the immune cells is converging to a Nash type of compromise. As a consequence, β is also allowed to decrease, but still preserving stability of the dormancy equilibrium in all three cases. Similarly, K_Z is increasing, at each step, back to the initial value, while R_T and R_Z were switched to initial values starting with σ_4.

For the initial system, for which the vector field plot is shown in Figure 3.6(b), it can be observed that for initial conditions corresponding to higher values of the state x_3, the trajectories of the system will converge to E_4^1 via the boundary of the positive orthant containing E_4^1. If the trajectories of $\dot{x} = f_1(x)$ reach this boundary before reaching the yellow set ($\mathcal{S}_2$), then they cannot be steered away from E_4^1. The same holds for $\dot{x} = f_2(x)$. Thus, convergence of the switched system cannot be guaranteed for initial conditions with a high or very low number of resting immune cells. However, this is not a limitation. Then an additional condition can be added to the switching law, i.e. to switch directly to the next set when the trajectory approaches a sufficiently small neighborhood of the (invariant) boundary of the positive orthant containing E_4^1, or E_4^2 in this case.

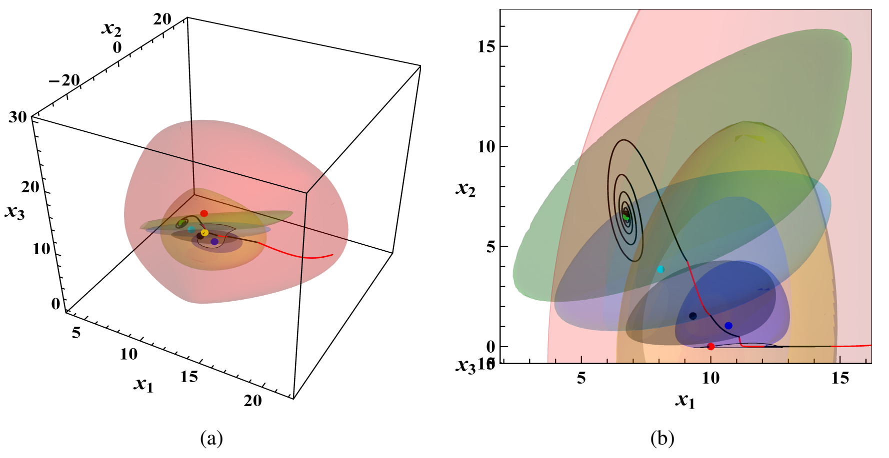

Figure 3.11: Sequence of the switching sets and equilibria of (3.3) together with a controlled trajectory–(a) and the left view–(b).

3.3.3.3 Discussion of results

If we consider the two models for which the switching control law was applied with the same purpose, to steer the tumor dynamics trajectories to tumor dormancy, for the case of the model proposed in [34], achieving dormancy was a much more difficult task. It required switching between all the system's parameters, not only the immunotherapy relevant ones as observed in the analysis part. This is due to increased complexity in the function describing the tumor dynamics. Once the number of hunting immune cells became nonzero in the equilibrium, steering the states to a "safer" dormancy equilibrium could not be achieved in one step, but by keeping K_T, R_T and R_Z at their initial values. Furthermore, in order to steer the states away from the stable invasive tumor equilibrium the tumor cells carrying capacity had to be slightly increased, while the resting immune cells carrying capacity had to be decreased. A possible explanation is that due to the increased value of β, there is an increase in the number of hunting cells which are converted from resting cells and for the environment to be able to sustain a larger population of hunting cells, the carrying capacity of the resting cells needed to be reduced. The fact that α_{NT}, which accounts for the effects of tumor cells on the immune cells was not decreased suddenly but in steps, is consistent with recent claims that aggressive forms of therapy aimed to completely eradicate tumor cells may act at making the tumor cells resistant to treatment. This will allow the ones that have survived the treatment to multiply faster and in an unbounded manner [42].

Furthermore, the proposed treatment strategy is clinically implementable due to the fact that the parameters of the system can be changed temporarily by external intervention by a medical doctor. For example, the immune system can be temporarily stimulated by drugs. Of course, the effect disappears over time but hopefully it will bring the state in the DOA of the target equilibrium. Nonetheless, since patient specific parameters need to be derived, estimating the parameters and measuring the states of the model might be difficult in real-life. In this sense, robustness may play a very important role to counteract uncertainty in the data.

3.4 Conclusions

In this chapter a new approach for tumor immunotherapy has been developed, by means of switching laws and rational LFs. The derived treatment plan, based on the studied models, is based on a switching control strategy defined on domains of attraction of equilibria of interest. Specifically, the problem of steering a stable invasive tumor to tumor dormancy has been investigated. This was addressed by means of a switching control law defined over successive parameterized DOAs which can steer trajectories initiated in the DOA of the invasive tumor equilibrium to the DOA of the tumor dormancy equilibrium, from which the solution converges autonomously to the desired equilibrium. The switching control law was illustrated on a model from the literature and on a new model from this thesis with the scope to illustrate the mechanism of resting immune cells to hunting ones when interacting with tumor cells.

The main contribution of this chapter is twofold. Firstly, to illustrate the benefits of Lyapunov based tools for analysis of tumor dynamics and secondly, to provide a formal mathematical framework for deriving the switching strategy for modifying not only the tumor dynamics, but also the steady state solutions, i.e. the set of equilibria (stable and unstable). This reasoning is in agreement with the new directions in cancer medical practice which focus on disrupting the interaction of tumor cells with their environment through a control–based approach [67]. By the proposed framework, information on the state at which the critical model parameters need to be altered is provided, and additionally, the outcome of the therapy is predicted. Certainly, in this work we dealt with one specific phase from tumor development. Nonetheless, the same procedure can be applied for example, when considering the post angiogenesis phase, when the critical parameter of interest is the carrying capacity of the tumor cells.

As for the theoretical tools used to design the control strategy, a similar switching strategy is applicable also to biological systems described by nonpolynomial models. This is an advantage with respect to the continuous polynomial feedback law developed in Chapter 2, since for nonpolynomial systems it would be based on approximations of the true dynamics. However, since the switching control law generates a DOA of the controlled system based on the union of the successive DOAs, in order to capture more states that can be steered to the desired equilibrium good DOA estimates are needed. If the RLFs are to be used to compute the DOA estimates for nonpolynomial systems, there is no guarantee that the resulting set estimates would be optimal, due to approximations. As such, a method to compute LFs that can deliver better estimates of the true DOA of a system (which is often unknown, in which case set estimates that capture more initial conditions, the better), also for nonpolynomial systems is needed. More specifically, tools for computing LFs irrespective of the nonlinearity type (as long as regularity conditions are satisfied) are required. This problem will be addressed in the next chapters.

Chapter 4

Computation of Lyapunov functions of Massera and Yoshizawa type

In this chapter we address the problem of computing LF's which can provide nonconservative DOA estimates for general nonlinear systems satisfying some regularity assumptions. As motivated in Chapter 1, in particular, the goal is to derive alternatives to the Massera/Yoshizawa LF converse results, which allow for computability and are applicable to general nonlinear systems. Consequently, the alternative converse LF formulations are related to the problem of relaxing the LF decrease condition. Therefore, we introduce two constructions which are enabled by imposing a finite–time criterion on the computed function, i.e. a finite time decrease condition. By means of this approach, we relax the assumptions of exponential stability on the system dynamics, while still allowing integration over a finite time interval. The resulting LF can be computed based on any $\mathcal{K}_\infty$–function of the norm of the solution of the system. In addition, we show how the developed converse theorem can be used to construct an estimate of the domain of attraction.

4.1 Introduction

The converse of Lyapunov's second method (or direct method) for general nonlinear systems is a topic of extensive ongoing research in the Lyapunov theory community. Work on the converse theorem started around the 1950s with the crucial result in [90], which states that if the origin of an autonomous differential equation is asymptotically stable, then the function defined by a semidefinite integral of an appropriately chosen function of the norm of the solution is a continuously differentiable LF. This construction, also known as the Massera construction, led to a significant amount of subsequent work, out of which we recall here [79]. It is well known that finding an explicit form of a LF for general nonlinear systems is a very difficult problem. One of the constructive results on answering the converse problem was introduced in [122]. Therein an analytic formula of a LF is provided, which approaches the value 1 on the boundary of the DOA of the considered system. Thus, simultaneously with constructing a LF, an estimate of the DOA is computed. This result, also known as the Zubov method is summarized in [60, Theorem 34.1] and [60, Theorem 51.1]. Stemming from Zubov's method, a recursive procedure for constructing a rational LF for nonlinear systems was proposed in [118]. This procedure has many computational advantages and it is directly applicable to polynomial systems, providing nonconservative DOA estimates (as illustrated in Chapter 2). An alternative construction (known as the Yoshizawa construction) to the one of Massera, was proposed in [121], where it was shown that the supremum of a function of the solutions of the system is a LF. Additionally, we refer to the books [78] and [80], and the survey [70].

As for more recent works, for the particular case of differential inclusions, a converse theorem for uniform global asymptotic stability of a compact set was provided in [87], and for the case of homogeneous systems it was shown in [97] that asymptotic stability implies the existence of a smooth homogeneous LF. Further converse results for differential inclusions for stability with two measures were provided in, for example, [115] and [76]. If control inputs are to be considered, an existence result of control LFs under the assumption of asymptotic controllability was derived in [104].

For what concerns computational, LF constructive methods, see the recent developments of the author of [57] and subsequent works, out of which we single out [12] and [15], where the Massera construction is exploited for generating piecewise affine LFs and [59] and [58] where the Yoshizawa construction is used. A more detailed historical survey on converse LF results can be found in the extensive paper [75].

Despite the comprehensive work on the topic of providing a converse to Lyapunov's theorem, the existing constructive approaches either rely on complex candidate LFs (rational, polynomial) or they involve state space partitions (for which scalability with the state space dimension is problematic), accompanied by correspondingly complex or large optimization problems. In turn, if we restrict strictly to analytical, Massera type of converse results, the construction in [77, Theorem 4.14], for example, involves integrating over a finite time interval, however with the assumption of exponential stability of the origin. A similar, relaxed construction was developed in [15], by using a Lipschitz, positive outside a neighborhood around the origin, (arbitrary) function of the state.

In this chapter, we develop a similar construction for the LF, by relaxing the exponential stability assumption to a richer type of $\mathcal{KL}$–stability property. This will allow a broader range of systems for which a LF can be computed. To enable a systematic, general computational approach, additionally, we allow for the LF to be generated by any $\mathcal{K}_\infty$ candidate function which satisfies a finite–time criterion. Nonetheless, this relaxation comes with a restriction on the $\mathcal{KL}$–stability condition indicated in the chapter by Assumption 4.1. Ultimately, the proposed solution makes use of an analytic relation between LFs and finite–time Lyapunov functions (FTLFs) to compute a LF. Thus, construction of LFs is brought down to verification that a candidate function is a FTLF, which is somewhat easier than identifying a candidate function for a true LF.

A similar finite–time criterion was introduced in [2] to provide a new asymptotic stability result for nonautonomous nonlinear differential equations. The discrete–time analog of this condition was first used in [45] to provide a converse Lyapunov theorem for nonlinear difference equations. The candidate LF therein is also of Massera type, but projected in discrete–time, thus defined by finite summation. Furthermore, for nonlinear discrete–time systems which are homogeneous, based on similar considerations, LF constructions which rely on vector norms were developed in [33].

The problem of relaxing the negative definite derivative requirement on the LF for stability analysis, based on three means is summarized in [71]. One mean is based on the

Krasovskii-LaSalle principle [77] which requires a LF with negative semidefinite derivative, or by allowing the LF to have positive definite derivatives in certain regions of the state space [72]. The second one is based on higher order derivatives of LF's. In [22], it is shown that a function with a higher order derivative which is negative definite implies stability, while in [4] it is shown that a linear combination of the function and its derivatives is a positive definite function with negative definite derivative. The downside of the above enumerated approaches is that they are not constructive towards nonconservative DOAs estimates; a positive definite candidate function needs to be somehow chosen. The third approach is the one used in this chapter, i.e. by means of a finite time decrease condition, or as it is called in [71], the "discretization approach", developed around the results in [2].

The approach in [2] has been further worked out and generalized in several directions in two results presented in [71]. Firstly, Proposition 2.3 offers an alternative to the periodic decrease condition in [2] (see also (4.7) in this chapter) by requiring the minimum over a finite time interval of a positive definite function of the state to decrease. Condition (2.2) in [71] always implies a decrease after a finite time interval, but it allows the length of the time interval to be state dependent. Proposition 2.3 of [71] shows that such a relaxed finite time decrease condition implies $\mathcal{KL}$-stability and exponential stability (under the usual global exponential stability assumptions plus a common time interval length for all states). The decrease condition (2.2) in [71] can be related to the Razumikhin decrease condition for time–delay systems, applied to a system without delays, which essentially requires a positive definite function to decrease compared to its maximum attained over a past finite time interval.

Secondly, another relevant result of [71] is presented in Remark 2.4, which provides a converse result for $\mathcal{KL}$–stable systems in terms of condition (2.2) in [71]. More precisely, therein it is proven that if the $\mathcal{KL}$–stability property holds, then any positive definite function satisfies inequality (2.2) in [71]. Compared to the converse results of [71], the converse theorem presented in this chapter shows that a stronger condition holds (inequality (4.7) with a common finite time d for all states $x(t)$) under Assumption 4.1 Interestingly, the proof of Remark 2.4 in [71] shows that Assumption 4.1 is naturally implied by $\mathcal{KL}$-stability and by the assumptions (H1)-(H3) therein (on compacts sets excluding the origin) when $d = d(x(t))$ is allowed to be state dependent.

From a technical point of view, the proofs of the corresponding results in this chapter (i.e., corresponding to Proposition 2.3 and Remark 2.4 in [71]) follow a different path, which exploits the existence of a d–invariant set, and yields simpler, more intuitive proofs and verifiable conditions that lead to constructive algorithms for computing LFs and estimating DOAs. It is also worth to point out that a direct relation between FTLFs and true LFs has not been established in [71].

We proceed by (re)introducing some concepts and results that will be subsidiary.

4.1.1 Preliminaries

Consider again autonomous continuous–time systems described by

$$\dot{x} = f(x), \tag{4.1}$$

where $f : \mathbb{R}^n \to \mathbb{R}^n$, is a locally Lipschitz function.

Remark 4.1 (Solution notation.) Let the solution of (4.1) at time $t \in \mathbb{R}_{\geq 0}$ with initial value $x(0)$ be denoted by $\phi(t, x(0))$, where $\phi : \mathbb{R}_{\geq 0} \times \mathbb{R}^n \rightarrow \mathbb{R}^n$. We assume that $\phi(t, x(0))$ exists and it is unique for all $t \in \mathbb{R}_{\geq 0}$ (see [77, Chapter 3] for sufficient smoothness conditions on f). The locally Lipschitz assumption on $f(x)$ implies that $\phi(t, x(0))$ is a continuous function of $x(0)$ [60, Chapter III]. Furthermore, the origin is an equilibrium point, i.e. $f(0) = 0$.

In what follows, for simplicity, unless stated otherwise, we will use the notation $x(t) := \phi(t, x(0))$ with the following interpretations:

- if $x(t)$ is the argument of $\dot{W}(x(t))$, then $x(t)$ represents the solution of the system as defined by $\phi(t, x(0))$;
- if $x(t)$ is the argument of $V(x(t))$ as in (4.7) and (4.8), for example, then $x(t)$ represents a point on the solution $\phi(t, x(0))$ for a fixed value of t; the same interpretation holds for $W(x(t))$; in other words we do not consider time-varying functions V or W.

Recall the definitions of AS from Definition 2.1 and of $\mathcal{KL}$–stability from Definition 2.2. In the remainder of this chapter we will use *$\mathcal{KL}$–stability* to refer to $\mathcal{KL}$–stability in $\mathcal{S}$ or, equivalently to AS, as defined above. When $\mathcal{S} = \mathbb{R}^n$, then we use the term global $\mathcal{KL}$–stability. Next we redefine the concept of LFs in an equivalent manner as in Definition 2.5.

Definition 4.1 A continuously differentiable function $W : \mathbb{R}^n \rightarrow \mathbb{R}_{\geq 0}$, for which there exist $\alpha_1, \alpha_2 \in \mathcal{K}_\infty$ and a $\mathcal{K}$ function $\rho : \mathbb{R}_{\geq 0} \rightarrow \mathbb{R}_{\geq 0}$ such that

$$\begin{aligned} \alpha_1(\|x\|) \leq W(x) &\leq \alpha_2(\|x\|), \quad \forall x \in \mathbb{R}^n && (4.2)\\ \dot{W}(x) &\leq -\rho(\|x\|), \quad \forall x \in \mathcal{S}, && (4.3) \end{aligned}$$

with $\mathcal{S} \subseteq \mathbb{R}^n$ proper, is called a Lyapunov function in $\mathcal{S}$ for the system (4.1). If $\mathcal{S} = \mathbb{R}^n$, then W is called a global LF.

The following concept is a relaxation of the classical concept of invariance as defined in Definition 2.4.

Definition 4.2 Given a positive, real scalar d, the proper set $\mathcal{S} \subseteq \mathbb{R}^n$ is called a d–invariant set for the system (4.1) if for any $t \in \mathbb{R}_{\geq 0}$, if $x(t) \in \mathcal{S}$, then it holds that $x(t+d) \in \mathcal{S}$.

Note that the d–invariance property does not imply that $x(t) \in \mathcal{S}$ for all $x(t) \in \mathcal{S}$ if $x(0) \in \mathcal{S}$.

We recall below Sontag's lemma on $\mathcal{KL}$–estimates [108, Proposition 7], as it will be instrumental.

Lemma 4.1 For each class $\mathcal{KL}$–function β and each number $\lambda \in \mathbb{R}_{\geq 0}$, there exist $\varphi_1, \varphi_2 \in \mathcal{K}_\infty$, such that $\varphi_1(s)$ is locally Lipschitz and

$$\varphi_1(\beta(s,t)) \leq \varphi_2(s)e^{-\lambda t}, \quad \forall s, t \in \mathbb{R}_{\geq 0}. \tag{4.4}$$

The following result was introduced in [60, Definition 24.3] to relate positive definite functions and $\mathcal{K}$–functions. A proof of this result was indicated in the Introduction of [74], however without providing a lower bound construction. In what follows we shall indicate results from $\mathcal{K}$–continuity characterizations which provide upper and lower bounds for a given continuous, positive definite function in terms of $\mathcal{K}$–functions. We recall the proof arguments, for completeness.

Lemma 4.2 Consider a function $W : \mathbb{R}^n \to \mathbb{R}_{\geq 0}$ with $W(0) = 0$.

1. If $W(x)$ is continuous and positive definite in some neighborhood around the origin, $\mathcal{N}(0)$, then there exist two functions $\hat{\alpha}_1, \hat{\alpha}_2 \in \mathcal{K}$ such that

$$\hat{\alpha}_1(\|x\|) \leq W(x) \leq \hat{\alpha}_2(\|x\|), \quad \forall x \in \mathcal{N}(0). \tag{4.5}$$

2. If $W(x)$ is continuous and positive definite in $\mathbb{R}^n$ and additionally, $W(x) \to \infty$, when $x \to \infty$ then (4.5) holds with $\hat{\alpha}_1, \hat{\alpha}_2 \in \mathcal{K}_\infty$ and for all $x \in \mathbb{R}^n$.

Proof: 1. For any $x \in \mathcal{N}(0)$, with $\mathcal{N}(0)$ sufficiently small, there exist r_1 and r_2 such that for $0 \leq r_1 \leq \|x\| \leq r_2$ and

$$W_u(\|x\|) := \max_{\xi} W(\xi)$$
$$\text{subject to } r_1 \leq \|\xi\| \leq \|x\|,$$

and

$$W_l(\|x\|) := \min_{\xi} W(\xi)$$
$$\text{subject to } \|x\| \leq \|\xi\| \leq r_2,$$

it holds that (by continuity of W)

$$W_l(\|x\|) \leq W(x) \leq W_u(\|x\|).$$

Additionally, $W_u(\cdot)$ and $W_l(\cdot)$ above are non–decreasing and continuous and $W_u(0) = W_l(0) = 0$. $W_u(\|x\|)$ and $W_l(\|x\|)$ can be upper and lower bounded, respectively, by $\mathcal{K}$–functions constructed as in [119, Lemma I] or in [39, Lemma A.2].

2. Since $W(x)$ is continuous and positive definite in $\mathbb{R}^n$ with $W(x) \to \infty$, by the same arguments as above, $\mathcal{K}_\infty$ functions can be constructed such that (4.5) holds.

■

Another instrumental result for this chapter is the Bellman–Gronwall Lemma. A proof is provided in [109, Lemma C. 3.1].

Lemma 4.3 Assume given an interval $\mathcal{I} \subseteq \mathbb{R}$, a constant $c \in \mathbb{R}_{\geq 0}$, and two functions $\alpha, \mu : \mathcal{I} \to \mathbb{R}_{\geq 0}$, such that α is locally integrable and μ is continuous. Suppose further that for some $\sigma \in \mathcal{I}$ it holds that

$$\mu(t) \leq \nu(t) := c + \int_\sigma^t \alpha(\tau)\mu(\tau)\mathrm{d}\tau$$

for all $t \geq \sigma$, $t \in \mathcal{I}$. Then it must hold that

$$\mu(t) \leq c e^{\int_\sigma^t \alpha(\tau)\mathrm{d}\tau}.$$

It is well known, from the direct method of Lyapunov, that the existence of a Lyapunov function for the system (4.1) implies that the origin is an AS equilibrium for (4.1). In the remainder of this chapter we propose some new alternatives to classical Lyapunov converse results, which are verifiable and constructive towards obtaining nonconservative DOA estimates. By nonconservative we mean set estimates of the DOA which manage to capture a larger region of the state space, as compared to existing results from literature, or, in the case of bistability, which get infinitesimally close to the stability boundary or separatrix [29].

4.2 A constructive Lyapunov converse theorem

4.2.1 Finite–time conditions

Let there be a continuous function $V : \mathbb{R}^n \to \mathbb{R}_{\geq 0}$, and a real scalar $d > 0$ for which the proper set $\mathcal{S} \subseteq \mathbb{R}^n$ is d–invariant and the conditions

$$\begin{aligned} \alpha_1(\|x\|) \leq V(x) &\leq \alpha_2(\|x\|), \quad \forall x \in \mathbb{R}^n, &(4.6)\\ V(x(t+d)) - V(x(t)) &\leq -\gamma(\|x(t)\|), \quad \forall t \geq 0, &(4.7)\end{aligned}$$

are satisfied with $\alpha_1, \alpha_2 \in \mathcal{K}_\infty$, and $\gamma \in \mathcal{K}$ and for all $x(t)$, with $x(0) \in \mathcal{S}$.

The function V which satisfies (4.6) and (4.7) is called a *finite–time Lyapunov function* (FTLF) in $\mathcal{S}$ for the system (4.1). If $\mathcal{S} = \mathbb{R}^n$, then V is a global FTLF.

In order for condition (4.7) to be well–defined, additionally to the locally Lipschitz property of the map $f(x)$, it is assumed that there exists no finite escape time in each interval $[t, t+d]$, for all $t \in \mathbb{R}_{\geq 0}$. However, as it will be shown later, it is sufficient to require that there is no finite escape time in the time interval $[0, d]$.

When $\mathcal{S} = \mathbb{R}^n$, a sufficient condition for existence of the solution for all $t \in \mathbb{R}_{\geq 0}$ (additional to continuity of f) is that the map $f(x)$ is Lipschitz bounded [60, Chapter III.16]. Furthermore, note that existence of a finite escape time for initial conditions in a given set in $\mathbb{R}^n$ implies that the origin is unstable in that set [60, Chapter III.16].

The following result relates inequality (4.7) with another known type of decrease condition, which will be instrumental.

Lemma 4.4 The decrease condition (4.7) on V is equivalent with

$$V(x(t+d)) - \rho(V(x(t))) \leq 0, \quad \forall t \in \mathbb{R}_{\geq 0}, \tag{4.8}$$

for all $x(t)$ with $x(0) \in \mathcal{S}$, where $\rho < \mathrm{id}$ for nonzero arguments, $\rho(0) = 0$ is a positive definite, continuous function.

Proof: The proof follows a similar reasoning as in [44, Remark 2.5]. Assume that V is such that (4.6) and (4.7) hold. Then, for all $x(t) \neq 0$:

$$\begin{aligned} 0 \leq V(x(t+d)) &\leq V(x(t)) - \gamma(\|x(t)\|) \\ &< V(x(t)) - 0.5\gamma(\|x(t)\|) \\ &\leq V(x(t)) - 0.5\gamma(\alpha_2^{-1}(V(x(t))) \\ &= (\mathrm{id} - 0.5\gamma \circ \alpha_2^{-1})(V(x(t)) \\ &=: \rho(V(x(t)). \end{aligned} \tag{4.9}$$

Similarly, for all $x(t) \neq 0$,

$$\begin{aligned} 0 \leq V(x(t+d)) &\leq V(x(t)) - \gamma(\|x(t)\|) \\ &< \alpha_2(\|x(t)\|) - 0.5\gamma(\|x(t)\|) \\ &= (\alpha_2 - 0.5\gamma)(\|x(t)\|), \end{aligned}$$

which implies that $(\alpha_2 - 0.5\gamma)(s) > 0$, for all $s \neq 0$. Furthermore, since $\alpha_2^{-1} \in \mathcal{K}_\infty$, then $(\alpha_2 - 0.5\gamma) \circ \alpha_2^{-1}(s) > 0$ and

$$0 < (\mathrm{id} - 0.5\gamma \circ \alpha_2^{-1})(s) < \mathrm{id}, \quad \forall s \neq 0.$$

Thus, by construction, the function $\rho : \mathbb{R}_{\geq 0} \to \mathbb{R}_{\geq 0}$ is a continuous, positive definite function. All involved functions are continuous by definition, thus the difference remains continuous. When $x(t) = 0$, then (4.8) trivially holds, since $\rho(0) = 0$.

Now assume that (4.8) holds. Then

$$\begin{aligned} V(x(t+d)) - V(x(t)) &\leq \rho(V(x(t))) - V(x(t)) \\ &= -(V(x(t)) + \rho(V(x(t))) \\ &= -((\mathrm{id} - \rho)(V(x(t)))) \\ &\leq -((\mathrm{id} - \rho)(\alpha_1(\|x(t)\|)) \\ &= -\tilde{\gamma}(\|x(t)\|), \end{aligned}$$

with $\tilde{\gamma} = (\mathrm{id} - \rho) \circ \alpha_1$. Since $\rho < \mathrm{id}$ by assumption, then $\tilde{\gamma}$ is positive definite, and furthermore continuous. Thus, by Lemma 4.2 $\tilde{\gamma}$ can be lower bounded by a $\mathcal{K}$–function $\gamma(\|x(t)\|)$, hence $V(x(t+d)) - V(x(t)) \leq -\gamma(\|x(t)\|), \quad \gamma \in \mathcal{K}$.

Next, we propose a version of [2, Theorem 1] for the time–invariant case and with the additional assumption that the set $\mathcal{S}$ is a d–invariant set for (4.1). This additional assumption enables a simpler proof, while the result is stronger, i.e., $\mathcal{KL}$–stability in $\mathcal{S}$ is attained as opposed to local (in some neighborhood around the origin) $\mathcal{KL}$–stability.

Theorem 4.1 If a function V defined as in (4.6) and (4.7) and a proper and compact d-invariant set $\mathcal{S}$ exist for the system (4.1), then the origin equilibrium of (4.1) is $\mathcal{KL}$–stable in $\mathcal{S}$.

Proof: For any $t \in \mathbb{R}_{\geq 0}$, there exists an integer $N \geq 0$ and $j \in \mathbb{R}_{\geq 0}$, $j < d$ such that $t = Nd + j$. By applying (4.7) in its equivalent form (4.8) recursively, we get that

$$\begin{aligned}
V(x(t)) &= V(x(Nd + j)) \\
&= V(x(((N-1)d + j) + d)) \\
&\leq \rho(V(x((N-1)d + j))) \\
&= \rho(V(x(((N-2)d + j) + d))) \\
&\leq \rho^2(V(x((N-2)d + j))) \\
&\dots \\
&\leq \rho^N(V(x(j))) \\
&\leq \rho^N(\alpha_2(\|x(j)\|)),
\end{aligned} \tag{4.10}$$

where ρ^N denotes the N–times composition of ρ. The solution at time $t = j$ is given by

$$x(j) = x(0) + \int_0^j f(x(s))\mathrm{d}s,$$

for any $j \geq 0$. Then,

$$\begin{aligned}
\|x(j) - x(0)\| &\leq \int_0^j \|f(x(s)) - f(x(0)) + f(x(0))\|\mathrm{d}s \\
&\leq \int_0^j \|f(x(s)) - f(x(0))\|\mathrm{d}s + \int_0^j \|f(x(0))\|\mathrm{d}s.
\end{aligned}$$

By using the local Lipschitz continuity property of f, with $L > 0$ the Lipschitz constant, and the Lemma 4.3 we obtain that

$$\begin{aligned}
\|x(j) - x(0)\| &\leq \int_0^j L\|x(s) - x(0)\|\mathrm{d}s + \int_0^j \|f(x(0))\|\mathrm{d}s \\
&\leq \left(\int_0^j \|f(x(0))\|\mathrm{d}s\right) e^{Lj}.
\end{aligned}$$

Thus,

$$\|x(j)\| \leq \|x(0)\| + \left(\int_0^j \|f(x(0))\|\mathrm{d}s\right) e^{Lj} =: F_j(\|x(0)\|).$$

Then $F_j(\|x(0)\|) \leq F_d(\|x(0)\|)$, for all $j \in [0, d]$. By the standing assumptions on f it results that $F_d(\|x(0)\|)$ is continuous with respect to $x(0)$. Furthermore, $F_d(0) = 0$ and $F_d(s)$ is positive definite and continuous and $F_d(s) \to \infty$, when $s \to \infty$, for any $s \geq 0$. By applying Lemma 4.2 to $F_d(\|x(0)\|)$ we obtain that there exists a function $\omega \in \mathcal{K}_\infty$ such that $F_d(\|x(0)\|) \leq \omega(\|x(0)\|)$, and consequently, $\|x(j)\| \leq \omega(\|x(0)\|)$, for all $0 \leq j < d$.

Thus, with $\hat{\alpha}_2 := \alpha_2 \circ \omega$ we get that

$$\begin{aligned} V(x(t)) &\leq \rho^N(\hat{\alpha}_2(\|x(0)\|)) = \rho^{\frac{t-j}{d}}(\hat{\alpha}_2(\|x(0)\|)) \\ &\leq \rho^{\lfloor \frac{t}{d} \rfloor - 1} \circ \hat{\alpha}_2(\|x(0)\|) \\ &= \rho^{\lfloor \frac{t}{d} \rfloor} \circ \rho^{-1} \circ \hat{\alpha}_2(\|x(0)\|) \\ &\leq \rho^{\lfloor \frac{t}{d} \rfloor} \circ \hat{\rho} \circ \hat{\alpha}_2(\|x(0)\|) =: \hat{\beta}(\|x(0)\|, t), \quad \hat{\rho} \in \mathcal{K}_\infty. \end{aligned}$$

Without loss of generality we can assume that ρ is a one–to–one (injective) and onto (surjective) function, thus invertible. Furthermore, since ρ is continuous, then by [20, Theorem 3.16], ρ^{-1} is continuous. Additionally, $\rho^{-1}(0) = \rho^{-1}(\rho(0)) = 0$. Thus, there exists a function $\hat{\rho} \in \mathcal{K}_\infty$, such that $\rho^{-1} \leq \hat{\rho}$, as follows from Lemma 4.2. We can conclude that $\hat{\beta} \in \mathcal{KL}$ since $\hat{\rho} \circ \hat{\alpha}_2(s) \in \mathcal{K}_\infty$ and $\rho^{\lfloor \frac{t}{d} \rfloor} \in \mathcal{L}$.

Finally,

$$\|x(t)\| \leq \alpha_1^{-1}(\hat{\beta}(\|x(0)\|, t)) =: \beta(\|x(0)\|, t),$$

for all $x(0) \in \mathcal{S}$ and for all $t \in \mathbb{R}_{\geq 0}$, thus we have obtained $\mathcal{KL}$–stability in $\mathcal{S}$.

We proceed by providing a converse finite–time Lyapunov function for $\mathcal{KL}$–stability in a compact set $\mathcal{S}$.

4.2.2 Alternative converse theorem

Assumption 4.1 There exists a pair $(\beta(\cdot, \cdot), d) \in \mathcal{KL} \times \mathbb{R}_{>0}$ with β satisfying (2.3) for the system (4.1) such that

$$\beta(s, d) < s \tag{4.11}$$

for all $s > 0$.

Theorem 4.2 If the origin is $\mathcal{KL}$–stable in some invariant subset of $\mathbb{R}^n$, $\mathcal{S}$[1] for the system (4.1) and Assumption 4.1 is satisfied, then for any function $\eta \in \mathcal{K}_\infty$ and for any norm $\|\cdot\|$, the function $V : \mathbb{R}^n \to \mathbb{R}_{\geq 0}$, with

$$V(x) := \eta(\|x\|), \quad \forall x \in \mathbb{R}^n \tag{4.12}$$

satisfies (4.6) and (4.7).

Proof: Let the pair (β, d) be such that Assumption 4.1 holds. Then, by hypothesis

$$\begin{aligned} \eta(\|x(t+d)\|) &\leq \eta(\beta(\|x(t)\|, d)) \\ &\leq \eta(\beta(\eta^{-1}(V(x(t))), d)) \\ &:= \rho(V(x(t))), \end{aligned}$$

where $\rho = \eta(\beta(\eta^{-1}(\cdot), d))$, for all initial conditions $x(0) \in \mathcal{S}$. By Assumption 4.1, we obtain that there exists a $d > 0$ such that $\rho < \eta(\eta^{-1}(\cdot)) = \mathrm{id}$, Thus, we get

$$V(x(t+d)) - \rho(V(x(t))) \leq 0, \quad \forall x(0) \in \mathcal{S}.$$

[1] Invariance is needed in order for (4.8) to hold for all $t \geq 0$.

From Lemma 4.4 this implies that (4.7) holds. Since V is defined by a $\mathcal{K}_\infty$ function, then let $\alpha_1(s) = \alpha_2(s) = \eta(s)$ such that (4.6) holds. ■

A similar converse theorem was provided in Remark 2.4 in [71]. Therein it was proven that when it is allowed that $d = d(x(t))$ to be state dependent, then Assumption 4.1 is implied by $\mathcal{KL}$-stability (and assumptions (H1)-(H3) in [71]) on compact sets excluding the origin and, a less conservative property than (4.7) (property (2.2) in [71]) holds for any candidate positive definite function V.

Consider the next function defined as

$$W(x(t)) := \int_t^{t+d} V(x(\tau))\mathrm{d}\tau, \tag{4.13}$$

for any V for which there exists a $d > 0$ such that (4.6) and (4.7) are satisfied.

Generally, in standard converse theorems the function φ_1 which defines the LF is a particular, special $\mathcal{K}_\infty$ function. In the finite–time converse theorem, η is any $\mathcal{K}_\infty$ function, which allows for more freedom in the construction. In turn, the developed finite–time converse theorem will be used to obtain an alternative converse Lyapunov theorem.

Lemma 4.5 There exists a V satisfying (4.6) and (4.7) for (4.1) and some $d > 0$, if and only if the function W as defined in (4.13) with the same $d > 0$ is a Lyapunov function in $\mathcal{S}$ for the system (4.1).

Proof: Let there be a function V satisfying (4.6) and (4.7). V is continuous, thus it is integrable over any closed, bounded interval $[t, t + d]$, $t \geq 0$. By Theorem 5.30 in [20], this implies that $W(x(t))$ is continuous on each interval $[t, t+d]$, for any t. Since V is also positive definite, by integrating over the bounded interval $[t, t + d]$ the resulting function $W(x(t))$ will also be positive definite. Since $W(x(t))$ is continuous and positive definite the result in Lemma 4.2 can be applied. Therefore, there exist two functions $\hat{\alpha}_1, \hat{\alpha}_2 \in \mathcal{K}_\infty$ such that

$$\hat{\alpha}_1(\|x\|) \leq W(x) \leq \hat{\alpha}_2(\|x\|), \quad \forall x \in \mathbb{R}^n, \tag{4.14}$$

holds. Next, by making use of the general Leibniz integral rule, we get that

$$\begin{aligned}\frac{\mathrm{d}}{\mathrm{d}t}W(x(t)) = &\int_t^{t+d} \underbrace{\frac{\mathrm{d}}{\mathrm{d}t}V(x(\tau))}_{=0}\,\mathrm{d}\tau + V(x(t+d))(\dot{\overline{t+d}}) - V(x(t))\dot{t} \\ =&V(x(t+d)) - V(x(t)) \leq -\gamma(\|x(t)\|).\end{aligned}$$

Thus, W is a Lyapunov function for (4.1).

Now assume that W is a Lyapunov function for (4.1), i.e. (4.14) holds and for $\gamma \in \mathcal{K}$ it holds that

$$\dot{W}(x) \leq -\gamma(\|x\|), \quad \forall x \in \mathcal{S}.$$

By the same Leibniz rule, we know that $\dot{W}(x(t)) = V(x(t + d)) - V(x(t))$, thus the difference $V(x(t + d)) - V(x(t))$ is negative definite, i.e. (4.7) holds. Now we have to show that (4.6) holds.

Assume that there exists an $x(t) \in \mathcal{S}$, $x(t) \neq 0$, such that $V(x(t)) \leq 0$. Then, this implies that

$$V(x(t+d)) < V(x(t) \leq 0,$$

and furthermore,

$$V(x(t+id)) < V(x(t+(i-1)d)) < \ldots < V(x(t+2d)) < V(x(t+d)) < V(x(t)) \leq 0,$$

for all integers $i > 0$, due to d-invariance of $\mathcal{S}$ and the assumption that $x(t) \in \mathcal{S}$. Then,

$$\lim_{i\to\infty} V(x(t+id)) = -\infty.$$

Since W is a LF for (4.1) in $\mathcal{S}$, then the origin is $\mathcal{KL}$–stable in $\mathcal{S}$, thus it implies that $\lim_{i\to\infty} x(t+id) = 0$. Then, because the solution of the system (4.1) is a continuous function of time and W is continuous, it follows that $\lim_{i\to\infty} W(x(t+id)) = W(0)$. Therefore, we have that

$$\lim_{i\to\infty} W(x(t+id)) = \lim_{i\to\infty} \int_{t+id}^{t+(i+1)d} V(x(\tau))\mathrm{d}\tau$$
$$\Leftrightarrow$$
$$W(0) = \int_{\infty}^{\infty} V(x(\tau))\mathrm{d}\tau = V(x(\infty)) = -\infty,$$

which is a contradiction since $W(0) = 0$, thus $V(x)$ must be positive definite on $\mathcal{S}$. By the definition of W, we have that V must be a continuous function, because it needs to be integrable for W to exist. By assumption, W is upper and lower bounded by $\mathcal{K}_\infty$ functions, thus for $x \to \infty$, $W(x) \to \infty$. This can only happen when $V(x) \to \infty$. Thus, using a similar reasoning as above, based on Lemma 4.2, this implies that V is upper and lower bounded by $\mathcal{K}_\infty$ functions, hence (4.6) holds in $\mathcal{S}$. ■

The next result summarizes the proposed alternative converse LF for $\mathcal{KL}$–stability in $\mathcal{S}$, enabled by the finite–time conditions (4.6) and (4.7).

Corollary 4.1 If the zero equilibrium of the system (4.1) is $\mathcal{KL}$–stable in some set $\mathcal{S}$ with the $\mathcal{KL}$–function β satisfying Assumption 4.1 for some $d > 0$, then by Theorem 4.2 and Lemma 4.5 for any function $\eta \in \mathcal{K}_\infty$ and any norm $\|\cdot\|$, the function $W(\cdot)$ defined as in (4.13) for the same $d > 0$, is a Lyapunov function for the system (4.1).

The above corollary provides a continuous–time counterpart of the converse result [45, Corollary 22]. The main line of reasoning relies on the Assumption 4.1, which is the same assumption needed for the discrete–time converse theorem. The main technical differences with [45] lie in the proofs of Theorem 4.1, the construction (4.13) and the proof of Lemma 4.5.

4.2.3 Remarks Massera construction

Notice that the function (4.13) with $V(x) = \eta(\|x\|)$ corresponds to a Massera type of construction, which in its original form is given by [90]

$$W(x(t)) = \int_t^\infty \alpha(\|x(\tau)\|)\mathrm{d}\tau, \tag{4.15}$$

with $\alpha : \mathbb{R}_{\geq 0} \to \mathbb{R}_{\geq 0}$ an appropriately chosen continuous function. In [12] the construction above is recalled as

$$W(x(0)) = \int_0^N \|x(\tau)\|_2\mathrm{d}\tau, \tag{4.16}$$

as an alternative to the construction in [77, Theorem 4.14], where the limits of the integral are t and $t+N$. This type of construction facilitated an extensive amount of converse results. Also, the converse proof in [90] set up a proof technique which is based on the so–called Massera's Lemma [90, p. 716] for constructing the function α in (4.15).

The formulation in [12] is based on the exponential stability assumption, though an extension for the asymptotic stability case is suggested. The extension relates to the construction in (4.13), where instead of the function η, a nonlinear scaling of the norm of the state trajectory is used. This scaling function is obtained from a $\mathcal{KL}$ estimate and Lemma 4.1 to provide an exponentially decreasing in time upper bound for the asymptotic stability estimate. In [15], a similar construction to the one in (4.13) is proposed, namely

$$W(x(0)) = \int_0^T \gamma(x(\tau))\mathrm{d}\tau, \tag{4.17}$$

with T a positive, finite constant and γ a positive definite function. While both the proposed construction and the one in (4.17) rely on arbitrary functions of the state, the main difference is in the choice of the integration interval, with d being such that (4.7) holds for the arbitrary η function.

By using the finite–time function V, we provide an alternative to Massera's construction via Corollary 4.1, whilst by defining W as in (4.13) we allow for a $\mathcal{KL}$–stability assumption with the $\mathcal{KL}$ function satisfying (4.11). The freedom in choosing any function of the state norm $\eta \in \mathcal{K}_\infty$ in the proposed construction facilitates an implementable verification procedure which is detailed in Section 4.4 and does not rely on a specific, possibly more complex form, which can add to the computational load, for a LF.

4.3 Expansion scheme

In [28] a scheme for constructing LFs starting from a given LF, which at every iterate provides a less conservative estimate of the DOA of a nonlinear system of the type (4.1) was proposed. The sequence of Lyapunov functions of the type

$$\begin{aligned} W_1(x) &= W(x + \alpha_1 f(x)) \\ W_2(x) &= W_1(x + \alpha_2 f(x)) \\ &\vdots \\ W_n(x) &= W_{n-1}(x + \alpha_n f(x)), \end{aligned} \tag{4.18}$$

with $\alpha_i \in \mathbb{R}_{\geq 0}$, $i = 1, 2 \ldots, n$ leads to the DOA estimates set inclusion

$$\mathcal{S}_W(c) \subset \mathcal{S}_{W_1}(c) \subset \ldots \subset \mathcal{S}_{W_n}(c),$$

where $\mathcal{S}_{W_i}(c) := \{x \in \mathbb{R}^n \,|\, W_i(x) \leq c\}$, $i = 1, 2 \ldots, n$ denote the largest level sets of the Lyapunov functions generated by the expansion sequence (4.18) with $\mathcal{S}_W(c) \subset \mathcal{S}$, where $\mathcal{S}$ is a d–invariant set. Note that the largest level set of the LF W, included in the d–invariant set $\mathcal{S}$ is a subset of the true DOA of the system (4.1). Thus, the expansion scheme (4.18) applied on a computed W will provide a better estimate of the true shape of the DOA contained in $\mathcal{S}$. However, a less conservative initial set $\mathcal{S}$ leads to a better estimate of the true DOA.

We propose to utilize the expansion idea in [28] to generate a sequence of FTLFs, with the purpose to generate a relevant d–invariant set. The next result follows as a consequence of Lemmas 4-1 and 4-2 from [28].

Corollary 4.2 Let V be a FTLF, i.e. conditions (4.6) and (4.7) hold with respect to the d–invariant set $\mathcal{S}$. Let

$$\mathcal{S}_V(c) := \{x \in \mathbb{R}^n \,|\, V(x) \leq c\} \subset \mathcal{S}.$$

Then, there exists an $\alpha \in \mathbb{R}_{\geq 0}$ such that for $V_1(x) = V(x + \alpha f(x))$ and $\mathcal{S}_{V_1}(c) := \{x \in \mathbb{R}^n \,|\, V_1(x) \leq c\}$, it holds that $\mathcal{S}_V(c) \subset \mathcal{S}_{V_1}(c)$ and $V(x + \alpha f(x))$ is a FTLF.

Proof: By hypothesis, $V(x)$ is a FTLF, thus it is assumed to be continuously differentiable, i.e. let V have continuous partial derivatives of order r higher or equal to 1. Then by [31, p.190] and [28, Lemma 2-1] we can write:

$$V_1(x(t)) = V(x(t)) + \alpha\dot{V}(x(t)) + \frac{\alpha^2}{2!}\ddot{V}(x(t)) + \ldots \frac{\alpha^{r-1}}{(r-1)!}V^{(r-1)}(x(t)) + \frac{\alpha^r}{r!}V^r(z(t)),$$

where V^r denotes the r-th derivative of V, i.e. $V^{(r)}(x) = \nabla^{(r-1)}V(x)^\top f(x)$ and $z(t) = x(t) + h\alpha f(x(t))$, for $h \in [0, 1]$.

Let $V(x(t)) = (V \circ x)(t) = \psi(t)$. Similarly, by the formula [31, p.190, (8.14.3)], we have that

$$\psi(t + d) = \psi(t) + d\dot{\psi}(t) + \frac{d^2}{2!}\ddot{\psi}(t) + \ldots \frac{d^{r-1}}{(r-1)!}\psi^{(r-1)}(t) + \frac{d^r}{r!}\psi^r(w),$$

where $w = t + hd$, $h \in [0, 1]$ and $\dot{\psi}(t) = \dot{V}(x(t)) = \nabla V(x)f(x)$. Then,

$$\begin{aligned} V(x(t + d)) =& V(x(t)) + d\dot{V}(x(t)) + \frac{d^2}{2!}\ddot{V}(x(t)) + \ldots + \frac{\alpha^{r-1}}{(r-1)!}V^{(r-1)}(x(t)) + \\ & \frac{\alpha^r}{r!}V^r(x(w)). \end{aligned}$$

From the expressions of $V_1(x(t))$ and $V(x(t+d))$, we can write

$$\begin{aligned}V_1(x(t)) \leq & V(x(t)) + V(x(t+d)) - V(x(t)) + |\alpha - d|\dot{V}(x(t)) + \frac{|\alpha^2 - d^2|}{2!}\ddot{V}(x(t)) + \\ & \ldots + \frac{|\alpha^{r-1} - d^{r-1}|}{(r-1)!}V^{(r-1)}(x(t)) + \left|\frac{\alpha^r}{r!}V^r(z(t)) - \frac{\alpha^r}{r!}V^r(x(w))\right| \\ \leq & V(x(t)) + V(x(t+d)) - V(x(t)) + |\alpha - d|\dot{V}(x(t)) + |\alpha - d|\epsilon.\end{aligned} \tag{4.19}$$

Since $V(x(t+d)) - V(x(t)) < 0$, there exists a $\beta \in \mathbb{R}_{>0}$ such that $V(x(t+d)) - V(x(t)) < -\beta$, for all $x(0) \in \mathcal{S} \setminus \mathcal{S}_V(c)$, where $\mathcal{S} \setminus \mathcal{S}_V(c)$ is a compact set containing no equilibrium point. Furthermore, on the compact set $\mathcal{S} \setminus \mathcal{S}_V(c)$, $\epsilon > 0$ is a bound on the sum of higher order continuous terms in the above expression. This is due to the fact that continuous functions are bounded on compact sets. As such, we obtain that

$$V_1(x(t)) < V(x(t)) - \beta + |\alpha - d|(\dot{V}(x(t)) + \epsilon)$$

Let $|\alpha - d| < \bar{\alpha}$ and let $\dot{V}(x(t)) + \epsilon \leq \nu$, $\nu \in \mathbb{R}_{>0}$ for all $x \in \mathcal{S} \setminus \mathcal{S}_V(c)$ since every continuous function is bounded on a compact set. Thus, we obtain that

$$V_1(x(t)) < V(x(t)) + \bar{\alpha}\nu - \beta.$$

If $(\bar{\alpha}\nu - \beta) < 0$, hence for $0 < |\alpha - d| < \beta/\nu$, it holds that

$$V_1(x(t)) < V(x(t)).$$

Similarly as in [28, Lemma 4-1], this implies that $\mathcal{S}_V(c) \subset \mathcal{S}_{V_1}(c)$.

Next we will show that V_1 is a FTLF. From Lemma 4.5 we know that the function $W(x(t)) = \int_t^{t+d} V(x(\tau))\mathrm{d}\tau$ is a LF for (4.1). From [28, Lemma 4-2] it is known that there exists some $\alpha > 0$ such that

$$W_1(x(t)) = W(x(t)) + \alpha f(x(t))) = \int_t^{t+d} V(x(\tau) + \alpha f(x(\tau)))\mathrm{d}\tau$$

is a LF. This implies that there exists some $\mathcal{K}$–function $\tilde{\gamma}(x(t))$ such that

$$\dot{W}_1(x(t)) = V(x(t+d) + \alpha f(x(t+d))) - V(x(t) + \alpha f(x(t))) \leq -\tilde{\gamma}(x(t)),$$

where the Leibniz integral rule was used. This further implies that $V_1(x(t+d)) - V_1(x(t)) \leq -\tilde{\gamma}(x(t))$, thus V_1 is a FTLF. ■

4.4 Construction of W based on linearization

In Section 4.2 it has been shown that if the equilibrium of a given system is $\mathcal{KL}$–stable, then a method to construct a Lyapunov function is provided by (4.13), for $V(x)$ defined by any function $\eta \in \mathcal{K}_\infty$ and any norm. The method is constructive starting with a given candidate d–invariant set $\mathcal{S}$ and a candidate function $V(x) = \eta(\|x\|)$. Due to the d–invariance property of $\mathcal{S}$ verifying condition (4.7) for the chosen V is reduced to verifying

$$V(x(d)) - V(x(0)) \leq -\gamma(\|x(0)\|) < 0, \tag{4.20}$$

for all $x(0) \in \mathcal{S}$. The difficulty in verifying (4.20) is given by the need to compute $x(d)$, for all $x(0) \in \mathcal{S}$. However if $x(d)$ is known analytically, then it suffices to verify (4.20) for all initial conditions in a chosen set $\mathcal{S}$. Then the largest level set of W, defined as in (4.13), which is included in $\mathcal{S}$, is a subset of the true DOA of the considered system. The verification of (4.20) translates into solving a problem of the type

$$\begin{aligned} &\max_{x(0)} \left[V(x(d)) - V(x(0))\right] \\ &\text{subject to } x(0) \in \mathcal{S}. \end{aligned} \tag{4.21}$$

The regularity assumptions on the map describing the dynamics (4.1) ensures that the solution is continuous for all $t \in [0, d]$. Furthermore, since $V(x) = \eta(\|x\|) \in \mathcal{K}_\infty$ and the d–invariant candidate set $\mathcal{S}$ is compact, the problem (4.21) will always have a global optimum.

When the analytical solution is not known, or obtaining a numerical approximation is computationally tedious, as it can be the case for higher order nonlinear systems, then we propose the following approach starting from the linearized dynamics of (4.1). In what follows we recall some relevant properties of the map f with respect to its linearization. The detailed derivations can be found in [77, Chaper 4.3]. Firstly, by the mean value theorem it follows that

$$f_i(x) = f_i(0) + \frac{\partial f_i}{\partial x}(z_i)x, \quad i = 1, \ldots, n, \tag{4.22}$$

where z_i is a point on the line connecting x to the origin. Since the origin is an equilibrium of (4.1),

$$f_i(x) = \frac{\partial f_i}{\partial x}(z_i)x = \frac{\partial f_i}{\partial x}(0)x + \left(\frac{\partial f_i}{\partial x}(z_i) - \frac{\partial f_i}{\partial x}(0)\right)x.$$

Then,

$$f(x) = Ax + g(x), \tag{4.23}$$

with

$$A = \frac{\partial f}{\partial x}(0) = \left[\frac{\partial f(x)}{\partial x}\right]_{x=0}, \quad g_i(x) = \left(\frac{\partial f_i}{\partial x}(z_i) - \frac{\partial f_i}{\partial x}(0)\right)x.$$

Furthermore,

$$\|g_i(x)\| \le \|\frac{\partial f_i}{\partial x}(z_i) - \frac{\partial f_i}{\partial x}(0)\|\|x\|$$

and

$$\frac{\|g(x)\|}{\|x\|} \to 0, \text{ as } \|x\| \to 0.$$

In this way, in a sufficiently small region around the origin we can approximate the system (4.1) with $\dot{x} = Ax$.

The next result is an analog to *Lyapunov's indirect method* [77, Theorem 4.7], but in terms of the FTLF concept. The aim is to provide a validity result for the FT condition (4.7) for the nonlinear system (4.1), whenever a (global) FT type condition is satisfied for the linearized system with respect to the origin.

Theorem 4.3 Let $V(x) = \|x\|$ be a global FTLF function for $\dot{x} = Ax$, i.e. there exists a $d > 0$ such that $\|e^{Ad}\| < 1$. Additionally, let

$$e^{d\mu(A)} - 1 = -\varsigma, \quad \varsigma \in \mathbb{R}_{>0}, \tag{4.24}$$

where $\mu(A)$ is the logarithmic norm of A, be satisfied. Then the following statements hold.

1. There exists a d–invariant set $\mathcal{S}$ for which $V(x)$ is a FTLF for (4.1).
2. There exists a set $\mathcal{A} \subseteq \mathcal{S}$ for which

$$W(x) = \int_0^d V(x + \tau f(x))\mathrm{d}\tau \tag{4.25}$$

is a LF for (4.1).

Proof: We start by proving point 1. As indicated in [77], from $\frac{\|g(x)\|}{\|x\|} \to 0$, as $\|x\| \to 0$, it follows that for any $\delta > 0$, there exists an $r > 0$ such that $\|g(x)\| < \delta\|x\|$, for $\|x\| < r$. Thus, the solution of the system defined with the map in (4.23) is bounded, whenever $g(x)$ is bounded [103], as shown below.

$$\begin{aligned}\|x(d)\| &\leq e^{d\mu(A)}\|x(0)\| + \int_0^d e^{(d-\tau)\mu(A)}\|g(x(\tau))\|\mathrm{d}\tau \\ &\leq e^{d\mu(A)}\|x(0)\| + \int_0^d e^{(d-\tau)\mu(A)}\delta\|x(\tau)\|\mathrm{d}\tau.\end{aligned}$$

By applying the Bellman–Gronwall Lemma 4.3 to the inequality above, we obtain

$$\begin{aligned}\|x(d)\| &\leq e^{d\mu(A)}\|x(0)\|e^{\int_0^d e^{(d-\tau)\mu(A)}\delta\mathrm{d}\tau} \\ &\leq e^{d\mu(A)}\|x(0)\|e^{\delta\frac{e^{d\mu(A)}-1}{\mu(A)}} \\ &\leq e^{d\mu(A)-\frac{\varsigma\delta}{\mu(A)}}\|x(0)\|.\end{aligned}$$

Thus, $V(x(d)) \leq \rho V(x(0))$, with $\rho := e^{d\mu(A)-\frac{\varsigma\delta}{\mu(A)}}$. For the equivalent FT condition (4.8) to hold, ρ must be subunitary, and equivalently

$$d\mu(A) - \frac{\varsigma\delta}{\mu(A)} < 0. \tag{4.26}$$

For equation (4.24) to hold, $\mu(A)$ must be negative. Thus, we obtain that

$$\delta \leq \frac{d\mu(A)^2}{\varsigma}, \tag{4.27}$$

which provides an upper bound on δ, and thus on r. Consequently, there exists a d–invariant set

$$\mathcal{S} \subseteq \{x \in \mathbb{R}^n \mid \|x\| < r\}.$$

As for the second item of the theorem, let us consider the Dini derivative expression for $\dot{W}(x(0))$,

$$\dot{W}(x(0)) = \mathscr{D}^+W(x(0)) = \limsup_{h\to 0^+} \frac{W(x(h)) - W(x(0))}{h}.$$

Then,

$$\begin{aligned}
\mathscr{D}^+W(x(0)) &= \limsup_{h\to 0^+} \frac{\int_h^{h+d} V(x(0)+\tau f(x(0)))\mathrm{d}\tau - \int_0^d V(x(0)+\tau f(x(0)))\mathrm{d}\tau}{h} \\
&= \limsup_{h\to 0^+} \frac{\int_d^{d+h} V(x(0)+\tau f(x(0)))\mathrm{d}\tau - \int_0^h V(x(0)+\tau f(x(0)))\mathrm{d}\tau}{h} \\
&=^2 V(x(0)+df(x(0))) - V(x(0)) \\
&< V(x(d)) - V(x(0)) \leq -\gamma(\|x(0)\|),
\end{aligned}$$

where we used the fact that $V_1(x(t)) < V(x(t))$ shown in the proof of Corollary 4.2.

■

In the theorem above, due to the equivalence result in Lemma 4.5, existence of a FTLF V is equivalent to existence of a true LF W defined as in (4.13). Since V is only valid in the region around the origin defined by δ, the LF W will also be a valid LF in some subset of that region. However, the expression of W in (4.13) still involves knowing the solution $x(d)$. In this case, relying on the solution of the linearized system might lead to conservative approximations of the DOA. In view of the fact that we want to construct LFs that lead to relevant DOA estimates, the construction in (4.25) is more suitable as it includes the nonlinear vector field.

The condition in (4.24), essentially requires that there should exist a (weighted) norm for which the induced logarithmic norm of the matrix obtained by evaluating the Jacobian associated to (4.1) at the origin is negative. The choice of the norm inducing the matrix measure is dictated by the choice of the norm defining the FTLF $V(x)$. A similar condition was introduced in [5] for characterizing infinitesimally contracting systems on a given convex set $\mathbb{X} \subseteq \mathbb{R}^n$. Therein, the logarithmic norm of the Jacobian at all points in the set $\mathbb{X}$ is required to be negative.

Remark 4.2 To overcome computing the pair (δ, r) in the above theorem, an a posteriori check on the validity domain of W constructed as in (4.25) is necessary. More precisely, similarly as in Theorem 2.1, this domain is provided by the largest level set of W included in the zero level set of its derivative with respect to (4.1). Consequently, this leads to an optimization problem as the one in (2.11), or the feasibility problem (5.6) in the computational procedure proposed in the next chapter.

4.4.1 An illustrative example with no polynomial LF

Consider the system

$$\begin{aligned}
\dot{x}_1 &= -x_1 + x_1 x_2 \\
\dot{x}_2 &= -x_2,
\end{aligned} \tag{4.28}$$

[2] Here we applied L'Hospital rule together with Leibniz integral rule.

with solutions $x_1(t) = x_1(0)e^{(x_2(0)-x_2(0)e^{-t}-t)}$ and $x_2(t) = x_2(0)e^{-t}$. In [3] it was shown that the system is GAS by using the Lyapunov function $V_{GAS}(x) = \ln(1 + x_1^2) + x_2^2$. Furthermore, it was shown that no polynomial LF exists for this system. We will illustrate our converse results on this system and we will show that the proposed constructive approach leads to local approximations of the DOA that cover a larger area of the state space compared to similar sublevel sets of V_{GAS}. Since the system is GAS, then it is $\mathcal{KL}$–stable with $\mathcal{S} = \mathbb{R}^n$, and by Theorem 4.2 we have that for any function $\eta \in \mathcal{K}_\infty$, there exists a set $\mathcal{S} \subseteq \mathbb{R}^n$ and a scalar d such that the function $V(x) = \eta(\|x\|)$, for any $x \in \mathcal{S}$ is a FTLF for the system (4.28).

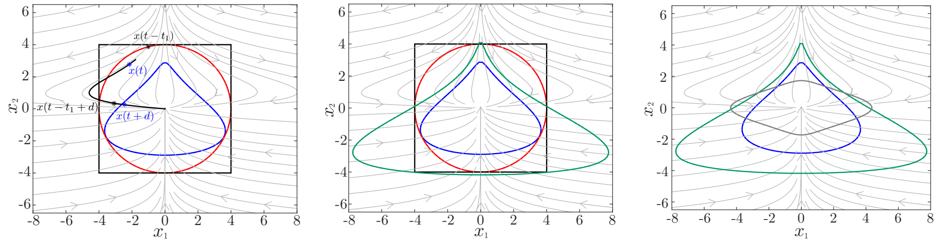

(a) (b) (c)

Figure 4.1: Plots of the level sets of the function V_{GAS}, V, W and W_1 computed for the system (4.28). (a)–The set $\mathbb{X}$–black, the set $\mathcal{S}$ defined by the level set $C_V = 1.6$ of FTLF V–red and the level set defined by $C_W = 0.415$ of the LF W–blue together with the vector field plot of (4.1). (b)–The same sets as in Figure 4.1(a) together with the level set defined by $C_{W_1} = 1.5$ of W_1–green. (c)–Comparison plot: $W(x) = 0.415$–blue, $W_1(x) = 1.5$–green and $V_{GAS} = 3$–gray.

Consider the set $\mathbb{X} := \{x \in \mathbb{R}^n \,|\, \|x\|_\infty \leq 4\}$, which is displayed in Figure 4.1 with the black contour. Pick $V(x) = x^\top Px$, where $P = \left(\begin{smallmatrix} 0.1 & 0 \\ 0 & 0.1 \end{smallmatrix}\right)$. For this choice of V, the feasibility problem (4.21) was solved using the `sqp` algorithm with `fmincon`. Since all involved functions are Lipschitz and we considered a polytopic, compact candidate set $\mathcal{S}$, the problem (4.21) has a global optimum. We found that condition (4.20) and consequently, (4.7) holds for $d = 2.4$ and we assume it is a valid result for any $x \in \mathcal{S}$, where $\mathcal{S}$ is the largest level set of V included in the set $\mathbb{X}$; $\mathcal{S}$ is shown in Figure 4.1(a) in red. By Lemma 4.5, we obtain that

$$W(x(t)) = \int_t^{t+d} x(\tau)^\top Px(\tau)\mathrm{d}\tau$$

is a Lyapunov function for (4.28), for any $t \in \mathbb{R}_{\geq 0}$. From (4.20) and the equivalence result in Lemma 4.5, it is sufficient to compute $W(x(0))$. For the computed d and chosen $\mathcal{S}$ and V, let $\mathcal{S}_V(C_V)$ denote the largest level set of V included in $\mathcal{S}$. Then, the largest level set of W in $\mathcal{S}_V(C_V)$ will be a subset of the true DOA of the system. In Figure 4.1(a) we show the level set of W defined by $C_W = 0.415$ in blue. Next, we will illustrate also the expansion method. Consider $W_1(x(t)) = W(x(t) + \alpha_1 f(x(t))$, with $\alpha_1 = 0.1$. The level set defined by $W_1(x) = C_{W_1}$, where $C_{W_1} = 1.5$ is shown in Figure 4.1(b) in green. Note that, by construction, $W_1(x) = 1.5$ is not restricted to the black set. For the sake of comparison we show in Figure 4.1(c) a plot of level sets of the two computed functions, W and W_1 and a relevant level set value of the logarithmic LF V_{GAS}.

4.5 Alternative construction: Yoshizawa type

The other classical converse result is derived in [121], and is based on computing the supremum of a function of the state of the system over an infinite time interval. In this section, similarly to the Massera case, we show how a Yoshizawa–type of LF can be constructed from a FTLF, with the advantage of computation over a finite time interval. Therefore, consider the function defined as

$$W(x(0)) = \sup_{\tau\in[0,d]} V(x(\tau))e^{\tau}, \tag{4.29}$$

for any V which satisfies (4.6) and (4.7) (or (4.8)) , for all $x(0) \in \mathcal{S}$.

Lemma 4.6 Let $V = \eta(\|x\|)$, with any $\mathcal{K}_\infty$–function η, be a continuously differentiable function satisfying (4.6) and (4.8) with $\rho < \mathrm{id}\cdot e^{-d}$, for some $d > 0$ and the proper d–invariant set $\mathcal{S}$ for (4.1). Then the function W defined as in (4.29) with the same value of d is a LaSalle type of LF for (4.1), i.e. $\mathscr{D}^+W(x(0)) \le 0$, for all $x(0) \in \mathcal{S}$.

Proof: From Theorem 4.1 it follows that the system (4.1) is $\mathcal{KL}$–stable in $\mathcal{S}$, thus for any $x(0) \in \mathcal{S}$, we have that

$$\begin{aligned} W(x(0)) &= \sup_{\tau\in[0,d]} \eta(\|x(\tau)\|)e^{\tau} \\ &\le \sup_{\tau\in[0,d]} \eta(\beta(\|x(0)\|,\tau))e^{\tau} \\ &\le \sup_{\tau\in[0,d]} \eta(\beta(\|x(0)\|,0))e^{\tau} \\ &= \eta\circ\beta(\|x(0)\|,0) \max_{\tau\in[0,d]} e^{\tau} \\ &= \alpha_2(\|x(0)\|)e^{d} =: \hat{\alpha}_2(\|x(0)\|), \end{aligned}$$

where $\hat{\alpha}_2 \in \mathcal{K}_\infty$.

$$\begin{aligned} W(x(0)) &= \sup_{\tau\in[0,d]} \eta(\|x(\tau)\|)e^{\tau} \ge \sup_{\tau\in[0,d]} \alpha_1(\|x(\tau)\|)e^{\tau}\Big|_{\tau=0} \\ &=: \hat{\alpha}_1(\|x(0)\|), \end{aligned}$$

with $\hat{\alpha}_1 \in \mathcal{K}_\infty$. Thus, we obtain (4.6). Notice that by the definition of $W(x(0))$, the derivative in the Dini sense needs to be considered for $\dot{W}(x)$, i.e.

$$\mathscr{D}^+W(x(0)) = \limsup_{h\to 0^+} \frac{W(x(h)) - W(x(0))}{h}.$$

Next, we will establish a relation between $W(x(t))$ and $W(x(0))$, which holds for any $t > 0$, based on (4.8) when $\rho < \mathrm{id} \cdot e^{-d}$.

Let $t = Nd + j$, where $N \in \mathbb{Z}_{\geq 0}$ and $j \in \mathbb{R}_{>0}$, $j < d$.

$$
\begin{aligned}
W(x(t)) &= \sup_{\tau \in [t,t+d]} V(x(\tau))e^{\tau} = \max_{\tau \in [t,t+d]} V(x(\tau))e^{\tau} \\
&= \max\Big\{ \max_{\tau \in [t,(N+1)d]} V(x(\tau))e^{\tau}, \max_{\tau \in [(N+1)d,t+d]} V(x(\tau))e^{\tau} \Big\} \\
&= \max\Big\{ \max_{\tau \in [t,(N+1)d]} V(x(\tau))e^{\tau}, \max_{\tau \in [Nd,t]} V(x(\tau+d))e^{\tau+d} \Big\} \\
&< \max\Big\{ \max_{\tau \in [t,(N+1)d]} V(x(\tau))e^{\tau}, \max_{\tau \in [Nd,t]} V(x(\tau))e^{\tau+d-d} \Big\} \\
&= \max_{\tau \in [Nd,(N+1)d]} V(x(\tau))e^{\tau} \qquad (4.30)\\
&= \max_{\tau \in [(N-1)d,Nd]} V(x(\tau+d))e^{\tau+d} \\
&< \max_{\tau \in [(N-1)d,Nd]} V(x(\tau))e^{\tau} \\
&\dots \\
&< \max_{\tau \in [0,d]} V(x(\tau))e^{\tau} = W(x(0)).
\end{aligned}
$$

Thus, it follows that

$$
\begin{aligned}
\mathscr{D}^{+}W(x(0)) &= \limsup_{h \to 0^{+}} \frac{W(x(h)) - W(x(0))}{h} \\
&\leq \limsup_{h \to 0^{+}} \frac{W(x(0)) - W(x(0))}{h} = 0
\end{aligned}
$$

and we have obtained that $\mathscr{D}^{+}W(x(t)) \leq 0$.

■

In the above lemma, the resulting condition $\mathscr{D}^{+}W(x) \leq 0$, does not represent a restriction when estimating the DOA of the system (4.1), because Theorem 2.1 in Chapter 2, which is a consequence of LaSalle's theorem [80, Theorem 1] can be applied to compute the largest level set of W contained in the set where $\mathscr{D}^{+}W(x) < 0$ and does not intersect the set $\{x \in \mathbb{R}^n : \mathscr{D}^{+}W(x) = 0\}$.

The next result summarizes the proposed alternative converse LF for $\mathcal{KL}$–stability in $\mathcal{S}$, enabled by the finite–time conditions (4.6) and (4.7).

Corollary 4.3 If the zero equilibrium of the system (4.1) is $\mathcal{KL}$–stable in some set $\mathcal{S}$ and Assumption 4.1 holds for some $d > 0$, then by Theorem 4.2 and Lemma 4.6 for any function $\eta \in \mathcal{K}_{\infty}$ and any norm $\|\cdot\|$, the function $W(\cdot)$ defined in (4.29) with the same value for $d > 0$ as in Assumption 4.1, is a Lyapunov function (of LaSalle type) for the system (4.1).

Consequently, an analogue of Theorem 4.3 in terms of constructing W starting from the linearization of (4.1) around the origin is provided below.

Theorem 4.4 Let $V(x) = \|x\|$ be a global FTLF function for $\dot{x} = Ax$, i.e. there exists a $d > 0$ such that $\|e^{Ad}\| < 1$. Additionally, let

$$e^{d\mu(A)} - 1 = -\varsigma, \quad \varsigma \in \mathbb{R}_{>0} \tag{4.31}$$

be satisfied. Then the following statements hold.

1. There exists a d–invariant set $\mathcal{S}$ for which $V(x)$ is a FTLF for (4.1).
2. There exists a set $\mathcal{A} \subseteq \mathcal{S}$ for which

   $$W_1(x) = \max_{\tau \in [0,d]} V(x + \tau f(x))e^{\tau} \tag{4.32}$$

   is a LF of LaSalle type for (4.1).

Proof: The first item of the theorem is the same as in Theorem 4.3.

For the second item of the theorem, observe that [31, p.190]

$$V(x(t+h)) = V(x(t) + hf(x(t)) + h\varepsilon),$$

where $\varepsilon \to 0$ as $h \to 0$. Furthermore, from [121, p.3], it follows that

$$V(x(t+h)) = V(x(t) + hf(x(t)) + h\varepsilon) \le V(x(t) + hf(x(t))) + Lh\|\varepsilon\|$$
$$V(x(t+h)) = V(x(t) + hf(x(t)) + h\varepsilon) \ge V(x(t) + hf(x(t))) - Lh\|\varepsilon\|$$

and

$$V(x(t-h)) = V(x(t) - hf(x(t)) - h\varepsilon) \le V(x(t) - hf(x(t))) + Lh\|\varepsilon\|$$
$$V(x(t-h)) = V(x(t) - hf(x(t)) - h\varepsilon) \ge V(x(t) - hf(x(t))) - Lh\|\varepsilon\|$$

where L is the Lipschitz constant of $V(x)$ for $x \in \mathcal{S}$ and $\varepsilon \to 0$ for $h \to 0^+$. Thus, for $h \to 0^+$, $V(x(h)) = V(x(0) + hf(x(0)))$, and, as shown in [98, Appendix I.4],

$$\begin{aligned}\mathscr{D}^+W_1(x(0)) &= \limsup_{h\to 0^+} \frac{W_1(x(h)) - W_1(x(0))}{h} \\ &= \limsup_{h\to 0^+} \frac{W_1(x(0) + hf(x(0))) - W_1(x(0))}{h}.\end{aligned}$$

We have to show that $\mathscr{D}^+W_1(x(0)) \le 0$. Then, by making use of the above relations we obtain the following:

$$\begin{aligned}\mathscr{D}^+W_1(x(0)) &= \limsup_{h\to 0^+} \frac{\max\limits_{\tau\in[h,h+d]} V(x(0) + \tau f(x(0)))e^{\tau} - \max\limits_{\tau\in[0,d]} V(x(0) + \tau f(x(0)))e^{\tau}}{h} \\ &= \limsup_{h\to 0^+} \frac{\max\limits_{\tau\in[0,d]} V(x(0) + (h+\tau) f(x(0)))e^{\tau+h} - \max\limits_{\tau\in[0,d]} V(x(0) + \tau f(x(0)))e^{\tau}}{h} \\ &= \limsup_{h\to 0^+} \frac{\max\limits_{\tau\in[0,d]} V(x(\tau) + h f(x(\tau)))e^{\tau+h} - \max\limits_{\tau\in[0,d]} V(x(0) + \tau f(x(0)))e^{\tau}}{h} \\ &= \limsup_{h\to 0^+} \frac{\max\limits_{\tau\in[0,d]} V(x(\tau+h))e^{\tau+h} - \max\limits_{\tau\in[0,d]} V(x(\tau))e^{\tau}}{h}\end{aligned}$$

and,

$$\begin{aligned}\mathscr{D}^+ W_1(x(0)) &= \limsup_{h\to 0^+} \frac{W(x(h)) - \max\limits_{\tau\in[0,d]} V(x(\tau))e^{\tau}}{h} = \limsup_{h\to 0^+} \frac{W(x(h)) - W(x(0))}{h} \\ &= \mathscr{D}^+ W(x(0)) \le 0,\end{aligned}$$

where $W(x)$ denotes the construction in (4.29), which it has been shown to be a LF of LaSalle type when V is a FTLF. ■

In the theorem above, due to the equivalence result in Lemma 4.6, existence of a FTLF V is equivalent to existence of a true LF W defined as in (4.29). Since V is only valid in the region around the origin defined by δ, the LF W will also be a valid LF in some subset of that region. However, the expression of W in (4.29) still involves knowing the solution $x(d)$. In this case, relying on the solution of the linearized system might lead to conservative approximations of the DOA. In view of the fact that we want to construct LFs that lead to relevant DOA estimates, the construction in (4.32) is more suitable as it includes the nonlinear vector field.

Remark 4.2 holds valid also in this case, when W_1 is constructed as in (4.32).

When comparing the construction (4.32) with the Massera–type one in (4.25), the advantage of the first one is that for complex systems it might be less computationally demanding to compute the maximum, rather than computing the integral.

4.5.1 An illustrative example with no polynomial LF

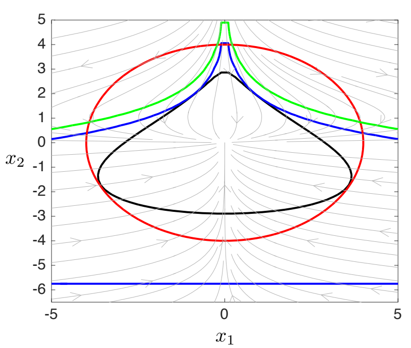

Figure 4.2: Plot of the the level set $W_{\tau^*}(x) = 0.3$–blue, $\dot{W}_{\tau^*}(x) = -1.2$–green, and the largest level set of the Massera–type function–black; with red the level set $V(x) = 1.6$ is plotted.

Consider again the system described in Example 4.4.1. We will illustrate also the Yoshizawa construction on this example. Again, since the system is GAS, then it is $\mathcal{KL}$–stable with $\mathcal{S} = \mathbb{R}^n$, and by Theorem 4.2 we have that for any function $\eta \in \mathcal{K}_\infty$, there exists a set $\mathcal{S} \subseteq \mathbb{R}^n$ and a scalar d such that the function $V(x) = \eta(\|x\|)$, for any $x \in \mathcal{S}$ is a FTLF for the system (4.28). Consider the set $\mathbb{X} := \{x \in \mathbb{R}^n \mid \|x\|_\infty \le 4\}$. Pick $V(x) = x^\top Px$, where where $P = \left(\begin{smallmatrix} 0.1 & 0 \\ 0 & 0.1\end{smallmatrix}\right)$. Let $\mathcal{S}$ be the largest level set of V included in $\mathbb{X}$, plotted with red in Figure 4.2. Then, condition (4.20) and consequently, (4.7) holds for $d = 2.4$ for any $x \in \mathcal{S}$. By Lemma 4.6, we obtain that

$$W(x(0)) = \sup_{\tau \in [0,d]} x(\tau)^\top P x(\tau) e^{\tau}$$

is a Lyapunov function for (4.28), for any $t \in \mathbb{R}_{\geq 0}$. For this system, we consider the maximum in (4.29) for all $x(0) \in \mathcal{S}$, which was attained for $\tau^* = d$, to facilitate the computation of an educated guess for W. Otherwise, if the true formula of (4.29) is used, note that the supremum (maximum) depends on each $x(0) \in \mathcal{S}$ and an analytic expression of W cannot be obtained. The largest level set of $W_{\tau^*}(x)$ which does not intersect the zero level set of $\dot{W}_{\tau^*}(x)$ is shown in Figure 4.2 with blue. Note that this set is not included in the red set any more, thus it is not included in $\mathcal{S}$. However, this is allowed since it is a valid estimate of the DOA (Theorem 2.1) as it is included in the zero level set of its corresponding derivative with respect to the dynamics (4.28).

4.6 Conclusions

In this chapter, a new Massera type of LF (and a Yoshizawa type alternative) have been derived. These constructions are enabled by imposing a finite–time condition on an arbitrary candidate function defined by a $\mathcal{K}_\infty$–function of the state norm. An advantage over classical constructions which for finite time interval integration (supremum calculation) require exponential stability or to allow for $\mathcal{KL}$–stability a specific function under the integral is imposed, is that we provide an approach with two more degrees of freedom. On one hand, we allow for $\mathcal{KL}$–stability (under Assumption 4.1) and on the other hand the construction of the LF is based on any $\mathcal{K}_\infty$ function of the norm of the solution of the system. While a similar formulation was previously introduced in [15], the main difference in the hereby proposed approach consists of the relation between the integration interval length and the finite–time decrease criterion imposed on the $\mathcal{K}_\infty$ function.

The motivation for choosing a constructive converse theorem approach to deriving LFs comes from the need to overcome the conservativeness of the RLFs (as introduced in Chapter 2) due to approximations of the dynamics. However, for either constructions the solution needs to be known up to some finite time value. In the next chapter we will address this problem by means of solution approximation techniques or by starting the computational procedure from the linearized system towards obtaining DOA estimates, as already indicated in this chapter.

Chapter 5

Verification of FTLFs for computing LFs and DOAs

In Chapter 4 we derived two alternatives for computing LFs based on FTLFs, with the downside that they require knowledge of the system solution for a finite time, in order to verify a corresponding finite time decrease property. In this chapter we will address the verification problem and develop two solutions. The first one relies on linearization and computation via an expanded FTLF and the second is based on a novel numerical approach for the computation of LFs via the Massera-type converse. The constructed LF is continuous and piecewise affine (CPA), computed via a FTLF evaluated at approximated trajectories. In both cases, by optimization, the obtained LF is verified and consequently we are able to give an estimate of the domain of attraction[1].

5.1 Introduction

Among the converse theorems, we have the early result of Massera [90], where it has been shown that the integral of a certain function of the norm of the solution of the system is a LF. Additionally, we have the result of Yoshizawa [121], where it has been shown that the supremum of a certain function of the norm of the solution of the system is a LF.

More recently, a stability criterion for dynamical systems in terms of a finite time difference condition has been established in [2]. In Chapter 4, a Massera-type of construction has been proposed, based on FTLFs. In fact, we allow any $\mathcal{K}_\infty$ function, that satisfies the finite–time criterion, to be a FTLF. Consequently, an analytic relation between a LF and a FTLF is stated.

Although the mentioned converse theorems are constructive, they all require the solution of the system to be known on a finite time interval. In general, obtaining the analytical solution for a nonlinear system is, just as obtaining a LF, difficult and therefore the computational contribution of the converse theorems is limited.

An approach for constructing LFs by partitioning the state space was introduced in [89], where linear programming is used to compute continuous and piecewise affine (CPA) LFs.

[1]Part of the work presented in this chapter was developed together with Tom Steentjes, during his internship [114].

In [12] an adjustment to this method was proposed, by making use of numerical approximations of the Massera construction instead of linear programming.

In Chapter 4, Theorems 4.3 and 4.4 provide alternative constructions of LFs starting from a FTLFs which is verified for the linearized system. These constructions provide directly computable analytical expressions and in this chapter we will simply state the computation steps. The main contribution is the construction of continuous and piecewise affine LFs by numerical approximations of the Massera-type converse. The proposed method differs from [12], and the later result in [15], in the sense that we allow any $\mathcal{K}_\infty$ function of the norm of the state to be a candidate FTLF. In [15], although a fairly arbitrary function is considered in the Massera formulation, the upper bound in the integration interval is not related to the properties of the function. Furthermore, by numerical approximations of the solution, we verify the finite–time condition for some candidate d-invariant set to obtain an upper bound for the integration interval, in contrast to [15], where the bound is chosen differently. Specifically, therein the integration bound is given by the smallest time instant for which states initiated in a given, chosen set reach a neighborhood of the equilibrium. Finally, an optimization problem is solved for verification of the constructed LF, aiming at nonconservative estimations of the domain of attraction.

5.2 Some preliminaries

Let $v_0, \ldots, v_m \in \mathbb{R}^n$ be a collection of vectors. The vectors in the collection $v_0, \ldots, v_m$ are said to be affinely independent if $\sum_{i=1}^{m} \lambda_i(v_i - v_0) = 0$, implies that $\lambda_i = 0$ for all $i \in \mathbb{N}_{[0:m]}$.

Definition 5.1 Given a collection of affinely independent vectors $v_0, \ldots, v_m$, an m-simplex in $\mathbb{R}^n$ is defined as its convex hull, i.e.

$$\operatorname{co}\{v_0, \ldots, v_m\} := \left\{ \sum_{i=0}^{m} \lambda_i v_i \,|\, \lambda_i \in [0,1],\ \sum_{i=0}^{m} \lambda_i = 1 \right\}.$$

Given a simplex $\mathfrak{S}$, let the diameter of $\mathfrak{S}$ be given by

$$\operatorname{diam}(\mathfrak{S}) := \max_{\alpha,\beta \in \mathfrak{S}} \|\alpha - \beta\|.$$

Additionally, we give a theorem serviceable for the estimation of the domain of attraction for biological systems, i.e. systems for which the positive orthant is positive invariant. To this end, we recall the definition of a practical set introduced in [16, Definition 4.9].

Definition 5.2 A set $\mathcal{S} \subset \mathcal{O}$, where $\mathcal{O}$ is an open set, is called a practical set if:

- it is defined by a finite set of inequalities:

$$\mathcal{S} = \{x \,:\, g_k(x) \leq 0,\ k = 1, \ldots, r\}, r \in \mathbb{Z}_{>0};$$

- for all $x \in \mathcal{S}$, there exists a z such that $g_i(x) = \nabla g_i(x)^\top z < 0$, for all i;

- there exists a Lipschitz continuous vector field $\phi(x)$ such that for all $x \in \partial\mathcal{S}$, it holds that $\nabla g_i(x)^\top \phi(x) < 0$, for all i.

Theorem 5.1 Let the positive orthant $\mathcal{P}$ be positively invariant and consider the system (4.1), but with an equilibrium $x^* \in \mathcal{P}$, such that $f(x^*) = 0$. Let $W(\cdot)$ be a LF for (4.1) and consider the sets

$$\mathcal{A} = \{x \in \mathbb{R}^n \,|\, \nabla W^\top(x) f(x) < 0\} \,\text{and}\, \mathcal{C} := \{x \in \mathbb{R} \,|\, W(x) \leq C^*\}.$$

Furthermore, let $C^* \in \mathbb{R}_{>0}$ be such that:

$$\mathcal{C} \cap \{\mathcal{P} \setminus \{x^*\}\} \subseteq \mathcal{A}.$$

Then the set

$$\mathcal{S}_\mathcal{A} = \mathcal{C} \cap \mathcal{P}$$

is positively invariant and contained in the DOA of (4.1), where $\mathcal{S}_\mathcal{A}$ is assumed to be practical.

Proof: First, we show that $\mathcal{S}_\mathcal{A}$ is positively invariant. Note that we can write this equivalently as

$$\mathcal{S}_\mathcal{A} = \{x \in \mathbb{R}^n \,|\, g_i(x) \leq 0,\ i \in \mathbb{N}_{[0:n]}\},$$

where $g_0(x) = W(x) - C^*$ and $g_i(x) = -x_i$, $i \in \mathbb{N}_{[1:n]}$.

Consider $\mathrm{Act}(x) := \{i \in \mathbb{N} \,|\, g_i(x) = 0\}$. Then for all $x \in \partial\mathcal{S}_\mathcal{A}$ the tangential cone is given by [16]

$$\mathcal{T}_{\mathcal{S}_\mathcal{A}}(x) = \{z \in \mathbb{R}^n \,|\, \nabla g_i^\top(x) z \leq 0, \quad \forall i \in \mathrm{Act}(x)\}.$$

Now, if $f(x) \in \mathcal{T}_{\mathcal{S}_\mathcal{A}}(x)$ for all $x \in \mathcal{S}_\mathcal{A}$, then by Nagumo's theorem, $\mathcal{S}_\mathcal{A}$ is positively invariant, [16]. Since $\mathcal{T}_{\mathcal{S}_\mathcal{A}}(x) = \mathbb{R}^n$ for all $x \in \mathcal{S}_\mathcal{A}^\circ$, we only have to show $f(x) \in \mathcal{T}_{\mathcal{S}_\mathcal{A}}(x)$ for all $x \in \partial\mathcal{S}_\mathcal{A}$.

On the boundary $\partial\mathcal{P} \cap \mathcal{C}^\circ$, the tangential cone is given by

$$\mathcal{T}_{\mathcal{S}_\mathcal{A}}(x) = \{z \in \mathbb{R}^n \,|\, z_i \geq 0 \quad, \forall i \text{ s.t. } x_i = 0\}.$$

Indeed, $f(x) \in \mathcal{T}_{\mathcal{S}_\mathcal{A}}(x)$ for all $x \in \partial\mathcal{P} \cap \mathcal{C}^\circ$, since $\dot{x}_i \geq 0$ for $x_i = 0$, which follows directly from the positive invariance property of $\mathcal{P}$.

On the boundary $\partial\mathcal{C} \cap \mathcal{P}^\circ$, the tangential cone is given by

$$\mathcal{T}_{\mathcal{S}_\mathcal{A}}(x) = \{z \in \mathbb{R}^n \,|\, \nabla W^\top(x) z \leq 0\}.$$

Indeed, we have that $f(x) \in \mathcal{T}_{\mathcal{S}_\mathcal{A}}(x)$ for all $x \in \partial\mathcal{C} \cap \mathcal{P}^\circ$, since $\nabla W^\top(x) f(x) \leq 0$ for all $x \in \mathcal{C} \cap \mathcal{P}$.

Finally, on the remaining intersections $\partial\mathcal{C} \cap \partial\mathcal{P}$, the tangential cone is given by

$$\mathcal{T}_{\mathcal{S}_\mathcal{A}}(x) = \{z \in \mathbb{R}^n \,|\, (z_i \geq 0,\ \forall i \text{ s.t. } x_i = 0) \wedge (\nabla W^\top(x) z \leq 0)\}.$$

We obviously have that $f(x) \in \mathcal{T}_{\mathcal{S}_\mathcal{A}}(x)$ for all $x \in \partial\mathcal{C} \cap \partial\mathcal{P}$, by the positive invariance property of $\mathcal{P}$ and since $\nabla W^\top(x)f(x) \leq 0$ for all $x \in \mathcal{C} \cap \mathcal{P}$. Concluding, we have shown that $f(x) \in \mathcal{T}_{\mathcal{S}_\mathcal{A}}(x)$ for all $x \in \partial\mathcal{S}_\mathcal{A}$ and thus $\mathcal{S}_\mathcal{A}$ is positively invariant.

Finally, $x(t) \to x^*$ as $t \to \infty$, since $\nabla W^\top(x)f(x) < 0$ for all $x \in \mathcal{C} \cap \mathcal{P} \setminus \{x^*\}$, by the Aymptotic Stability Theorem, [80].

As introduced in Chapter 4, while the construction of classical LFs from a FTLF allows the freedom to choose any $\mathcal{K}_\infty$–function of the norm of the state, two problems arise, related to the verification of a FTLF and construction of a true LF.

Firstly, as opposed to verifying (4.3), verifying (4.7) requires knowledge of the solution of system (4.1). Indeed, if we consider a d-invariant set candidate $\mathcal{S}$ and a candidate map $V(x) = \eta(\|x\|)$, then we need to verify

$$V(x(d)) - V(x(0)) \leq -\gamma(\|x\|) < 0, \tag{5.1}$$

for all $x(0) \in \mathcal{S}$. If the solution for (4.1) is known (analytically), then verifying (5.1) can be done easily. However, $x(d)$ is not known for non-linear systems, in general.

Secondly, once a FTLF $V(x) = \eta(\|x\|)$ is verified, i.e. (5.1) is satisfied for some $d \in \mathbb{R}_{>0}$, one wants to compute a classical LF $W(x)$ using

$$W(x(0)) = \int_0^d V(x(\tau))\mathrm{d}\tau \quad \forall x(0) \in \mathcal{S}. \tag{5.2}$$

Again, we need the solution $x(t)$, $t \in [0, d]$. Although obtaining approximate solutions for a finite set of initial conditions is possible, and thus a finite set containing numerical approximations of $W(x(0))$, finding a complete LF W is not straightforward. So we need a way to "connect" values of W. One way of constructing a complete LF is the CPA method, introduced in [89], where a unique continuous and piecewise affine function is determined from a finite set containing numerical approximations of $W(x(0))$. In [89], numerical values of W are obtained using linear programming.

Finally, a computed candidate function should be verified. That is, we need to verify the region for which the computed function is a classical LF. Consequently, the domain of attraction can be estimated.

5.3 Construction of a LF by means of linearization

5.3.1 Computation of a d for which the finite–time condition holds for the linearized system with respect to the origin

Let

$$\dot{\delta x} = \left[\frac{\partial f(x)}{\partial x}\right]_{x=0} \delta x,$$

be the linearized system. Then condition (5.1) can be verified as:

$$\eta(\|e^{d\left[\frac{\partial f(x)}{\partial x}\right]_{x=0}} x(0)\|) - \eta(\|x(0)\|) < 0,$$

for all $x(0)$ in some compact, proper set $\mathcal{S}$. As such, for a given value of d, (5.1) can be verified via a feasibility problem (see (4.21)). If $\eta = \mathrm{id}$ then the feasibility problem above translates into verifying the matrix norm condition:

$$\|e^{d\left[\frac{\partial f(x)}{\partial x}\right]_{x=0}}\| < 1. \tag{5.3}$$

Note that if there exists a $d > 0$ such that the condition (4.24) holds for some $\varsigma > 0$, then condition (5.3) is implicitly satisfied since it holds that $\|e^{dA}\| \leq e^{d\mu(A)}$ for some real matrix A [103].

5.3.2 Computation of $W(x)$

$$W(x) = \int_0^d V(x + \tau f(x))\mathrm{d}\tau. \tag{5.4}$$

Or, alternatively

$$W(x) = \max_{\tau\in[0,d]} V(x + \tau f(x))e^{\tau}\mathrm{d}\tau. \tag{5.5}$$

In this construction we exploit the results in Corollary 4.2 and Theorem 4.3, which guarantee that $V(x + \tau f(x))$ remains a FTLF for (4.1) for all $\tau \in [0, d]$.

5.3.3 Finding the best DOA estimate of (4.1) provided by W

Let C be such that the set $\{x \in \mathbb{R}^n \mid W(x) \leq C\}$ is included in the set

$$\{x \in \mathbb{R}^n \mid \nabla W^\top f(x) = 0\}.$$

Finding C, implies solving an optimization problem, which involves rather complex nonlinear functions. However, feasibility problems (for example by using bisection) can be solved successfully to obtain the best C which leads to a true DOA estimate. The feasibility problem is as follows:

$$\begin{aligned} &\max_x \ \nabla W(x)^\top f(x) \\ &\text{subject to } W(x) \leq C, \end{aligned} \tag{5.6}$$

for a given C value. The largest C value for which $\dot{W}(x)$ remains negative renders the best DOA estimate provided by a true LF $W(x)$, which is valid for (4.1) since $\dot{W}(x) = \nabla W(x)^\top f(x)$. The optimization problem (5.6) has been addressed in Chapter 2 and it is standard in checking validity regions of LFs a posteriori to construction.

The bound (4.27), via r, provides an implicit, a priori theoretical indication of the region where W is a valid LF, or in other words of a subset of the DOA. An explicit estimate can be obtained a posteriori to computing W by solving the problem above.

5.3.4 Further improve the DOA estimate by expansion of W

The DOA estimate obtained above can be further improved by making use of expansion methods as introduced in [28]. More specifically, the expansion method states that the C–level set of $W_1(x) = W(x + \alpha f(x))$ for some $\alpha \in \mathbb{R}_{>0}$ is a subset of the true DOA of the considered system and it will contain the estimate of the DOA obtained by the C–level set of W.

In summary, the proposed method starts by verifying the finite–time decrease condition (5.1) for a candidate function $V(x) = \eta(\|x\|)$, $\eta \in \mathcal{K}_\infty$ and a candidate d–invariant set $\mathcal{S}$.

The simplest way to do this, while avoiding solution approximations, given in Step 5.3.1, is to verify (5.1) globally ($x \in \mathbb{R}^n$) for the linearization of (4.1) around the origin. Then, it is known by Theorem 4.3, that there exists a set $\mathcal{S} \subseteq \{x \in \mathbb{R}^n \,|\, \|x\| < r\}$ which is d–invariant, such that (5.1) holds for the true nonlinear system.

Next, in the second step of the procedure, W is computed via the analytic formula (5.4), which yields an educated guess of a true LF. Thus, the final check in the third step is a verification of the standard Lyapunov condition on W, with W known, and with the aim to maximize the level C of W where the condition is satisfied, which in turn maintains the DOA approximation induced by W.

In contrast, most of the other proposed methods in the literature, compute the LF W simultaneously with verifying the derivative negative definiteness condition, which is in a general a more difficult task, even because it is not clear how to select an appropriate W.

Remark 5.1 As for the Yoshizawa–type formulation (4.29), and corresponding one (5.5), due to the $\max$ function W is no longer differentiable and we cannot obtain an analytic expression. Therefore in the illustrative Example 4.5.1 we consider a heuristic path by taking $\tau^* = d$ to be the time value for which the maximum, W^*, is attained for all $x(0) \in \mathcal{S}$, thus rendering an analytical, differentiable function $W^*(x(0))$. By solving the optimization problem (5.6) for the constructed W^*, we can guarantee that $W^*(x(0)) = C$ is a valid estimate of the DOA of the considered system. Alternatively, numerical values of the non-differentiable function W can be computed for the vertices of a simplicial partition of the state space, yielding a CPA Yoshizawa–type of function, as described in the next section for a CPA Massera–type LF.

5.4 Construction of a LF by means of approximated trajectories

We start with the definition of a (proper) triangulation, which will be used later on in this section for the verification of a finite–time Lyapunov candidate function and construction of a classical CPA LF via a converse theorem.

Definition 5.3 Let $\mathfrak{M}$ be a proper subset of $\mathbb{R}^n$ and let $\mathfrak{T} = \{\mathfrak{S}_1, \ldots, \mathfrak{S}_z\}$, where $\mathfrak{S}_i,\ i \in \mathbb{N}_{[1:z]}$ is an n-simplex. Suppose $\mathfrak{M} = \cup_{i \in \mathbb{N}_{[1:z]}} \mathfrak{S}_i$. If for all $\mathfrak{S}_a, \mathfrak{S}_b \in \mathfrak{T}$, $a \neq b$, we have $\mathfrak{S}_a \cap \mathfrak{S}_b = \emptyset$ or $\mathfrak{S}_a \cap \mathfrak{S}_b$ is a q-simplex and a face of $\mathfrak{S}_a$ and of face of $\mathfrak{S}_b$, where $q \in \mathbb{N}_{[0:n-1]}$, then $\mathfrak{T}$ is called a triangulation of $\mathfrak{M}$. If, additionally, the origin is contained in a simplex $\mathfrak{S}_i$ and it is a vertex of $\mathfrak{S}_i$, then $\mathfrak{T}$ is called a proper triangulation of $\mathfrak{M}$.

For a (proper) triangulation as defined above, we also define the set containing all vertices of the simplices in the triangulation. This set is defined as

$$\mathcal{V}_{\mathfrak{T}} = \left\{ x \in \mathbb{R}^n \,|\, x \text{ is a vertex of a simplex } \mathfrak{S}_i \in \mathfrak{T},\ i \in \mathbb{N}_{[1:z]} \right\}.$$

Note that a triangulation of a proper set $\mathfrak{M}$, even with uniform simplex diameter, is not unique. Indeed, the orientation of simplices can be chosen in various ways. For the remainder of this chapter, we will consider triangulations with two types of orientations; mono–oriented (as shown in Figure 5.1(a)) and poly–oriented (as shown in Figure 5.1(b)) triangulations. A triangulation is called mono–oriented on $\mathfrak{M}$, if all hypercubes formed by simplices in $\mathfrak{T}$ are equivalent. A triangulation is called poly–oriented if it is mono–oriented on each $\mathcal{P}\cap\mathfrak{M}$, $\mathcal{P}$ being an orthant of $\mathbb{R}^n$, and the hypercubes in orthant $\mathcal{P}$ are not equivalent to hypercubes in $\mathfrak{M} \setminus (\mathcal{P} \cap \mathfrak{M})$, for all orthants $\mathcal{P}$.

As stated in Section 5.2, solution approximations are needed for both verification and construction of a finite–time and classical LF, respectively. Thereto, we state two methods for obtaining numerical approximations of trajectories. The first method is called the piecewise affine vector field method, described in Appendix A.1. The second method is the fourth-order Runge-Kutta method, described in Appendix A.2. Both methods are illustrated by examples in Appendix A.3. Consider the map $W_{\mathcal{V}} : \mathcal{V}_{\mathfrak{T}} \to \mathbb{R}_{\geq 0}$. Similarly to the

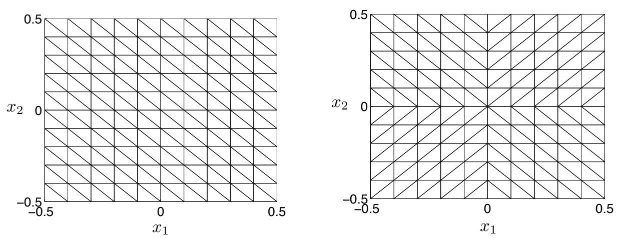

(a) Example of a mono–oriented triangulation in $\mathbb{R}^2$.

(b) Example of a poly–oriented triangulation in $\mathbb{R}^2$.

Figure 5.1: Triangulation examples in $\mathbb{R}^2$.

piecewise affine construction for the vector field in Appendix A.1, $W_{\mathcal{V}}$ can be extended to a unique piecewise affine map $W : \mathfrak{M} \to \mathbb{R}_{\geq 0}$. Indeed, for each simplex $\mathfrak{S}_i \in \mathfrak{T}$, $i \in \mathbb{N}_{[1:z]}$, the unique affine interpolation that interpolates $W_{\mathcal{V}}$ at the vertices $v_0, \ldots, v_n$ of $\mathfrak{S}_i$ is given by

$$W_{\mathfrak{S}_i}(x) = \sum_{j=0}^{n} \lambda_j(x) f(v_j) = a_i^\top x + b_i,$$

where

$$x = \sum_{j=0}^{n} \lambda_j(x) v_j, \quad \sum_{j=0}^{n} \lambda_j(x) = 1, \quad \forall x \in \mathfrak{S}_i.$$

The continuous piecewise affine function is now given by $W(x) = W_{\mathfrak{S}_i} := a_i^\top x + b_i$ for all $x \in \mathfrak{S}_i$. Note that $W(x) = W_{\mathcal{V}}(x)$ for all $x \in \mathcal{V}_{\mathfrak{T}}$. Moreover, note that $\nabla W_{\mathfrak{S}_i}^\top = a_i^\top$.

5.4.1 Construction in the Massera case

The construction of a LF for the system (4.1) can be achieved by first considering a FTLF candidate $\eta(\|x\|)$, $\eta \in \mathcal{K}_\infty$, with a candidate d-invariant set $\mathfrak{M}$, and consequently computing a classical LF using (5.2). When the analytical solution to (4.1) is not known, the following procedure is proposed to obtain a CPA LF using numerical approximations:

1. Let $\mathfrak{M} \subset \mathbb{R}^n$ be a proper candidate d-invariant set and let $V(x) = \eta(\|x\|)$ be a candidate FTLF. Create a (proper) triangulation $\mathfrak{T}$ of $\mathfrak{M}$ with corresponding vertex

set $\mathcal{V}_{\mathfrak{T}}$. Compute a $d \in \mathbb{R}_{>0}$ for which the finite–time condition

$$V(x(d)) - V(x(0)) < 0, \tag{5.7}$$

holds for all $x(0) \in \mathcal{V}_{\mathfrak{T}}$, by means of numerical approximations of the solution $x(t)$, using the piecewise affine vector field method.

2. Compute the map $W_{\mathcal{V}} : \mathcal{V}_{\mathfrak{T}} \to \mathbb{R}_{\geq 0}$. That is, compute

$$W_{\mathcal{V}}(x(0)) = \int_0^d V(x(\tau))\, \mathrm{d}\tau,$$

for all $x(0) \in \mathcal{V}_{\mathfrak{T}}$, where $x(\tau)$ is the numerical approximation of the solution of (4.1) initiated in $x(0)$, using the fourth-order Runge-Kutta method.

3. Compute a continuous piecewise affine map $W : \mathfrak{M} \to \mathbb{R}_{\geq 0}$ from $W_{\mathcal{V}}$ by interpolation.

In the preceding algorithm, we use the piecewise affine vector field method in Step 1, because of the analytical expression of the solution. That is, we can determine d precisely, in contrast to the fourth-order Runge-Kutta method, where we are limited by a fixed time step h. In Step 2, we use the Runge-Kutta method to reduce computational effort.

5.4.2 Verification

We know that the function computed using (5.2) is a true classical LF for (4.1). However, due to numerical approximations of the trajectories and affine interpolation of $W_{\mathcal{V}}$, W is not guaranteed to be a LF on $\mathfrak{M}$. Therefore, we need verification of the derivative of W along the trajectories being negative definite, $\dot{W}(x(t)) < 0$, for some proper set. Since the CPA LF W is continuous, and in general not continuously differentiable, the orbital derivative $\dot{W}(x(t))$ is replaced by the Dini derivative of W, which is equal to $\nabla W_{\mathfrak{S}_i}^\top f(x)$ for all $x \in \mathfrak{S}_i$, $\mathfrak{S}_i \in \mathfrak{T}$ [49]. We state two methods for verification.

The following theorem [13] states that we only need to verify a condition at the vertices of a simplex, to verify whether the derivative of the affine LF along trajectories is negative definite on the whole simplex.

Theorem 5.2 Consider the system (4.1), let $\mathfrak{T} = \{\mathfrak{S}_1, \ldots, \mathfrak{S}_z\}$ be a triangulation of $\mathfrak{M}$ and assume that $f(\cdot)$ is twice continuously differentiable on $\mathfrak{M}$. Let $W : \mathfrak{M} \to \mathbb{R}_{\geq 0}$, $W_{\mathfrak{S}_i}(\xi) := a_i\xi + b_i$ for all $\xi \in \mathfrak{S}_i$, be the continuous and piecewise affine interpolation of $W_{\mathcal{V}} : \mathcal{V}_{\mathfrak{T}} \to \mathbb{R}_{\geq 0}$. For each $\mathfrak{S}_i \in \mathfrak{T}$, let constants be defined by $h_i := \mathrm{diam}(\mathfrak{S}_i)$,

$$E_i := \frac{nB_i}{2} h_i^2,$$

where

$$B_i \geq \max_{j \in \mathbb{N}_{[1:n]}} \sup_{\xi \in \mathfrak{S}_i} \|H_{f^j}(\xi)\|_{\max},$$

with H_{fj} the Hessian of the j-th entry of f. Then, for every simplex $\mathfrak{S}_i = \mathrm{co}\{v_0, \cdots, v_n\}$ where the inequality

$$\nabla W_{\mathfrak{S}_i}^\top f(v_k) + E_i \|\nabla W_{\mathfrak{S}_i}^\top\|_1 < 0$$

holds for all $k \in \mathbb{N}_{[0:n]}$, the inequality

$$\nabla W_{\mathfrak{S}_i}^\top f(\xi) < 0$$

holds for all $\xi \in \mathfrak{S}_i$.

While the above theorem provides a way to verify the continuous and piecewise affine function W, it may not yield satisfactory results regarding estimation of the domain of attraction, because it can be conservative. We propose a method that is in fact not conservative. Clearly, we have that

$$\max_{\xi \in \mathfrak{S}_i} \nabla W_{\mathfrak{S}_i}^\top f(\xi) < 0 \Leftrightarrow \nabla W_{\mathfrak{S}_i}^\top f(\xi) < 0, \quad \forall \xi \in \mathfrak{S}_i.$$

Thereto, we propose to solve the following optimization problem

$$\begin{aligned} \max_{\xi} \quad & \nabla W_{\mathfrak{S}_i}^\top f(\xi) < 0 \\ \text{s.t.} \quad & \xi \in \mathfrak{S}_i, \end{aligned}$$

on each simplex $\mathfrak{S}_i \in \mathfrak{T}$. Using the definition of the simplex (Definition 5.1) and thus barycentric coordinates $\lambda = (\lambda_0, \ldots, \lambda_n)^\top$, the problem is rewritten as

$$\begin{aligned} \min_{\lambda} \quad & -\nabla W_{\mathfrak{S}_i}^\top f\left(\sum_{i=0}^{n} \lambda_i v_i\right) > 0 \\ \text{s.t.} \quad & 0 \leq \lambda_i \leq 1, \quad i \in \mathbb{N}_{[0:n]}, \\ & \sum_{i=0}^{n} \lambda_i = 1. \end{aligned}$$

To guarantee that the global minimum for the nonlinear problem is found, we need the objective function to be either concave or convex on the simplex $\mathfrak{S}_i$. Thereto, since the simplex diameter is chosen "small" in general, we state the following reasonable assumption.

Assumption 5.1 The map $\nabla W_{\mathfrak{S}_i}^\top f : \mathfrak{S}_i \to \mathbb{R}$ is either concave or convex, for all $\mathfrak{S}_i \in \mathfrak{T}$.

Indeed, if the objective function is convex, a local minimum is equal to the global minimum. Moreover, if the function is concave, the minimum will be attained at an extreme point (vertex) v_i [64].

5.5 Numerical examples

In what follows, a step size of $h = 0.05$ and simplex diameter of $h\sqrt{n}$ are used for the fourth-order Runge Kutta and piecewise affine vector field method, respectively, where n is denotes the state dimension.

5.5.1 *Example 1: 2D example from literature - Approach 5.3*

Consider the system in [48, Example 1], described by

$$\begin{cases} \dot{x}_1 &= x_2, \\ \dot{x}_2 &= -x_1 + \frac{1}{3}x_1^3 - x_2. \end{cases} \tag{5.8}$$

This system has an exponentially stable equilibrium at the origin and two saddle equilibria at $\pm(\sqrt{3}\;0)^\top$. We let the candidate d-invariant set be $\mathfrak{M} = \{x \in \mathbb{R}^n \mid \|x\|_\infty \le 3\}$ and create a proper poly–oriented triangulation $\mathfrak{T}$ of $\mathfrak{M}$ with uniform simplex diameter $h = 0.05\sqrt{2}$. Let the candidate FTLF be $V(x) = \|x\|_1$. We find that for all $x \in \mathcal{V}_\mathfrak{T}$, for which there exists a d such that the finite–time condition holds, the condition (5.1) holds for $d = 2.6651$. Next,

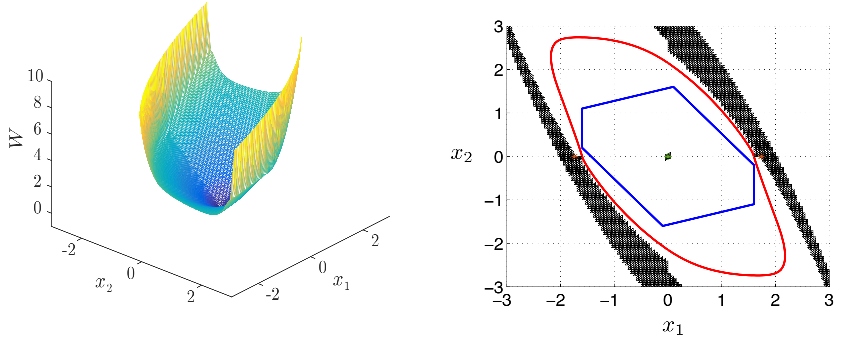

(a) Computed LF W for (5.8).

(b) Level set $W(x) = 4.25$-red, polytope containing approximation of domain of attraction from [48]-blue and the simplices where $W(x)$ is not verified-black.

Figure 5.2: LF computed for (5.8).

we compute the function $W_\mathcal{V}$, i.e.

$$W_\mathcal{V}(x(0)) = \int_0^d \|x(\tau)\|_1 \,\mathrm{d}\tau,$$

for all $x(0) \in \mathcal{V}_\mathfrak{T}$, from the approximated trajectories and construct its unique continuous piecewise affine interpolation W. In Figure 5.2(a) we show the computed LF for (5.8).

In Figure 5.2(b) we show the simplices where $\nabla W_{\mathfrak{S}_i}^\top f(x)$ is not negative definite together with the level set $W(x) = 4.25$. By analyzing the Hessian of $\nabla W_{\mathfrak{S}_i}^\top f(x)$, it is easily seen the function is indeed concave or convex on each simplex $\mathfrak{S}_i$ and the obtained results are thus guaranteed. Utilizing Theorem 2.1, we find that $\mathcal{S}_\mathcal{A} = \{x \in \mathbb{R}^n \mid W(x) < C^* = 4.25\}$ is an approximation of the domain of attraction, i.e. a subset of the true domain of attraction of the system. For this system a CPA LF was computed using the RBF method and the Massera construction in [48] and [12], respectively. The approximation of the domain of attraction obtained using the method proposed in this report shows improvement, cf. [48, Figure 4] and [12, Figure 11].

5.5.2 *Example 2: 3D example from literature*

Consider the system in [14, Example 5], given by

$$\begin{cases} \dot{x}_1 &= x_1(x_1^2 + x_2^2 - 1) - x_2(x_3^2 + 1), \\ \dot{x}_2 &= x_2(x_1^2 + x_2^2 - 1) + x_1(x_3^2 + 1), \\ \dot{x}_3 &= 10x_3(x_3^2 - 1). \end{cases} \tag{5.9}$$

This system has an exponentially stable equilibrium in the origin with the true domain of attraction given by the cylinder [48]

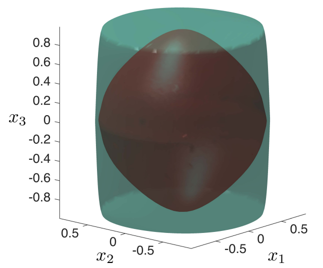

(a) Level set $W(x) = 1.20$-green and the domain of attraction approximation from [14]-red.

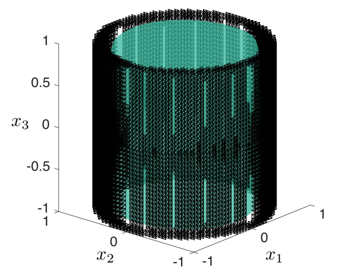

(b) Level set $W(x) = 1.20$-green and the simplices for which W is not verified-black.

$$\mathcal{A} = \{x \in \mathbb{R}^n \mid x_1^2 + x_2^2 < 1, |x_3| < 1\}. \tag{5.10}$$

In [14], a CPA Lyaponov function was computed using the RBF method, resulting in the domain of attraction shown in Figure 5.3(a) in red, available at `www.ru.is/kennarar/sigurdurh/MICNON2015CPP.rar`. The blue dots represent the midpoints of the simplices where the CPA LF is not verified.

5.5.2.1 Construction of a LF by means of approximated trajectories

Let $\mathfrak{M} = \{x \in \mathbb{R}^n \mid \|x\|_\infty \leq 1\}$ and consider the function $V(x) = \|x\|_1$. The proper poly–oriented triangulation of $\mathfrak{M}$ is given by $\mathfrak{T}$, with uniform simplex diameter $h = 0.05\sqrt{3}$. For the corresponding vertex set $\mathcal{V}_\mathfrak{T}$, it is found that for all initial conditions in $\mathcal{V}_\mathfrak{T}$ for which there exists a d such that (5.1) holds, inequality (5.1) is satisfied for $d = 1.5481$.

From the obtained map $W_\mathcal{V} : \mathcal{V}_\mathfrak{T} \to \mathbb{R}_{\geq 0}$, the continuous piecewise affine interpolation W is obtained. In Figure 5.3(b) we show the tetrahedra for which the derivative along the trajectories of W is positive definite, together with the level set $W(x) = 1.20$. Figure 5.3(a) shows the level set $W(x) = 1.20$, i.e. the approximated domain of attraction, in green. Comparing with the true domain of attraction (5.10), the approximated domain of attraction $\mathcal{S}_\mathcal{A}$ has a “cylinder like” shape with $\max_{x \in \mathcal{S}_\mathcal{A}} x_1^2 + x_2^2 \approx 0.87^2$ and $\max_{x \in \mathcal{S}_\mathcal{A}} |x_3| \approx 0.99$.

5.5.2.2 Construction of a LF by means of linearization

We apply the steps described in Section 5.3 for verification starting with the linearized dynamics corresponding to (5.9). Let $V(x) = x^\top Px$ where P is the identity matrix. Then, the condition (5.3) holds with $d = 0.2$. In Figure 5.3 the level set defined by $W(x) = 0.19$ is plotted with green (inner set) together with the zero level set of $\dot{W}(x)$ in red. The value of $C = 0.19$ was obtained by solving the feasibility problem (5.6).

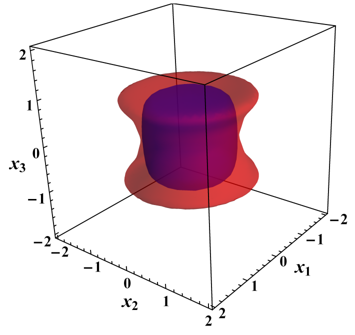

Figure 5.3: Validation of level set of W: $\nabla^\top W f = 0$–red, level set of $W(x) = 0.19$–green.

5.5.3 *Example 3: 2D example from literature*

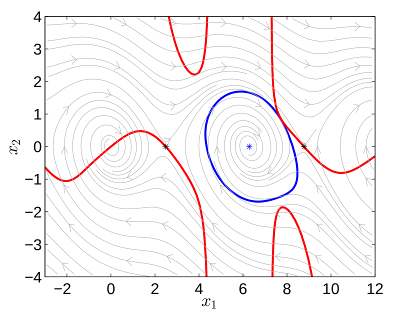

Figure 5.4: The level set $W(x) = 5$–blue, its derivative $\dot{W} = 0$–red, the stable equilibrium E_1–blue and the unstable ones E_1, E_2–black together with the vector field plot for (5.11).

Consider the system:

$$\begin{aligned} \dot{x_1} &= x_2 \\ \dot{x_2} &= 0.301 - \sin(x_1 + 0.4136) + 0.138 \sin 2(x_1 + 0.4136) - 0.279 x_2, \end{aligned} \tag{5.11}$$

with the stable equilibrium $E_1 = (6.284098 \quad 0)^\top$, and the two unstable equilibria $E_2 = (2.488345 \quad 0)^\top$, $E_2 = (8.772443 \quad 0)^\top$. This system was studied in [29] with the purpose to compute the stability boundary of E_1. By applying the steps described in Section 5.3 for verification starting with the linearized dynamics, for $V(x) = x^\top P x$ where $P = \left(\begin{smallmatrix} 1.6448 & 0.3430 \\ 0.3430 & 2.1255 \end{smallmatrix}\right)$, the condition (5.3) holds with $d = 0.8$. The resulting LF $W = \int_0^d V(x + \tau f(x)) \mathrm{d}\tau$ leads to the DOA estimate defined by $C = 5$ and plotted in Figure 5.4

with blue contour. The zero level set of the corresponding derivative $\dot{W} = \nabla W(x)^\top f(x) = 0$ is shown with red.

5.6 Conclusions

We have developed an algorithm for the construction of a continuous and piecewise affine LF based on a novel Massera–type converse, enabled by a candidate $\mathcal{K}_\infty$ function of the norm of the state, verifying a finite–time condition. Albeit by numerical approximations, we verify the finite–time condition on a candidate d-invariant set, yielding an upper limit for the integral in the converse theorem. Together with an extra degree of freedom for the construction of the LF, i.e. based on any $\mathcal{K}_\infty$ function of the norm of the solution, the algorithm delivers promising results towards obtaining nonconservative approximations of the domain of attraction. By two- and three-dimensional examples, we have shown that our method can deliver better results than existing CPA methods. Furthermore, we obtained nonconservative estimates of the domain of attraction for the illustrative, theoretical examples.

As for possible improvements for the proposed method, one may consider local refinements in the triangulation for the domain of the CPA LF to obtain even less conservative estimates of the domain of attraction, and to reduce overall computational effort, such that the domain $\mathfrak{M}$ could be enlarged, if necessary.

Chapter 6

Application to biological systems

In this chapter the procedures derived in Chapters 4 and 5 will be applied to a range of models describing biological systems, to illustrate the solutions proposed in this thesis for the analysis and stabilization problems described in Chapter 1.

6.1 Toggle switch in Escherichia coli

Consider the genetic toggle switch in Escherichia coli constructed in [40],

$$\begin{aligned} \dot{x}_1 &= \frac{\alpha_1}{1+x_2^{\beta}} - x_1 \\ \dot{x}_2 &= \frac{\alpha_2}{1+x_1^{\gamma}} - x_2. \end{aligned} \tag{6.1}$$

The genetic toggle switch is a synthetic, bistable gene–regulatory network, constructed from any two repressible promoters arranged in a mutually inhibitory network. The model (6.1), proposed in [40] for description of a synthetic toggle switch in Escherichia coli (E. coli), was derived from a biochemical rate equation formulation of gene expression. For this model, the set of parameters for which bistability is ensured is especially of interest, as it accommodates the real behavior of the toggle switch. The switching behavior is ensured by flipping the system between the stable states. The implications of the toggle switch circuit as an addressable memory unit are in biotechnology and gene therapy. When at least one of the parameters $\beta, \gamma > 1$, bistability occurs. In (6.1), x_1 denotes the concentration of repressor 1, x_2 is the concentration of repressor 2, α_1 is the effective rate of synthesis of repressor 1, α_2 is the effective rate of synthesis of repressor 2, β is the cooperativity of repression of promoter 2 and γ is the cooperativity of repression of promoter 1. The rational terms in the above equations represent the cooperative repression of constitutively transcribed promoters and the linear terms represent the degradation/dilution of the repressors.

The two possible stable states are one in which promoter 1 transcribes repressor 2, which we denote by E_1 and corresponds to a high value for the x_2 state, and one in which promoter 2 transcribes repressor 1, which we denote by E_3 and corresponds to a high value for the x_1 state. Let the parameters be defined by $\alpha_1 = 1.3$, $\alpha_2 = 1$, $\beta = 3$ and $\gamma = 10$. For this set of parameters the stable equilibria are $E_1 = \begin{pmatrix} 0.668 & 0.9829 \end{pmatrix}^\top$

and $E_3 = \begin{pmatrix}1.2996 & 0.0678\end{pmatrix}^\top$. The unstable equilibrium is $E_2 = \begin{pmatrix}0.8807 & 0.7808\end{pmatrix}^\top$. The separation between the DOAs corresponding to E_1 and E_3 is achieved by the stability boundary or separatrix. It is known that the unstable equilibrium E_2 belongs to the stability boundary [29]. Note that although (6.1) is not a system of the form in (4.1), as its stable equilibria are not located at the origin, we can still apply the tools derived in Chapters 4 and 5 by applying the change of variable $\xi_i := x_i - E_i$, $i = 1, 3$.

In [40], the necessary conditions for bistability were analyzed based on the model (6.1) and validated by implementation on E. coli plasmids. In the same paper, it is argued that synthetic gene circuits, such as the toggle switch, can serve as highly simplified, highly controlled models of natural gene networks.

For controlling the behavior of the toggle switch such that it achieves certain properties, it is important to compute the two DOAs corresponding to the stable equilibria. This problem was addressed in the literature, specifically for gene regulation, by means of PWA approximating dynamics [120] and by computing reachable sets via a linear temporal logic formalism. Since the PWA approximation is based on modeling gene regulation by ramp functions, they will induce three regions of different dynamics. In the end, for the toggle switch example this leads to nine polyhedral regions. While the approach in [120] leads to a close estimate of the separatrix, as pointed out by the authors of the paper, the method is very computationally expensive.

In what follows we will apply the methods proposed in Chapter 5 for computing the DOAs of E_1 and E_3.

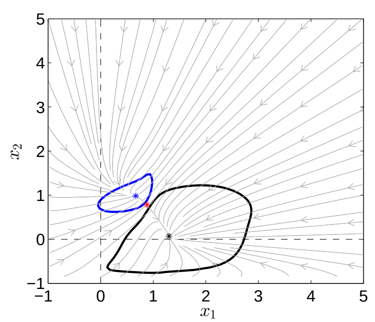

Figure 6.1: Level sets of the computed LFs corresponding to E_1–blue and E_3–black for the toggle switch system (6.1) together with vector field plots. The unstable equilbrium E_2 is plotted with the red marker.

6.1.1 Construction of a LF by means of linearization

By following the procedure in Section 5.3, the DOAs corresponding to E_1 and E_3 were computed and are shown in Figure 6.1. Note that the computation procedure needs to be carried out for the origin equilibrium. As such, by translating each nonzero equilibrium to the origin a different system is obtained. For each system corresponding to E_1 and E_3, a quadratic FTLF candidate was considered, where the matrix P is the solution of the classical Lyapunov inequality $A^\top P + PA < -I_2$, where I_2 denotes the identity matrix and $A = \left[\frac{\partial f(x)}{\partial x}\right]_{x=E_i}$ for each $i = 1, 3$. The blue level set defined by $C_1 = 0.07$ and $d = 1.2$ corresponds to E_1 and the black level set defined by $C_3 = 0.8$ and $d = 0.4$ corresponds to E_3. The trajectories starting from initial conditions close to the stability boundary will go to E_2 and from there via its unstable directions, they will converge either to E_1 or E_3. As shown in Figure 6.1, the DOA estimates go very close to E_2 (red), thus close to the stability boundary. However, the computed sets seem conservative with respect to the directions of the vector fields for initial conditions far from the equilibria in the positive orthant. This is due to the fact that higher level sets of the corresponding LFs would intersect with the unstable equilibrium and violate the stability boundary. In fact, this is not an issue for the toggle switch as the real–life behavior is centred around the three equilibria and stability boundary.

6.1.2 Construction of a LF by means of approximated trajectories

Consider E_1 and the candidate finite–time Lyapunov function $V_1(x) = \|x - E_1\|_1$ on the candidate d-invariant set $\mathfrak{M}_1 = [-1, 1] \times [-1, 1.2]$ for the shifted variable $\xi_1 = x - E_1$. We create a proper mono–oriented triangulation $\mathfrak{T}_1$ of $\mathfrak{M}_1$ with a uniform simplex diameter $h = 0.025\sqrt{2}$. The corresponding vertex set is $\mathcal{V}_{\mathfrak{T}_1}$. Then for all $x \in \mathcal{V}_{\mathfrak{T}_1}$, for which there exists a d such that the finite–time condition holds, the condition (5.7) holds for $d = 5.4352$. We compute the map $W_{1,\mathcal{V}} : \mathcal{V}_{\mathfrak{T}_1} \to \mathbb{R}_{\geq 0}$ and its unique continuous piecewise affine interpolation W_1. Figure 6.2(a) shows the computed Lyapunov function W_1 and Figure 6.3(a) shows some relevant level sets of W_1. Note that the figures show the plots for the original system and not the translated system. In Figure 6.3(b) the level

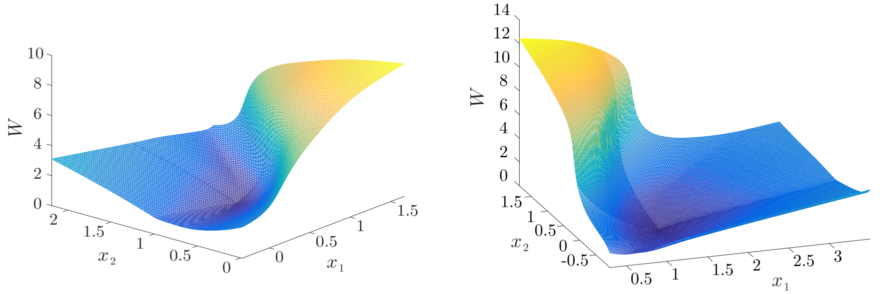

(a) (b)

Figure 6.2: (a)–Computed Lyapunov function W_1 for E_1 of (6.1); (b)–Computed Lyapunov function W_3 for E_3 of (6.1).

set $W_1(x) = 0.98$ is plotted in red together with the simplices in the triangulation $\mathfrak{T}_1$ for which the derivative of W_1 along the trajectories is not negative definite. The set $\mathcal{S}_{\mathcal{A}_1} = \{x \in \mathbb{R}^n \,|\, W_1(x) < 0.98\}$ is contained in the true domain of attraction. Similarly, we compute a Lyapunov function and an approximation of the domain of attraction for the equilibrium E_3. Let the candidate d-invariant set for the shifted variable $\xi_3 = x - E_3$ be

$\mathfrak{M}_3 = [-1,\, 2.2] \times [-1,\, 1.8]$ and take $V_3(x) = \|x - E_3\|_1$. We let the triangulation of $\mathfrak{M}_3$, $\mathfrak{T}_3$, be proper and poly–oriented with the same simplex diameter as for E_1. We find $d = 6.7507$ and consequently compute $W_{3,\mathcal{V}} : \mathcal{V}_{\mathfrak{T}_1} \to \mathbb{R}_{\geq 0}$. We show the computed Lyapunov function W_3 in Figure 6.2(b) and some level sets in Figure 6.4(a). In Figure 6.4(b) the

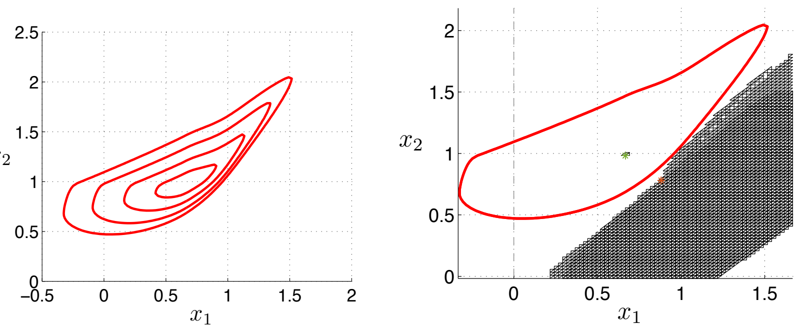

(a) Some level sets of the computed Lyapunov function W_1 for (6.1).

(b) Level set $W_1(x) = 0.98$-red and the simplices where $W_1(x)$ is not verified-black.

Figure 6.3: Computation of the DOA of E_1 for (6.1).

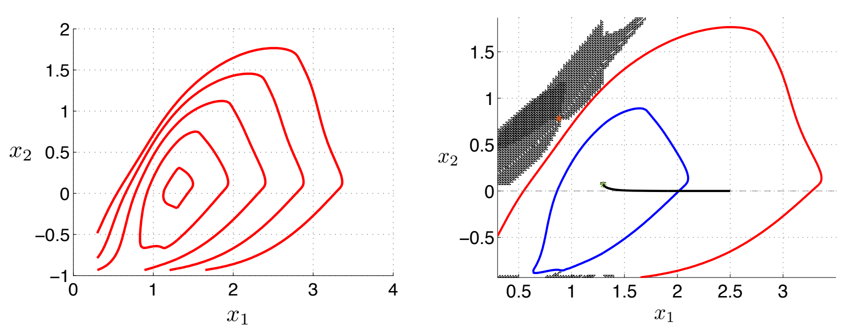

(a) Some level sets of the computed Lyapunov function W_3 for (6.1).

(b) Level set $W_3(x) = 2.25$-red and the simplices where $W_3(x)$ is not verified-black.

Figure 6.4: Computation of the DOA of E_3 for (6.1).

level set $W_3(x) = 2.25$ is plotted in red together with the simplices in the triangulation $\mathfrak{T}_3$ for which the derivative of W_3 along the trajectories is not negative definite. Since the positive orthant $\mathcal{P}$ is positive invariant, we conclude using Theorem 5.1, that the set $\mathcal{S}_{\mathcal{A}_3} = \{x \in \mathbb{R}^n \mid W_3(x) \leq 2.25\} \cap \mathcal{P}$ is contained in the domain of attraction for E_3.

6.1.3 Discussion

The resulting DOA estimates computed by the two verification approaches are rather similar, with the sets in Subsection 6.1.2 capturing slightly larger areas outside the stability boundary. Thus, we can provide guarantees that once a trajectory is initiated in one of the two sets it will remain in that set for all time and converge to either E_1 or E_2 correspondingly. If a certain behavior is desired, for example that a trajectory converges to E_1 and after some time it is steered away to E_3, then a stabilizing feedback control which globally (or at least in the positive orthant) stabilizes E_3 is needed. This will be addressed in Section 6.4.

6.2 The hypothalamic-pituitary-adrenal gland (HPA) axis

The following model was proposed in [6] to illustrate the behavior of the Hypothalamic-Pituitary-Adrenal (HPA) axis which was schematically described in Chapter 1.

$$\begin{aligned}
\dot{x}_1 &= \left(1 + \xi \frac{x_3^\alpha}{1 + x_3^\alpha} - \psi \frac{x_3^\gamma}{x_3^\gamma + \tilde{c}_3^\gamma}\right) - \tilde{w}_1 x_1 \\
\dot{x}_2 &= \left(1 - \rho \frac{x_3^\alpha}{1 + x_3^\alpha}\right) x_1 - \tilde{w}_2 x_2 \\
\dot{x}_3 &= x_2 - \tilde{w}_3 x_3.
\end{aligned} \tag{6.2}$$

The HPA axis is a system which acts mainly at maintaining body homeostasis by regulating the level of cortisol. The three hormones involved in the HPA axis are the CRH (x_1), the ACTH (x_2) and the cortisol (x_3).

For certain parameter values the system (6.2) has a unique stable equilibrium, which relates to cortisol level returning to normal after periods of mild stress in healthy individuals. When the parameters are perturbed, bifurcation can occur which leads to bistability. The stable states correspond to hypercortisolemic and hypocortisolemic equilibria, respectively.

There are several models developed in the literature aimed at matching observations from patient data by including different mechanisms in the HPA model. We recall here the models developed and studied in [55], [10], and [54]. The model (6.2) includes the effects from the hippocampus on the HPA axis via its influence on the CRH (x_1) in the hypothalamus. For physiologically reasonable parameter values, no oscillations were found, thus the authors of [6] concluded that the ultradian rhythm observed in data is generated by different mechanisms influencing the HPA axis.

In [55] a different approach is considered, which includes the glucocorticoid receptor (GR) in the pituitary gland which is influenced by cortisol. In this case, bistability is also observed, but the stable equilibria correspond to low GR concentrations (normal of healthy steady state) and high GR concentrations (nonhealthy steady state). The cortisol levels corresponding to each of the stable states do not differ as much as in the case of the system (6.2).

In [54], a four states model is considered, where the additional state corresponds to a regulatory substance describing the processes that occur in the hypothalamus, which further interacts with CRH. The therein derived model was capable of capturing circadian and ultradian oscillations of the hormone concentrations related to the HPA axis and matches data from patients. Similarly to the model discussed in this chapter, a relation between abnormal cortisol values and depression is emphasized.

In what follows, the model (6.2) developed in [6] will be studied. The motivation from choosing this model comes from the following arguments. The model (6.2) is able to capture bistability corresponding to low and high cortisol levels, which have been observed in chronically depressed people. Based on the comparison between different models carried out in [65] on data from 17 patients (i.e., values of ACTH (x_2) and cortisol), the considered model performed the best. Finally, since it has three states, it is suitable for illustrating our tools, since the DOA set estimates can be visualized in plots.

As such, for the parameter values $\tilde{w}_1 = 4.79$, $\tilde{w}_2 = 0.964$, $\tilde{w}_3 = 0.251$, $\tilde{c}_3 = 0.464$, $\psi = 1$, $\xi = 1$, $\rho = 0.5$, $\gamma = \alpha = 5$, the HPA system has three equilibria,

$$E_1 = \begin{pmatrix} 0.1170 & 0.1199 & 0.4778 \end{pmatrix}^\top,$$
$$E_2 = \begin{pmatrix} 0.2224 & 0.2017 & 0.8039 \end{pmatrix}^\top,$$
$$E_3 = \begin{pmatrix} 0.7833 & 0.4316 & 1.7196 \end{pmatrix}^\top,$$

with E_1 and E_3 stable and E_2 unstable. By following the same steps as those indicated in the case of the toggle switch system, for the E_1 equilibrium the level set defined by $C_1 = 0.08$ and $d = 0.4$ is plotted in Figure 6.5 (the lower set) and for the E_2 equilibrium the level set defined by $C_2 = 1$ and $d = 0.4$ is plotted in Figure 6.5 (the upper set). It is worth noting that

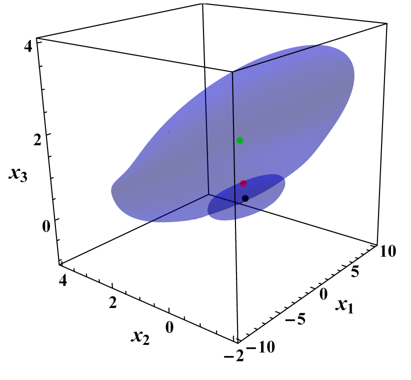

Figure 6.5: Level sets of the computed LFs corresponding to E_1 and E_3 for the HPA system (6.2). The corresponding equilibria are E_1–green marker, E_2–red marker and E_3–black marker.

for this system, the logarithmic norm defined by taking the 2–norm, $\mu_2(A)$ is positive, with $A = \left[\frac{\partial f}{\partial x}\right]_{x=E_1}$. Thus, equality (4.24) will not be satisfied. However, since the considered FTLF is $V(x) = x^\top Px$, then the weighted logarithmic norm satisfies $\mu_{2,P}(A) < 0$.

6.3 The repressilator

Regulatory molecular networks, especially the oscillatory networks, have attracted a lot of interest from biologists and biophysiscists because they are found in many molecular pathways. Abnormalities of these processes lead to various diseases, from sleep disorders to cancer. The naturally occurring regulatory networks are very complex, so their dynamics have been studied by highly simplified models [21], [37]. These models are particularly valuable because they can provide an understanding of the important properties in the naturally occurring regulatory networks and, thus, support the engineering of artificial ones. Moreover, these rather simple, models can describe behaviors observed in experiments rather well [37].

An example of such a network is the repressilator. Its genetic implementation uses three proteins that cyclically repress the synthesis of one another. A model for the reprissilator

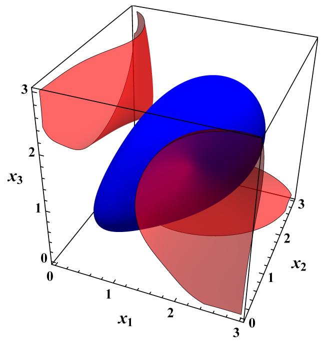

(a) The level set $W(x) = 0.32$–blue and $\dot{W} = 0$–red.

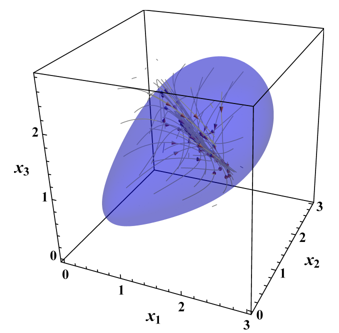

(b) The level set $W(x) = 0.32$ and some trajectories of (6.3).

Figure 6.6: Computation of the DOA of $E = (1.516, 1.516, 1.516)^\top$ for (6.3).

was first proposed in [37] and we consider here the simplified version from [21]:

$$\begin{aligned}\dot{x}_1 &= \frac{\alpha}{1+x_2^\beta} - x_1\\ \dot{x}_2 &= \frac{\alpha}{1+x_3^\beta} - x_2\\ \dot{x}_3 &= \frac{\alpha}{1+x_1^\beta} - x_3.\end{aligned} \tag{6.3}$$

The states x_1, x_2, and x_3 are proportional to protein concentrations. All negative terms in the right–hand side represent degradation of the molecules. The nonlinear function $h(x) = \frac{1}{1+x^\beta}$ reflects synthesis of the mRNAs from the DNA controlled by regulatory elements called promoters. β is called cooperativity and reflects multimerization of the protein required to affect the promoter. The three proteins are assumed to be identical, rendering the model symmetric and the order in choosing the states x_1, x_2 and x_3 does not influence the analysis outcome.

In [21] it was shown that for $\alpha > 0$ and $\beta > 1$, there is only one equilibrium point for the system (6.3), of the type $E = (r, r, r)^\top$, where r satisfies the equation $r^{\beta+1} + r - \alpha = 0$.

For the values $\alpha = 5$ and $\beta = 2$, $r = 1.516$ and the eigenvalues of its corresponding linearized matrix are $\lambda = (-2.3936, -0.3032+1.2069i, -0.3032-1.2069i)$. By following the procedure in Section 5.3 with the FTLF candidate $V(x) = x^\top P x$, with P the identity matrix the value $d = 0.4$ was obtained. For the obtained function $W = \int_0^d V(x + \tau f(x))\mathrm{d}\tau$ the level set given by $C = 0.32$ was checked to be a subset of the true DOA of the system and it is plotted in Figure 6.6(a) with blue. The zero level set of $\dot{W} = \nabla W^\top f(x)$, where $f(x)$ denotes the map describing (6.3) is plotted in Figure 6.6(a) with red. In Figure 6.6(b) the level set $W(x) = 0.32$ is shown together with some trajectories of (6.3).

6.4 Feedback stabilization via Sontag's "universal" controller

For systems subject to control inputs, of the type

$$\dot{x} = f(x) + g(x)u \tag{6.4}$$

where $u \in \mathbb{U} \subseteq \mathbb{R}^m$ denotes the input and $f : \mathbb{R}^n \to \mathbb{R}^n$ and $g : \mathbb{R}^n \to \mathbb{R}^{n\times m}$ with $f(0) = 0$ and $g(0) = 0$, recall the concept of a CLF defined by Definition 2.10.

For systems defined as in (6.4), when a CLF W is known, an explicit formula for a state feedback control that renders the system asymptotically stable, was provided in [106]. We recall it below as defined in [106]. Note that in the remainder of this chapter we consider the case when u is a scalar.

Let $u = k(a(x), b(x)^\top)$, where $a(x) := \nabla W(x)^\top f(x)$, $b(x) = \nabla W(x)^\top g(x)$, and k is a function $k : \mathbb{R} \times \mathbb{R}^m \to \mathbb{R}$ defined by

$$k(a, b) := \begin{cases} -\frac{a+\sqrt{a^2+b^4}}{b}, & \text{if } b \neq 0 \\ 0, & \text{if } b = 0. \end{cases} \tag{6.5}$$

The above feedback law is a consequence of an explicit proof provided in [106] for a result from [7] stating that if there exists a CLF, smooth, then there must exists a feedback law $u = k(x)$, $k(0) = 0$, which globally stabilizes the system and which is smooth on $\mathbb{R}^n \setminus \{0\}$, if the functions f and g are smooth. Moreover, from [106] it is known that k is also continuous in the origin if V satisfies a small control property, defined in the same paper. The analytic construction (5.4) will yield a Lyapunov function for autonomous systems which is valid in the set where $\dot{W} = \nabla W(x)^\top f(x) < 0$ as discussed in Chapters 4 and 5. By using the expression of $W(x)$ for the uncontrolled case in (6.5), a global stabilizer $u = k(a, b)$ will be determined for systems of the type (6.4).

6.4.1 Control of the genetic toggle switch

We apply the formula (6.5) for stabilizing the equilibrium E_1 of the toggle switch system (6.1) and we consider the input $u = k(x)$ to act on the x_2 state, thus let $g(x) = (0\ 1)^\top$ and $f(x)$ be the function describing the autonomous system (6.1). By using the feedback stabilizer defined in (6.5), the LF $W_1(x)$ computed in Section 6.1.1 was used as a CLF candidate, in the expression of $k(a, b)$. In Figure 6.7(a) we show the vector field plot of the controlled toggle switch together with some level sets of W_1. In Figure 6.7(b) we show a plot of $k(x(t))$, corresponding to the initial condition which generates the trajectory shown with black in Figure 6.7(a). It can be observed that all trajectories converge to the E_1 equilibrium.

6.4.2 Control of the HPA axis

The feedback stabilizer defined in (6.5) will be applied in what follows for the stabilization of the healthy equilibrium of the HPA axis system, E_2. Differently than in the toggle switch case, E_2 is an unstable equilibrium. In this case we consider the CLF candidate $W(x) = (x - E_2)^\top P(x - E_2)$, where P is computed such that the linearized

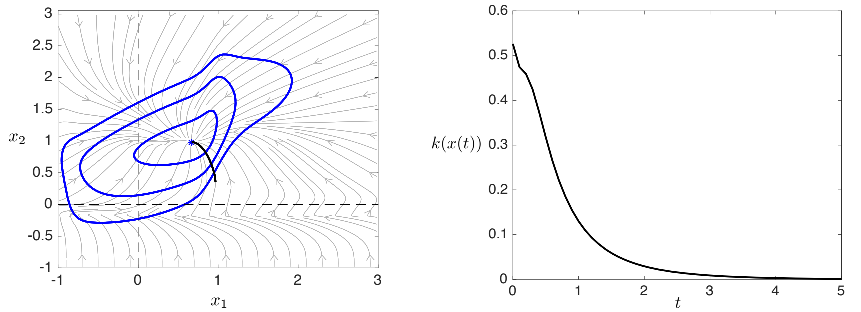

(a) Different level sets of the CLF $W_1(x)$, vector field plot of the controlled toggle switch and one trajectory initiated in $x(0) = (0.9682\ \ 0.3513)^\top$.

(b) The feedback stabilizer $k(x(t))$ for the initial state $x(0) = (0.9682\ \ 0.3513)^\top$.

Figure 6.7: CLF and feedback stabilizer results for the toggle switch.

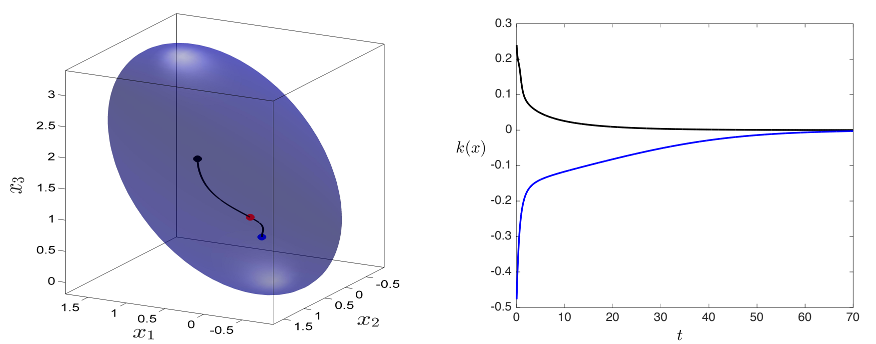

(a) Plot of the level set $W(x) = 1$, and two trajectories initiated in $x_0 = E_1$–blue dot and in $x_0 = E_3$–black dot.

(b) The feedback stabilizer $k(x(t))$ for the initial states $x(0) = E_1$–black and $x_0 = E_3$–blue.

Figure 6.8: CLF and feedback stabilizer results for the HPA axis.

system around E_2 is stabilized by a linear feedback [18]. The resulting matrix P is defined by $P = \begin{pmatrix} 0.8737 & -0.0714 & -0.3720 \\ -0.0714 & 0.5611 & 0.0670 \\ -0.3720 & 0.0670 & 0.4715 \end{pmatrix}$. We consider again the system to be of the type $\dot{x} = f(x) + g(x)u$, where $g(x) = (0\ 0\ 1)^\top$, illustrating that the control input will act on the cortisol state x_3. A plot of the level set $W(x) = 1$ is shown in Figure 6.8(a) together with two trajectories initiated in the stable, unhealthy equilibria of the system with $u = 0$, which are now destabilized by $u = k(x)$. In Figure 6.8(b) plots of the values of $u = k(x)$ corresponding to the trajectories in Figure 6.8(a) are shown. In [10] it has been shown that manipulating cortisol concentrations is a plausible strategy for redirecting the HPA axis to a healthy steady state, in particular since only ACTH and cortisol concentrations (x_2 and x_3 states in (6.2)) can be measured in real life. Although the model used therein is different, the same reasoning applies to the well functioning of the HPA axis. Furthermore, in [10], a model predictive control approach was used to stabilize the healthy HPA equilibrium. Similarly as in this chapter, for an initial state in the nonhealthy equilibrium, the control input computed in [10] has been shown to steer the HPA axis trajectory to the desired one. However, it has been noted that the resulting control input was too aggressive in the initial time instants (of order -4) and a scaled down (up to level -0.25) suboptimal, clinical realistic input, was applied instead. In contrast, the input values corresponding to the two initial conditions considered in Figure 6.8(a) appear to be clinically realistic. Furthermore, extensions of the stabilizer (6.5) such that bounded inputs are considered have been derived in the literature, in, for example, [86].

6.5 Implications of the obtained results

6.5.1 Clinical interpretations for the HPA axis results

As a consequence of the results in Section 6.2 and Subsection 6.4.2, the following remarks can be drawn with respect to possible clinical interpretations.

The computed DOA estimates shown in Figure 6.5 for each of the stable high and low cortisol level equilibria represent invariant sets for the HPA axis. This implies that once a trajectory enters such a set, it will be trapped for all times in that set and eventually converge to the stable equilibrium. Consequently, if the measured hormone values of a patient are found to belong to one of the two sets, then it can be predicted that his/hers HPA axis will eventually converge to a nonhealthy steady state. Thus, it won't be able to regulate the cortisol level back to an admissible concentration range. The information provided by the two DOA estimates can be useful for treatment assignment. If a patient's cortisol level belongs to the upper set, then a medical doctor can decide to prescribe drugs which act at lowering the cortisol level. Therefore, nonconservative DOA estimates which come arbitrarily close to the stability boundary between the convergence regions of the two equilibria are needed.

Although nonconservative DOA estimates are needed for accurate diagnostics, as shown in Subsection 6.4.2, when using the feedback stabilizer (6.5) simpler CLF candidates can be used, such as the quadratic function. From Figure 6.8(b) it follows that for destabilizing E_3 corresponding to the high level cortisol steady state, a negative input value is applied which acts at decreasing the cortisol concentration. Although this can be a logical treatment choice of a clinician, the plot in Figure 6.8(b), additionally provides an indication for quantifying the treatment level such that stabilization is guaranteed.

6.5.2 Insights for the synthetic gene systems

The genetic toggle switch and the reprissilator circuits were designed in [40] and [37] with the help of the mathematical models which were also considered in this chapter. These systems have been designed from genetic components to illustrate how novel regulatory circuits can be obtained. Such artificially constructed networks can serve as testing models in biotechnologies [69]. One of the advantages of using dynamical models is that model parameters can be varied systematically and corresponding properties observed. The DOA estimates computed in this chapter can be used to predict the behavior of a proposed circuit. The use of feedback stabilizers computed via CLFs is relevant for indicating input signals which provide a guarantee for a certain behavior corresponding to the stability of a desired steady state.

6.6 Conclusions

This chapter provides a counterpart to Chapter 3 where the computation of DOAs and stabilizing control laws were addressed for evolutionary biological systems. In this chapter we presented two examples which are known from synthetic biology, namely the genetic toggle switch and the repressilator and one example from the biomedical area. These three systems were modelled from a biochemical reaction systems perspective, thus leading to rational systems. The procedures described in Chapter 5 were applied for the above mentioned systems in order to compute Massera type LFs, and thus DOA estimates based on the level sets of these functions. In particular, the construction in Section 5.3 leads to an analytical expression for the LF W. Finally, the obtained W in combination with Sontag's "universal" feedback stabilizer was used to illustrate the stabilization problem on the toggle switch and for stabilizing the healthy equilibrium of the HPA axis.

Chapter 7

On computing ISS Lyapunov functions and stabilizers

In this chapter we propose an input to state stability (ISS) criterion based on a finite–time decrease condition for a $\mathcal{K}_\infty$ function of the norm of the state. This condition enables the construction of a Massera–type ISS classical Lyapunov function (LF). Furthermore, for the problem of designing a state feedback control law that yields the closed loop system ISS we show how the constructed ISS LF can be used in combination with Sontag's "universal" formula for ISS stabilization.

7.1 Introduction

The stability analysis and stabilization tools developed in the previous chapters are applicable to deterministic models of considered biological systems. However, the estimated model parameters are subject to errors, the developed models are simplified and proposed control inputs based on feedback stabilization can be affected by perturbations or inaccuracies in measurements. Then it is important to study the stability and stabilization problems with respect to disturbance inputs. The property of input to state stability (ISS), first introduced in [105] was proposed to study such problems. In a later paper, [111], equivalences between the ISS property and a range of other concepts such as robustness and Lyapunov–like functions, called ISS LFs, were introduced. The ISS concept was further extended for stability with respect to compact sets in [110] and [112].

Since it was shown that the ISS property is equivalent with existence of an ISS LF, the problem of constructing such functions needs to be addressed. In [23], a Zubov approach is proposed to compute ISS LFs, followed by [83] where an alternative Zubov type approach was derived. Both papers rely on the idea that ISS LFs can be obtained by computing robust LFs for suitably designed auxiliary systems. The robust LF is computed as the numerical solution of a Zubov type of equation, thus yielding a numerical approximation of an ISS LF.

Recently, in [81] and [82], a linear programming based algorithm for computing continuous, piecewise affine ISS LFs for local ISS systems was developed. The ISS LF computed therein is a viscosity subsolution of a Hamilton–Jacobi–Bellman partial differential equation.

In the case of discrete–time systems, for the ISS concept formulation, we refer to [68].

As for computing ISS LFs, in [52] for example, a similar auxiliary system procedure was used to compute ISS LFs via a set oriented approach.

The finite–time decrease condition for a $\mathcal{K}_\infty$ function of the norm of the state, which was used to compute LFs for continuous–time systems in Chapter 4, was used previously for computing ISS LFs but for discrete–time systems. In [17] it was shown that for sufficiently regular dynamics inherent global ISS can be established via finite–step LFs. In [46] the concept of dissipative finite–step ISS LFs is introduced, where similarly as in [17], the function is assumed to decrease after a finite time, rather than at each time step. This approach eases somewhat the search for an ISS LF. Moreover, therein an equivalent characterization of ISS in terms or existence of a dissipative finite–step ISS Lyapunov functions is shown for discrete–time systems.

In this chapter, we introduce the concept of finite–time ISS LFs for continuous–time, nonlinear systems and we show that existence of such a function implies ISS for systems which are described by $\mathcal{K}$–bounded maps. As for the converse result, when the ISS property is known, under a certain assumption on the solution estimate of the system subject to disturbance inputs, we show that any $\mathcal{K}_\infty$–function of the norm of the state is a finite time ISS LF function. Furthermore, similarly as in the case without inputs, a classical ISS LF can be constructed via a Massera type function based on the finite–time ISS LF.

When the considered finite–time function candidate is the norm of the state, i.e. let $V(x) = \|x\|$, for verification purposes, we show that V is an inherent finite–time ISS LF if it is a FTLF for the system with zero inputs.

Lastly, for the problem of designing a state feedback control law that renders the closed loop system ISS we show how the constructed ISS LF can be used with Sontag's "universal" formula for ISS stabilization.

7.1.1 Preliminaries

Consider systems of the form

$$\dot{x} = f(x, v), \tag{7.1}$$

where $f : \mathbb{R}^n \times \mathbb{R}^m \to \mathbb{R}^n$, is a locally Lipschitz function and $v(\cdot) : [0, \infty) \to \mathbb{R}^m$, a measurable locally essentially bounded map represents the disturbance input. We denote the solution of the system (7.1) with initial value $x(0)$ at time $t = 0$, under disturbance input $v(t)$, by $x(t)$ and we assume that $x(t)$ exists and it is unique for all $t \in \mathbb{R}_{\geq 0}$ (see [77, Chapter 3] for sufficient smoothness conditions on f). The locally Lipschitz assumption on $f(x, v)$ implies that $x(t)$ is a continuous function of $x(0)$ and $v(0)$ [60, Chapter III]. Furthermore, $f(0, 0) = 0$.

We will use the following notations for the disturbance signal v: $|v| = \sup_{s \geq 0} \|v(s)\|$, $|v_{[t_1,t_2]}| = \sup_{t_1 \leq s \leq t_2} \|v(s)\|$, $t_1, t_2 \geq 0$, with $v(s) \in \mathbb{R}^m$, for all s in the corresponding interval. Furthermore, $\|v\|$ denotes the regular Holder norm. Next, we proceed by recalling some subsidiary notions and definitions, starting with the input–to–state stability concept as introduced in [111].

Definition 7.1 The system (7.1) is said to be input–to–state stable (ISS) with respect to v if given a proper set $\mathcal{S} \subseteq \mathbb{R}^n$, there exist a function $\beta \in \mathcal{KL}$ and $\gamma \in \mathcal{K}_\infty$ such that for all

$x(0) \in \mathcal{S}$, and every v, the corresponding solution of (7.1) satisfies

$$\|x(t)\| \leq \beta(\|x(0)\|, t) + \gamma(|v|), \quad \forall t \in \mathbb{R}_{\geq 0}, \tag{7.2}$$

If the set $\mathcal{S} = \mathbb{R}^n$, then we call the ISS property global ISS.

The characterization in (7.2) is equivalent with [111]:

$$\|x(t)\| \leq \max\big(\beta(\|x(0)\|, t), \gamma(|v|)\big), \quad \forall t \in \mathbb{R}_{\geq 0}. \tag{7.3}$$

Definition 7.2 A continuously differentiable function $V : \mathbb{R}^n \to \mathbb{R}_{\geq 0}$, for which there exist $\alpha_1, \alpha_2, \alpha, \chi \in \mathcal{K}_\infty$ such that for all $v \in \mathbb{R}^m$ it holds that

$$\begin{aligned} \alpha_1(\|x\|) \leq V(x) &\leq \alpha_2(\|x\|), & \forall x \in \mathbb{R}^n \quad (7.4)\\ \dot{V}(x) &\leq -\alpha(\|x\|) + \chi(|v|), & \forall x \in \mathcal{S}, \quad (7.5) \end{aligned}$$

with $\mathcal{S} \subseteq \mathbb{R}^n$ proper, is called an ISS Lyapunov function in $\mathcal{S}$ for the system (7.1).

Equivalently, (7.5) can be restated as [111]

$$\dot{V}(x) \leq -\alpha(\|x\|), \quad \forall x \in \mathcal{S} \tag{7.6}$$

and for any $v \in \mathbb{R}^m$ such that $\|x\| \geq \hat{\chi}(|v|)$, where $\hat{\chi}(\cdot) = (\alpha^{-1} \circ \chi)(\cdot) \in \mathcal{K}_\infty$.

7.2 Finite–time ISS Lyapunov functions

Let there be a continuous function $V : \mathbb{R}^n \to \mathbb{R}_{\geq 0}$, and a real scalar $d > 0$ for which the proper set $\mathcal{S} \subseteq \mathbb{R}^n$ is d–invariant and the conditions

$$\alpha_1(\|x\|) \leq V(x) \leq \alpha_2(\|x\|), \; \forall x \in \mathbb{R}^n, \tag{7.7}$$

$$V(x(t+d)) - V(x(t)) \leq -\alpha(\|x(t)\|) + \chi(|v|), \tag{7.8}$$

are satisfied for all $t \in \mathbb{R}_{\geq 0}$ and α_1, $\alpha_2, \alpha, \chi \in \mathcal{K}_\infty$, and for all $x(t)$, with $x(0) \in \mathcal{S}$ and $v(s) \in \mathbb{R}^m$, for any $s \in \mathbb{R}_{\geq 0}$,

By similar arguments as in [111, Remark 2.4.], the equivalent form of (7.8) is

$$V(x(t+d)) - V(x(t)) \leq -\alpha(\|x(t)\|), \tag{7.9}$$

whenever $\|x(t)\| \geq \hat{\chi}(|v|)$, with $\hat{\chi}(\cdot) = (\alpha^{-1} \circ \chi)(\cdot) \in \mathcal{K}_\infty$.

The function V which satisfies (7.7) and (7.8) ((7.9)) is called an *ISS finite–time Lyapunov function* (ISS–FTLF) for the system (7.1).

In order for condition (7.8) to be well–defined, additionally to the locally Lipschitz property of the map $f(x)$, it is assumed that there exists no finite escape time in each interval $[t, t+d]$, for all $t \in \mathbb{R}_{\geq 0}$. However, as it will be shown later, it is sufficient to require that there is no finite escape time in the time interval $[0, d]$, if the set $\mathcal{S}$ is d–invariant.

The following result relates inequality (7.8) with another known type of decrease condition, which will be instrumental.

Lemma 7.1 The decrease condition (7.8) on V is equivalent with

$$V(x(t+d)) \leq \rho(V(x(t))) + \chi(|v|), \quad \forall t \in \mathbb{R}_{\geq 0}, \tag{7.10}$$

for all $x(t)$ with $x(0) \in \mathcal{S}$, where ρ is a positive definite, continuous function such that $(\mathrm{id} - \rho) \in \mathcal{K}_\infty$.

Proof: The proof follows similarly as in [46, Remark 3.17]. We provide it below for completeness.
(7.8)⇒(7.10):

$$\begin{aligned}
0 \leq V(x(t+d)) &\leq V(x(t)) - \alpha(\|x(t)\|) + \chi(|v|) \\
&\leq V(x(t)) - \alpha(\alpha_2^{-1}(V(x(t)))) + \chi(|v|) \\
&= (\mathrm{id} - \alpha \circ \alpha_2^{-1})(V(x(t))) + \chi(|v|) \\
&= \rho(V(x(t))) + \chi(|v|),
\end{aligned}$$

where $\rho = \mathrm{id} - \alpha \circ \alpha_2^{-1}$ can be assumed to be positive, since one can always take $\alpha_2(s) \geq 2\alpha(s) > \alpha(s)$, for all $s > 0$, thus $\rho = \mathrm{id} - \alpha \circ \alpha_2^{-1} > 0$. Additionally, $\mathrm{id} - \rho = \alpha \circ \alpha_2^{-1} \in \mathcal{K}_\infty$.

(7.10)⇒(7.8):

$$\begin{aligned}
V(x(t+d)) - V(x(t)) &\leq \rho(V(x(t))) - V(x(t)) + \chi(|v|) \\
&= -(-\rho + \mathrm{id})(V(x(t))) + \chi(|v|) \\
&= -\hat{\alpha}(V(x(t))) + \chi(|v|) \\
&\leq -\hat{\alpha}(\alpha_1(\|x(t)\|)) + \chi(|v|) \\
&= -\alpha(\|x(t)\|) + \chi(|v|),
\end{aligned}$$

where $\hat{\alpha} = \mathrm{id} - \rho \in \mathcal{K}_\infty$, by hypothesis and $\alpha = \hat{\alpha} \circ \alpha_1 \in \mathcal{K}_\infty$. ■

Assumption 7.1 The function $f(\cdot, \cdot)$ in (7.1) satisfies

$$\|f(x, v)\| \leq \mu_1(\|x\|) + \mu_2(\|v\|) \tag{7.11}$$

for all $x \in \mathbb{R}^n$, $v \in \mathbb{R}^m$, and some $\mu_1, \mu_2 \in \mathcal{K}$.

The above assumption is a natural consequence of the Lipschzitz continuity requirement for f at the origin. In fact, it implies $\mathcal{K}$–boundedness with respect to each argument of f.

Remark 7.1 For some fixed $t > 0$, the solution of the system (7.1) is given by

$$x(t) = x(0) + \int_0^t f(x(s), v(s))\mathrm{d}s.$$

Let the locally Lipschitz condition be

$$\|f(x, v) - f(y, u)\| \leq L(\|x - y\| + \|v - u\|), \quad L > 0$$

for $x, y \in \mathcal{N}(0, r)$, where $\mathcal{N}(0, r)$ denotes a neighborhood around the origin of radius r and $v \in \mathbb{R}^m$ and $u \in \mathbb{U}$, $\mathbb{U}$ a compact subset of $\mathbb{R}^m$. Then,

$$\begin{aligned}
\|x(t) - x(0)\| &\leq \int_0^t (\|f(x(s), v(s)) - f(x(0), v(0)) + f(x(0), v(0)))\|\mathrm{d}s \\
&\leq L \int_0^t \|x(s) - x(0)\|\mathrm{d}s + L \int_0^t \|v(s) - v(0)\|\mathrm{d}s + \int_0^t \|f(x(0), v(0)\|\mathrm{d}s \\
&\underset{(7.11)}{\leq} L \int_0^t \|x(s) - x(0)\|\mathrm{d}s + L \int_0^t \|v(s) - v(0)\|\mathrm{d}s + \int_0^t \mu_1(\|x(0)\|)\mathrm{d}s + \\
&\quad \int_0^t \mu_2(\|v(0)\|)\mathrm{d}s.
\end{aligned}$$

By applying the Gronwall Lemma above, we obtain that

$$\begin{aligned}
\|x(t) - x(0)\| &\leq \big(L \int_0^t \|v(s) - v(0)\|\mathrm{d}s + \int_0^t \mu_2(\|v(0)\|)\mathrm{d}s + \int_0^t \mu_1(\|x(0)\|)\mathrm{d}s\big)e^{Lt} \\
&\leq G_t(|v_{[0,t]}|) + \int_0^t \mu_1(\|x(0)\|)\mathrm{d}s e^{Lt},
\end{aligned}$$

and further,

$$\begin{aligned}
\|x(t)\| &\leq G_t(|v_{[0,t]}|) + \|x(0)\| + \int_0^t \mu_1(\|x(0)\|)\mathrm{d}s e^{Lt} \\
&= G_t(|v_{[0,t]}|) + F_t(\|x(0)\|).
\end{aligned}$$

From the inequalities above and the standing assumptions on f we know that $F_t(\|x(0)\|)$ and $G_t(|v_{[0,t]}|)$ are continuous with respect to $x(0)$ and $v(t)$, respectively. Furthermore, $F_t(0) = 0$, $G_t(0) = 0$ and $F_t(\|x(0)\|), G_t(|v_{[0,t]}|)$ are positive definite and continuous as $\mu_1, \mu_2 \in \mathcal{K}$.

Remark 7.2 In [46, Theorem 4.1], it is shown that the set

$$\mathcal{S}_v := \{x \in \mathbb{R}^n \,|\, V(x) \leq (\mathrm{id} - \rho)^{-1} \circ \nu^{-1} \circ \chi(|v|)\}, \tag{7.12}$$

where $\nu \in \mathcal{K}_\infty$ and $\mathrm{id} - \nu \in \mathcal{K}_\infty$ is d–invariant for the system (7.1) and for all $v(s) \in \mathbb{R}^m$, $s \geq 0$. Following from the proof (7.8)⇒(7.10) of Lemma 7.1, we have that $\rho = \mathrm{id} - \alpha \circ \alpha_2^{-1}$. If one takes ν in (7.12) to be such that $\alpha = \nu^{-1}$, we obtain that

$$\begin{aligned}
(\mathrm{id} - \rho)^{-1} \circ \nu^{-1} \circ \chi(|v|) &= (\alpha \circ \alpha_2^{-1})^{-1} \circ \alpha \circ \chi(|v|) \\
&= \alpha_2 \circ \alpha^{-1} \circ \alpha \circ \chi(|v|) \\
&= \alpha_2 \circ \chi(|v|).
\end{aligned}$$

The set $\mathcal{S}_v$ defined in (7.12) can be written equivalently (with respect to condition (7.8)) as

$$\mathcal{S}_v := \{x \in \mathbb{R}^n \,|\, V(x) \leq \alpha_2 \circ \chi(|v|)\}, \tag{7.13}$$

which corresponds to the construction with classical LFs in [111, Lemma 2.14], where $\mathcal{S}_v$ is an invariant set when V is a classical LF.

Theorem 7.1 If a function V defined as in (7.7) and (7.8) and a proper and compact d-invariant set $\mathcal{S}$ exist for the system (7.1) satisfying Assumption 7.1, then the system (7.1) is ISS in $\mathcal{S}$.

Proof: Consider the set $\mathcal{S}_v$ defined as in (7.12). Let

$$t_1 = \inf\{t \geq 0 \,|\, x(j) \in \mathcal{S}_v, j \in [t, t+d)\}.$$

Then, when $\underline{t \geq t_1}$, $x(t) \in \mathcal{S}_v$ and

$$V(x(t)) \leq (\mathrm{id} - \rho)^{-1} \circ \nu^{-1} \circ \chi(|v|) =: \hat{\gamma}(|v|)$$

implies that

$$\|x(t)\| \leq \alpha_1^{-1} \circ \hat{\gamma}(|v|) =: \tilde{\gamma}(|v|).$$

When $\underline{t < t_1}$, it is possible that $x(t) \in \mathcal{S}_v$ which implies that $\|x(t)\| \leq \tilde{\gamma}(|v(t)|)$, and that $x(t) \notin \mathcal{S}_v$. For the latter case, let $t = Nd + j$, with $N \in \mathbb{N}$ and $0 \leq j < d$. The d–invariance of $\mathcal{S}_v$ implies that for $x(j) \in \mathcal{S}_v$, $x(d+j) \in \mathcal{S}_v$ and $x(Nd+j) \in \mathcal{S}_v$. Thus, $x(Nd+j) \notin \mathcal{S}_v$ implies that $x(j) \notin \mathcal{S}_v$. Hence,

$$\begin{aligned}
V(x(j)) &> (\mathrm{id} - \rho)^{-1} \circ \nu^{-1} \circ \chi(|v|) \\
(\mathrm{id} - \rho)V(x(j)) &> \nu^{-1} \circ \chi(|v|) \\
\nu \circ (\mathrm{id} - \rho)V(x(j)) &> \chi(|v|),
\end{aligned}$$

and

$$\begin{aligned}
V(x(j+d)) &\leq \rho(V(x(j))) + \chi(|v|) \\
&< \rho(V(x(j))) + \nu \circ (\mathrm{id} - \rho) \circ V(x(j)) \\
&= (\rho + \nu \circ (\mathrm{id} - \rho)) \circ V(x(j)) \\
&=: \hat{\rho}(V(x(j))),
\end{aligned}$$

where $\hat{\rho} = \rho + \nu \circ (\mathrm{id} - \rho)$ satisfies $\mathrm{id} - \hat{\rho} = \mathrm{id} - \rho - \nu \circ (\mathrm{id} - \rho) = (\mathrm{id} - \nu) \circ (\mathrm{id} - \rho)$, thus we can write $\hat{\rho} = \mathrm{id} - (\mathrm{id} - \nu) \circ (\mathrm{id} - \rho)$. $\hat{\rho} < \mathrm{id}$ since $(\mathrm{id} - \nu), (\mathrm{id} - \rho) \in \mathcal{K}_\infty$, thus $\mathrm{id} - \hat{\rho} \in \mathcal{K}_\infty$, which implies that $\mathrm{id}(s) - \hat{\rho}(s) > 0$ for $s \neq 0$. Furthermore, $\hat{\rho}$ is positive definite, continuous and $\hat{\rho}(0) = 0$.

Let $N^* := \sup\{N \in \mathbb{N} \,|\, V(x(Nd+j)) \notin \mathcal{S}_v\}$. Then for all $\underline{N \leq N^*}$ we have:

$$\begin{aligned}
V(x(t)) &= V(x(Nd+j)) \\
&= V(x(((N-1)d+j)+d)) \\
&\leq \hat{\rho}(V(x((N-1)d+j))) \\
&= \hat{\rho}(V(x(((N-2)d+j)+d))) \\
&\leq \hat{\rho}^2(V(x((N-2)d+j))) \\
&\dots \\
&\leq \hat{\rho}^N(V(x(j))) \\
&\leq \hat{\rho}^N(\alpha_2(\|x(j)\|)),
\end{aligned} \tag{7.14}$$

where $\hat{\rho}^N$ denotes the N–times composition of $\hat{\rho}$. Following from Remark 7.1, by applying Lemma 4.2 we obtain that there exist functions $\omega_1, \omega_2 \in \mathcal{K}_\infty$, such that $F_j(\|x(0)\|) \leq \omega_1(\|x(0)\|)$ and $G_j(|v_{[0,j]}|) \leq \hat{\omega}_2(|v_{[0,j]}|)$ and consequently,

$$\|x(j)\| \leq \omega_1(\|x(0)\|) + \omega_2(|v_{[0,j]}|),$$

for all $0 \leq j < d$. Thus

$$\begin{aligned}
V(x(t)) &\leq \hat{\rho}^N(\alpha_2(\omega_1(\|x(0)\|) + \omega_2(|v_{[0,j]}|))) \\
&\leq \hat{\rho}^N(\alpha_2(2\omega_1(\|x(0)\|)) + \alpha_2(2\omega_2(|v_{[0,j]}|))) \\
&= \hat{\rho}^N(\sigma_1(\|x(0)\|) + \sigma_2(|v_{[0,j]}|)) \\
&\leq \hat{\rho}^N(2\sigma_1(\|x(0)\|)) + \hat{\rho}^N(2\sigma_2(|v_{[0,j]}|)) \\
&\leq \hat{\rho}^N(2\sigma_1(\|x(0)\|)) + \hat{\rho}^N(2\sigma_2(|v_{[0,j]}|)), \quad \forall t \geq j \\
&= \hat{\rho}^N(\hat{\sigma}_1(\|x(0)\|)) + \hat{\rho}^N(\hat{\sigma}_2(|v_{[0,j]}|)) \\
&= \hat{\rho}^{\frac{t-j}{d}}(\hat{\sigma}_1(\|x(0)\|)) + \tilde{\gamma}_1(|v_{[0,j]}|) \\
&\leq \hat{\rho}^{\lfloor \frac{t}{d} \rfloor - 1} \circ \hat{\sigma}_1(\|x(0)\|) + \tilde{\gamma}_1(|v_{[0,j]}|) \\
&= \hat{\rho}^{\lfloor \frac{t}{d} \rfloor} \circ \hat{\rho}^{-1} \circ \hat{\sigma}_1(\|x(0)\|) + \tilde{\gamma}_1(|v_{[0,j]}|) \\
&\leq \hat{\rho}^{\lfloor \frac{t}{d} \rfloor} \circ \tilde{\rho} \circ \hat{\sigma}_1(\|x(0)\|) + \tilde{\gamma}_1(|v_{[0,j]}|), \quad \tilde{\rho} \in \mathcal{K}_\infty \\
&=: \hat{\beta}(\|x(0)\|, t) + \tilde{\gamma}_1(|v_{[0,j]}|) \\
&\leq \hat{\beta}(\|x(0)\|, t) + \tilde{\gamma}_1(|v|).
\end{aligned}$$

Without loss of generality we can assume that $\hat{\rho}$ is a one–to–one (injective) and onto (surjective) function, thus invertible. Furthermore, since $\hat{\rho}$ is continuous, then by [20, Theorem 3.16], $\hat{\rho}^{-1}$ is continuous. Additionally, $\hat{\rho}^{-1}(0) = \hat{\rho}^{-1}(\rho(0)) = 0$. Thus, there exists a function $\tilde{\rho} \in \mathcal{K}_\infty$, such that $\hat{\rho}^{-1} \leq \tilde{\rho}$, as follows from Lemma 4.2. We can conclude that $\hat{\beta} \in \mathcal{KL}$ since $\tilde{\rho} \circ \hat{\sigma}_1(s) \in \mathcal{K}_\infty$ and $\hat{\rho}^{\lfloor \frac{t}{d} \rfloor} \in \mathcal{L}$. Next, $\tilde{\gamma}_1 = \hat{\rho}^N \circ 2\alpha_2 \circ 2\omega_2$, thus $\tilde{\gamma}_1 > 0$ is continuous and $\tilde{\gamma}_1(0) = 0$. Therefore, there exists a function $\hat{\gamma}_1 \in \mathcal{K}_\infty$ such that $\tilde{\gamma}_1 < \hat{\gamma}_1$. We obtain

$$\begin{aligned}
\|x(t)\| &\leq \alpha_1^{-1}(2\hat{\beta}(\|x(0)\|, t)) + \alpha_1^{-1}(2\hat{\gamma}_1(|v|)) \\
&:= \beta(\|x(0\|, t) + \tilde{\gamma}_2(|v|),
\end{aligned}$$

with $\beta \in \mathcal{KL}$ and $\tilde{\gamma}_2 \in \mathcal{K}_\infty$.

For $\underline{N > N^*}$ it holds that $V(x(Nd + j)) \in \mathcal{S}_v$, thus $\|x(Nd + j)\| \leq \tilde{\gamma}(|v|)$.

For all $N \in \mathbb{N}^*$ it follows that

$$\|x(t)\| \leq \beta(\|x(0\|, t) + (\tilde{\gamma}_2 + \tilde{\gamma})(|v|),$$

thus, also for all $t \geq t_1$

$$\|x(t)\| \leq \beta(\|x(0\|, t) + (\tilde{\gamma}_2 + 2\tilde{\gamma})(|v|).$$

Hence, for all $t \geq 0$ it holds that

$$\|x(t)\| \leq \beta(\|x(0\|, t) + (\tilde{\gamma}_2 + 2\tilde{\gamma})(|v|),$$

which implies ISS for (7.1).

7.3 Alternative ISS converse theorem

Assumption 7.2 There exists a pair $(\beta(\cdot,\cdot),d) \in \mathcal{KL} \times \mathbb{R}_{>0}$ with β satisfying (7.2) for the system (7.1) such that

$$\beta(s,d) < s \tag{7.15}$$

for all $s > 0$.

Theorem 7.2 If the system (7.1) is ISS in some invariant set $\mathcal{S}$ with $d > 0$ as in (7.15) and Assumption 7.2 is satisfied, then for any function $\eta \in \mathcal{K}_\infty$ and for any norm $\|\cdot\|$, the function $V : \mathbb{R}^n \to \mathbb{R}_{\geq 0}$, with

$$V(x) := \eta(\|x\|), \quad \forall x \in \mathbb{R}^n \tag{7.16}$$

satisfies (7.7) and (7.8) with the same $d > 0$ as in (7.15).

Proof: Let the pair (β,d) be such that Assumption 7.2 holds. Then, from the ISS hypothesis we obtain that for all initial conditions $x(0) \in \mathcal{S}$, it holds that

$$\begin{aligned}\|x(t+d)\| &\leq \max(\beta(\|x(t)\|,d),\gamma(|v|))\\ &= \beta(\|x(t)\|,d),\end{aligned}$$

whenever $\alpha_d(\|x(t)\|) := \beta(\|x(t)\|,d) \geq \gamma(|v|)$, where $\alpha_d \in \mathcal{K}_\infty$, or equivalently, whenever $\|x(t)\| \geq (\alpha_d^{-1} \circ \gamma)(|v|) = \hat{\gamma}(|v|)$. Consequently,

$$\begin{aligned}\eta(\|x(t+d)\|) &\leq \eta(\beta(\|x(t)\|,d))\\ &\leq \eta(\beta(\eta^{-1}(V(x(t))),d))\\ &:= \rho(V(x(t))),\end{aligned}$$

where $\rho = \eta(\beta(\eta^{-1}(\cdot),d))$. Then, via Assumption 7.2, it follows that $\rho < \eta(\eta^{-1}(\cdot)) = \mathrm{id}$ and $\mathrm{id} - \rho \in \mathcal{K}_\infty$. Thus, we get

$$V(x(t+d)) - \rho(V(x(t))) \leq 0,\ \forall x(0) \in \mathcal{S},\ \|x(t)\| \geq \hat{\gamma}(|v(t)|).$$

Next, this implies

$$\begin{aligned}V(x(t+d)) - V(x(t)) &\leq \rho(V(x(t))) - V(x(t))\\ &= -(V(x(t)) + \rho(V(x(t)))\\ &= -((\mathrm{id}-\rho)(V(x(t))))\\ &\leq -((\mathrm{id}-\rho)(\alpha_1(\|x(t)\|))\\ &= -\alpha(\|x(t)\|), \quad \|x(t)\| \geq \hat{\gamma}(|v|),\end{aligned}$$

with $\alpha = (\mathrm{id}-\rho) \circ \alpha_1$. Since $\mathrm{id} - \rho \in \mathcal{K}_\infty$, then $\alpha \in \mathcal{K}_\infty$ and we have obtained (7.9) which further yields (7.8). Furthermore, since V is defined by a $\mathcal{K}_\infty$ function, then there exist $\alpha_1, \alpha_2 \in \mathcal{K}_\infty$ such that (7.7) holds.

7.3.1 An ISS Lyapunov Function

Consider the function defined as

$$W(x(t)) := \int_t^{t+d} V(x(\tau))\mathrm{d}\tau, \tag{7.17}$$

for any V that satisfies (7.7) and (7.8).

Lemma 7.2 There exists a V satisfying (7.7) and (7.8) for some $d > 0$ for (7.1) if and only if the function W as defined in (7.17) with the same $d > 0$ is an ISS Lyapunov function for the system (7.1).

Proof: Let there be a function V satisfying (7.7) and (7.8). $V(x(t))$ is continuous, thus it is integrable over any closed, bounded interval $[t, t+d]$, $t \geq 0$. By Theorem 5.30 in [20], this implies that $W(x(t))$ is continuous on each interval $[t, t+d]$, for any t. Since V is also positive definite, by integrating over the bounded interval $[t, t+d]$ the resulting function $W(x(t))$ will also be positive definite. Since $W(x(t))$ is continuous, $W(0) = 0$ and it positive definite the result in Lemma 4.2 can be applied. Therefore, there exist two functions $\hat{\alpha}_1, \hat{\alpha}_2 \in \mathcal{K}_\infty$ such that

$$\hat{\alpha}_1(\|x\|) \leq W(x) \leq \hat{\alpha}_2(\|x\|), \quad \forall x \in \mathbb{R}^n, \tag{7.18}$$

holds. Next, by making use of the general Leibniz integral rule, we get that

$$\begin{aligned}
\frac{\mathrm{d}}{\mathrm{d}t}W(x(t)) = \int_t^{t+d} &\underbrace{\frac{\mathrm{d}}{\mathrm{d}t}V(x(\tau))}_{=0}\mathrm{d}\tau + V(x(t+d))(\dot{t+d}) - V(x(t))\dot{t} \\
&= V(x(t+d)) - V(x(t)) \\
&\leq -\alpha(\|x(t)\|) + \chi(|v|).
\end{aligned}$$

In $\frac{\mathrm{d}}{\mathrm{d}t}V(x(\tau))$ note that $x(\tau) = x(\tau, v(\tau))$, which implies that

$$\begin{aligned}
\frac{\mathrm{d}}{\mathrm{d}t}V(x(\tau, v(\tau))) &= \frac{\partial V}{\partial x}\frac{\mathrm{d}x}{\mathrm{d}t} \\
&= \frac{\partial V}{\partial x}\left(\frac{\partial x}{\partial \tau}\frac{\mathrm{d}\tau}{\mathrm{d}t} + \frac{\partial x}{\partial v}\frac{\mathrm{d}v}{\mathrm{d}t}\right) \\
&= \frac{\partial V}{\partial x}\left(\frac{\partial x}{\partial \tau}\cdot 0 + \frac{\partial x}{\partial v}\cdot 0\right) \\
&= 0.
\end{aligned}$$

Thus, W is an ISS Lyapunov function for (7.1).

Now assume that W is an ISS Lyapunov function for (7.1), i.e. (7.4) holds and for some $\hat{\alpha}, \hat{\chi} \in \mathcal{K}_\infty$ it holds that

$$\dot{W}(x(t)) \leq -\hat{\alpha}(\|x(t)\|) + \hat{\chi}(|v|), \quad \forall x(t) \in \mathcal{S}, \forall v \in \mathbb{R}^m.$$

By the same Leibniz rule, we know that $\dot{W}(x(t)) = V(x(t+d)) - V(x(t))$, thus for the difference $V(x(t+d)) - V(x(t))$ (7.8) holds. Now we have to show that (7.7) holds.

Assume that there exists an $x \in \mathbb{R}^n$ such that $V(x) < 0$. Then we obtain that $W(x) = \int_t^{t+d} V(x(\tau))\mathrm{d}\tau < 0$. But this is a contradiction since we assumed that W satisfies (7.18) on $\mathbb{R}^n$, thus $V(x)$ must be positive definite on $\mathbb{R}^n$. By the definition of W, we have that V must be a continuous function, because it needs to be integrable for W to exist. By assumption, W is upper and lower bounded by $\mathcal{K}_\infty$ functions, thus for $x \to \infty$, $W(x) \to \infty$. This can only happen when $V(x) \to \infty$. Thus, using a similar reasoning as above, based on Lemma 4.2, this implies that V is upper and lower bounded by $\mathcal{K}_\infty$ functions, hence (7.7) holds.

The next result summarizes the proposed alternative converse theorem for ISS of (7.1) in $\mathcal{S}$, enabled by the finite–time conditions (7.7) and (7.8).

Corollary 7.1 If the the system (7.1) is ISS in some invariant set $\mathcal{S}$ and Assumption 7.2 holds for $(\beta, d) \in \mathcal{KL} \times \mathbb{R}_{>0}$, then by Theorem 7.2 and Lemma 7.2 for any function $\eta \in \mathcal{K}_\infty$ and any norm $\|\cdot\|$, the function $W(\cdot)$ as defined in (7.17) with $V(x) = \eta(\|x\|)$ for the same $d > 0$ as in Assumption 7.2, is an ISS Lyapunov function for the system (7.1).

7.3.2 Computation of W

In Section 7.2 it was shown that if a system is ISS, then a method to construct an ISS LF is provided by (7.17), for $V(x)$ defined by any function $\eta \in \mathcal{K}_\infty$ and any norm. The method is constructive starting with a given candidate d–invariant set $\mathcal{S}$ and a candidate function $V(x) = \eta(\|x\|)$. Due to the d–invariance property of $\mathcal{S}$ verifying condition (7.8) for the chosen V is reduced to verifying

$$V(x(d)) - V(x(0)) \leq -\alpha(\|x(0)\|) + \chi(|v|), \tag{7.19}$$

for all $x(0) \in \mathcal{S}$. The difficulty in verifying (7.19) is given by the need to compute $x(d)$, for all $x(0) \in \mathcal{S}$. However if $x(d)$ is known analytically and the disturbance input v is a known or estimated signal in some analytic form, then it suffices to verify (7.19) for all initial conditions in a chosen set $\mathcal{S}$. Since V is a continuous function of time and the integral in (7.17) is defined over a closed time interval, the expression of W becomes

$$W(x(0)) = \int_0^d V(x(\tau))\mathrm{d}\tau. \tag{7.20}$$

Since v is however not known in general, we propose to compute a value for d when $v = 0$ and rely on inherent ISS. As such, we will make use of the next result, which enables the verification of the finite–time condition (7.19) for the system (7.1) with $v = 0$.

Lemma 7.3 Let $V(x) = \|x\|$. If $V(x)$ satisfies (7.8) for $\dot{x} = f(x, 0)$ and $v(t) = 0$ for all $t \in \mathbb{R}_{\geq 0}$, then $V(x)$ satisfies the condition (7.8) for $\dot{x} = f(x, v)$.

Proof: We shall write the proof for t in the interval $[0, d]$. Let $\bar{x}(d)$ denote the solution of $\dot{x} = f(x, 0)$ for $x(0) \in \mathcal{S}$. It follows from (7.8) that

$$\|\bar{x}(d)\| - \|x(0)\| \leq -\alpha(\|x(0)\|),$$

for all $x(0) \in \mathcal{S}$, where $\mathcal{S}$ a d–invariant set. Then,

$$\begin{aligned}\|x(d)\| - \|x(0)\| &\leq \|x(d)\| - \|\bar{x}(d)\| - \alpha(\|x(0)\|) \\ &\leq \|x(d) - \bar{x}(d)\| - \alpha(\|x(0)\|),\ \forall x(0) \in \mathcal{S}.\end{aligned}$$

$$x(d) - \bar{x}(d) = \int_0^d f(x(s), v(s))\mathrm{d}s - \int_0^d f(x(s), 0)\mathrm{d}s.$$

This implies, by using the local Lipschtiz condition on f with respect to its both arguments, that

$$\begin{aligned}\|x(d) - \bar{x}(d)\| &\leq \int_0^d \|f(x(s), v(s)) - f(x(s), 0)\|\mathrm{d}s \\ &\leq \int_0^d L\|v(s) - 0\|\mathrm{d}s\end{aligned}$$

where $L > 0$ is the Lipschitz constant. Since $\int_0^d L\|v(s) - 0\|\mathrm{d}s$ is positive definite, zero at zero and continuous then via Lemma 4.2, there exists $\chi \in \mathcal{K}_\infty$ such that

$$\|x(d) - \bar{x}(d)\| \leq \int_0^d L\|v(s)\|\mathrm{d}s \leq \chi(\|v(d)\|) \leq \chi(|v|).$$

As such, we have that

$$\|x(d)\| - \|x(0)\| \leq \chi(|v|) - \alpha(\|x(0)\|),\ \forall x(0) \in \mathcal{S},$$

which recovers (7.19), and further (7.8) for $V(x) = \|x\|$.

The result of Lemma 7.3 allows us to obtain a d for which a candidate function $V(x) = \|x\|$, with any norm, is an ISS FTLF in a much simpler way than verifying (7.19) directly.

Remark 7.3 In [28] a scheme for constructing LFs starting from a given LF, which at every iterate provides a less conservative estimate of the DOA of a nonlinear system of the type (7.1) was proposed and it was based on iterative constructions of the type $W_1(x) = W(x + \alpha_1 f(x))$. In Chapter 4, the expansion idea in [28] was used to generate a sequence of FTLFs, with the purpose to generate a relevant d–invariant set for constructing Massera–type of LFs. Thus the sequence of functions

$$\begin{aligned}V_1(x) &= V(x + \alpha_1 f(x, 0)) \\ V_2(x) &= V_1(x + \alpha_2 f(x, 0)) \\ &\vdots \\ V_n(x) &= V_{n-1}(x + \alpha_n f(x, 0)),\end{aligned} \tag{7.21}$$

with $\alpha_i \in \mathbb{R}_{\geq 0}$, $i = 1, 2 \ldots, n$ yields FTLFs, when V is FTLF. From Lemma 7.3, we know that $V_1(x) = V(x + \alpha_1 f(x, v))$ for example is an inherent ISS FTLF. This fact will be relevant in the computation of an ISS LF, W from (7.20) as it involves knowledge of the solution of (7.1) up to time d.

7.3.3 Computational procedure FTLF candidates $V(x) = \|x\|$

The procedure can be summarized as follows.

7.3.3.1 Verify the FT conditions for $\dot{x} = f(x, 0)$

When the analytical solution is not known, or obtaining a numerical approximation is computationally tedious, as it can be the case for higher order nonlinear systems, then we propose to use the approach in Chapter 5 starting from the linearized dynamics of (7.1) with $v = 0$:

$$\|e^{d\left[\frac{\partial f(x,0)}{\partial x}\right]_{x=0}} x(0)\| - \|x(0)\| < 0, \tag{7.22}$$

for all $x(0)$ in some compact, proper set $\mathcal{S}$. Then, for the computed d, the approach in Chapter 4 relies on constructing W as

$$W(x) = \int_0^d V(x + \tau f(x, 0))\mathrm{d}\tau, \quad \forall x \in \mathcal{S}. \tag{7.23}$$

7.3.3.2 Compute an ISS LF

Let $\bar{W}(x) = \int_0^d V(x + \tau(f(x, 0))\mathrm{d}\tau$ and $\mathcal{S}(c) = \{x \in \mathbb{R}^n \,|\, \bar{W}(x) \leq c\}$ with $c > 0$ such that $\mathcal{S}(c) \subseteq \{x \in \mathbb{R}^n \,|\, \dot{\bar{W}}(x) < 0\}$. Now consider $\dot{\bar{W}}(x) \leq -\alpha(\|x\|)$, for any $x \in \mathcal{S}(c)$. By the Leibniz integral rule, this implies that

$$V(x + df(x, 0)) - V(x) \leq \alpha(\|x\|) \quad \forall x \in \mathcal{S}(c).$$

For $V(x) = \|x\|$, by a similar reasoning as in the proof of Lemma 7.3 it can be seen that

$$V(x + df(x, v)) - V(x) \leq \alpha(\|x\|) + dL|v| \quad \forall x \in \mathcal{S}(c),$$

which implies that

$$W(x) = \int_0^d V(x + \tau f(x, v))\mathrm{d}\tau, \quad \forall x \in \mathcal{S}(c) \tag{7.24}$$

is an ISS Lyapunov function.

7.4 Control Lyapunov functions and ISS stabilization

For systems subject to control inputs, of the type

$$\dot{x} = f(x) + g(x)u \tag{7.25}$$

where $u \in \mathbb{U} \subseteq \mathbb{R}^m$ denotes the input and $f : \mathbb{R}^n \to \mathbb{R}^n$ and $g : \mathbb{R}^n \to \mathbb{R}^m$ with $f(0) = 0$ and $g(0) = 0$, recall the concept of a CLF defined in Definition 2.10.

When a CLF W is known, an explicit formula for a state feedback control that makes the system asymptotically stable or $\mathcal{KL}$–stable in $\mathcal{A}$ was provided in [106] and it was recalled in Chapter 6 in (7.26). In this chapter we will use a slightly modified version for the expression of $k(a, b)$ defined in [85]. Let $u = k(a(x), b(x)^\top)$, where $a(x) := \nabla W(x)^\top f(x)$, $b(x) = \nabla W(x)^\top g(x)$, and k is a function $k : \mathbb{R} \times \mathbb{R}^m \to \mathbb{R}^m$ defined by

$$k(a, b) := \begin{cases} -\frac{a+\sqrt{a^2+\|b\|^4}}{\|b\|^2} b, & \text{if } b \neq 0 \\ 0, & \text{if } b = 0. \end{cases} \tag{7.26}$$

In the remainder of this chapter we consider the case when u is a scalar.

Let there be disturbance inputs acting on (7.25), as described by

$$\dot{x} = f(x, v) + g(x)u, \tag{7.27}$$

where v, u and $g : \mathbb{R}^n \to \mathbb{R}^{n\times m}$ are defined as in (7.1) and (7.25), respectively with $v \in \mathbb{R}^p$ and $f : \mathbb{R}^n \times \mathbb{R}^p \to \mathbb{R}^n$.

For the problem of disturbance attenuation by choice of feedback in terms of ISS, it is necessary to define the notion of an ISS CLF. We recall the definition from [85].

Definition 7.3 Let $W : \mathbb{R}^n \to \mathbb{R}$, be a continuously differentiable function for which there exist $\alpha_1, \alpha_2, \alpha, \chi \in \mathcal{K}_\infty$, such that

$$\alpha_1(\|x\|) \leq W(x) \quad \leq \alpha_2(\|x\|), \ \forall x \in \mathbb{R}^n \tag{7.28}$$

$$\nabla W(x)^\top (f(x, v) + g(x)u) \quad \leq -\alpha(\|x\|) + \chi(|v|), \tag{7.29}$$

for all $x \neq 0$, and $v \in \mathbb{R}^p$. Then W is an ISS CLF for the system (7.27).

Note that the second condition above is equivalent with the statement that

$$\nabla W(x)^\top g(x) = 0 \Rightarrow \nabla W(x)^\top f(x, v) < 0, \quad \forall x \in \mathbb{R}^n.$$

Consider as candidate ISS CLF, the function $W(x)$ defined in (7.23) computed for (7.27) when the control input is $u = 0$. In [85], a similar “universal” construction as in (7.26) was proposed for computing feedback stabilizers for (7.27). We propose to use $W(x)$ to compute a feedback stabilizer as constructed in [85] for (7.27) with $f(x, v) = \hat{f}(x) + \hat{g}(x)v$. Thus, let us consider systems described by

$$\dot{x} = \hat{f}(x) + \hat{g}(x)v + g(x)u. \tag{7.30}$$

Let $a(x)$ be redefined as $a(x, v) := \nabla W(x)^\top \hat{f}(x) + \nabla W(x)^\top \hat{g}(x)v = \hat{a}(x) + \hat{b}(x)v$. Then W is an ISS CLF for (7.30) if

$$\hat{a}(x) + \hat{b}(x)v + b(x)u \leq -\alpha(\|x\|) + \chi(|v|). \tag{7.31}$$

In [85], the condition (7.31) was equivalently written so as not to involve v as

$$\hat{a}(x) + \|\hat{b}(x)\|\varrho^{-1}(\|x\|) + b(x)u \leq -\tilde{\alpha}(\|x\|), \tag{7.32}$$

where $\varrho, \tilde{\alpha} \in \mathcal{K}_\infty$ are such that it holds that $\|x\| \geq \varrho(|v|)$ implies that

$$\hat{a}(x) + \hat{b}(x)v + b(x)u \leq \tilde{\alpha}(\|x\|).$$

Then a feedback stabilizer can be computed by using the same formula (7.26) with

$$a(x, d) = \hat{a}(x) + \|\hat{b}(x)\|\varrho^{-1}(\|x\|). \tag{7.33}$$

7.4.1 *Computation of an ISS feedback stabilizer*

In this subsection we summarize the steps required for computing an ISS feedback stabilizer.

7.4.1.1 Compute a CLF candidate function W for $\dot{x} = \hat{f}(x)$

Find a d and compute W similarly as in (7.22) and (7.23), i.e.

$$V(e^{d\left[\frac{\partial \hat{f}(x)}{\partial x}\right]_{x=0}}x) - V(x) \leq -\alpha(\|x\|)$$

and

$$W(x) = \int_0^d V(x + \tau\hat{f}(x))\mathrm{d}\tau, \quad \forall x \in \mathcal{S}.$$

7.4.1.2 Compute $k(x)$ via (7.26) with W and $a(x, d)$ from (7.33)

Compute $\tilde{\alpha}$ and ϱ such that (7.32) holds. From (7.31) it follows that

$$\varrho(|v|) = \alpha^{-1} \circ \chi(|v|)$$

and via the inherent ISS FT LF lemma, Lemma 7.3 we have that $\chi(\cdot)$ can be any $\mathcal{K}_\infty$–function such that $\chi(|v|) \geq \int_0^d L\|v(s)\|\mathrm{d}s$.

7.5 Examples

7.5.1 *Example 1: whirling pendulum*

We consider the system below, which was studied in [25] with the purpose to compute the DOA of the zero equilibrium when the system is autonomous ($u = v = 0$).

$$\begin{aligned} \dot{x}_1 &= x_2 \\ \dot{x}_2 &= \frac{-k_f}{mb}x_2 + \omega^2 \sin(x_1)\cos(x_1) - \frac{g}{l_p}\sin(x_1) + c(u+v). \end{aligned} \tag{7.34}$$

Therein a polynomial LF was computed, whose level set rendering a DOA estimate is shown in Figure 7.1(a) with the black contour. Following Step 7.4.1.1 (for more details we refer to Chapter 5), a LF W was computed from a quadratic FTLF, $V(x) = x^\top Px$, with $P = \left(\begin{smallmatrix} 3.6831 & 2.3169 \\ 2.3169 & 14.7694 \end{smallmatrix}\right)$ and $d = 1.1$ and $\alpha(\|x\|) = \|x\|$. The level set $C = 3.55$ of $W(x)$ defines an estimate of the true DOA of the origin of (7.34) and it is shown with blue in Figure 7.1(a) together with a vector field plot of the system. Then, as suggested in Step 7.4.1.2 we consider the above computed W as a CLF candidate for computing an ISS feedback stabilizer $u = k(x)$. Let $\tilde{\alpha}(\|x\|) = \|x\|$. Next we have to compute ϱ. Since the proposed computational procedure relies on an inherent ISS FTLF, the result in Lemma 7.3 will be used to compute $\chi(|v|)$ which is needed in the expression of ϱ, and consequently in the feedback stabilizer.

Let the disturbance signal be a generated as an uniformly distributed sequence in the interval $(-0.5, 0.5)$. Thus $|v| = \sup_{s\in[0,t]}\|v(s)\| \leq 0.5$ for some $t \in \mathbb{R}_{\geq 0}$. As such we have that

$$L\int_0^d \|v(s)\|\mathrm{d}s \leq L\int_0^d |v_{[0,d]}|\mathrm{d}s \leq Ld|v_{[0,d]}| = Ld\bar{v}, \tag{7.35}$$

where L is the Lipschitz constant and $\bar{v} = 0.5$ for the considered system and disturbance signal. L can be approximated as suggested in [77], from the fact that $\|\frac{\partial f}{\partial v}\| \leq L$ implies that $\|f(x,v) - f(x,u)\| \leq L\|v-u\|$. In this case $L = c = 0.2$. However, to compute $k(x)$ we need $\varrho^{-1}(\|x\|)$. We know that $\varrho(|v|) = \alpha^{-1} \circ \chi(|v|)$, thus $\varrho^{-1}(s) = \chi^{-1}(s) \circ \alpha = \chi^{-1}(s) \circ \mathrm{id} = \chi^{-1}(s)$. Following from (7.35) we shall take $\varrho^{-1}(s) = \frac{1}{Ld}s$, thus $\varrho^{-1}(\|x\|) = \frac{1}{Ld}\|x\|$ in (7.32). Furthermore, since the computed $W(x)$ is based on a FTLF

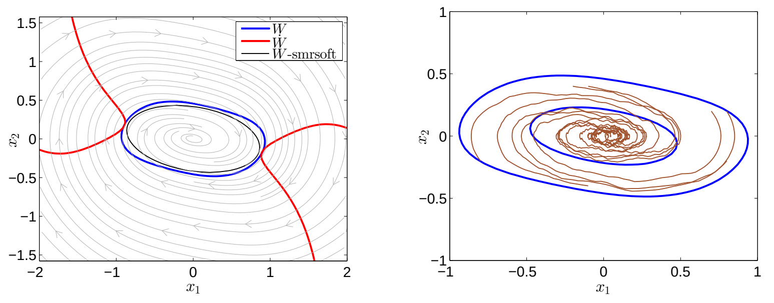

(a) (b)

Figure 7.1: (a)–level set of W for $C = 3.55$ computed for (7.34) with $v = u = 0$, $d = 1.1$, plotted in blue, its corresponding derivative–red and the level set computed in Chesi with smrsoft; (b)–level set of W for $C = 3.55$ computed for (7.34) with $v \neq 0$ plotted in blue and simulations from the same $x(0)$ different cases.

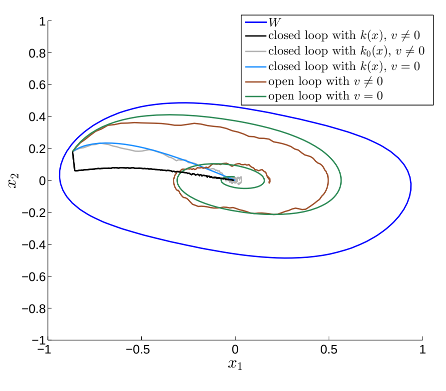

Figure 7.2: Level set of W for $C = 3.55$ computed for (7.34) with $v \neq 0$ plotted in blue and simulations from the same $x(0)$ different cases.

which is an inherent ISS LF, it follows from the equivalence in Lemma 7.2 that $W(x)$ is an (inherent) ISS Lyapunov function. From [111, Lemma 2.14] it follows that the set

$$\mathcal{S}_v = \{x \in \mathbb{R}^n \,|\, W(x) \leq \alpha_2 \circ \chi(|v|)\}$$

is an invariant set for (7.34). If we consider $\chi(|v|) = Ld\bar{v}$ and we know that $W(x)$ can be upper bounded by $\varepsilon V(x) = x^\top \varepsilon P x$ such that the level set $V(x) = \frac{1}{\varepsilon}$ is included in the level set $W(x) = C$, then $\alpha_2(\|x\|) = \lambda_1(\varepsilon P)\|x\|$, where λ_1 is the largest eigenvalue of P. Then we obtain $\alpha_2 \circ \chi(|v|) = \lambda_1(\varepsilon P)Ld\bar{v}$. For this example $\varepsilon = 0.4762$ and a plot of the resulting level set is shown in Figure 7.1(b) together with several trajectories of the system.

The same level set defined by $C = 3.55$ of W is shown in Figures 7.1(a), 7.1(b) and 7.2. Next, we compute $k(x)$ from (7.26) with $a(x, d)$ from (7.33) on basis of the computed $W(x)$. As the expression of $k(x)$ is rather lengthy we provide a plot of $u = k(x)$ for the initial condition $x_0 = \begin{pmatrix} -0.8680 & 0.1810 \end{pmatrix}^\top$ in Figure 7.3(d). For comparison, we show also a plot of $u = k_0(x)$, where $k_0(x)$ is computed without considering v in the dynamics, i.e. in the computation of a in (7.26).

A trajectory of the closed loop system is shown in Figure 7.3(d) for a particular initial condition, together with trajectories initiated at the same initial condition for different cases: the closed loop system with $u = k(x)$–black, the closed loop system with $u = k_0(x)$ and $v \neq 0$–grey, the closed loop system with $u = k_0(x)$ and $v = 0$–blue, the open loop system with $v \neq 0$–brown and the open loop system with $v = 0$–green. For the same initial

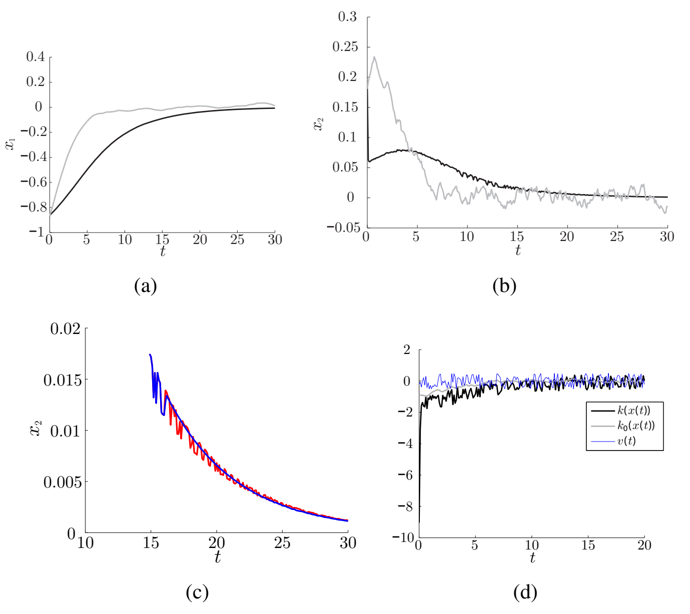

Figure 7.3: The corresponding states for k computed without considering v–grey and k computed with $v \neq 0$ via the function ϱ ((a)-(b)). In (c): plot of x_2 when the disturbance becomes zero for $t = 16$; (d): v, $k(x)$ and $k_0(x)$ as functions of the solution of (7.34) initiated at $x_0 = (-0.8680 \quad 0.1810)^\top$.

condition, we show each of the states of the closed–loop system for $u = k(x)$–black and for $u = k_0(x)$–grey in Figure 7.3(a) and Figure 7.3(b). We also illustrate the case when the disturbance becomes zero after some time in Figure 7.3(c) for the x_2 state. It can be observed that the trajectory corresponding to the disturbance becoming zero–blue recovers asymptotic stability.

7.6 Conclusions

In this chapter, we provided an equivalent characterization of the ISS property in terms of existence of an ISS–FTLF. For what concerns the converse result, when the ISS property is known, under a certain assumption on the solution estimate of the system subject to disturbance inputs, we showed that any $\mathcal{K}_\infty$–function of the norm of the state is an ISS–FTLF. Furthermore, inspired by classical converse results, we showed how an ISS LF can be computed via a construction of the Massera type.

When the considered finite–time function candidate is the norm of the state, i.e. let $V(x) = \|x\|$, for verification purposes, we show that V is an inherent finite–time ISS LF if it is a FTLF for the system with zero inputs. Finally, we proposed a procedure to construct an ISS feedback stabilizer by using Sontag's "universal" formula for ISS stabilization and a Massera–type of function constructed for the system without disturbances.

The main motivation for the results in this chapter comes from the need to ensure some robustness properties for the tools developed in the previous chapters, when applied to biological systems. Furthermore, the ISS theory provides a suitable framework for dealing with large scale systems (which can be met in biology, although not treated in this thesis). If such systems can be written as interconnected small scale systems, then the individual ISS property together with small gain type of conditions can be used for analysis of the large scale system [23].

Chapter 8

Conclusions and future perspectives

8.1 Discussion of the results

In this thesis a Lyapunov functions outlook on answering problems emerging from biological applications, which are described by nonlinear continuous–time dynamical systems has been developed. In particular, we derive and demonstrate the use of nonlinear systems theory tools for analysis and stabilization of the dynamical description of the considered class of systems. Consequently, the purpose of the developed framework is to assist biologists/clinicians in addressing issues such as disease or dysfunctions diagnosis, time evolution predictions and treatment evaluation and synthesis.

As advocated in this thesis, there is a one–to–one relation between properties of the equilibria and trajectories of the continuous–time nonlinear differential equation systems used as models for biological systems and their real life interpretations. We recall the case of the HPA axis for which a stable equilibrium with an acceptable value of the cortisol state corresponds to a well functioning HPA axis. Therefore, in this thesis we have sought to provide relevant solutions to the analysis and stabilization problems in the context of nonlinear dynamical systems, which answer the above mentioned biological problems.

Specifically, by relevant solutions it is meant: as good as possible DOA estimates in the case of the analysis problems and which allow destabilizing certain equilibria and stabilizing others, in the case of the stabilization problem. Accordingly, the classical problems of computing LFs and estimating the DOA for nonlinear systems have been addressed in the thesis.

In order to derive systematic procedures which are computationally applicable in the field of systems biology and are based on LFs, two different perspectives were considered with respect to the nonlinearity type. Therefore, the subproblems addressed in this thesis can be classified as follows.

8.1.1 Analysis and design tools for polynomial (approximated) systems

Many biological systems, especially those describing diseases as a consequence of the time evolving interaction between native cells and invader cells, whether they are from bacteria, viruses or they develop from genetic mutations, can be and are usually modelled in the literature by following evolutionary principles. This approach generally leads to polynomial systems. Although the problem of computing LFs for polynomial systems has been studied in the literature, leading to polynomial LFs, for computing nonconservative DOA estimates a different approach was needed. As such, in Chapter 2, a Zubov type of procedure has been revisited, for the reason that it iteratively works at improving the DOA estimate. In the interest of answering the stabilization problems from Chapter 1, Table 1.1, this procedure was further extended to generate a feedback stabilizer and a control Lyapunov function. In particular, the coefficients of a polynomial feedback stabilizer are computed together with the coefficients of a rational polynomial CLF, both with a predefined structure. While this procedure is systematic and theoretically should render a maximal LF, which is associated with the true DOA for a system, in practice it will provide an estimate, similar to all computational methods from the literature.

As for a representative biological application, tumor dynamics have been considered and in Chapter 3 we discussed two population computation type of models from the literature and we derived a new one which contains relevant information for immunotherapeutic treatment strategies. The analysis of these models has been carried by means of RLFs and for treatment design we proposed an alternative to the continuous, polynomial feedback stabilizer. The alternative proposed treatment course is based on a switching control strategy defined on domains of attraction of equilibria of interest. Specifically, the problem of steering a stable invasive tumor to tumor dormancy has been investigated. This has been addressed by means of a switching control law defined over successive parametrized DOAs which can steer trajectories initiated in the DOA of the invasive tumor equilibrium to the DOA of the tumor dormancy equilibrium, from which the solution converges autonomously to the desired equilibrium.

For nonpolynomial systems, the same procedures for computing DOAs and stabilizing control laws can be applied. However, in addition to the estimation errors, polynomial approximations errors will introduce conservativeness in the results. The switching control law will then be based on DOAs which are computed for polynomial approximations of the individual switching dynamics and the continuous feedback stabilizer on the approximation of the system whose steady state is to be stabilized.

8.1.2 Analysis and design tools for general nonlinear systems

The research question posed in Chapter 1 is concerned with a broader class of nonlinear systems emerging from biological processes, not only polynomial ones. With regard to overcoming the conservativeness of RLFs based tools, which is due to approximations of the functions describing the dynamics, approaches which are not dependent on the system class have been considered. Thereupon, in Chapter 4 alternative constructive converse theorems to the classical ones, known as the Massera and Yoshizawa constructions have been developed. Alternative constructions were needed for developing a framework which allows for computation feasibility, and thus can be applied to models for biological systems. Otherwise, restrictions on the considered class of systems such as exponential stability, or the use of specific functions within the constructions, which are generally difficult to find, are imposed.

In Chapter 4 we allow for $\mathcal{KL}$–stability (though under one assumption) and the construction of the LF is based on any $\mathcal{K}_\infty$ function of the norm of the solution of the system. A finite–time decrease criterion was imposed on the $\mathcal{K}_\infty$ function which generates a finite computation interval in both Massera and Yoshizawa type of constructions. However, for either constructions, the freedom in the LF construction is counteracted by the fact that the solution of the system needs to be known up to some finite time value. This problem was addressed in Chapter 5 by means of solution approximation techniques or by developing a computational procedure starting from the linearized system towards obtaining DOA estimates.

The stability analysis and stabilization tools developed in the previous chapters are applicable to deterministic models of considered biological systems. However, the estimated model parameters are subject to errors, the developed models are simplified and proposed control inputs based on feedback stabilization can be affected by perturbations or inaccuracies in measurements. Then it is important to study the stability and stabilization problems with respect to disturbance inputs.

Since biological models are subject to input disturbances coming from parameter estimation errors or inaccuracies in measurements, the problem of robustness of the tools developed in Chapter 4 was addressed in Chapter 7. The ISS framework has been chosen, since it fits to the nonlinear context of our problems and allows formulations in terms of LFs. Hence, in Chapter 4 we provided an equivalent characterization of the ISS property in terms of existence of an ISS–FTLF. For what concerns the converse result, when the ISS property is known, under certain assumptions, we showed that any $\mathcal{K}_\infty$–function of the norm of the state is an ISS–FTLF, allowing computation for a Massera–type ISS LF.

When the considered finite–time function candidate is the norm of the state, for verification purposes, we showed that V is an inherent finite–time ISS LF if it is a FTLF for the system with zero inputs. Finally, we proposed a procedure to construct an ISS feedback stabilizer by using Sontag's "universal" formula for ISS stabilization and a Massera–type of function constructed for the system without disturbances.

8.1.3 Verification and applicability of the developed theory in the biological field

Based on the theoretical tools developed in Chapter 4, the problems of computing DOAs and stabilizing control laws for biological systems with general (Lipschitz) nonlinearities can be addressed without requiring approximations of the dynamics. However, for computational purposes approximations of the system solutions over a finite time interval are required. In Chapter 5, two solutions were proposed. The first one relies on linearization and computation via an expanded FTLF and the second is based on a numerical approach for the computation of LFs via the Massera–type converse. The constructed Lyapunov function is continuous and piecewise affine (CPA), computed via a finite–time Lyapunov function evaluated at approximated trajectories. In both cases, by optimization, the obtained LF is verified and consequently we are able to give an estimate of the DOA. Both proposed procedures delivered promising results towards obtaining nonconservative approximations of the DOA. By two- and three-dimensional examples, we have shown that the proposed method can deliver comparable results with state–of–art computational methods from the literature. The improvements in the DOA estimation validate the nonconservativeness of the developed method. A possible advantage of the proposed solution originates from the fact that Lyapunov functions are constructed based on finite–time Lyapunov functions and the corresponding finite time decrease time.

Chapter 6 is dedicated strictly at applying the procedures derived in Chapters 4 and 5 to some representative examples of biological applications. In the case of the HPA example or the genetic toggle switch, for which bistability is either a property of a dysfunction (in the HPA case) or desired, engineered behaviour, a measure of the "nonconservativeness" is provided by the bistability property. It is known that the boundary of the DOAs of the two stable equilibria contains the unstable equilibrium. Thus, DOA estimates which get very close to the unstable equilibrium are also very close to the true DOAs. In both examples, by means of the developed procedures, DOA estimates which satisfy this criterion were obtained. This allows for fairly accurate disease evolution predictions. For example, in the case of the HPA axis, if measurements of the three hormone levels (or at least cortisol level) indicate that the state of the patient is inside the hypercortisolic DOA or hypocortisolic DOA, one can infer that without treatment intervention, the patient will converge to a stable nonhealthy state which in turn will lead, for example, to type 2 diabetes.

8.2 Future perspectives and extensions

In this thesis a nonlinear systems theory based approach was proposed for answering problems from biological applications which are related to diagnosis and predictions and treatment design strategies. The derived LF computation procedures were aimed at issues arising from the specific classes of systems considered in this thesis. The majority of possible extensions of the developed results come from a biological perspective, however they reflect on nonlinear systems theory classical problems.

8.2.1 Dynamical properties of biological systems

A large range of biological systems are characterized by oscillatory behaviour, which in turn is represented by stable limit cycles of their corresponding models. Therefore, in order to address this type of systems as well, an extension of the developed tools in this thesis for computing LFs for attractors or invariant sets (as formulated for example in [15], [110]) is necessary.

An inherent property of biological systems is that they are positive, thus the positive orthant is an invariant set for such systems. When a stable equilibrium is on the boundary of the positive orthant, or the positive orthant is an attractor for certain equilibria, the resulting DOAs based on level sets of LFs will also contain initial states outside the positive orthant if $\dot{W}(x) < 0$ holds in those points. While this is not a concern for computing DOAs, when computing stabilizing controllers based on such LFs it is possible that the control input will steer trajectories outside the positive orthant before converging to the desired equilibrium. Thus, mechanisms which restrict the computation of CLFs inside the positive orthant need to be included in the procedures.

8.2.2 Validation and application to real life cases

In the case of synthetically engineered biological systems, like the genetic toggle switch or the reprissilator, the models discussed in this thesis have been experimentally validated to capture real life properties of the systems [40], [37]. The methods developed in this thesis can be directly employed to analyze certain synthesized behaviours or indicate the optimal operating areas for the systems as well as for computing control inputs which achieve the desired behavior.

In the case of biomedical systems, while a model type can be validated against measurements gathered from patients, in certain cases parameter models are specific to each person and need to be measured or estimated. The parameters of the HPA axis model considered in Chapter 6 used in this thesis have been derived based on available experimental data from multiple patients in [6]. The parameters of the tumor growth models from Chapter 3 have been chosen to illustrate certain behaviours which correspond to a range of parameter values. Predator–prey models have been shown to be able to describe very well the stages of cancer evolution [41] and explain phenomena which, without an understating of the nonlinear interactions between the tumor cells in immune cells, cannot be explained by medical doctors. In this sense, effects of treatment can be incorporated in the model parameters to analyze the influence of treatment on the tumor dynamics. This approach can provide a supporting mechanism for medical doctors when deriving personalized treatment strategies. However, again the model parameters are specific to each tumor and not all are measurable. Take for example the parameter representing the influence of immune cells on tumor cells. To the best of our knowledge, it can only be estimated from analyzing data of a tumor evolution in time. As a possible solution we propose for example the use of (noninvasive) ultrasound data, gathered for a period of time from the same patient.

As many diseases which have a nonlinear dynamical behavior are becoming more and more prevalent, and with the increase number of applications of the “big data” and “data analytics” concepts in the healthcare field, extracting dynamical information from the gathered data becomes more and more relevant. This will allow for more accurate, patient specific models which need to be analyzed and possibly, used for optimal personalized treatment design.

Appendix A

Approximation of solutions

A.1 Approximate solutions using piecewise affine vector fields

The method of approximating the solution of (4.1) using piecewise affine vector fields, was proposed in [51]. A 2D version of the algorithm called CASCADE has been implemented in MATLAB by the author of [51] and is available online at: `http://ljk.imag.fr/CASYS/LOGICIELS/CASCADE/`. A 3D version of the algorithm has been implemented in MATLAB by the first author of [114]. Unlike classical methods for approximating solutions (Runge-Kutta, Taylor, etc.), which use a discretization of the time space, this method uses a discretization of the phase space. More precisely, consider system (4.1) with $f : \mathfrak{M} \to \mathbb{R}^n$, $\mathfrak{M} \subset \mathbb{R}^n$; given a simplicial subdivision of the phase space, we let f_h be the interpolate piecewise affine vector field of f on the triangulation. To obtain the approximate solutions, the following steps have been followed [51]. [1]

A.1.1 Algorithm

First, we define a subdivision of $\mathfrak{M}$, $\mathfrak{T} = \{\mathfrak{S}_1, \dots, \mathfrak{S}_z\}$, where $\mathfrak{S}_i,\ i \in \mathbb{N}_{[1:z]}$, is an n-simplex. A simplex $\mathfrak{S}_i$ is delimited by the $(n-1)$-simplices $\mathfrak{F}_{0,i}, \dots, \mathfrak{F}_{n,i}$, called facets. For all $\mathfrak{S}_i$, $i \in \mathbb{N}_{[1:z]}$ the unique affine interpolate vector field that interpolates $f(x)$ at the vertices $v_0, \dots, v_n$ of $\mathfrak{S}_i$ is given by

$$f_i(x) = \sum_{j=0}^{n} \lambda_j(x) f(v_j) = A_i x + B_i,$$

where $\lambda_j(x) \in [0,1]$ are the barycentric coordinate functions with respect to the vertices $v_0, \dots, v_n$, such that

$$x = \sum_{j=0}^{n} \lambda_j(x) v_j, \quad \sum_{j=0}^{n} \lambda_j(x) = 1, \quad \forall x \in \mathfrak{S}_i.$$

Then the piecewise affine vector field is given by

$$f_h(x) = f_i(x), \quad \text{if } x \in \mathfrak{S}_i.$$

[1] The work presented in this Appendix was developed by Tom Steentjes, during his internship [114].

Next, we find the approximated solution on a simplex $\mathfrak{S}_i$. If $x(t) \in \mathfrak{S}_i$, then it verifies

$$\dot{x} = A_{i_k} x + B_{i_k},$$

which is equivalent to

$$\begin{pmatrix} \dot{x} \\ 0 \end{pmatrix} = \underbrace{\begin{pmatrix} A_{i_k} & B_{i_k} \\ 0 & 0 \end{pmatrix}}_{=:M_{i_k}} \begin{pmatrix} x \\ 1 \end{pmatrix}. \tag{A.1}$$

The solution of (A.1) is given by

$$\begin{pmatrix} x(t) \\ 1 \end{pmatrix} = e^{(t-t_k)M_{i_k}} \begin{pmatrix} x(t_k) \\ 1 \end{pmatrix},$$

for all t such that $x(t) \in \mathfrak{S}_{i_k}$, where t_k is the time at which $x(t)$ entered $\mathfrak{S}_{i_k}$.

To determine t such that $x(t) \in \mathfrak{S}_{i_k}$, we need to determine the time t_{k+1} at which $x(t)$ exits simplex $\mathfrak{S}_{i_k}$. There does not exist an algebraic expression for the exit time for n-dimensional systems, as it does for 1-dimensional systems [51]. Therefore, numerical computation of the exit time is used instead. The problem can be stated equivalently as follows

$$\begin{aligned} &\text{For } \dot{x} = Ax + B, \quad x(0) =: x_0 \in \mathfrak{S}, \\ &\text{find the time when } x(t) \text{ leaves } \mathfrak{S}, \\ &t^* \in \mathbb{R}_{>0} \text{ (if it exists).} \end{aligned} \tag{A.2}$$

The simplex $\mathfrak{S}$ is delimited by the facets $\mathfrak{F}_0, \ldots, \mathfrak{F}_n$. Consider the unitary vectors k_j being orthogonal with respect to $\mathfrak{F}_j$ and directed towards the interior of $\mathfrak{S}$. Then there exist scalars $r_0, \ldots, r_n \in \mathbb{R}$, such that $x \in \mathfrak{S}$, if and only if

$$k_j^\top x - r_j \geq 0, \quad \forall j \in \mathbb{N}_{[0:n]}.$$

Consequently, the distance of $x(t)$ to $\mathfrak{F}_j$ is defined as $l_j(t) := k_j^\top x(t) - r_j$, $j \in \mathbb{N}_{[0:n]}$. Now, the series τ_k converges to the solution t^* of (A.2) quadratically [50]

$$\begin{cases} \tau_0 & = 0, \\ \tau_{k+1} & = \tau_k + \min_{j \in \mathbb{N}_{[0:n]}} s_{k_j}, \end{cases}$$

where s_{k_j} is the smallest positive solution of the equation

$$l_j(\tau_k) + s\dot{l}_j(\tau_k) + \frac{1}{2}s^2 m_j = 0, \tag{A.3}$$

with

$$m_j = \min_{i \in \mathbb{N}_{[0:n]}} k_j^\top (A^2 v_i + AB).$$

When there does not exist a solution for (A.3) in $\mathbb{R}_{>0}$, then we set $s_{k_j} = \infty$. Since we are looking for an approximate solution on a finite time interval $\mathcal{T}$, the algorithm will stop whenever for some finite k, $\tau_k \notin \mathcal{T}$.

Based on the exit time t_{k+1}, one can easily compute the position $x(t_{k+1})$ at which it exits the simplex $\mathfrak{S}_{i_k}$. Next, the following active simplex $\mathfrak{S}_{i_{k+1}}$ is created. Since the state exits the simplex through a face,

$$\exists j \in \mathbb{N}_{[0:n]} \quad x(t_{k+1}) \in \mathfrak{F}_{j,i_k}.$$

Since we know j, we then create a new simplex $\mathfrak{S}_{i_{k+1}}$ such that

$$\mathfrak{S}_{i_{k+1}} \cap \mathfrak{S}_{i_k} = \mathfrak{F}_{j,i_k},$$

i.e. the current and "new" simplex have a common facet ($(n-1)$-simplex). The listed steps will be repeated, until $t \notin \mathcal{T}$.

Now, we have determined finite series of time instants and exit states, $\{t_k\}$ and $\{x(t_k)\}$, respectively. The approximate solution is now given by an analytic expression given by

$$\begin{pmatrix} x(t) \\ 1 \end{pmatrix} = e^{(t-t_k)M_{i_k}} \begin{pmatrix} x(t_k) \\ 1 \end{pmatrix}, \quad \forall t \in [t_k, t_{k+1}].$$

A.1.2 Error bound on approximate solutions

In this section it will be shown that the approximate solutions of the piecewise affine vector field method converge to the exact solutions of (4.1), when the simplex diameter $\mathrm{diam}(\mathfrak{S}_{i_k}) \to 0$ for all i. We recall the so-called Fundamental Inequality [66], which provides a way to compute an upperbound on the norm of the difference of two trajectories. This theorem will be used in the proof of Corollary A.1, which provides an upperbound on the error of the approximated solution.

Theorem A.1 Let $\mathcal{T} \subset \mathbb{R}$ be a nonempty interval and let $\mathcal{U} \subset \mathbb{R}^n$ be a domain. Let $f : \mathcal{T} \times \mathfrak{M} \to \mathbb{R}^n$ be a continuous mapping and assume there exists a constant L such that f satisfies the Lipschitz condition, i.e. there exists a constant $L \in \mathbb{R}_{>0}$ such that

$$\|f(t,x) - f(t,y)\| \le L\|x-y\| \quad \forall t \in \mathcal{T} \quad \forall x, y \in \mathfrak{M}.$$

If for ε_i, $\delta \in \mathbb{R}$, $\xi_1(t)$ and $\xi_2(t)$ are continuous piecewise differentiable functions on $\mathcal{T}$ into $\mathbb{R}^n$ with

$$\|\dot{\xi}_i(t) - f(t, \xi_i(t))\| \le \varepsilon_i$$

and let $t_0 \in \mathcal{T}$ with

$$\|\xi_1(t_0) - \xi_2(t_0)\| \le \delta,$$

then

$$\|\xi_1(t) - \xi_2(t)\| \le \delta e^{L|t-t_0|} + \frac{\varepsilon_1 + \varepsilon_2}{L}\left(e^{L|t-t_0|} - 1\right).$$

Corollary A.1 Let $\mathcal{T} \subset \mathbb{R}$ be a nonempty interval and let $\mathcal{U}$ be a domain in $\mathbb{R}^n$. Let $f : \mathfrak{M} \to \mathbb{R}^n$ be a mapping that satisfies the Lipschitz condition

$$\|f(t,x) - f(t,y)\| \leq L\|x - y\| \quad \forall t \in \mathcal{T},\ \forall x, y \in \mathfrak{M},$$

for some $L \in \mathbb{R}_{>0}$. Let $t_0 \in \mathcal{T}$ and let $x_0 \in \mathfrak{M}$ and denote the solution of the initial value problem

$$\dot{x}(t) = f(x(t)), \quad x(t_0) = x_0,$$

by $\xi(t)$ and denote the solution of

$$\dot{x}_h(t) = f_h(x_h(t)), \quad x_h(t_0) = x_0,$$

by $\xi_h(t)$, where $f_h : \cup_{i \in \mathbb{N}_{[1:z]}} \mathfrak{S}_i \to \mathbb{R}^n$ denotes the piecewise affine interpolate vector field of f with regard to the simplicial subdivision $\cup_{i \in \mathbb{N}_{[1:z]}} \mathfrak{S}_i$ of $\mathfrak{M}$. Let the error in the interpolation have an upper bound $\varepsilon \in \mathbb{R}_{\geq 0}$, i.e.

$$\|f(x) - f_h(x)\| \leq \varepsilon, \quad \forall x \in \cup_{i \in \mathbb{N}_{[1:z]}} \mathfrak{S}_i.$$

Then for all t where ξ and ξ_h are defined,

$$\|\xi(t) - \xi_h(t)\| \leq \frac{\varepsilon}{L}\left(e^{L|t-t_0|} - 1\right).$$

Proof: We have

$$\|\dot{\xi}(t) - f(\xi(t))\| = 0$$

and

$$\|\dot{\xi}_h(t) - f(\xi_h(t))\| = \|f_h(\xi_h(t)) - f(\xi_h(t))\|.$$

As $\xi_h(t) \in \cup_{i \in \mathbb{N}_{[1:z]}} \mathfrak{S}_i$ for all $t \in \mathcal{T}$, we have

$$\|f(x) - f_h(x)\| \leq \varepsilon,\ \forall x \in \cup_{i \in \mathbb{N}_{[1:z]}} \mathfrak{S}_i \\ \Rightarrow \|f_h(\xi_h(t)) - f(\xi_h(t))\| \leq \varepsilon,\ \forall t \in \mathcal{T}.$$

Moreover,

$$\|\xi(t_0) - \xi_h(t_0)\| = 0,$$

and thus using Theorem A.1 we conclude that

$$\|\xi(t) - \xi_h(t)\| \leq \frac{\varepsilon}{L}\left(e^{L|t-t_0|} - 1\right).$$

The following lemma will provide a way to compute a lower bound on the Lipschitz constant $L \in \mathbb{R}_{>0}$ for some convex domain in $\mathbb{R}^n$, such that the upper bound on the error in Corollary A.1 can be computed.

Lemma A.1 Let $\mathcal{T} \subset \mathbb{R}$ be a nonempty interval and let $\mathcal{D}$ be a domain in $\mathbb{R}^n$. Let $f : \mathcal{T} \times \mathcal{D} \to \mathbb{R}^n$ be a mapping and suppose that $\frac{\partial f}{\partial x}$ exists and is continuous on $\mathcal{T} \times \mathcal{D}$. If for a convex subset $\mathcal{W} \subset \mathcal{D}$, there is a constant $L \in \mathbb{R}_{>0}$ such that

$$\left\| \frac{\partial f}{\partial x}(t, x) \right\| \leq L,$$

on $\mathcal{T} \times \mathcal{W}$, then

$$\|f(t, x) - f(t, y)\| \leq L\|x - y\|, \quad \forall t \in \mathcal{T},\ \forall x, y \in \mathcal{W}.$$

A proof of the above lemma can be found in [77, Chapter 3]. In the following theorem, an upper bound on the error ε of the piecewise affine vector field f_h with respect to the exact vector field f is provided. Let the norm $\|\cdot\|_{\max}$ be defined by $\|A\|_{\max} = \max\{|a_{ij}|\}$.

Theorem A.2 Let $\mathfrak{S}_i$ be an n-simplex satisfying $\operatorname{diam}(\mathfrak{S}_i) = h$, $h \in \mathbb{R}_{\geq 0}$. Let $f : \cup_{i \in \mathbb{N}_{[1:z]}} \mathfrak{S}_i \to \mathbb{R}^n$ be a vector-valued multivariate function of class C^2 and $f_i : \mathfrak{S}_i \to \mathbb{R}^n$ the affine map that interpolates f at the vertices of $\mathfrak{S}_i$. Now let $f_h : \cup_{i \in \mathbb{N}_{[1:z]}} \mathfrak{S}_i \to \mathbb{R}^n$ denote the piecewise affine vector field

$$f_h(x) = f_i(x) \quad \text{if } x \in \mathfrak{S}_i.$$

Then

$$\|f(x) - f_h(x)\| \leq K h^2 M, \quad \forall x \in \cup_{i \in \mathbb{N}_{[1:z]}} \mathfrak{S}_i,$$

where

$$M = \max_{i \in \mathbb{N}_{[1:z]}} \max_{j \in \mathbb{N}_{[1:n]}} \sup_{x \in \mathfrak{S}_i} \|H_{f^j}(x)\|_{\max},$$

with H_{f^j} the Hessian of the j-th entry of f, and

$$K = \frac{n^2 \sqrt{n}}{4(n+1)}.$$

Proof: As

$$\|f(x) - f_h(x)\| = \|f(x) - f_i(x)\|, \quad \forall x \in \mathfrak{S}_i,$$

we have

$$\|f(x) - f_h(x)\| \leq \max_{i \in \mathbb{N}_{[1:z]}} \{\|f(x) - f_i(x)\|\},$$

for all $x \in \cup_{i \in \mathbb{N}_{[1:z]}} \mathfrak{S}_i$.

Consider a single simplex $\mathfrak{S}_i$, $i \in \mathbb{N}_{[1:z]}$, and corresponding interpolation $f_i : \mathfrak{S}_i \to \mathbb{R}^n$. According to [113]

$$\|f(x) - f_i(x)\| \leq Kh^2 \max_{j \in \mathbb{N}_{[1:n]}} \sup_{x \in \mathfrak{S}_i} \|H_{f^j}(x)\|_{\max},$$

and thus

$$\begin{aligned}
\|f(x) - f_h(x)\| &\leq \max_{i \in \mathbb{N}_{[1:z]}} Kh^2 \max_{j \in \mathbb{N}_{[1:n]}} \sup_{x \in \mathfrak{S}_i} \|H_{f^j}(x)\|_{\max} \\
&= Kh^2 \max_{i \in \mathbb{N}_{[1:z]}} \max_{j \in \mathbb{N}_{[1:n]}} \sup_{x \in \mathfrak{S}_i} \|H_{f^j}(x)\|_{\max} \\
&= Kh^2 M.
\end{aligned}$$

We have shown that the upper bound on the error of approximate solutions for the considered algorithm converges to zero, when the simplex size goes to zero. Indeed, using Corollary A.1 and Theorem A.2, we see that

$$\|\xi(t) - \xi_h(t)\| = \mathcal{O}(h^2).$$

A.2 Approximate solutions using the Runge-Kutta method

One of the classical methods for approximating the solution of (1) is the Runge-Kutta method. We consider t on the finite time interval $t \in [t_0, t_z]$. Note that this method does not provide an analytic expression of the approximate solution. Indeed, we find an approximate solution $x(t)$ on a finite set of time instants $t_0, \ldots, t_z$, where $t_i < t_j$ for all $j > i$. The sample time will be taken constant, that is

$$t_k = t_0 + kh, \quad k \in \mathbb{N}_{[0:z]}.$$

The general form for a Runge-Kutta method is given by

$$x(t_{k+1}) = x(t_k) + hF(t_k, x(t_k), h), \quad k \in \mathbb{R}_{\geq 0}.$$

An explicit Runge-Kutta method of $s-$th order for $\dot{x} = f(t, x)$ has the following form [8]:

$$\begin{aligned}
z_1 &= x(t_k), \\
z_2 &= x(t_k) + ha_{2,1} f(t_k, z_1), \\
z_3 &= x(t_k) + h(a_{3,1} f(t_k, z_1) + a_{3,2} f(t_k + c_2 h, z_2)), \\
&\vdots \\
z_s &= x(t_k) + h(a_{s,1} f(t_k, z_1) + a_{s,2} f(t_k + c_2 h, z_2) \\
&\qquad + \cdots + a_{s,s-1} f(t_k + c_{s-1} h, z_{s-1})), \\
x(t_{k+1}) &= x(t_k) + h(b_1 f(t_k, z_1) + b_2 f(t_k + c_2 h, z_2) + \cdots \\
&\qquad + b_{s-1} f(t_k + c_{s-1} h, z_{s-1}) + b_s f(t_k + c_s h, z_s)).
\end{aligned}$$

Equivalently, we write

$$z_i = x(t_k) + h\sum_{j=1}^{i-1} a_{i,j} f(t_k + c_j h, z_j), \quad i \in \mathbb{N}_{[1:s]},$$
$$x(t_{k+1}) = x(t_k) + h\sum_{j=1}^{s} b_j f(t_k + c_j h, z_j).$$

Note that the next state $x(t_{k+1})$ depends only on the current state $x(t_k)$ and not on the previous states $x(t_{k-1})$ etcetera. Therefore, this method is called a one-step method. Since we only consider autonomous systems (4.1), the algorithm is reduced to

$$z_i = x(t_k) + h\sum_{j=1}^{i-1} a_{i,j} f(z_j), \quad i \in \mathbb{N}_{[1:s]}, \tag{A.4}$$
$$x(t_{k+1}) = x(t_k) + h\sum_{j=1}^{s} b_j f(z_j). \tag{A.5}$$

In this thesis, we mainly focus on the fourth-order Runge-Kutta method (RK4) given by

$$\begin{aligned} z_1 &= x(t_k), \\ z_2 &= x(t_k) + \frac{1}{2} h f(z_1), \\ z_3 &= x(t_k) + \frac{1}{2} h f(z_2), \\ z_4 &= x(t_k) + h f(z_3), \\ x(t_{k+1}) &= x(t_k) + \frac{1}{6} h (f(z_1) + 2f(z_2) + 2f(z_3) + f(z_4)). \end{aligned}$$

A.2.1 Error bound on approximate solutions

Consider the truncation error defined by

$$E_{k+1}(\xi(t)) := \xi(t_{k+1}) - (\xi(t_k) + hF(t_k, \xi(t_k), h)),$$

where $\xi(t)$ denotes the true solution to (4.1). According to [8] we have the following result regarding the convergence.

Corollary A.2 If the Runge-Kutta method (A.4), (A.5) has a truncation error $\mathcal{O}(h^{m+1})$, then the error in the convergence of $x(t_k)$ to $\xi(t)$ on $[t_0, t_z]$ is $\mathcal{O}(h^m)$.

For the fourth-order Runge-Kutta method, we have that $E_{k+1} = \mathcal{O}(h^5)$. Therefore, the error in the convergence of the approximate solution to the exact solution is $\mathcal{O}(h^4)$ and thus for $h \to 0$, we have that the approximate solution converges to the true solution.

A.3 Numerical examples of approximate solutions

In this section we show two examples to illustrate the piecewise affine vector field method and the RK4 method. The two examples considered, represent models of biochemical processes. As the states of the models represent concentrations, they are considered to be biologically feasible if they are contained in the positive orthant $\mathcal{P}$, which is defined as

$$\mathcal{P} := \{(x_1, x_2, x_3) \in \mathbb{R}^3 | x_1 \geq 0,\ x_2 \geq 0,\ x_3 \geq 0\}.$$

In what follows the simplex diameter $h = 0.05\sqrt{2}$ has been used for all simplices $\mathfrak{S}_i$ generated along the trajectory for the piecewise affine vector field method. For the RK4 method a step size $h = 0.05$ has been used.

A.3.1 Model of hypothalamic-pituitary-adrenal gland axis

Consider again the dimensionless model representing the HPA-axis (6.2), with the parameters given in section (6.2). Approximations of the solutions of (6.2) are made using both the

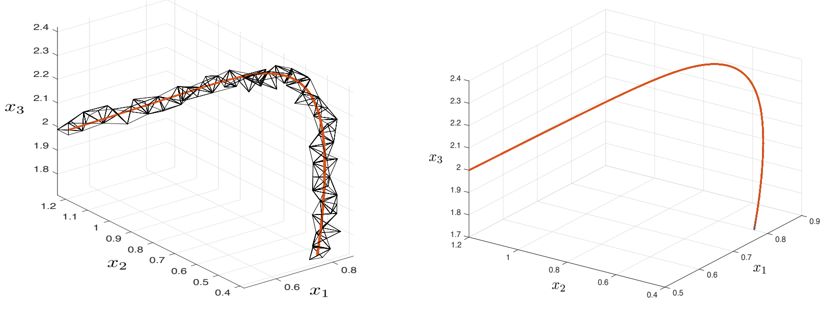

(a) Simulation results for (6.2) with the PWA vector field method-red, including simplices-black.

(b) Simulation results for (6.2) with the PWA vector field method-red and RK4 method-blue.

Figure A.1: Trajectory approximations for (6.2).

3D implementation of the piecewise affine vector field method and the fourth-order Runge-Kutta algorithm. In Figure A.1(a) we show the trajectory of the approximated solution of (6.2), initialized in $x_0 = (0.5\ 1.2\ 2.0)^\top \in \mathcal{P}$, generated by the PWA vector field method, together with the corresponding simplices. For the same initial condition, a simulation is made using the RK4 method. We show the trajectories generated by both methods in Figure A.1(b) where it can be observed that they fully overlap.

A.3.2 Model of tumor growth dynamics

Consider the system described by

$$\begin{cases} \dot{x}_1 &= 1 + a_1 x_1(1 - x_1) - x_1 x_2, \\ \dot{x}_2 &= a_2 x_2 x_3 - a_3 x_2, \\ \dot{x}_3 &= a_4 x_3(1 - x_3) - a_5 x_2 x_3 - a_6 x_3, \end{cases} \tag{A.6}$$

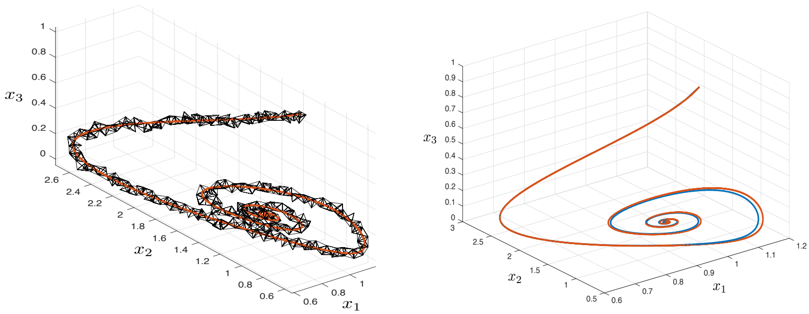

(a) Simulation results for (A.6) with the PWA vector field method-red, including simplices-black.

(b) Simulation results for (A.6) with the PWA vector field method-red and RK4 method-blue.

Figure A.2: Trajectory approximations for (A.6).

representing a prey-predator type model for tumor growth dynamics [100]. We consider the parameters $a_1 = 2.5$, $a_2 = 4.8$, $a_3 = 0.6$. $a_4 = 3.5$, $a_5 = 2.4$ and $a_6 = 0.1$.

Approximations of the solutions of (A.6) are made using both the 3D implementation of the piecewise affine vector field method and the fourth-order Runge-Kutta algorithm. In Figure A.2(a) we show the trajectory of the approximated solution of (A.6), initialized in $x_0 = (1\ 1\ 1)^\top \in \mathcal{P}$, generated by the PWA vector field method, together with the corresponding simplices. For the same initial condition, a simulation is made using the RK4 method. We show the trajectories generated by both methods in Figure A.2(b).

Appendix B

Numerical values from Chapter 3

B.1 Numerical values for the system in Section 3.2.1

The LF $V_4(x)$ for system (3.1) is defined by

$$V_4(x) = \frac{R_2(x) + R_3(x) + R_4(x)}{1 + Q_1(x) + Q_2(x)},$$

with the following polynomials.

$$\begin{aligned}
R_2(x) =& 0.0742x_1^2 - 0.0042x_1x_2 + 12.8175x_2^2 - 0.0003x_1x_3 + 50.0419x_2x_3 + 61.571x_3^2.\\
R_3(x) =& -0.00826194x_1^3 - 0.0992636x_1^2x2 + 0.00579408x_1x_2^2 - 18.2006x_2^3\\
&+ 0.34662x_1^2x_3 - 0.0196204x_1x_2x_3 - 7.11137x_2^2x_3 - 0.00145815x_1x_3^2\\
&+ 47.7474x_2x_3^2.\\
R_4(x) =& 0.00105993x_1^4 + 0.0110812x_1^3x_2 + 0.0466955x_1^2x_2^2 - 0.00275097x_1x_2^3\\
&+ 8.96691x_2^4 - 0.0385862x_1^3x_3 - 0.224657x_1^2x_2x_3 + 0.0131018x_1x_2^2x_3\\
&- 18.0608x_2^3x_3 + 0.0100365x_1^2x_3^2 + 0.00026071x_1x_2x_3^2 + 13.836x_2^2x_3^2\\
&+ 0.000156139x_1x_3^3 - 0.170002x_2x_3^3 + 0.000643478x_3^4.\\
Q_1(x) =& -1.33826x_2 + 4.67002x_3.\\
Q_2(x) =& 0.000339616x_1^2 - 0.0000193332x_1x_2 + 0.571608x_2^2 - 3.25913x_2x_3 - 0.1483x_3^2.
\end{aligned}$$

B.2 Numerical values for the system in Section 3.2.2

Numerical values for each LF V_4, corresponding to system (3.2) in the cases discussed in Section 3.2.2.

- Case 1: $V_1(x) = (29.8 + 6.45x_1 + 1.16x_1^2 - 0.0272x_1^3 - 0.000275x_1^4 - 1.81x_2 - 1.18x_1x_2 - 0.073x_1^2x_2 + 0.0016x_1^3x_2 - 0.69x_2^2 + 0.0707x_1x_2^2 + 0.00197x_1^2x_2^2 + 0.0731x_2^3 - 0.0017x_1x_2^3 - 0.00158x_2^4)/(-0.0659 + 0.0432x_1 - 0.00123x_1^2 + 0.129x_2 - 0.00153x_1x_2 - 0.00219x_2^2)$ with $C_1 = 37$.

- Case 2: $V_2(x) = (57.9 + 31.3x_1 + 8.26x_1^2 - 0.596x_1^3 + 0.0231x_1^4 - 19.8x_2 - 11.4x_1x_2 - 0.349x_1^2x_2 + 0.0125x_1^3x_2 + 3.05x_2^2 + 0.901x_1x_2^2 + 0.00921x_1^2x_2^2 - 0.21x_2^3 - 0.0239x_1x_2^3 + 0.00591x_2^4)/(0.517 + 0.434x_1 - 0.0425x_1^2 - 0.0743x_2 + 0.00157x_1x_2 + 0.00576x_2^2)$.

- Case 3: $V_3(x) = (44.7 - 6.13x_1 + 2.72x_1^2 - 0.19x_1^3 + 0.00523x_1^4 - 6.13x_2 - 4.84x_1x_2 + 0.213x_1^2x_2 - 0.00212x_1^3x_2 + 2.72x_2^2 + 0.213x_1x_2^2 - 0.00781x_1^2x_2^2 - 0.19x_2^3 - 0.00212x_1x_2^3 + 0.00523x_2^4)/(0.204 + 0.0671x_1 - 0.00248x_1^2 + 0.0671x_2 + 0.00273x_1x_2 - 0.00248x_2^2)$.

- Case 4: $V_4(x) = (29.8 - 1.81x_1 - 0.69x_1^2 + 0.0731x_1^3 - 0.00158x_1^4 + 6.45x_2 - 1.18x_1x_2 + 0.0707x_1^2x_2 - 0.0017x_1^3x_2 + 1.16x_2^2 - 0.073x_1x_2^2 + 0.00197x_1^2x_2^2 - 0.0272x_2^3 + 0.0016x_1x_2^3 - 0.000275x_2^4)/(-0.0659 + 0.129x_1 - 0.00219x_1^2 + 0.0432x_2 - 0.00153x_1x_2 - 0.00123x_2^2)$.

Bibliography

[1] J. Adam and N. Bellomo. *A Survey of Models on Tumor Immune Systems Dynamics*. Birkhauser, Boston, 1996.

[2] D. Aeyels and J. Peuteman. A new asymptotic stability criterion for nonlinear time-variant differential equations. *IEEE Transactions on Automatic Control*, 43(7):968–971, Jul 1998.

[3] A. A. Ahmadi, M. Krstic, and P. A. Parrilo. A globally asymptotically stable polynomial vector field with no polynomial Lyapunov function. In *50th IEEE Conference on Decision and Control and European Control Conference (CDC-ECC)*, pages 7579–7580, Dec 2011.

[4] A. A. Ahmadi and P. A. Parrilo. On higher order derivatives of Lyapunov functions. In *Proceedings of the 2011 American Control Conference*, pages 1313–1314, 2011.

[5] Z. Aminzare and E. D. Sontag. Contraction methods for nonlinear systems: A brief introduction and some open problems. In *53rd IEEE Conference on Decision and Control (CDC)*, pages 3835–3847, 2014.

[6] M. Andersen, F. Vinther, and J. T. Ottesen. Mathematical modeling of the hypothalamic-pituitary-adrenal gland (hpa) axis, including hippocampal mechanisms. *Mathematical Biosciences*, 246(1):122 – 138, 2013.

[7] Z. Artstein. Stabilization with relaxed controls. *Nonlinear Analysis: Theory, Methods & Applications*, 7(11):1163 – 1173, 1983.

[8] K. Atkinson, W. Han, and D. Stewart. *Numerical solution of ordinary differential equations*. Wiley-Interscience, John Wiley & Sons, Inc., Hoboken, New Jersey, 2009.

[9] R. Baier and S.F. Hafstein. Numerical computation of control Lyapunov functions in the sense of generalized gradients. In *Proceedings of the 21st International Symposium on Mathematical Theory of Networks and Systems (MTNS 2014), July 7-11, 2014, University of Groningen, Groningen, Netherlands*, pages 1173 – 1180, 2014.

[10] A. Ben-Zvi, S. D. Vernon, and G. Broderik. Model-based therapeutic correction of hypothalamic-pituitary-adrenal axis dysfunction. *PLOS Computational Biology*, 5(1), 2009.

[11] A. Berman, M. Neumann, and R. J. Stern. *Nonnegative Matrices in Dynamic Systems: A Wiley Series of Texts, Monographs and Tracts*. Wiley-Interscience; 1 edition, 1989.

[12] J. Bjornsson, P. Giesl, S. F. Hafstein, C. M. Kellett, and H. Li. Computation of continuous and piecewise affine Lyapunov functions by numerical approximations of the Massera construction. In *53rd IEEE Annual Conference on Decision and Control (CDC)*, pages 5506–5511, Dec 2014.

[13] J. Bjornsson, S. Gudmundsson, and S. F. Hafstein. Algorithmic verification of approximations to complete Lyapunov functions. In *Proceedings of the 21st International Symposium on Mathematical Theory of Networks and Systems (MTNS)*, pages 1181–1188, 2014.

[14] J. Bjornsson, S. Gudmundsson, and S. F. Hafstein. Class library in C++ to compute Lyapunov functions for nonlinear systems. *IFAC-PapersOnLine*, 48(11):778 – 783, 2015. 1st IFAC Conference on Modelling, Identification and Control of Nonlinear Systems, 2015.

[15] J. Björnsson, P. Giesl, S. F. Hafstein, and C. M. Kellett. Computation of Lyapunov functions for systems with multiple local attractors. *Discrete and Continuous Dynamical Systems*, 35(9):4019–4039, 2015.

[16] F. Blanchini and S. Miani. *Set-theoretic methods in control*. Systems & Control: Foundations & Applications. Birkhäuser, Boston, MA, 2008.

[17] R. V. Bobiti and M. Lazar. On input-to-state stability analysis of discrete-time systems via finite-time Lyapunov functions. In *the 19th World Congress The International Federation of Automatic Control Cape Town, South Africa*, pages 8623–9628, 2014.

[18] S. Boyd and L. Vandenberghe. *Convex optimization*. Cambridge University Press, 2004.

[19] M. S. Branicky. Multiple Lyapunov functions and other analysis tools for switched and hybrid systems. *IEEE Transactions on Automatic Control*, 43(4):475–482, Apr 1998.

[20] A. Browder. *Mathematical analysis. An introduction*. Springer, 1996.

[21] O. Buse, R. Pérez, and A. Kuznetsov. Dynamical properties of the repressilator model. *Phys. Rev. E*, 81:066206–1–066206–7, June 2010.

[22] A. Butz. Higher order derivatives of Liapunov functions. *IEEE Transactions on Automatic Control*, 14(1):111–112, 1969.

[23] F. Camilli, L. Grüne, and F. Wirth. Domains of attraction of interconnected systems: A Zubov method approach. In *European Control Conference (ECC)*, pages 91–96, Aug 2009.

[24] F. Camilli, L. Grüne, and F. Wirth. Control Lyapunov Functions and Zubov's Method. *Siam Journal on Control and Optimization*, 47:301–326, 2008.

[25] G. Chesi. Estimating the domain of attraction for non-polynomial systems via LMI optimizations. *Automatica*, 45(6):1536 – 1541, 2009.

[26] G. Chesi. *Domain of Attraction: Analysis and Control via SOS Programming*. Lecture Notes in Control and Information Sciences. Springer, 2011.

[27] G. Chesi. Rational Lyapunov functions for estimating and controlling the robust domain of attraction. *Automatica*, 49(4):1051 – 1057, 2013.

[28] H. D. Chiang and J. S. Thorp. Stability regions of nonlinear autonomous dynamical systems: a constructive methodology. *IEEE Transactions on Automatic Control*, 34:1229–1241, 1989.

[29] H.D. Chiang, M.W. Hirsch, and F. W. Wu. Stability regions of nonlinear autonomous dynamical systems. *IEEE Transactions on Automatic Control*, 33:16–27, 1988.

[30] E. J. Davison and E. M. Kurak. A computational method for determining quadratic Lyapunov functions for non-linear systems. *Automatica*, 7(5):627 – 636, 1971.

[31] J. Dieudonné. *Treatise on Analysis, Vol. I, Foundations of Modern Analysis*. Academic Press, New York and London, 1969.

[32] A. I. Doban and M. Lazar. Domain of attraction computation for tumor dynamics. In *53rd IEEE Conference on Decision and Control (CDC)*, pages 6987–6992, Los Angeles, 2014.

[33] A. I. Doban and M. Lazar. Stability analysis of discrete-time general homogeneous systems. In *the 19th IFAC World Congress*, pages 8642–8647, 2014.

[34] A. I. Doban and M. Lazar. An evolutionary-type model for tumor immunotherapy. In *The 9th IFAC Symposium on Biological And Biomedical Systems (BMS)*, pages 575–580, Berlin, 2015.

[35] A. I. Doban and M. Lazar. A switched systems approach to cancer therapy. In *the 14th annual European Control Conference (ECC)*, pages 2723–2729, Linz, 2015.

[36] L. Edelstein-Keshet. *Mathematical Models in Biology*. Society for Industrial and Applied Mathematics, 2005.

[37] M. B. Elowitz and S. Leibler. A synthetic oscillatory network of transcriptional regulators. *Nature*, 403(6767):335–338, 2000.

[38] H. Enderling, N. Almog, and L. Hlatky. *Systems Biology of Tumor Dormancy*. Advances in Experimental Medicine and Biology, Volume 734, Springer, 2013.

[39] R. A. Freeman and P.V. Kokotović. *Robust Nonlinear Control Design.* Birkhäuser, Boston, MA, 2008. reprint of the 1996 edition.

[40] T. S. Gardner, C. R. Cantor, and J. J. Collins. Construction of a genetic toggle switch in Escherichia coli. *Nature*, 403(6767):339–342, 2000.

[41] R. A. Gatenby. Models of tumor-host interaction as competing populations: Implications for tumor biology and treatment. *Journal of Theoretical Biology*, 176(4):447 – 455, 1995.

[42] R. A. Gatenby. A change of strategy in the war on cancer. *Nature*, 459:508–509, 2009.

[43] R. A. Gatenby and T. L. Vincent. Application of quantitative models from population biology and evolutionary game theory to tumor therapeutic strategies. *Molecular Cancer Therapeutics*, 2(9):919–927, 2003.

[44] R. Geiselhart. *Advances in the stability analysis of large-scale discrete-time systems*. PhD thesis, The Julius Maximilians University of Wurzburg, 2015.

[45] R. Geiselhart, R. H. Gielen, M. Lazar, and F. R. Wirth. An alternative converse Lyapunov theorem for discrete-time systems. *Systems & Control Letters*, 70:49 – 59, 2014.

[46] R. Geiselhart and F. Wirth. Relaxed ISS small-gain theorems for discrete-time systems. *ArXiv e-prints*, nov 2015.

[47] R. Genesio and A. Vicino. Some results on the asymptotic stability of second-order nonlinear systems. *Automatic Control, IEEE Transactions on*, 29(9):857–861, 1984.

[48] P. Giesl and S. F. Hafstein. Computation and Verification of Lyapunov Functions. *SIAM Journal on Applied Dynamical Systems*, 14(4):1663–1698, 2015.

[49] P. Giesl and S.F. Hafstein. Construction of Lyapunov functions for nonlinear planar systems by linear programming. *Journal of Mathematical Analysis and Applications*, 388(1):463 – 479, 2012.

[50] A. Girard. Etude de Systèmes Dynamiques Hybrides Affines par Morceaux. Master's thesis, ENSIMAG, DEA de Mathématiques Appliquées, 2001.

[51] A. Girard. Approximate solutions of ODEs using piecewise linear vector fields. In *5th International Workshop on Computer Algebra in Scientific Computing, Yalta, Ukraine*, pages 107–120, 2002.

[52] L. Grüne and M. Sigurani. Numerical ISS controller design via a dynamic game approach. In *52nd IEEE Conference on Decision and Control*, pages 1732–1737, 2013.

[53] L. Grüne, F. Camilli, and F. Wirth. Homogeneous control Lyapunov functions for homogeneous control systems. In *Mathematical Theory of Networks and Systems (MTNS)*, Perpignan, 2000.

[54] J. Gudmand-Hoeyer, S. Timmermann, and J. T. Ottesen. Patient-specific modeling of the neuroendocrine HPA-axis and its relation to depression: Ultradian and circadian oscillations. *Mathematical Biosciences*, 257:23 – 32, 2014.

[55] S. Gupta, E. Aslakson, B. M. Gurbaxani, and S. D. Vernon. Inclusion of the glucocorticoid receptor in a hypothalamic pituitary adrenal axis model reveals bistability. *Theoretical Biology and Medical Modelling*, 4(1):1–12, 2007.

[56] O. Hachicho. A novel LMI-based optimization algorithm for the guaranteed estimation of the domain of attraction using rational Lyapunov functions. *Journal of the Franklin Institute*, 344(5):535 – 552, 2007.

[57] S. F. Hafstein. An algorithm for constructing Lyapunov functions. *Electronic Journal of Differential Equations, Monograph 08*, 2007.

[58] S. F. Hafstein, C. M. Kellett, and H. Li. Computing continuous and piecewise affine Lyapunov functions for nonlinear systems. `https://epub.uni-bayreuth.de/1962/`, 2015.

[59] S. F. Hafstein, C. M. Kellett, and Huijuan Li. Continuous and piecewise affine Lyapunov functions using the Yoshizawa construction. In *American Control Conference (ACC), 2014*, pages 548–553, June 2014.

[60] W. Hahn. *Stability of motion*. Die Grundlehren der mathematischen Wissenschaften, Band 138, Springer, Berlin, 1967.

[61] D. Han and M. Althoff. Control synthesis for non-polynomial systems: A domain of attraction perspective. In *54th IEEE Conference on Decision and Control (CDC)*, pages 1160–1167, 2015.

[62] J. Hofbauer and K. Sigmund. *Evolutionary Games and Population Dynamics*. Cambridge University Press, 1998.

[63] L. Hormander. *The Analysis of Linear Partial Differential Operators II*. Springer-Verlag, Berlin, 1983.

[64] R. Horst. On the global minimization of concave functions. *Operations-Research-Spektrum*, 6(4):195–205, 1984.

[65] N. Hosseinichimeh, H. Rahmandad, and A. K. Wittenborn. Modeling the hypothalamus-pituitary-adrenal axis: A review and extension. *Mathematical Biosciences*, 268:52 – 65, 2015.

[66] J. H. Hubbard and B. H. West. *Differential Equations: A Dynamical Systems Approach - Higher-Dimensional Systems*. Springer, 1995.

[67] G. Jansen, R. Gatenby, and C. A. Aktipis. Control vs. eradication: Applying infectious disease treatment strategies to cancer. *Proceedings of the National Academy of Sciences of the United States of America*, 112(4):937–938, 2015.

[68] Z. P. Jiang and Y. Wang. Input-to-state stability for discrete-time nonlinear systems. *Automatica*, 37(6):857 – 869, 2001.

[69] E. M. Judd, M. T. Laub, and H. H. McAdams. Toggles and oscillators: New genetic circuit designs. *BioEssays*, 22(6):507–509, 2000.

[70] R. Kalman and J. Bertram. Control system analysis and design via the "second method" of Lyapunov: Part I, continuous-time systems. *Transactions of the AMSE, Series D: Journal of Basic Engineering*, 82(2):371–393, 1960.

[71] I. Karafyllis. Can we prove stability by using a positive definite function with non sign-definite derivative? *IMA Journal of Mathematical Control and Information*, 29(2):147–170, 2012.

[72] I. Karafyllis and J. Tsinias. Control Lyapunov functions and stabilization by means of continuous time-varying feedback. *ESAIM: Control, Optimisation and Calculus of Variations*, 15(3):599–625, 2009.

[73] J. Keener and J. Sneyd. *Mathematical physiology*. Springer-Verlag, 1998.

[74] C. M. Kellett. A compendium of comparison function results. *Mathematics of Control, Signals, and Systems*, 26(3):339–374, 2014.

[75] C. M. Kellett. Classical converse theorems in Lyapunov's second method. *Discrete and Continuous Dynamical Systems - Series B*, 20(8):2333–2360, 2015.

[76] C. M. Kellett and A. R. Teel. Weak converse Lyapunov theorems and Control-Lyapunov functions. *SIAM Journal on Control and Optimization*, 42(6):1934–1959, 2004.

[77] Hassan K. Khalil. *Nonlinear Systems*. Prentice Hall, 2002.

[78] N. N. Krasovskii. *Stability of motion: Applications of Lyapunov's second method to differential systems and equations with delay*. Stanford University Press, 1963.

[79] J. Kurzweil. On the inversion of Ljapunov's second theorem on stability of motion. *Czechoslovak Mathematical Journal*, 81:455 – 484, 1956. English transaltion in Americal Mathematical Society Transaltions (2), v.24, pp. 19-77.

[80] J. LaSalle and S. Lefschetz. *Stability by Liapunov's Direct Method with Applications*. Academic Press, New York, London, 1961.

[81] H. Li, R. Baier, L. Grüne, S. F. Hafstein, and F. Wirth. Computation of local ISS Lyapunov functions via linear programming. In *the 21st International Symposium on Mathematical Theory of Networks and Systems (MTNS), Groningen, The Netherlands*, pages 1189–1195, no.158, 2014.

[82] H. Li, R. Baier, L. Grüne, S. F. Hafstein, and F. Wirth. Computation of local ISS Lyapunov functions with low gains via linear programming. *Discrete and Continuous Dynamical Systems - Series B*, 20(8):2477–2495, 2015.

[83] H. Li and F. Wirth. Zubov's method for interconnected systems - a dissipative formulation. In *the 20th Int. Symp. Math. Theory of Networks and Systems (MTNS 2012)*, pages 8, paper no. 184, 2012.

[84] A. Liapounoff. Problème général de la stabilité du mouvement. *Annales de la faculté des sciences de Toulouse*, 9:203–474, 1907.

[85] D. Liberzon, E. D. Sontag, and Y. Wang. Universal construction of feedback laws achieving ISS and integral-ISS disturbance attenuation. *Systems & Control Letters*, 46(2):111 – 127, 2002.

[86] Y. Lin and E. D. Sontag. A universal formula for stabilization with bounded controls. *Systems & Control Letters*, 16(6):393 – 397, 1991.

[87] Y. Lin, E. D. Sontag, and Y. Wang. A smooth converse Lyapunov theorem for robust stability. *SIAM Journal on Control and Optimization*, 34(1):124–160, 1996.

[88] A. H. Maas, Y. J. W. Rozendaal, C. Pul, van, P. A. J. Hilbers, E. J. E. Cottaar, H. R. Haak, and N. A. W Riel, van. A physiology-based model describing heterogeneity in glucose metabolism: the core of the Eindhoven Diabetes Education Simulator (E-DES). *Journal of Diabetes Science and Technology*, 9(2):282–292, 2015.

[89] S. F. Marinósson. Lyapunov function construction for ordinary differential equations with linear programming. *Dynamical Systems*, 17(2):137–150, 2002.

[90] J. L. Massera. On Liapounoff's conditions of stability. *Annals of Mathematics*, 50(3):705–721, 1949.

[91] L. G. Matallana, A. M. Blanco, and J. A. Bandoni. Estimation of domains of attraction: A global optimization approach. *Mathematical and Computer Modelling*, 52(3-4):574 – 585, 2010.

[92] A. Merola, C. Cosentino, and F. Amato. An insight into tumor dormancy equilibrium via the analysis of its domain of attraction. *Biomedical Signal Processing and Control*, 3(3):212 – 219, 2008.

[93] J. Muller and C. Kuttler. *Methods and Models in Mathematical Biology. Deterministic and Stochastic Approaches*. Springer, 2015.

[94] J. D. Murray. *Mathematical Biology I: An introduction*. Springer, 2002. Third edition.

[95] C. Phang, Y. Wu, and B Wiwatanapataphee. Computation of the domain of attraction for suboptimal immunity epidemic models using the maximal Lyapunov function method. *Abstract and Applied Analysis*, 2013, Article ID 508794, 7 pages, 2013.

[96] S. Prajna, A. Papachristodoulou, and P. A. Parrilo. Introducing sostools: a general purpose sum of squares programming solver. In *Decision and Control, 2002, Proceedings of the 41st IEEE Conference on*, volume 1, pages 741–746 vol.1, Dec 2002.

[97] L. Rosier. Homogeneous Lyapunov function for homogeneous continuous vector field. *Syst. Control Lett.*, 19(6), December 1992.

[98] N. Rouche, P. Habbets, and M. Lalloy. *Stability theory via Liapunov's direct method*. Springer-Verlag, 1977.

[99] S. Rozgonyi, K. M. Hangos, and G. Szederkényi. Determining the domain of attraction of hybrid nonlinear systems using maximal Lyapunov functions. *Kybernetika*, 46(1):19–37, 2010.

[100] R. R. Sarkar and S. Banerjee. Cancer self remission and tumor stability - a stochastic approach. *Mathematical Biosciences*, 196(1):65 – 81, 2005.

[101] R. Sepulchre and D. Aeyels. Homogeneous Lyapunov functions and necessary conditions for stabilization. *Mathematics of Control, Signals and Systems*, 9(1).

[102] C. Sloth and R. Wisniewski. Control to facet for polynomial systems. In *Proceedings of the 17th ACM international conference on Hybrid Systems: Computation and Control*, pages 123–132, 2014.

[103] G. Söderlind. The logarithmic norm. History and modern theory. *BIT Numerical Mathematics*, 46(3):631–652, 2006.

[104] E. D. Sontag. A Lyapunov-like characterization of asymptotic controllability. *SIAM Journal on Control and Optimization*, 21(3):462–471, 1983.

[105] E. D. Sontag. Smooth stabilization implies coprime factorization. *IEEE Transactions on Automatic Control*, 34(4):435–443, 1989.

[106] E. D. Sontag. A "universal" construction of Artstein's theorem on nonlinear stabilization. *Systems* & *Control Letters*, 13:117–123, 1989.

[107] E. D. Sontag. Feedback stabilization of nonlinear systems. In *Robust control of linear systems and nonlinear control (Amsterdam, 1989)*, volume 4 of *Progr. Systems Control Theory*, pages 61–81. Birkhäuser Boston, Boston, MA, 1990.

[108] E. D. Sontag. Comments on integral variants of ISS. *Systems & Control Letters*, 34(1-2):93 – 100, 1998.

[109] E. D. Sontag. *Mathematical Control Theory: Deterministic Finite Dimensional Systems. Second Edition*. Textbooks in Applied Mathematics. Springer, New York, 1998.

[110] E. D. Sontag and Y. Wang. On characterizations of input-to-state stability with respect to compact sets. In *The IFAC Non-Linear Control Systems Design Symposium (NOLCOS'95), Tahoe City, CA*, pages 226–231, 1995.

[111] E. D. Sontag and Y. Wang. On characterizations of the input-to-state stability property. *Systems & Control Letters*, 24(5):351 – 359, 1995.

[112] E. D. Sontag and Y. Wang. New characterizations of input-to-state stability. *IEEE Transactions on Automatic Control*, 41(9):1283–1294, 1996.

[113] M. Stämpfle. Optimal Estimates for the Linear Interpolation Error on Simplices. *Journal of Approximation Theory*, 103(1):78 – 90, 2000.

[114] T. R. V. Steentjes, A. I. Doban, and M. Lazar. Construction of continuous and piecewise affine Lyapunov functions via a finite-time converse. Accepted to *the 10th IFAC Symposium Nonlinear Control Systems, (NOLCOS)*, 2016.

[115] A. R. Teel and L. Praly. A smooth Lyapunov function from a class-$\mathcal{KL}$ estimate involving two positive semidefinite functions. *ESAIM: Control, Optimisation and Calculus of Variations*, 5:313–367, 2000.

[116] G. J. Tortora and B. H. Dickinson. *Principles of Anatomy and Physiology. Control Systems of the Human Body*. John Wiley & Sons, 2009.

[117] A. van der Schaft, S. Rao, and B. Jayawardhana. On the mathematical structure of balanced chemical reaction networks governed by mass action kinetics. *SIAM Journal on Applied Mathematics*, 73(2):953–973, 2013.

[118] A. Vannelli and M. Vidyasagar. Maximal Lyapunov functions and domains of attraction for autonomous nonlinear systems. *Automatica*, 21(1):69–80, 1985.

[119] M. Vidyasagar. *Nonlinear Systems Analysis (2Nd Ed.)*. Prentice-Hall, Englewood Cliffs, NJ, 1993.

[120] N. Yordanov, J. Tumova, I. Cerna, J. Barnat, and C. Belta. Formal analysis of piecewise affine systems through formula-guided refinement. *Automatica*, 49(1):261 – 266, 2013.

[121] T. Yoshizawa. *Stability Theory by Liapunov's Second Method*. Publications of the Mathematical Society of Japan, No. 9, 1966.

[122] V. I. Zubov. *Methods of A. M. Lyapunov and their application*. Noordhoff, Groningen, 1964.

Acknowledgements

First of all I would like to thank Mircea for his constant support and guidance starting with my M.Sc. studies in Eindhoven in 2010, then writing a Ph.D. project proposal together and pursuing such a challenging research topic. I am very grateful for the many scientific and nonscientific discussions we had during this period, including our disagreements. Challenging personalities only add up to keep the work interesting! They all have significantly contributed to my development as a researcher, but also as a person. Thank you for being such a devoted supervisor and for all the time invested in my project.

Next, I would like to thank my promoter, Paul, for his advice and being an inspiring example of stability when dealing with people. Thank you for your suggestions which have improved a lot the readability of this thesis. I also want to acknowledge DISC for facilitating this research, which otherwise wouldn't have happened, and NWO for financing it. I also want to thank Jan van Schuppen for his involvement in preparing the proposal and the time spent in my project.

I am very grateful to the members of my committee, whose comments have greatly improved my thesis. I would like to especially thank Dr. Sigurdur Hafstein, for reading my thesis so carefully and pointing out very important remarks, which have added considerably to the thesis. Thank you as well for the wonderful time at the Lyapunov workshop in Reykjavik, where I went together with Mircea and Nikos. The trip at the end of the workshop was great! I also want to thank Dr. Ralf Peeters, for his insightful remarks and the nice discussion in Maastricht. Next I want to thank Dr. Natal van Riel and Dr. Arjan van der Schaft for being part of the committee. Natal, thank you for the nice discussion we had on emerging healthcare challenges and Arjan thank you for bringing physical Lyapunov functions to my attention! Finally, a special thanks goes to Dr. Octavian Pastravanu. Thank you for accepting to be part of the committee and your guidance during my B.Sc. studies, which has had a major influence on my career path. If it wasn't for you, I would have probably never studied Lyapunov theory.

My time as Ph.D student wouldn't have been the same without my colleagues! Thank you guys for the nice conference trips, lunches, coffee breaks and abs classes! I want to especially thank Ruxandra, for many fun moments and discussions and to my original office mate, Koen. It was very nice having you as office mate in Potentiaal, and afterwards in Flux, also partially due to Jennifer's cakes (especially the carrot cake)! Ruben, thanks for being a very good housemate! Barbara, Will and Udo thank you for all your help during these years. Also, I would like to thank Paul van den Bosch for his helpful advice since I started as an M.Sc. student in the CS group. Working with you on the Control course was

a very nice experience. A word of thanks goes also to Tom Steentjes. It was a pleasure to co-supervise you, your work lead to some nice plots in my thesis. I wish you the best of luck for the future!

I would like to thank Bianca for her friendship and support for almost 10 years! Thank you for the advice during the difficult times, but also for the very nice time during our visits and trips. The last trip in Barcelona was definitely a highlight for our Spanish skills. As for new friends, I want to thank Lieneke for being my friend since my first weeks in the Netherlands! I truly enjoyed all our activities together, especially going on trips, to concerts and nice dinners. I will miss a lot our coffee breaks and weekly lunches at TU/e!

Of course, none of this would be possible without my family. I want to thank my parents for all their support and for giving me the freedom and independence for making my own choices! I am grateful to my sister and brother and their families for always making my trips back home so nice! I want to especially thank my sister for all the advice she has given me through the years and to my nephew Razvan for designing my thesis cover.

Alina Doban,
Eindhoven, 16 August, 2016.

Curriculum Vitae

Alina I. Doban was born in Târgu Frumos, Romania on December 28, 1987. She received her B.Sc. degree in Automatic Control from the Technical University “Gh. Asachi” of Iasi, Romania. In 2010, she started her M.Sc. studies with a scholarship from the Eindhoven University of Technology, Eindhoven, The Netherlands as part of the Talent Scholarship Program and received her M.Sc. degree (cum laude) in Electrical Engineering in 2012. Thereafter, she started working towards a Ph.D. degree in the Control Systems group of the Electrical Engineering Department at the same institution with a NWO financed personal grant as part of the DISC Graduate Programme.

Her research interests include the computation of domains of attraction and stabilization of nonlinear continuous–time systems and she has studied the application of these techniques to the domain of mathematical biology, in particular disease dynamics, systems regulating substances produced in the body, such as cortisol and gene regulatory networks.